THE STEAM REFORMING OF HYDROCARBONS WITH SPECIAL REFERENCE TO METHANE.

A THESIS SUBMITTED BY

CHRISTOPHER JOHN WOODCOCK

FOR THE DEGREE OF Ph.D.

JULY 1971

THE UNIVERSITY OF ASTON IN BIRMINGHAM

CHEMICAL ENGINEERING DEPARTMENT.

SUMMARY.

From an examination of the literature relating to the catalytic steam reforming of hydrocarbons, it is concluded that the kinetics of high pressure reforming, particularly steam-methane reforming, has received relatively little attention. Therefore because of the increasing availability of natural gas in the U.K., this system was considered worthy of investigation.

An examination of the thermodynamics relating to the equilibria of steam-hydrocarbon reforming is described. The reactions most likely to have influence over the process are established and from these a computer program was written to calculate equilibrium compositions. A means of presenting such data in a graphical form for ranges of the operating variables is given, and also an operating chart which may be used to quickly check feed ratios employed on a working naphtha reforming plant is presented.

For the experimental kinetic study of the steam-methane system, cylindrical pellets of ICI 46-1 nickel catalyst were used in the form of a rod catalyst. The reactor was of the integral type and a description is given with the operating procedures and analytical method used.

The experimental work was divided into two parts, qualitative and quantitative. In the qualitative study

the various reaction steps are examined in order to establish which one is rate controlling. It is concluded that the effects of film diffusion resistance within the conditions employed are negligible.

In the quantitative study it was found that at 250 psig and 650°C the steam-methane reaction is much slower than the CO shift reaction and is rate controlling. Two rate mechanisms and accompanying kinetic rate equations are derived, both of which represent 'chemical' steps in the reaction and are considered of equal merit. However the possibility of a dual control involving 'chemical' and pore diffusion resistances is also expressed.

C O N T E N T S.

INDEX OF FIGURES.

INDEX OF FIGURES (Cont.).

INDEX OF FIGURES (Cont.).

INDEX OF TABLES.

INDEX OF TABLES (Cont.).

INDEX OF PLATES.

ACKNOWLEDGEMENTS.

I would like to thank the following who have helped make this thesis possible.

The Gas Council for awarding the scholarship.

Dr.B.Thompson of the Gas Council Midlands Research Station for his help in arranging the loan of apparatus.

Mr. R.A. Cross of the Gas Council Midlands Research Station for advice on chromatographic methods.

Mr. C.L. Maxey for allowing access to the process records at the W.M.G.B. Coleshill works.

Prof. G.V.Jeffreys for a place in the research school at the University of Aston in Birmingham.

Mr. N.Roberts and the technical staff at Aston for assistance in the construction of apparatus.

My Supervisor, Mr. A.R.Cooper for his advice, encouragement, and support throughout.

NOMENCLATURE.

B_G	-	film thickness.
Cp	-	specific heat at constant pressure.
C_I	-	concentration of component I adsorbed on the catalyst surface.
Cl	-	concentration of unoccupied active sites on the catalyst surface.
D_{AV}	-	average diffusivity of the controlling component.
E_A	-	activation energy.
F	-	methane flow rate g moles h^{-1}.
ΔG_T^o	-	free energy at temperature T.
ΔH_T^o	-	heat of formation at temperature T.
Kp	-	partial pressure equilibrium constant.
K_α	-	fugacity coefficient equilibrium constant.
K_T	-	thermodynamic equilibrium constant.
K_{SR}	-	surface reaction equilibrium constant.
K_I	-	adsorption equilibrium constant for component I.
L	-	total number of active sites on the catalyst surface.
P	-	total pressure atm.
R	-	gas constant lit atm. $^oK^{-1}$, and steam-methane feed ratio (mole : mole).
T	-	temperature.
W	-	mass of catalyst gm.
W/F	-	time factor gm catalyst, h, gm mole methane $^{-1}$.

NOMENCLATURE (Cont.).

a	-	catalyst external area available for mass transport.
f	-	fractional conversion.
k_G	-	mass transfer coefficient.
k	-	reaction velocity constant.
l	-	active site on the catalyst surface.
p_I	-	bulk partial pressure of component I.
p_{I_i}	-	partial pressure of I at the gas/solid interface.
p_f	-	film pressure factor.
r	-	reaction rate.
α	-	fugacity coefficient.
ρ	-	density.
μ	-	viscosity.

INTRODUCTION.

The catalytic reforming of hydrocarbons in the presence of steam has developed in recent years into one of the major routes for producing towns gas, synthesis gas, and hydrogen. The rapid growth in the U.K. and other countries without supplies of natural gas can be directly attributed to the development of high pressure naphtha reforming processes such as the ICI lean gas, ICI towns gas, Gas Council Catalytic Rich Gas (C.R.G.), and Topsøe 500, which give high continuous outputs at relatively low capital and running costs (8,80,97). This growth is illustrated in Figure 1 which shows the naphtha usage in the U.K. by steam-reforming plant.

Overall, the reforming process may be considered essentially as sulphur removal from the hydrocarbon feed followed by reforming with steam.

Since reforming catalysts are sensitive to sulphur poisoning (8,9,23,49,82) it is necessary to remove sulphur compounds from the feed, which usually exist as H_2S, COS, CS_2, and mercaptans. Furthermore, by removing sulphur at this stage it does eliminate the need to remove H_2S from the reformed product gas, which provides a saving in capital costs since in the latter case the volumetric throughput is considerably larger and therefore larger capacity absorbing plant would be required.

Figure 1

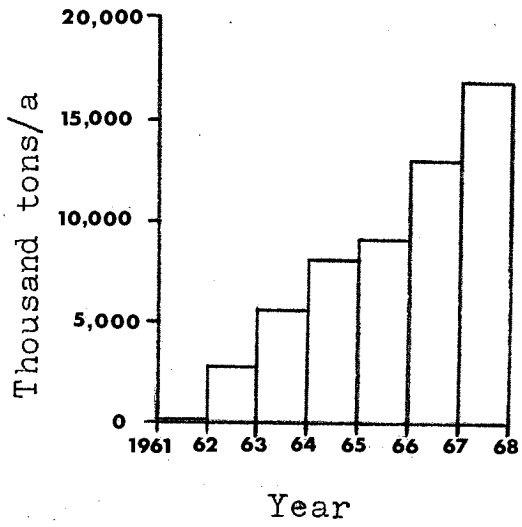

NAPHTHA USAGE IN STEAM REFORMING PLANTS FOR THE U.K.

Removal can be achieved in a number of ways, a common method employed involves passing the vapourised feed hydrocarbon with hydrogen recycle gas over a converting catalyst, followed by absorption of the resulting H_2S in a zinc oxide bed.

Following sulphur removal, the feedstock is mixed with steam and passed into the reformer itself. Since the overall reforming reaction is highly endothermic, the reformer generally consists of a number of catalyst filled alloy tubes suspended vertically inside a refractory lined furnace. Heat is supplied by burning a suitable fuel within the furnace, which in many cases is the same as the hydrocarbon feedstock. Various types of furnace have been built such as downwards firing, sidewall firing, and christmas tree; all these are well described in the book 'Gasmaking' (22).

Tube sizes are usually between 3.5 and 8 inches

internal diameter, and between 20 and 40 feet heated length. Reformer outlet temperatures are in the range 700 - 900°C, the higher temperatures being used for hydrogen production and the lower for Gas manufacture. Inlet temperatures are usually in the region of 500 - 600°C, but desulphurisation is carried out at approximately 400°C.

Because of the increasing demand for the products as mentioned above (17,97,98) along with the increasing availability of natural gas in this country, reforming can be expected to play an even larger role in the above fields (98). Towns gas production will no doubt be the exception to this in the long term. However, the rate of conversion of appliances to burn natural gas by area Gas Boards is such that the reforming of natural gas and other hydrocarbon feeds to a towns gas will be carried out for a number of years to come (15).

The USA has natural gas reserves estimated to be sufficient up to the year 2,000 (99), but due to the rapid growth in usage of natural gas, with an increase of 400% in the last nineteen years (100) at a max.: min. load ratio of up to 15 : 1 in some areas (20), work in the U.S. has been directed towards developing supplimental pipe line processes to ensure adequate supplies and help in peak load shaving (99,101,107). It is therefore likely that the U.K. gas industry will retain some reforming plant for similar purposes.

The overall reforming reaction may be represented by:- $C_nH_m + XH_2O \longrightarrow aCO + bCO_2 + cH_2 + dCH_4$ which when carried out over a nickel catalyst at high temperatures is very fast with a high equilibrium constant for the initial decomposition. This results in the complete conversion of the feedstock, with methane as the only surviving hydrocarbon in the product. The total product composition is controlled by the equilibria of the following two reactions:-

(i) methane-steam reaction

$$CH_4 + H_2O \rightleftharpoons CO + 3H_2$$

(ii) CO shift reaction

$$CO + H_2O \rightleftharpoons CO_2 + H_2$$

which permits exit compositions to be predicted entirely from a knowledge of thermodynamic data and operating conditions alone.

Nickel has been found the most practicable catalyst (18,49,82,102,103), and is used commercially on a support material consisting mainly of ceramic materials. Nickel is the active component in the ICI naphtha catalyst, in which it is distributed on a mixture of alumina, silica, and magnesia, bonded together with a calcium aluminate hydraulic cement (49).

Reisz (104) in examining various thermally stable ceramics as supports for the dispersion of nickel, found that periclase (fused magnesium oxide) and alumina (fused aluminium oxide) were particularly effective. Addition of

small amounts of magnesium oxide or aluminium oxide as promoters greatly enhanced the activity of stable, but relatively low-active catalysts.

The formation of carbon has been found to be a function of the catalyst support material. In particular the inclusion of alkali metal inhibits carbon deposition even when high molecular weight hydrocarbons are reformed at low feed ratios (49,105).

Work with basic and neutral catalysts has shown that product compositions are considerably changed with the catalyst pH, and the reactivity with respect to feeds of different molecular weights is also changed (42).

As mentioned above, reforming catalysts are easily poisoned by sulphur compounds. These are readily hydrogenated by the catalyst to H_2S which then forms a poisoning sulphide with the nickel sites:-

$$2H_2S + 3Ni \rightleftharpoons Ni_3S_2 + 2H_2$$

Sulphur poisoning has been found (106) to manifest itself in two distinct ways:-

(i) By accelerating the normal rates of carbon deposition on and within the catalyst structure.

(ii) By lessening the completeness of the hydrocarbon conversion.

Although sulphur concentrations as low as 0.5 ppm in the feedstock can poison a catalyst, the process

is reversible, and may be rectified by regenerative treatment with hydrogen (82).

To design and operate reforming plants effectively it is essential to have a sound understanding of the process principles involved. Since the overall reaction is such that an accurate assessment of the thermodynamics of the process can be made, part of this thesis is devoted to such studies in order to make some contribution towards this understanding.

Although the reforming process is now well established, attention is still being paid to process design. The cost of catalyst and the alloy required for tube manufacture is such that even small reductions in requirement can result in significant savings. Therefore, in any optimisation exercise directed towards this end it is essential to know all the parameters involved, including those governing the kinetics and the transfer of heat. With the latter consideration it has been found (48) that data from heat transfer work done in other fields can be successfully applied; however kinetic parameters must be derived from experimental work and to a certain extent, analysis of industrial data.

Because of the increasing availability of North Sea gas it is reasonable to assume that its use as an industrial feedstock will increase. It follows therefore that kinetic work based on steam-natural gas

reforming at pressure would be topical. However, since natural gas is made up of a number of components, some in appreciable quantities, it was decided that an examination of the constituent of interest, i.e.methane, should be carried out in order to establish a basis for comparison with any future work on natural gas or higher hydrocarbons.

The second part of this thesis is therefore devoted to a kinetic study of the steam-methane system, and an attempt has been made to establish some of the controlling factors and the kinetic relationship prevailing. Also a tentative examination of the carbon deposition phenomenon is described.

CHAPTER I.

REVIEW OF THE LITERATURE.

1.1. Process Development.

The first reforming plants to operate commercially were installed in the U.S. during the early 1930's by the Standard Oil Company. They were used to produce hydrogen for the hydrogenation of petroleum at their plants at Bayway N.J., and Baton Rouge La. (1,2,3). These plants utilised natural gas as a feedstock and operated at atmospheric pressure.

Because of the abundance of natural gas in the U.S. and the inherent advantages of continuous operation, the change from solid fuel to natural gas as a feedstock for hydrogen production continued. In the early 1940's the process was adopted by the American ammonia industry to supply the hydrogen required for synthesis (4). Like the petroleum industry, the process was rapidly adopted, and by 1949, 40% of the hydrogen required by the industry was being manufactured by the steam-natural gas reforming process (5). During this period the process was also adopted by other U.S. hydrogen consumers, notably the edible oil and methanol industries (6,7).

The first reforming plant to be commissioned in Britain for commercial operation was at the ICI Billingham plant in 1936, and this reformed propane and butane waste gases from a synthetic petrol refinery (8,9,10). Despite the advantages this process had over existing ones, the rate of development in the U.K. was

much slower than its counterpart in the U.S., mainly because of the limited availability of a suitable feedstock. A second ICI plant was commissioned at Heysham in 1942 using a propane feed, and this like its forerunner at Billingham operated at atmospheric pressure.

A great deal of the development of the process can be attributed to the fertiliser industry, especially in terms of pressure operation and extension of the range of feedstocks useable.

Eickmeyer and Marshall (11) in examining the synthesis process pointed out the advantages in operating at pressure, the main ones being the saving in subsequent compression costs and better heat transfer from the product gas.

Although operating at pressure is economically attractive it does impose some limitations on the process. The endothermic reforming reaction is accompanied by an increase in the number of molecules, and therefore increased pressure reduces the maximum conversion attainable (equilibrium), and higher operating temperatures are required to offset this detrimental effect and maintain the required conversion levels. However, increased temperature operation changes the rupture stress characteristics of the tube metal considerably (12) and imposes a severe limitation on the operating pressure.

Because no suitable materials were available for high pressure operation, plants were still operated at

relatively low pressure up to the late 1950's and early 1960's (4,13,14).

To overcome the problem of temperature-pressure limitations, Shell, and also Texaco moved away from the multi-tube concept and developed high pressure non-catalytic partial oxidation processes which used a single, refractory lined reactor.

Although these processes could operate with almost any hydrocarbon feedstock at high pressure, the advantages were offset by the need for an oxygen supply which resulted in high running and capital costs (15,16).

Although ICI had successfully reformed sulphur free hydro-petrols on a pilot scale as early as 1932, it was not until the last decade that hydrocarbons above butane were used on a commercial scale. It was during this period when world ammonia prices were dropping and coal costs started to rise coupled with a steady fall in petroleum prices, that ICI turned their attention towards using liquid hydrocarbons as a feedstock (9, 15, 17).

The options involved at this time in using a liquid feedstock such as naphtha, have been summarised as follows (18):-

(i) Operation at elevated feed ratios - up to 8 : 1.

(ii) Cyclic operation with alternate reforming and burning off the deposited carbon.

(iii) Partial combustion processes - i.e. Shell and Texaco processes.

Since none of these options was particularly attractive, attention was turned towards developing a new nickel based catalyst capable of working at low feed ratios and elevated pressures (10,16,18).

In 1954 the ICI Heysham plant was adapted to use a sulphur free hydro-petrol as feed, and later in 1957 after the development of a sulphur removal process, the feed was changed to naphtha. A second ICI installation followed, but like the first one it operated at atmospheric pressure (8).

After considerable work in overcoming the tube metallurgical difficulties imposed by high temperature - pressure operation, resulting in the use of 25/20 and 35/25 Cr/Ni alloys with a high carbon content (17,19), the first pressure reformer was commissioned in 1962 operating at about 25 atm with tube wall temperatures in the range 800 - 900°C (9). This was quickly followed by other installations in the following year.

The gas industry has been using hydrocarbons and gas oils for many years in water-gas sets, cyclic cracking plant, and low capacity, low pressure L.P.G. or methane reformers. But it was not until the advent of the ICI high pressure lean gas process that the industry used a hydrocarbon feed to a large extent.

Under similar economic pressures to the fertiliser industry, coupled with a growing shortage of high grade carbonising coal (20,21,22), the gas industry quickly recognised the potential of the ICI naphtha process. Since it offered a far greater output at less capital and operating costs than other processes and also saved on compression costs for distribution in a national grid system (21), it was quickly adopted.

By operating at lower temperatures than those required for hydrogen production, followed by CO conversion, partial CO_2 removal, and then enrichment, a product gas can be made having the required characteristics suitable for towns gas distribution.

The application of the process expanded rapidly and between 1962 and 1964 the plant capacity installed accounted for almost half of the gas industry's total production, and outstripped the installed capacity for ammonia manufacture (20).

One of the notable developments resulting from the Gas Council's own research work has been the Catalytic Rich Gas (C.R.G.) process, which uses a steam-naphtha feed to produce a rich gas having a calorific value of about 950 Btu/s.cu.ft. The process operates autothermically at about 500°C and high pressure in a packed bed reactor, thus avoiding the metallurgical problems associated with externally

heated tubular reactors. The activity of the catalyst developed for the process coupled with the low temperature of operation allows very low feed-ratios to be employed, approximately 1.5:1 mole steam/atom C.

Subsequent autothermic or more conventional reforming of part of a rich gas product followed by recombination of the process streams and suitable 'clean-up' operations give a towns gas product. Commercial installations of the C.R.G. process have been made at Bromley (25) and Stoke on Trent (26).

The various gas making processes outlined above, as well as the more recent developments like the ICI Towns Gas and Topsøe 500 processes are well described in the literature (15,20,22,27).

1.2. Reactions of Hydrocarbons.

The reactions of hydrocarbons either thermally or catalytically, with or without the presence of other reactants, have received considerable attention over the past years. Despite this there still exists a diversity of opinion as to which reactions take place.

Steacie and Puddington (28, 29, 30) who studied the thermal decomposition of n-butane, isobutane, and propane, in the temperature range 500 - 600°C, found that the initial products of the reaction contained hydrogen and methane together with

other saturated and unsaturated hydrocarbons. In the case of propane they also detected small amounts of polymer and a deposit of carbon on the quartz reaction vessel. Kassel (31), who also worked with a quartz reactor at 700 - 850°C, concluded a reaction scheme for the dehydrogenation of methane giving products of unreacted methane, hydrogen, carbon, and other hydrocarbons. Others (32, 33) using methane over carbon filaments in the temperature range 1457 - 2000°C have come to similar conclusions.

Marschner (34) found that the thermal decomposition of n-octane at 571°C led to a long but simple series of products including methane and hydrogen. Above this temperature CH_4 and H_2 increased with the exclusion of heavier hydrocarbons. Below 571°C, products were obtained containing large amounts of CH_4. Since it is shown above that even at high temperatures CH_4 and H_2 are formed from thermal decompositions, Marschner's results at temperatures above 571°C are thus consistent with those of other workers. At temperatures below this, methane is essentially thermally stable and hence CH_4 decomposition will be reduced and its percentage in the product will increase.

Roberts (35) who studied the reaction of ethane over a clean Rhodium film at 27°C, observed that it

decomposed to yield a single gaseous product, methane, and an adsorbed residue having a hydrogen to carbon ratio of 1.5:1 (atom:atom). Kemball and Taylor (36) also examined the decomposition of ethane but over a supported nickel catalyst at about 200°C, found that the decomposition products were methane and carbon, the reaction being represented by :-

$$2C_2H_6 \longrightarrow 3CH_4 + C$$

The carbon was found to be deposited reversibly and could be converted to methane by treatment with hydrogen. Using ethylene as a feed at approximately 190°C they found ethane as an additional product to CH_4.

These latter observations are supported by McKee (37) who found at temperatures below 60°C ethylene self-hydrogenated to give ethane, but above 60°C methane appeared in the product. However, above 200°C, CH_4 was found to be the sole gaseous product accompanied by a carbon residue on the catalyst. Similarly for butane, McKee found that methane and ethane were the gaseous products; however, the carbonaceous residue formed in this case was of variable composition.

Greensfelder and Voge (38) studying the catalytic cracking of hydrocarbons ranging from C_3 - C_{24} between 500 and 600°C compared their catalytic results with thermal cracking data. They found that

the catalytic process led to less production of CH_4 and C_2 species. Also with large paraffins i.e. C_{16} and higher, the catalysis was found to operate leaving very little cracked material above C_{10}, which was not the case thermally. A further conclusion they made was that the presence of catalyst accelerated the cracking, with the acceleration more pronounced for the higher hydrocarbons. The rupture was found selective, with the first and second carbon-carbon bonds at the ends of the hydrocarbon chains relatively inert, thus accounting for the low amounts of CH_4 and C_2 species found.

Geniesse and Reuter (39) also examined the catalytic cracking of petroleum fractions and pure light hydrocarbons, and they too found that the rates of decomposition increased as the molecular weight of the feedstock increased. Anderson and Baker (40) concluded similarly.

In contrast to this Yoshiro et.al.(41) working with hydrocarbon - air - steam mixtures over a supported nickel catalyst found that the reactivity of paraffins decreased with increasing molecular weight. While this result is difficult to accept on a thermodynamic basis, Suehiko (42) observed similar results using a range of hydrocarbons and steam over a neutral catalyst. However, in the case of basic catalysts, Suehiko (42) found the reactivity to increase with carbon atoms.

A number of people have examined the hydrocarbon

reactions in the presence of steam with the view of establishing the reactions that take place, and in particular the initial products.

Cryder and Porter (43), investigated the steam-ethane pyrolysis catalysed and uncatalysed, and found that carbon monoxide and hydrogen were present in the initial products, but for a given temperature the relative amounts of each increased considerably for the catalysed reaction. They also found that the threshold temperature for pyrolysis was 600°C, but in the presence of a nickel catalyst the reaction started at 430°C. These facts, coupled with the behavious of the feed ratio - composition curves for carbon monoxide and carbon dioxide (the latter found to result from secondary reaction), indicated to them that in the presence of catalyst the mechanism of the reaction changes from one of thermal pyrolysis to one of reforming.

Slovokhotova et.al. (44) also working with steam-ethane mixtures over a nickel catalyst obtained conversions at slightly lower temperatures than Cryder, the range being 350 - 420°C. More significantly the initial products in this case were found to be CO_2, H_2, CH_4, and carbon which was deposited on the catalyst. The same author working with cyclohexane (45) found that the hydrocarbon underwent three simultaneous parallel reactions:-

(i) dehydrogenation yielding $C_6 H_6$ and H_2

(ii) hydrogenolysis yielding CH_4

and (iii) steam reforming yielding CO_2 and H_2.

But the dehydrogenation and carbon-carbon bond rupture were found to be inhibited by the presence of steam more than the rupture of carbon-hydrogen bonds.

Yarze and Lockerbie (46) who studied steam-butane reactions over a nickel catalyst, like above (44) found that as well as CO and H_2, carbon dioxide was also an initial product. Extrapolation of their conversion curves indicated that methane was not a primary product of the reaction, and was only produced when the butane conversion exceeded 15%. They assumed therefore, that CH_4 arises as the result of a subsequent methanation reaction. This view is also shared by Rakovskii (47), working with steam-propane-butane mixtures over a supported catalyst. Further, Yarze found that a comparison of rate constants for butane disappearance by steam reforming and by thermal cracking indicated that the reforming reaction is approximately 100 times faster. Hence, like Cryder they concluded that thermal cracking is not a major reaction.

Topsøe (48) found the rate constant for the naphtha-steam catalytic reaction much higher than for thermal cracking. But he differs from Yarze with regard to the origin of methane. In his work with

propane, butane, and heptane, he found in all cases a methane concentration in excess of the thermodynamic equilibrium value, and therefore concluded that CH_4 must be a primary product of the overall reforming reaction.

Bridger and Wyrwas (49) also postulate that CH_4 is an original product along with unsaturated hydrocarbons resulting from thermal and catalytic cracking of the feedstock on the catalyst. These then undergo steam reforming to CO, CO_2, and H_2.

Dent (23) favours an initial reaction between the hydrocarbon and steam yielding methane and carbon dioxide as products. This view is shared by Lihou (50).

Thus, the reactions that occur when hydrocarbons are reformed are probably numerous, and with regard to those occurring initially, somewhat speculative. Nevertheless, whatever the basic reforming reactions may be, most workers (23,24,50,51,52) are agreed that the reforming reactions quickly reach equilibrium over a sufficiently active catalyst - such as used in modern plant.

The equilibria which control the final gas product composition can be represented by the following two reactions:-

$$\text{(i)} \quad CH_4 + H_2O \rightleftharpoons CO + 3H_2$$

$$\text{(ii)} \quad CO + H_2O \rightleftharpoons CO_2 + H_2$$

these being the steam-methane reaction and the carbon monoxide shift reaction respectively.

It follows therefore that the final product composition is governed by the process operating variables, pressure, feed ratio, and temperature.

1.3 Reaction Mechanisms.

As shown in Sec. 1.2, there exists some difference of opinion as to which products are formed initially or secondly when hydrocarbons react with or without the presence of steam. Examination of the various mechanism schemes that have been proposed can help in explaining some of the differences that have been highlighted.

Kassel (31) who found hydrogen and other hydrocarbons as the products of methane thermal decomposition, proposed the following mechanism scheme:-

$$CH_4 \rightleftharpoons CH_2 + H_2$$

$$CH_2 + CH_4 \rightleftharpoons C_2H_6$$

$$C_2H_6 \rightleftharpoons C_2H_4 + H_2$$

$$C_2H_4 \rightleftharpoons C_2H_2 + H_2$$

$$C_2H_2 \rightleftharpoons 2C + H_2$$

His results showed that the rate of decomposition was greatly retarded by hydrogen, and hence assumed that all of the reactions in the scheme are reversible. Similarly the data obtained by Storch (32) was satisfactorily explained by this mechanism.

Belchetz (33), also concluded that methane decomposes to give methylene radicals and hydrogen, with the radicals then reacting together to form ethylene. No evidence for the formation of methyl radicals was found in this work.

Kiyoshi et.al. (53, 54, 55) however, examining the dissociative catalytic adsorption of methane, ethane, and propane, concluded that the process did proceed via the formation of methyl radicals. In the cases of ethane and propane they found that the radicals so formed reacted with adsorbed hydrogen to give methane. The mechanisms proposed in the three papers can be summarised as follows:-

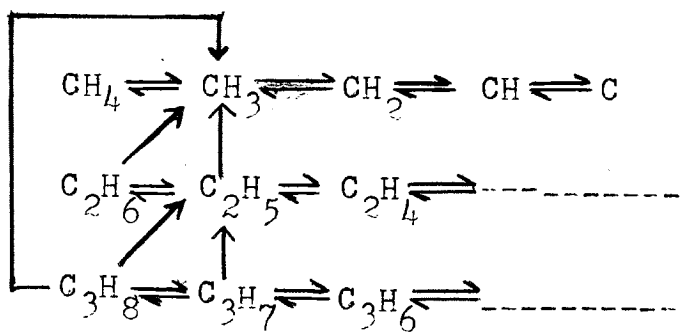

(hydrogen omitted for clarity).

In the limit, they found the dissociative process to proceed to the state where all of the C - H bonds are broken yielding carbon and hydrogen. In the work with ethane in the range 157 - 300°C, they found carbon and methane were the products in very large amounts.

McKee (56), was not as explicit in his proposed mechanism for butane cracking. The products of methane and a CxHy surface residue were explained by the following scheme:-

$$C_3H_{8(g)} \longrightarrow C_3H_{8(ads)} \begin{cases} \longrightarrow C_2H_x + CH_y \\ \longrightarrow C_3H_n + (8-n)H \end{cases} \quad (ads)$$

$$\text{and } CH_{y(ads)} + (4-y)\,H\,(ads) \longrightarrow CH_{4(g)}$$

Since no hydrogen was detected in their experiments they suggested that propane is initially and rapidly chemisorbed on the surface, followed by dissociation into mono and di-carbon fragments.

Others (37, 57, 58, 59, 60, 61, 62, 63) who have examined the adsorptive dissociation of hydrocarbons on nickel catalysts and films, generally agree with the

conclusions reported above, namely that the mechanism goes via adsorptive radical and hydrogen formation, with methane and a carbon-hydrogen residue as the products.

However, the work of Wright (57), and also Galway (63) has some significance since they both detected a hydrogen liberation whereas all of the others workers did not.

The former (57), using methane and a number of different types of metal film, concluded that the methane is adsorbed as a methyl radical and a hydrogen atom, with the subsequent breakdown of the radical being the rate controlling step. The scheme is represented by:-

$$CH_3 \longrightarrow CH_2 \longrightarrow CH \longrightarrow C$$

with all of the dissociations contributing to the liberation of hydrogen. As the temperature was increased towards 200°C the H_2 liberation was enhanced.

Galway (63) using a supported nickel catalyst found that hydrocarbons adsorb and react on the catalyst surface irreversibly, and may subsequently be removed after reaction has taken place as methane. Adsorbed hydrogen formed in the dissociation was found to desorb partially and reversibly on heating. In an earlier paper (62) the adsorption was represented by:-

$$CxHy + \text{surface} \longrightarrow CxHy\text{-}n\ (ads) + nH(ads)$$

and the adsorbed species so formed could only be removed from the surface by using relatively forcing conditions, and the process was usually accompanied by secondary reactions.

The methane-water vapour reaction has received the attention of a number of workers (64,65,66,67,68, 69,70,71). In particular, Leibush (65) working at temperatures up to 900°C using nickel, concluded that a chain reaction occurs in which the methane decomposes to CH_2, C_2H_6, C_2H_4, C_2H_2, and finally C. The final stable products of CO, CO_2, and H_2 are then formed by reaction of steam with the various intermediates.

Bodrov (66), in comparing the rate of decomposition of methane to carbon and hydrogen with the reaction of methane and water vapour, found that the former was many times slower. They therefore decided when the latter reaction takes place over a catalyst the likelihood of intermediate carbon formation is relatively improbable. The reaction mechanism proposed is represented by:-

$$CH_4(g) \rightleftharpoons CH_2(ads) + H_2(g)$$

$$CH_2(ads) + H_2O(g) \rightleftharpoons CO(ads) + 2H_2(g)$$

$$CO(ads) \rightleftharpoons CO(g)$$

$$H_2O(g) \rightleftharpoons O(ads) + H_2(g)$$

$$CO(g) + O(ads) \rightleftharpoons CO_{2(g)}$$

thus giving initial products of carbon monoxide and hydrogen via the initial step of CH_2 radical formation.

Similarly, Akers and Camp (68) favour a mechanism involving the formation of CH_2 radicals

which subsequently react with steam to give CO, CO_2, and H_2 as products.

Gordon (70) on the other hand suggests that the methane-steam reaction is a combination of CH_4 decomposition followed by the steam-carbon reaction and until carbon is formed the steam behaves as an inert gas.

This view is shared by others to some extent. Thus Yarze and Lockerbie (46) who used a butane-steam mixture concluded that the hydrocarbon molecule is adsorbed, then catalytically cracked, dehydrogenated and polymerised resulting in a carbon or coke. These deposits are then removed by adsorbed steam reacting to give the final stable products. Dirksen (73), and Goldstein (72), also postulate a mechanism involving the degradation to carbon and hydrogen, followed by a steam-carbon reaction.

1.4. Kinetics of the Hydrocarbon Reactions.

As indicated in the previous sections, the reactions of hydrocarbons have received considerable attention. Likewise, a number of kinetic rate expressions have been postulated for various systems, but because of the complexity that exists when hydrocarbons react, rate expressions tend to be empirical in nature.

In Kemball's work (36) with ethane and ethane-hydrogen mixtures over a nickel catalyst, the rate for

the ethane-hydrogen decomposition was found to be represented by:-

$$r = k p_{C_2H_6}^{0.7} / p_{H_2}^{1.2}$$

with a reaction activation energy of 52 Kcal/mole. Ethane alone was found to decompose to methane and carbon, the rate in this case being:-

$$r = k p_{C_2H_6}^{0.7}$$

with a somewhat lower activation energy of 40 Kcal/mole. Comparing the two rate expressions shows that the presence of hydrogen in the reactant mixture retards the rate.

Similar activation energies for hydrocracking over catalytic surfaces have been reported (40,54).

Roberts (35) working with ethane in a temperature range 27-100°C found that over a rhodium film the kinetics for the decomposition were first order, and an activation energy of 16 Kcal/mole was reported.

A low activation energy, 15 Kcal/mole was found by McKee (56) for butane cracking over nickel, and like Roberts, the temperature range investigated was relatively low 100 - 200°C; and similar products were obtained. However, in this case a zero order dependence on the butane partial pressure was generally found.

Low pressure, high temperature work on the thermal decomposition of methane (31,32,69,70,71,74) has generally indicated first order kinetic relationships. Although Storch (32) found that above 8 cm Hg pressure the reaction order increased to second, since no increase was obtained in isothermal static experiments, it was concluded that the increase was due to a rapid change in the temperature gradient in the immediate vicinity of the carbon filament used.

The effect of hydrogen addition to the methane feed gives rise to some confliction between the results of these workers. Like Kemball working with ethane, Kassel (31) found that hydrogen retarded the reaction rate of methane and it changed from 1st. order to:-

$$r = k \, CH_4^{\,2} \,/\, H_2^{\,3}$$

in the presence of hydrogen.

Gordon (71), on the other hand, found that overall, hydrogen increased the reaction rate. Since he had concluded that acetylene catalysed the cracking reaction, and that hydrogen addition to the feed resulted in increased acetylene production, it was assumed that any retarding effect hydrogen may have is compensated for by an increased acetylene catalysis.

No other evidence for acetylene catalysis has been found, and the more recent work (74,75,76) supports

the former view that hydrogen retards the reaction rate.

Accepting a mechanism scheme that involves reversible dehydrogenation steps, from a thermodynamic standpoint hydrogen would be expected to retard the overall reaction rate.

First order relationships have also been reported for steam methane reforming. Akers and Camp (68), working in the temperature range 336 - 638°C found that over a nickel catalyst the reaction was first order with respect to methane, and the velocity constant was represented by:-

$$k = 127e^{-15.8/RT}$$

the activation energy being 15,800 Btu/lb mole or 28.4 Kcal/mole.

Obolentsev (77) however, found that only at a temperature of 800°C, and a feed ratio of 3:1 did the reaction approximate to first order. Otherwise the rate data was expressed by:-

$$\frac{dp}{d\tau} = (p - p_f)\, ab\tau^{b-1}$$

where p is the partial pressure of methane

τ the contact time

p_f the partial pressure of methane at $\tau = 0$

a and b are parameters and functions of the volume and surface energies respectively.

However, Rozhdestuenskii (76), who also used an identical empirical relationship, found that at a feed ratio of 2:1 the parameter b was equal to 0.99 and 0.98 at temperatures of 600°C and 700°C respectively, thus giving a rate equation approximating to a first order relationship.

Again in contrast, Leibush (64), working in a similar temperature range to Akers, found the reaction rate to be described by the equation:-

$$r = kp_{CH4}p_{H2O} / (10p_{H2} + p_{H2O})$$

the activation energy being equal to 22.7 Kcal/mole. From the above expression it can be seen that a first order relationship holds only when the hydrogen present is extremely low, i.e. at the start of the reaction.

Bodrov (66), who made a detailed study of the reaction mechanism found that the kinetic data was expressed by:-

$$r = \frac{kp_{CH4}}{1 + \frac{ap_{H2O}}{pH2} + bp_{CO}}$$

where b is an adsorption equilibrium constant and a, a surface reaction equilibrium constant.

At 900°C however, and with low values of the ratio pH_2O/pH_2, the reaction approximated to first order, and the rate was represented by:-

$$r = 4,300\ p\ CH_4$$

from which an activation energy of 31 Kcal/mole was

calculated. In a later paper (67), Bodrov reported a first order relationship in the temperature region 700 - 900°C for three types of nickel catalyst. The three activation energies obtained for the different types of catalyst were close at 18.3, 19.4, and 24.0 Kcal/mole.

Yarze (46) did not obtain sufficiently precise data for a detailed kinetic analysis, but the rate of butane disappearance appeared to be approximately proportional to the butane concentration.

Bhatta and Dixon (78) using a similar system but at high pressure (30 atm), found zero order dependence with respect to butane and first order with respect to steam:-

$$\frac{d\left[C_4H_{10}\right]}{dt} = k\left[C_4H_{10}\right]^0\left[H_2O\right]^1$$

In their kinetic work considerable coke formation was encountered, and as a result of this they found it difficult to reproduce their results on fresh catalyst and obtain a reliable value for the activation energy.

Very little work is reported on the kinetics of reforming higher hydrocarbons than C_5. That which has been reported (48,79) is of an empirical nature relating the main parameters of the process for use in the design of commercial installations.

1.5 Carbon Deposition.

One of the major problems that had to be overcome in the development of the liquid hydrocarbon reforming process was the deposition of carbon. With the catalysts employed up to the late 1950's carbon was unavoidable with liquid feeds, resulting in the choking of the tubes and shattering of the pellets. This could be avoided only by using high and uneconomic feed ratios (10,16,80,81).

Other of the more obvious effects of carbon deposition may be briefly summarised as follows:-

(i) Decrease in the catalyst activity resulting in lower conversions.

(ii) Hot spots on the reactor tube metal caused by reduced internal heat transfer characteristics.

(iii) A feedstock material loss.

It is generally recognised (24,82,83) that carbon deposition on the catalyst during the course of reforming can be attributed to two sources:-

(i) From the direct decomposition of the hydrocarbon feed

and (ii) by the effect of the relative partial pressure of the components in the system on the equilibrium of the carbon forming reactions.

In both of these situations the presence or absence of carbon is not only a function of the conditions of operation, but also of the catalyst itself (49). In particular its acidic or alkaline nature is important.

1.5.1. Direct decomposition.

It is evident from the previous sections that the decomposition of a hydrocarbon whether thermal or catalytic, with or without the presence of steam, can lead to gaseous products with a possible carbon or carbonaceous residue. It follows therefore, as long as the removal of any such deposits by steam is continuous and at a rate equal to the deposition, the overall effect will not be detrimental to the catalyst or process as a whole.

Achieving this was, in fact, the difficulty encountered in the early development of the process. At that stage a high feed ratio was the only solution found to keep the catalyst surface clear of permanent residues. The advent of the high pressure steam-naphtha process was due to the development of a catalyst capable of promoting the desired reforming reaction whilst inhibiting the naphtha decomposition to carbon, thus permitting economic feed ratios to be employed with no carbon deposited.

Bridger and Wyrwas (49) working with the ICI naphtha catalyst 46/1, found at temperatures around

500°C the reforming of naphtha was catalytic resulting in no carbon formation. Therefore in the top region of a reformer tube where the initial reaction takes place at temperatures below 600°C (10,49,84) carbon cannot deactivate the catalyst since it will not be formed.

Although under normal conditions of operation using modern catalysts, carbon deposition of this nature can be avoided, it is worthwhile noting the effects that such depositions are found to have.

Bhatta and Dixon (78), found that the initial decomposition of butane at 500°C was very rapid resulting in a carbonaceous deposit which deactivated the catalyst. A typical pattern for the decline in activity with time was given and is reproduced in Figure 2.

Although the catalyst activity was rapidly and significantly reduced, it was found that subsequent treatment with hydrogen could restore the activity to its original value, and the authors concluded that the reduction in activity was due to a coverage or blanketing of the catalyst sites.

Levintner (84), examining the kinetics of coke formation for various hydrocarbons also concluded that at low temperatures the catalyst is chemically poisoned but at higher temperatures choked.

In the light of this and what others (36,54)

Figure 2.

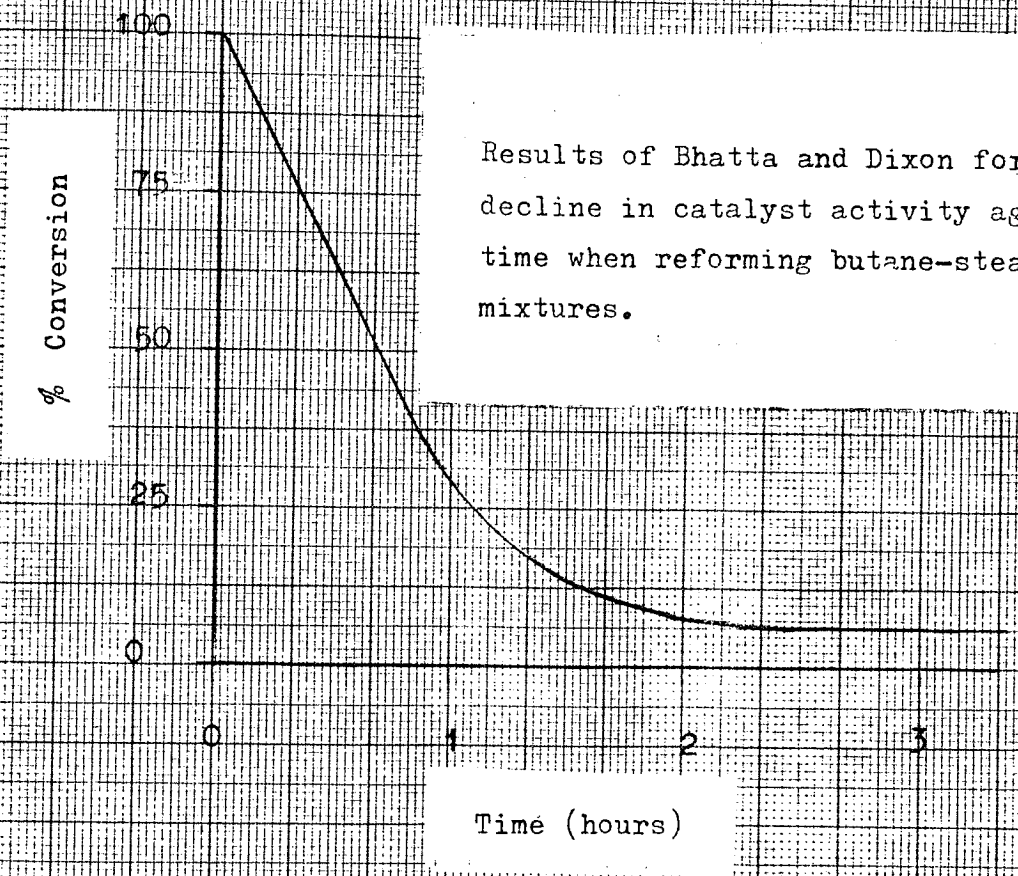

Results of Bhatta and Dixon for the decline in catalyst activity against time when reforming butane-steam mixtures.

have found it would appear that carbon formed by the initial decomposition is not detrimental to the catalyst since the activity can be restored by suitable treatment. However, Bridger (82) stated that the life of the ICI 46/1 catalyst can be terminated in minutes, if exposed to hydrocarbons in the absence of steam, due to carbon formation causing catalyst disintegration.

1.5.2. Equilibrium carbon.

It is generally accepted (23,24,50,52,85) that for this type of deposition the Bouduard reaction is the one of major importance:-

$$2CO \rightleftharpoons CO_2 + C$$

Holland and Wan (85) examined thermodynamically a number of reactions likely to form carbon, and concluded that the Bouduard controls the lower limit for deposition.

For the purpose of establishing conditions that cause carbon participating reactions to move in the direction of carbon deposition, use is made of the equilibrium pertaining to the Bouduard reaction. However, it has been pointed out by Hebden (86), and also Dent (23), that over a nickel catalyst this is not governed by the equilibrium constant for carbon in the form of β-graphite. This fact has frequently been overlooked by others and Figure 3 shows the equilibrium constants experimentally obtained by Dent over the temperature range 300-900°C

Figure 3.

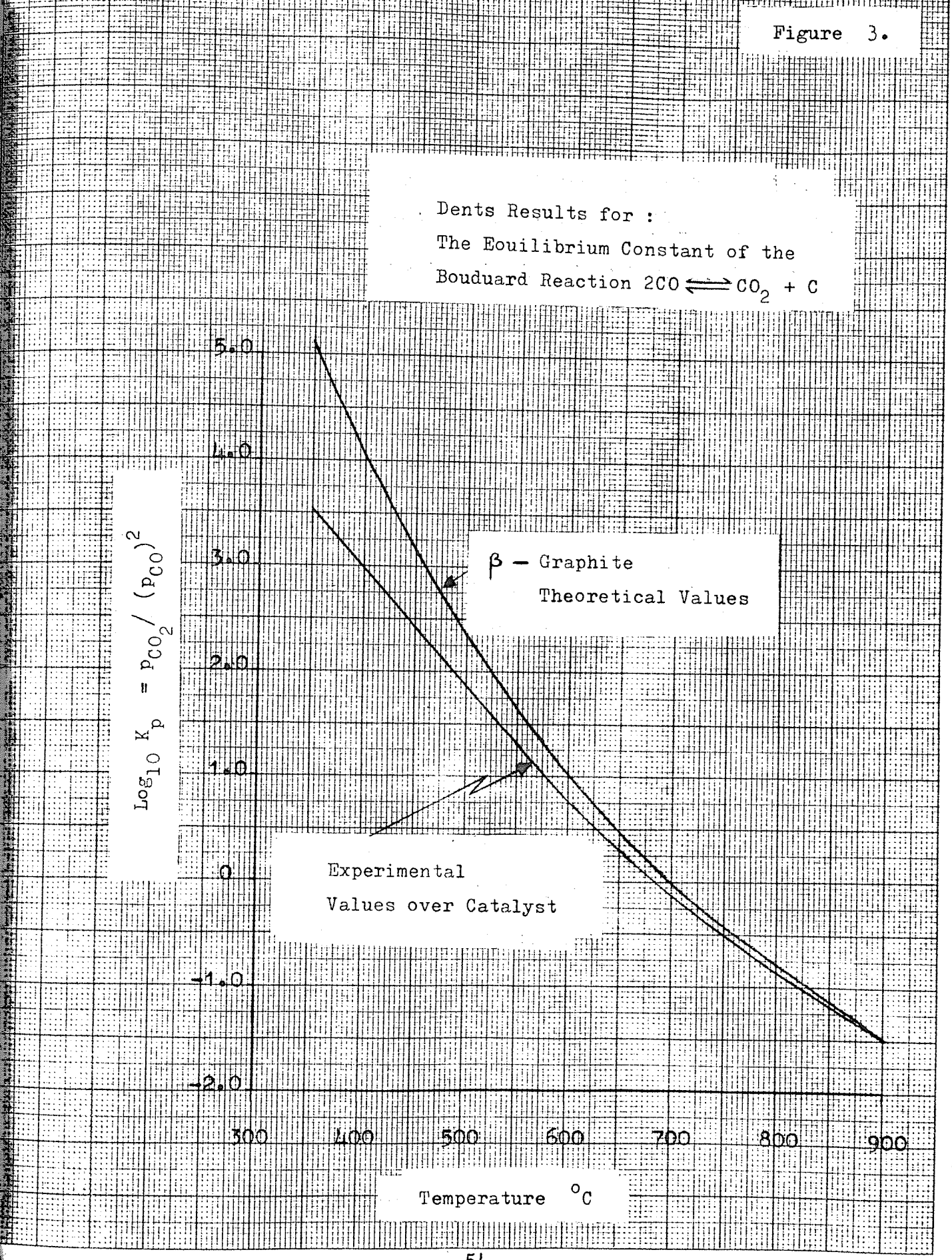
Dents Results for :
The Eouilibrium Constant of the
Bouduard Reaction $2CO \rightleftharpoons CO_2 + C$
β – Graphite
Theoretical Values
Experimental
Values over Catalyst
$\log_{10} K_p = p_{CO_2} / (p_{CO})^2$
5.0
4.0
3.0
2.0
1.0
0
-1.0
-2.0
300
400
500
600
700
800
900
Temperature °C

compared with the theoretical values for β-graphite formation.

From Figure 3 it can be seen that the difference in the two constants is significant, especially at the lower temperatures, and they are approximately equal only at about 900°C. It follows therefore, within the temperature range of reforming that the equilibrium constant for the Bouduard reaction will be lower than the β-graphite theoretical value, and since the ratio $p\,CO_2\,equ/(pCOequ)^2$ decreases with feed ratio at a given temperature and pressure, the limiting feed ratio will also be lower.

Carbon deposition has been the subject of a number of experiments by Kiyoshi (87,88,89,90). The feed employed in all of the tests was methane plus steam, but in some, O_2, CO_2, ethane, and propane were included. In all cases the β-graphite theoretical minimum feed ratio was found to be greater than the experimental, and also the amounts of carbon deposited were less than theoretically predicted. With methane-steam mixtures alone (87), the differences reported between the theoretical and minimum feed ratios were 0.005, 0.025, 0.32, and 1.1 at 926, 816, 706, and 595°C respectively. Qualitatively these results confirm Dent's findings since the sequence is exactly as would be expected from Figure (2).

Reitmeir (91) using a steam-CO_2-CH_4 mixture at

about 800°C also found that carbon was not deposited when theoretically predicted.

In considering the above conclusions it must be mentioned that with the possible exception of methane reforming and the Catalytic Rich Gas (C.R.G.) process, they have little practical significance. The reasons for this are as follows:-

(i) In the temperature region of operation, above 700°C, the difference between the two constants is not excessively great.

(ii) The limiting feed ratios required to prevent a carbon build-up due to an initial decomposition is greater than the minimum ratio required to prevent equilibrium carbon.

When methane is the feedstock, the decomposition at tube inlet will be catalytic rather than thermal since methane is thermodynamically stable at temperatures corresponding to those at tube inlet.

With the C.R.G. process, operational temperatures are lower than with tubular reformers, thus reducing the likelihood of an initial thermal decomposition. Hence, in these cases any deposition will be due to the establishment of equilibrium.

Nevertheless, the findings of Hebden and Dent are interesting with regard to the mechanism of carbon formation. The former concluded that chemisorbed

carbon atoms formed on the catalyst surface diffuse into the bulk to form a lattice carbide. Further, a saturation point for the carbide was assumed, and when reached, carbon is ejected from the lattice as graphite. A delay observed prior to the rapid onset of deposition was attributed to the initial formation of the lattice involving readjustment of the structure, which once achieved permitted the rapid formation and decomposition to take place.

Kemball and Moss (92) working with mixtures of methylamine and hydrogen, found that carbon disappeared from the surface by absorption into the catalyst.

McD Baker and Rideal (93) examining the adsorption of carbon monoxide on nickel metal, observed a rapid initial uptake of CO followed by a slower disappearance from the gas phase - during which CO_2 was formed. Since the added gas (CO) exceeded that required to cover the surface with nickel carbide according to the reaction $2CO \longrightarrow CO_2 + C \equiv Ni$, it was assumed that the carbide was able to diffuse from the surface. The slow rate of CO adsorption was associated with a slow diffusion of the carbide into the lattice.

Galway (63), also supported the theory that carbon may diffuse into the bulk catalyst and proposed the following scheme by which a tetradsorbed radical is in equilibrium with carbon which enters the lattice.

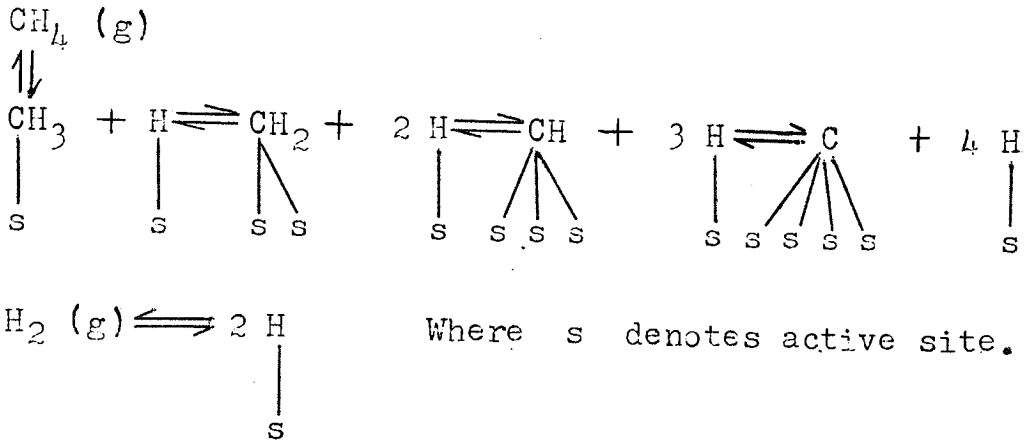

$H_2\ (g) \rightleftharpoons 2\ H\text{-}s$ Where s denotes active site.

Hoffer, Cohn, and Peebles (94), examined the decomposition of nickel carbide at 350°C, and found that it proceeded according to the reaction:-

$$Ni_3C \longrightarrow 3Ni + C$$

but only after an induction period. However, during this period no structural change in the carbide could be detected. Nagakura (95), found at 500°C the decomposition of nickel carbide was more rapid than at 400°C, and at the higher temperature, the decomposition to carbon predominates over reactions with hydrogen that yield methane.

1.6. Summary.

In comparing the results reported for thermal and catalytic decomposition of hydrocarbons alone, it is evident that in the former situation hydrogen is readily liberated as a detectable gaseous product,

whereas in the latter case this is not so. This indicates that the catalyst sites have a strong affinity for hydrogen as well as for the hydrocarbon, and hence the marked absence of hydrogen.

For all feedstocks reacting catalytically, methane is reported as a major product. Since the hydrogen:carbon ratio of saturated hydrocarbons is greatest for methane, it must be concluded that adsorbed hydrogen reacts with adsorbed carbonaceous species in preference to being liberated as H_2 gas. This hypothesis is in general agreement with Galway's findings (63) in that hydrogen could be removed from a catalyst surface partially and reversibly but only under forcing conditions, i.e. high temperatures.

Whilst there is a marked absence of hydrogen as a product in the catalytic decomposition of a hydrocarbon alone, the situation is reversed when steam is present in the feed. In all of the papers studied for this latter system, hydrogen is reported as a product.

It is difficult to make a direct comparison between the work reported on the two systems since that for hydrocarbons alone is generally at much lower temperatures. However, it is concluded that at temperatures of the order of 350°C, adsorbed hydrogen resulting from an initial decomposition simultaneously desorbes

as H_2 gas and also reacts with carbonaceous species. Hydrogen production must also result from reactions between steam and the surface species giving oxides of carbon also.

The different conclusions on the initial products of reforming are probably due to the relative rates and equilibria of the competing reactions. A number of researchers have reported that methane is not an initial product of reforming; however, most are agreed that the steam-methane and CO shift reactions approach equilibrium very rapidly, and even at partial conversion of the original feed the CO shift reaction is near equilibrium. Under such conditions where the steam concentration is relatively high, equilibrium concentrations of methane will be low and therefore may go undetected. Similarly CO may go undetected as an original product, and depending upon the sensitivity of the analytical methods used these products may only be found after substantial conversion of the original feed (46).

In examining the various studies on reaction mechanisms, there seems little doubt about the fact that the reactions of hydrocarbons proceed via adsorbed radical formation. There is however some disagreement as to which radicals are actually formed. Methylene radical formation upon the initial adsorption is postulated by some workers (31,32,33,66), whilst others

(53,54,55,57) have found evidence indicating the formation of methyl radicals. It is likely that the situation that exists is that proposed by Kiyoshi (53) and also by Wright (57), which for the case of methane is represented by :-

$$CH_4(g) \xrightarrow[1]{} CH_3(ads) \xrightarrow[2]{} CH_2(ads) \xrightarrow[3]{} CH(ads) \xrightarrow[4]{} C$$

where the product of each stage reacts to some degree with steam.

Each step in the dissociation will have a reaction rate depending on the operating condition, and perhaps more significantly the catalyst itself. Therefore with different catalysts at given conditions of operation a single step could be very fast and also have a high equilibrium constant thus causing false conclusions to be made. For example, if this applies to Step 2 in the above scheme, CH_2 radicals will appear to be the initial decomposition radicle. Similarly if all of the steps are rapid and outstrip the rate of interactions with steam, it is equally likely that carbon would appear to be the initial product, which in fact has been found to be the case (46,70,73). However, thermal reactions resulting in carbon formation must be accounted for, and it is possible that initial carbon deposition found in the above studies arose from thermal cracking since the temperatures employed were relatively high.

Similar diversity extends into the conclusions that have been drawn from kinetic work. Although a number of first order relationships with respect to the feed hydrocarbon have been reported, intuitively one would expect otherwise. For a kinetically controlled reaction over an active catalyst, it seems unlikely that the steam does not exert an influence over the reaction rate, and in fact a steam dependence has been found by some workers (64,66).

There is sufficient evidence available to accept that adsorbed carbon may diffuse into the catalyst bulk to form a nickel carbide, and that the presence or absence of carbon as graphite, other than that deriving from thermal decomposition, depends on the equilibrium relationships of the carbide.

Induction periods prior to carbon deposition observed by Hebden (86) were attributed to a structural rearrangement of the catalyst lattice. However, Hoffer (94) who observed a similar period could not detect any such rearrangement.

Kiyoshi (96) working with reduced 'spent' catalyst, found that in the range 595 - 982°C the quantities of carbon deposited were far greater than those obtained using fresh catalyst. The activity at the lower temperatures was considerably less, and minimum feed ratios for deposition were found to lie between the β-graphite theoretical

minima and the experimental minima for fresh catalyst.

These results could be attributed to a structural rearrangement as suggested by Hebden, which having taken place as in the 'spent' catalyst reduces the induction period and permits greater and earlier depositions. At the same time the activity is significantly and permanently reduced, which was found not to be the case following thermal decompositions (36, 54, 78)since hydrogen treatment was found to restore the activity almost completely.

It is difficult to reconcile such a hypothesis to Hoffers results. However his work was carried out at much lower temperatures than that of Kiyoshi or Hebden and it is possible that at low temperatures the rearrangement is very slow or alternatively that there exists a temperature threshold for this phenomenon, and Hoffer was working below this.

It is well established that when hydrocarbons decompose and react on a catalytic surface in the presence of steam the reactions that take place are numerous. In any complex system such as this where simultaneous and competitive reactions are taking place at different rates, there will be a great number of variables controlling the overall outcome. Hence variation of any single factor can influence the results such that completely different conclusions are drawn. This makes the task of comparing different works extremely difficult, and any conclusions made by so doing must be viewed in this light.

A great number of experimental studies of the rates and mechanisms of hydrocarbon reactions have been reported in the literature. However, of the general areas of interest, the catalytic reforming reaction is the least reported. In addition it is noticeable that the majority of reforming systems that have been studied, were confined to low pressure operation, and the more notable (46, 78, 123) high pressure studies used hydrocarbon feeds other than methane.

In view of the likelihood of methane or natural gas becoming the major feedstock for reforming plant in the U.K., it was considered that an experimental study at an elevated pressure using a methane feed, could lead to a worthwhile contribution.

It is likely that some of the knowledge gained from catalytic studies of saturated paraffins higher than methane in the homologous series, can be used to predict the behaviour of a steam-methane system. However, it is equally likely that reactions which occur in other systems, do not occur at all or to the same extent as when methane is the feedstock. For example, methane is the most thermally stable saturated paraffin, therefore the possibility of a thermal and catalytic decomposition to a carbonaceous deposit on the catalyst, which was found to be the case for a steam-butane system (46, 73), is unlikely when methane is the feedstock.

It follows that reaction mechanisms and rate

expressions that govern the overall steam-methane reforming reaction need not necessarily be the same as those that have been found to apply to other hydrocarbon systems. Therefore it was decided to study the steam-methane system at pressure, with the object of establishing which of the various steps involved in the catalytic reaction controls the overall rate, the controlling mechanism, and the relevant rate equation.

A cylindrically pelletted industrial catalyst was selected so that in the experimental work it could be threaded onto a former and used in a rod form. It was not envisaged that for the proposed work, the arrangement would have an advantage over a granulated catalyst used in a packed bed form. However, it was considered that for future studies that may involve the effects of superficial gas flow velocities and pellet diameter, the rod arrangement would be advantageous.

CHAPTER 2.

REFORMING APPARATUS AND PROCEDURES.

2.1. Reforming Apparatus.

2.1.1. General description.

The apparatus was constructed to reform methane with steam so that all of the experimental operating conditions, temperature, , pressure, flow rates and feed ratios, could be used as variables. The front and rear views of the apparatus are shown in Plates I and 2 respectively, and a simplified flow diagram is given in Figure 4. A detailed flow diagram is given in Appendix A with a full specification of the equipment used.

Methane feedstock obtained from a cylinder supply was metered by means of a variable area flowrater, from which the methane passed into the Feedstock Preheater where it was heated to approximately 330°C. From the preheater it passed into the Steam Generator into which pre-heated water was simultaneously injected. In the generator the feed water evaporated and formed a homogeneous gaseous mixture with the methane.

From the Steam Generator, the steam-methane mixture passed into the main Superheater and then into a second heater (Line Heater) which added further superheat prior to the mixture passing into the Reactor containing the catalyst.

The exit reactor product gases passed into a water cooled condenser where unreacted steam was condensed out

SIMPLIFIED FLOW DIAGRAM

Figure 4

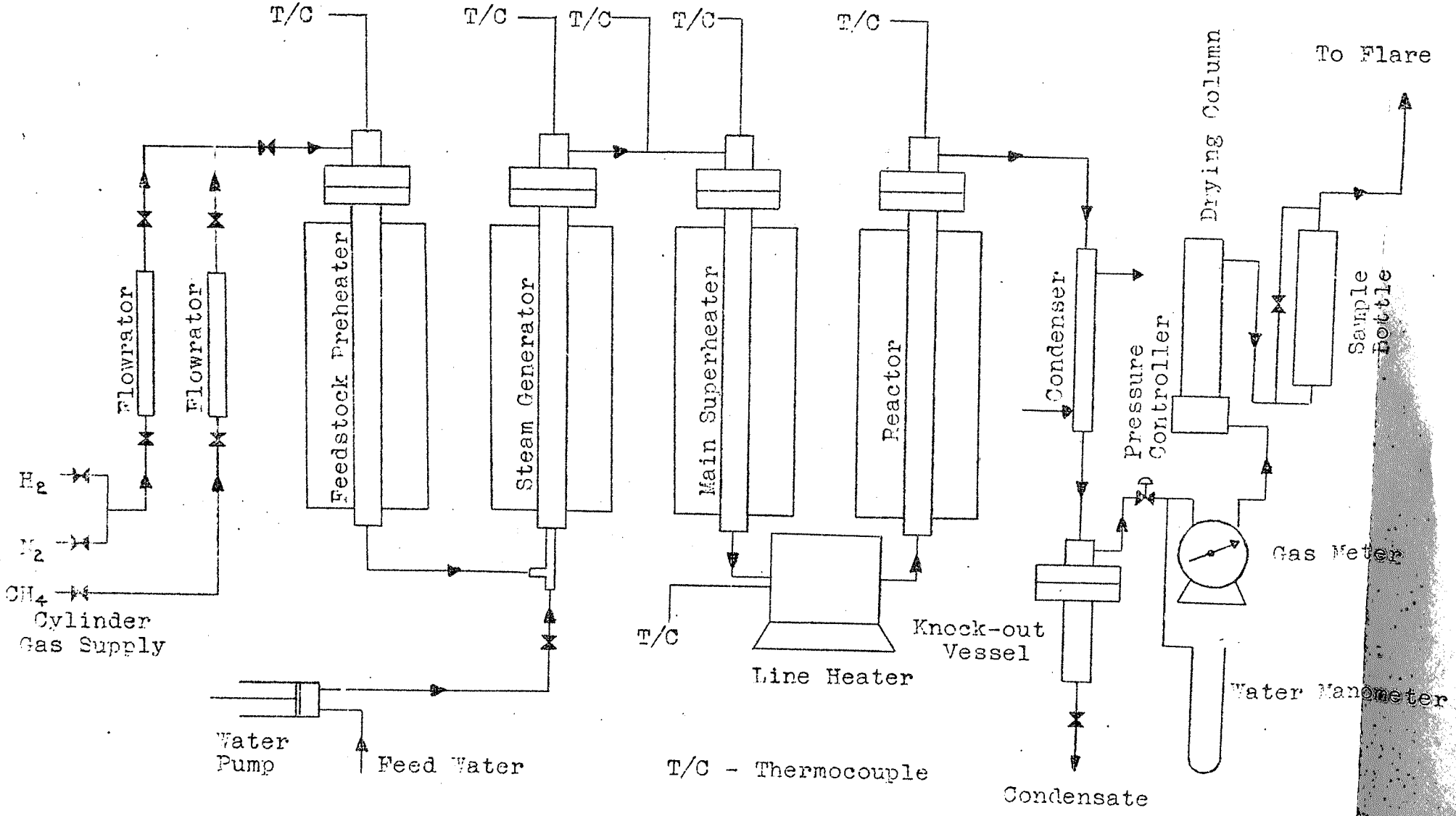

PLATE 1

THE EXPERIMENTAL APPARATUS (FRONT)

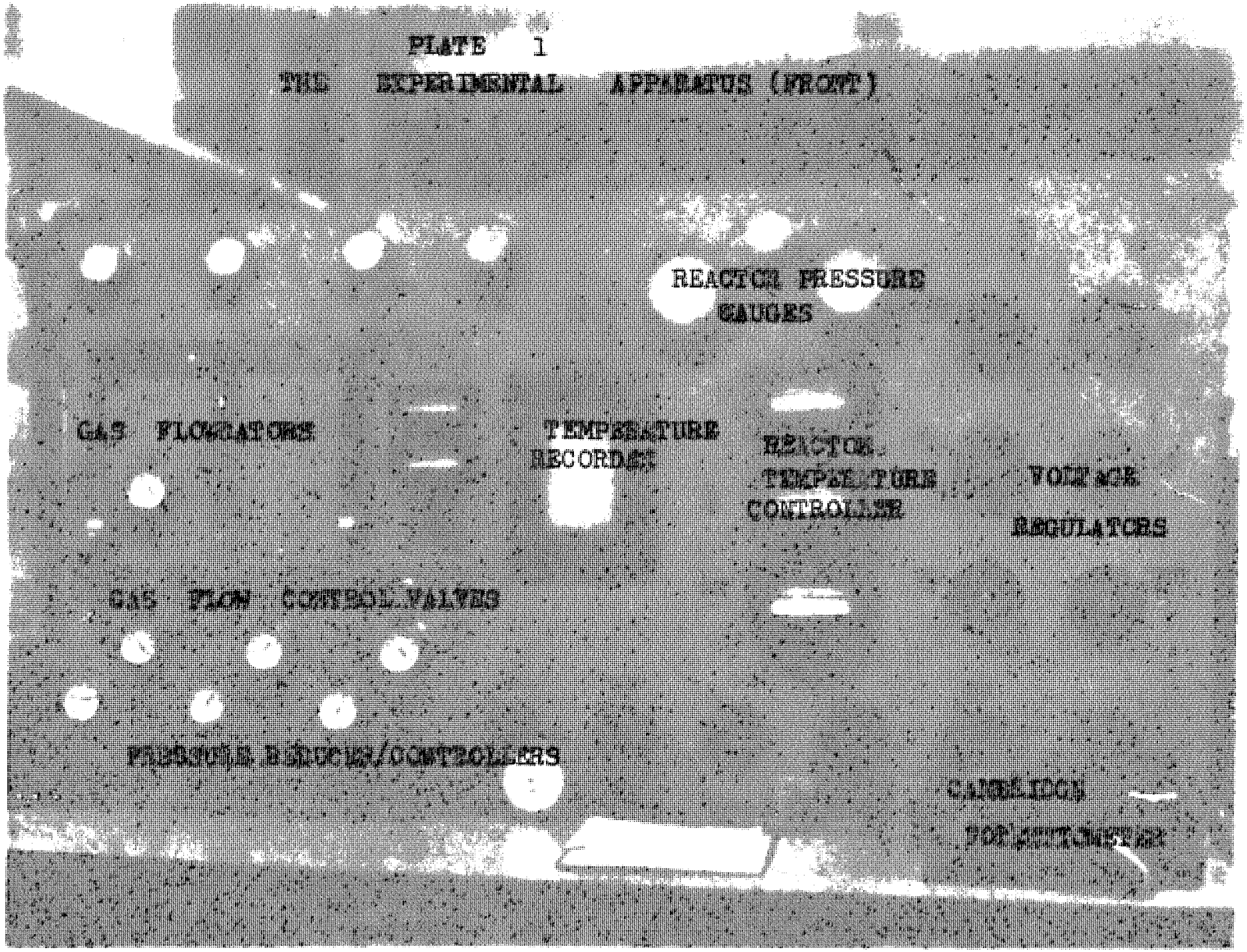

PLATE 2

THE EXPERIMENTAL APPARATUS (REAR)

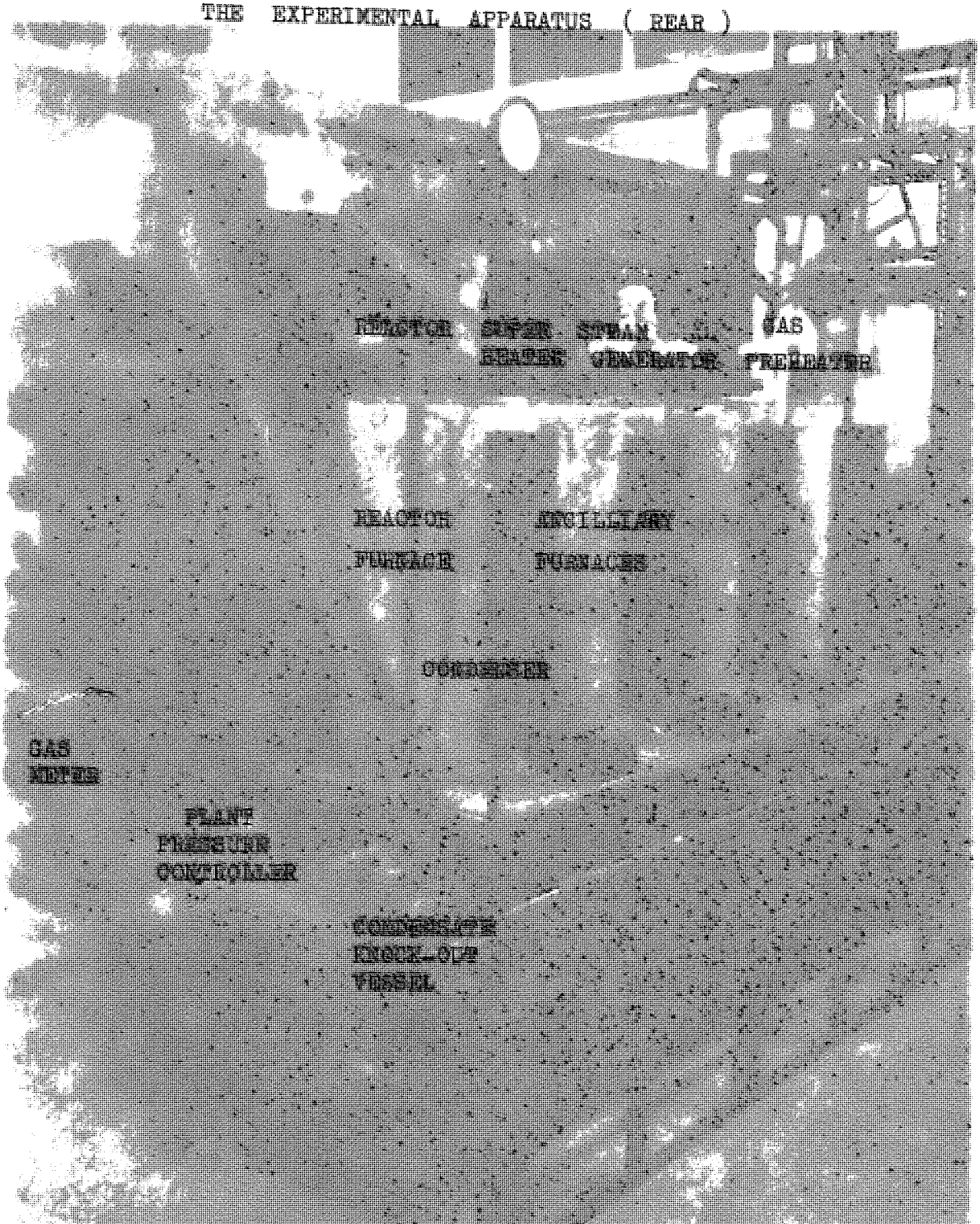

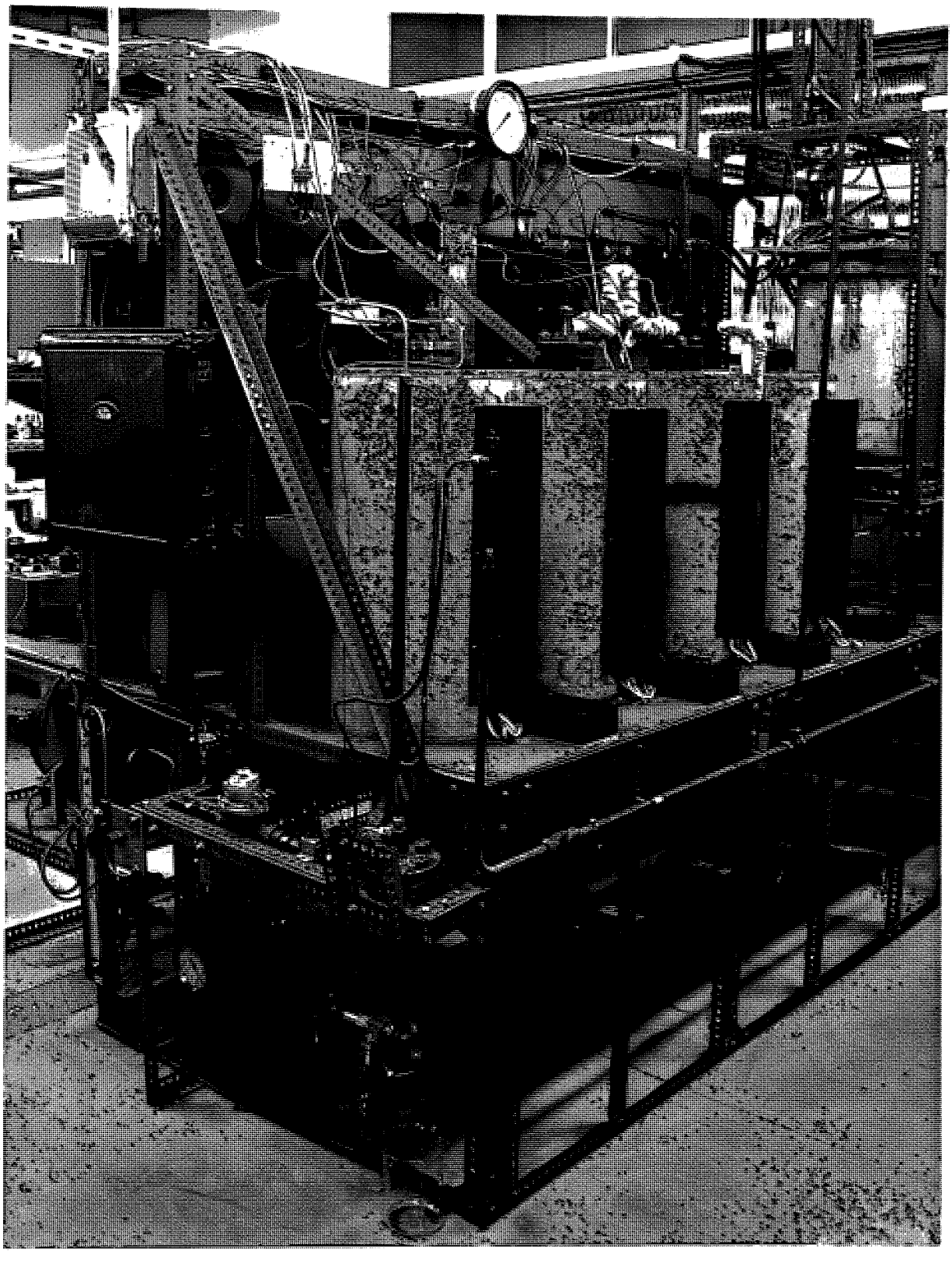

and then collected by means of a Knock-out vessel. The product gas then underwent pressure reduction, metering, and drying. Finally, prior to flaring, the gas flowed through a sample bottle which allowed samples to be taken for analysis.

The pipe-work for the liquid water line was constructed from $\frac{1}{4}$ inch O.D. copper tube, and for all other pipe work $\frac{1}{4}$ and $\frac{1}{8}$ inch O.D. stainless steel tube was used. Exposed hot pipe work was lagged with a crinkled aluminium foil/glass fibre laminate, and further wrapped with electrical heating tape to keep heat losses to a minimum.

Stainless steel 'Ermeto' high pressure fittings were used for all tube joints, and following consultation with the manufacturers, the maximum hot working pressure was set at 250 psig. However, pressure testing with soap solution was carried out at 400 psig at ambient temperature.

The electric furnaces providing the heating media for the heating vessels consisted of three windings, a main one plus two end-loss compensators, all wound on a $2\frac{1}{2}$ inch diameter silica tube. The Line Heater was a Wild-Barfield 0.75 KW horizontal furnace. Variac type voltage regulators were used to control the heating rate on all of the ancillary furnaces and heating tapes, whereas the reactor had 'Ether Transitrol' temperature controllers incorporated into the winding circuits.

High pressures were indicated on Bourdon Gauges, and the pressure of the product gas downstream of the

pressure controller was measured on a water manometer, which also acted as a relief valve on the low pressure line.

Thermowells extending down the centre of the four main vessels allowed internal temperatures to be measured. These were monitored by means of Chromel/Alumel thermocouples and an indicator-multipoint switch unit; an Electroflow six point recorder was also incorporated in the temperature measurement circuits. Reactor temperatures were measured using a moveable thermocouple in conjunction with a 'Cambridge' portable potentiometer.

The catalyst used for the experiments was pelleted ICI 46/1 catalyst and was threaded on a stainless steel tube to form a rod. With the exception of reducing the outside diameter, the cylindrical pellets were used as commercially supplied:

i.e.	Outside diameter (machined down)	1.524 cm
	Inside diameter	0.645 cm
	Length (variable)	1.68 cm (ave.)

2.1.2. Feed section.

The gases used were all of high purity and supplied by B.O.C. at cylinder pressures up to 2,500 psig. In addition to methane, a nitrogen supply was installed to provide an inert purging medium, and a hydrogen supply to provide an atmosphere for catalyst reduction.

Pressure reduction was achieved by means of Hale-Hamilton pressure controllers, and gas flowrates were

measured with Fischer and Porter variable area flow-rators. To provide various flow ranges, combinations of different tube sizes and float materials were used. Tube sizes employed were 1/16 and 1/8 inch bore with floats made of either steel, sapphire, glass, or tantulum. Ermeto needle valves located at the flow-rator inlets were used to regulate gas flows.

As can be seen from Figure 4, feed gas after metering, flowed through the pre-heater and then into the Steam Generator into which pre-heated water was simultaneously injected. Feed water was delivered at pressure by means of metering pumps, and although they were of the reciprocating type, the plant volume was sufficient to absorb the pulsations, and hence, no pressure oscillations within the apparatus were produced. Deionised water, used for the feed, was drawn by the pump from a 2 litre burette through an interchangeable fritted glass filter. For low water flows (15 - 150 ml/h) a 'Micro' pump was used, and for higher flows (75-750 ml/h) an 'M' type pump was employed. An adjustable relief valve in the high pressure water line allowed calibration of the pumps to be carried out at working pressures. During experimental runs the valve was adjusted to relieve at approximately 50 psi above the operating pressure. Feed water pre-heat was obtained from an electrical heating tape wrapped round the high pressure water pipe, a voltage controller was incorporated in the wiring circuit.

The three main ancillary heating vessels, i.e. Feed Preheater, Steam Generator, and Superheater, were all of similar construction, and are specified in Appendix A. In order to increase the heat transfer areas within these vessels, they were packed with silica chips for about two thirds of their heated length. In the Steam Generator (illustrated in Figure 5), the feed gases passed upwards through the bed of silica whilst the water cascaded from a feed pipe fitted axially and through the bed. As the delivered water cascaded down through the silica chips it evaporated and was mixed and carried away with the feed gas.

After undergoing superheating the feed mixture entered the reactor at approximately 600°C.

2.1.3. Reactor Section.

For preliminary tests the reactor used was identical in construction to the ancillary heating vessels, the head joint on these being made up of 'gramaphone record' flanges sandwiching a 1/16 inch 'Klingerit' gasket. However, at temperatures in excess of 600°C with a hydrogen feed, this type of joint was not able to hold pressure, and appreciable leaks occurred at the reactor. Therefore a second reactor was obtained, identical in size but with a 'Rushton' metal to metal head joint which proved very successful.

The steel former supporting the catalyst pellets

STEAM GENERATOR - FEED END

Figure 5

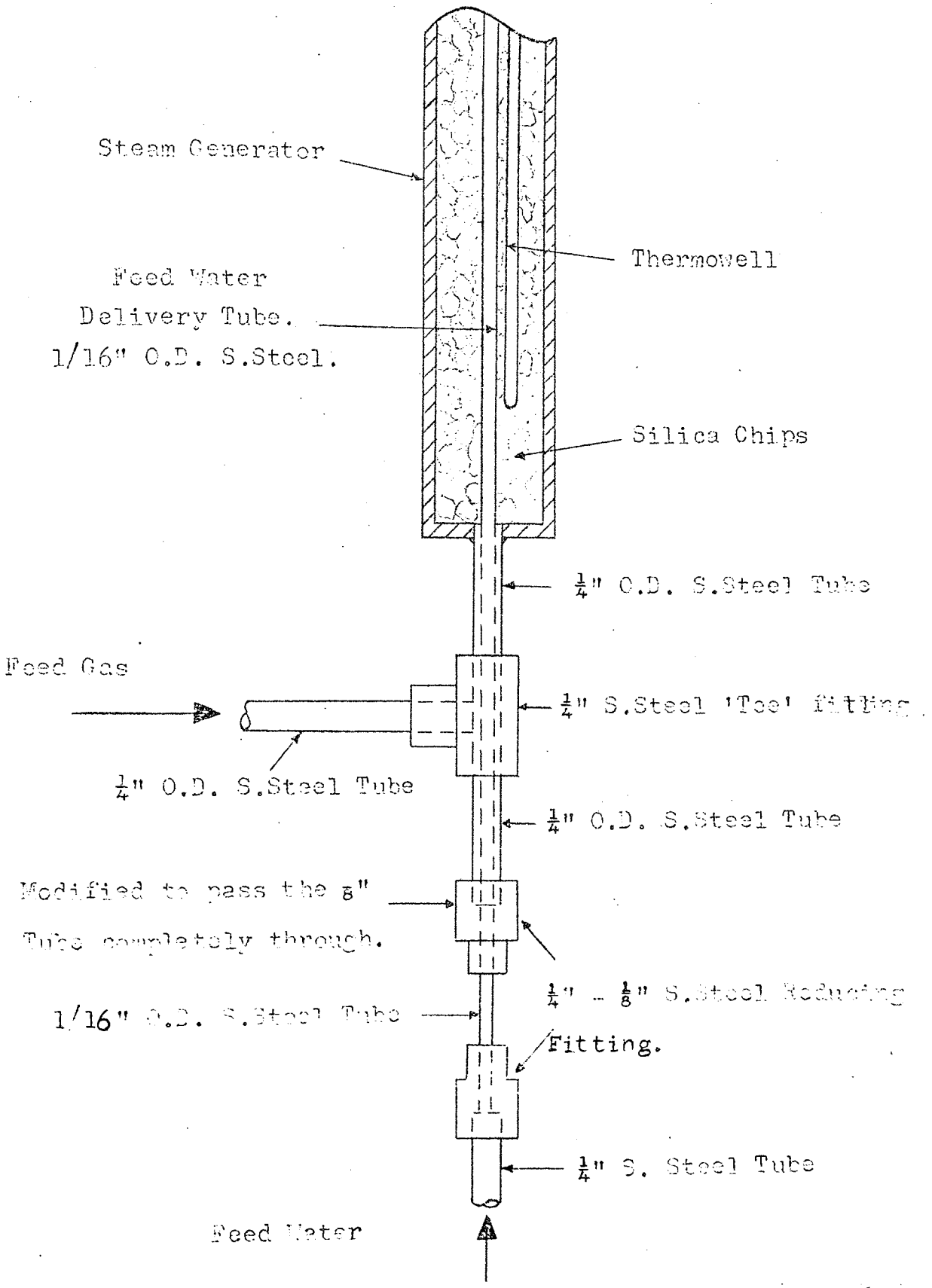

was mounted axially in the reactor, and since an upward gas flow was used in the experimentation, a bridge was fitted to the closed end of the Former so that the reactor inlet was not obstructed. Figure 6 shows the catalyst assembly in the reactor. The thermowell which extended down the centre of the catalyst Former allowed a thermocouple to be moved axially along the catalyst in order to monitor longitudinal temperatures.

2.1.4. Product handling section.

The first function of the product handling section was to condense excess steam out of the product gas. This was achieved using a water cooled copper condenser with a $\frac{1}{4}$ inch O.D. stainless steel centre tube carrying the product gases.

From the condenser the water/gas mixture passed into the knock-out vessel which separated the two phases and allowed the condensate to be removed from the system for collection. A needle valve was used to control the condensate out-flow; this system of removal was preferred to an automatic steam trap type arrangement since the amounts of water to be handled were relatively small and removal could be achieved without any appreciable gas losses, which would not be the case with a steam trap system.

Following phase separation, pressure reduction was carried out using a Hale-Hamilton pressurised dome

CATALYST ROD ASSEMBLY. Figure 6

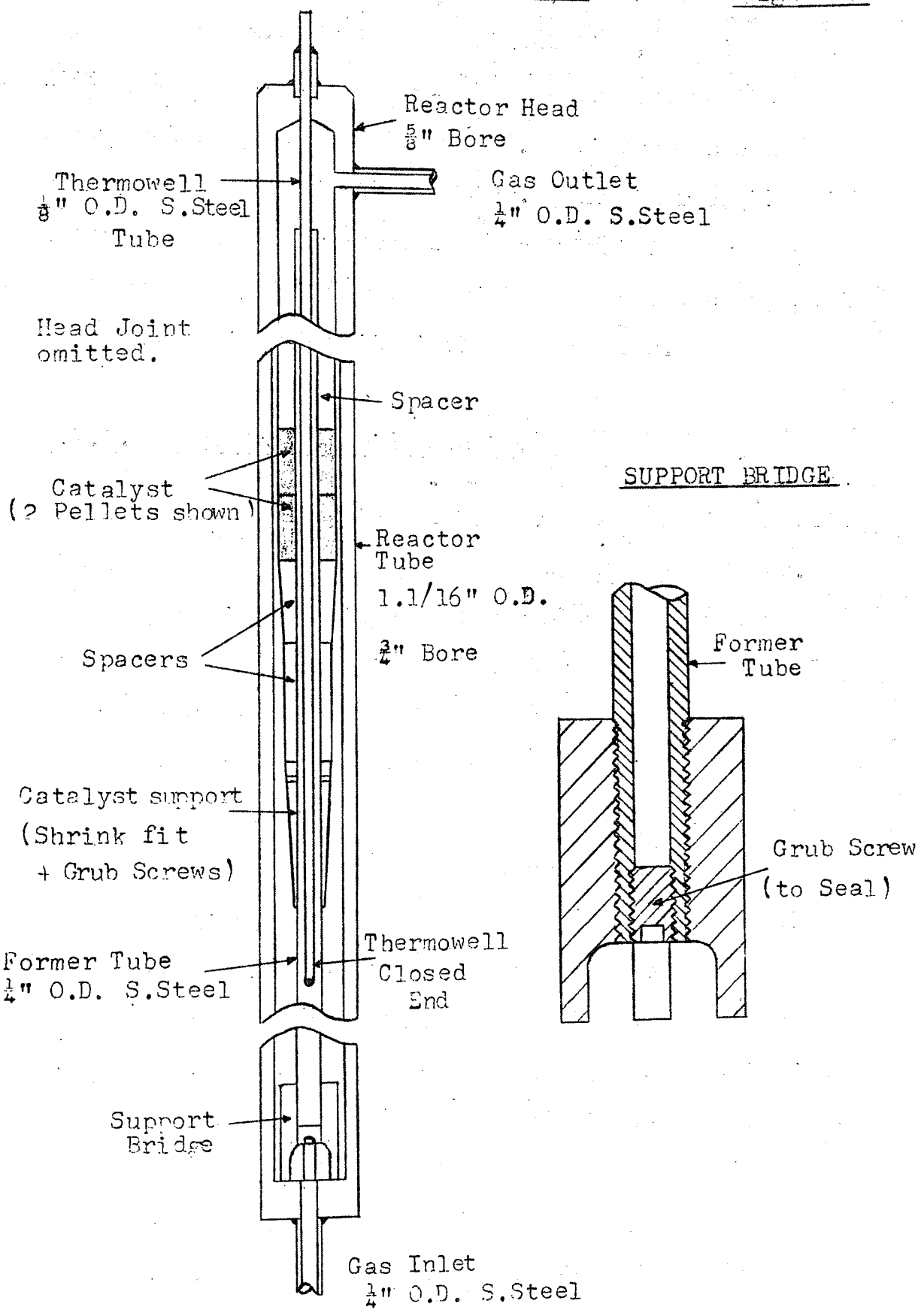

regulator. After pressure reduction the product was metered through a Parkinson-Cowan wet test meter which measured the volumetric flow rate to an accuracy of ± 0.1%. A 0-10 inch water manometer immediately upstream of the test meter allowed the metering pressure to be noted for subsequent reading correction. A thermometer was inserted in the gas stream at the meter exit so that similar corrections could be made for temperature.

The gas at this stage was still saturated with water vapour, and since the analytical technique required a dry sample, the product gas was dried prior to sampling. Drying was carried out using an aluminium oxide drying column, downstream of which was a silica-gel column for indication purposes. Two oxide columns were installed, one being used during start-up, and the second for actual runs.

Gas sampling was achieved by installing a gas bottle in the product stream immediately following the drying columns. A by-pass fitted round the sample bottle allowed the gas flow to be directed to the flare when the bottle was removed for content analysis.

2.2. Calibration Procedures.

2.2.1. Fischer and Porter flowrators.

As stated previously, combinations of tube sizes and float materials were used to obtain different gas flowrate ranges. For each combination used, a

calibration curve was prepared, and in the case of the methane flowrator, experimental checks also performed.

The calibrations were carried out according to the method given in the Fischer and Porter handbook (108), which involved calculating flowrates at tube scale readings for given operating conditions. A model calculation for the calibration of a $\frac{1}{8}$ inch tube incorporating a sapphire float operating with methane at 250 psig and at ambient temperature is given in Appendix B. The calculation method for a given tube and float may be summarised as follows:-

(i) Calculate the viscosity μ_{OPT} and density ρ_{OPT} of the gas to be metered at the temperature and pressure of metering.

(ii) From the Fischer and Porter handbook (108) obtain the float density ρ_f and tube size factors A and B.

(iii) Calculate a Viscous Influence Number N, where

$$N = \frac{A}{\mu_{OPT}} \sqrt{(\rho_f - \rho_{OPT})\rho_{OPT}}$$

(iv) From given float characteristic curves (108), obtain Flow Coefficients, C, at each tube scale reading, corresponding to the value of N.

(v) Using the relationship $W = CB\sqrt{(\rho_f - \rho_{OPT})\rho_{OPT}}$ calculate the gas flowrate W g/min.

Thus the flowrate - scale reading calibration curve may be drawn from the calculated data.

The calibrations obtained by the above method for nitrogen and hydrogen were considered accurate enough for the applications. In the case of methane however it was considered necessary to check the curves experimentally.

The checks were carried out using the whole of the reforming apparatus as described earlier, operated at ambient temperature and test pressure. For given flowrator scale readings, methane flows obtained over a test period were noted from the gas meter. The volumetric throughputs so obtained, were converted to mass flowrates after temperature and pressure correction, and then the results were compared with the theoretical calibrations.

In all cases the experimental curves were within ±1% of the theoretical for 90% of the tube scale, and only at the maximum scale readings did the discrepencies become appreciable ($\simeq \pm 5\%$). Therefore, since it was not intended to operate any flowrator combination at maximum flow, the theoretical curves were accepted as accurate.

2.2.2. Water Pump calibration.

The pumps used to deliver the feed water at pressure, are manufactured with a calibrated micrometer type stroke adjustment barrel, which allows fine control

of delivery rates. Calibration of the micrometer barrels was carried out by isolating the water feed section at the Steam Generator and controlling delivery pressure at the relief valve installed in the line. For given pump settings, the water delivered during a test period was collected at the relief valve, thus allowing calibration curves to be constructed.

In order to protect the pump valves from foreign matter, a fritted glass filter was incorporated in the pump feed line, a cleaned filter being installed on each occasion the pumps were used. It was found that the pump delivery varied slightly with each filter, therefore prior to every reforming run a secondary calibration was always carried out.

2.2.3. Reactor temperature control.

To carry out the proposed kinetic work it was necessary to be able to maintain the catalyst at set temperatures, therefore the reactor was fitted with a temperature control system. Since the furnace used for heating the reactor had three windings, and three 'Ether Transtrol' controllers were available, it was decided to incorporate a controller in each of the individual winding circuits; each had an independent thermocouple suitably sited within the reactor system.

The siting of the controller thermocouples proved

very critical from the standpoint of maintaining a constant temperature zone, and a number of locations were tried before satisfactory control could be obtained. The testing of the control system was carried out using a nitrogen feed at 250 psig pressure, the catalyst former was fitted within the reactor but without any catalyst pellets.

In the first test carried out the three thermocouples were placed at 1 inch spaces within the thermowell, the lower one being $1\frac{1}{2}$ inches above the catalyst support. The uppermost thermocouple was connected to the top winding controller, the centre couple to the main winding controller, and the bottom couple to the bottom controller. All of the ancillary heaters were used in the test, and a control point of 600°C was attempted.

This arrangement proved totally unsatisfactory since a $\pm$ 20°C oscillation about the set point was obtained with all three controllers, and therefore was considered too inaccurate for the subsequent work. The oscillations produced were assumed to be the culmination of: a closed loop control system, a long delay lag, and on-off controllers. Therefore the thermocouples were resited for a second test using open loop control in an attempt to reduce the delay lag.

For the second system tried, the three thermocouples were spaced $1\frac{1}{2}$ inches apart and secured to the

outer wall of the reactor, the lower couple being 17½ inches from the top of the thermowell. The reactor internal temperatures were measured with a potentiometer and moveable couple inserted down the thermowell. It was realised that for this arrangement guess work would be involved in setting the controllers to give a required reactor temperature, but it was rightly assumed that with practice, required temperatures could be readily achieved. The test carried out was essentially the same as the previous one, but in this case reactor temperatures were taken with the potentiometer at 1 inch increments upwards from the point where the catalyst support was fitted. Temperature surveys were made every 10 minutes following the reactor attaining the control temperature.

The degree of control obtained in this test was much better than that obtained with the first arrangement, and a 4 inch zone having a reasonably constant temperature was achieved; the maximum deviations from the average temperature were $+4^{o}C$ and $-2^{o}C$. However, temperature variation at any one position within the zone with time was considerably greater, this being $\pm 7^{o}C$ about the average. Hence, this arrangement was also rejected.

In the final arrangement tried, the controller thermocouples were placed in a steel sheath which was suspended against the inner wall of the furnace. The couples were spaced and located in positions corresponding to those used in the second test, and the procedure used

in testing was also the same.

This latter arrangement proved very satisfactory, and an extract of the reactor temperature survey is given in Table 1.

It can be seen that for the zone between 4 and 8 inches from the catalyst support, the temperatures obtained were essentially constant. The maximum deviations to the average throughout the constant zone were about $\pm$ 1°C, and therefore it was considered satisfactory to use this control arrangement for the subsequent experimental work.

2.3. Operating Procedures.

2.3.1. Catalyst loading.

For convenience, catalyst reduction was carried out as an entirely separate operation in which 21 pellets were reduced together. After activating, the pellets were removed from the reactor and stored in a nitrogen atmosphere ready for subsequent use. A full description of the reduction procedure is given in a separate section to follow.

In the preparation for a reforming run, the reactor was removed from the apparatus, stripped down, and the Catalyst Former removed for loading. The required number of pellets, taken from the reduced stock, were weighed

TABLE 1

REACTOR TEMPERATURE SURVEY

(Temperatures given in degrees centigrade)

Distance up from Catalyst Support.	Time (min.) from Reactor attaining Control Temperature.										
	20	30	40	50	60	70	80	90	105	120	135
4 inches	601.5	600	600	600	600	600	600.5	600	600.5	600	600
5 "	601.5	600.5	600.5	601.5	601.5	601.5	601	601	600.5	601	600.5
6 "	600.5	600.5	600.5	601.5	601.5	602	601.5	601.5	601	600.5	601
7 "	600	600	600.5	602	601.5	602	601.5	601.5	601.5	600.5	601.5
8 "	600.5	600	600.5	601.5	601.5	601.5	602	602	601.5	601	601.5

and sized, then threaded on to the Former, preceded by steel spacers to position the catalyst 'rod' within the constant temperature zone obtainable with the reactor controllers.

Prior to placing the catalyst rod assembly into the reactor, the catalyst location on the Former was measured and then related to the top of the thermowell after loading the vessel. This was necessary in order to take catalyst temperature profiles with the moveable thermocouple during the reforming runs.

After sealing, the loaded reactor was placed back into the apparatus and the pipe joints re-made. Pressure testing with nitrogen was carried out at this stage, and when the equipment proved pressure tight, the pipe work was lagged ready for an experimental run.

2.3.2. Start-up procedure.

Commissioning tests with the equipment provided the necessary experience to obtain Variac setting required to give the necessary temperatures within the ancillary heating equipment. Hence, at the start-up the Variacs were adjusted prior to switching on power. The set points on the reactor controllers were increased from ambient by 100°C increments so that the reactor operating temperature was achieved in approximately $2\frac{1}{2}$ hours.

During the warm-up period the valves immediately downstream of the flowraters, water pump, and reactor were all closed until the required temperatures in the various heating vessels were achieved. At this point the dome of the plant pressure control valve was pressurised with nitrogen, to a level necessary to maintain operating pressure, and then the appropriate valves were opened allowing a stream of nitrogen to pass through the equipment. This situation was maintained for at least $\frac{1}{2}$ hour to obtain thermal equilibrium. At this stage the reactor controllers were adjusted to give a catalyst temperature of about 25°C above that required, to allow for the subsequent drop in temperature due to the endothermicity of the reforming reaction. Also during the warm-up period the pump calibration was checked following the installation of a clean filter in the pump feed line.

Once thermal equilibrium was attained, the nitrogen flow was replaced with hydrogen. Then, after switching on the pump and pressurising the water feed line, the water inlet valve on the Steam Generator was opened. The pump delivery was increased incrementally to the required final delivery at a rate that allowed about 5°C of superheat to be maintained within the Steam Generator exit mixture.

As soon as the required water delivery was achieved and the reactor had attained the necessary

temperature, the hydrogen supply was halted and replaced with methane. When a fully developed methane flame could be observed at the flare, final adjustments to the set points on the reactor controllers were made, and after putting the tared test drying column on stream, the experiment was considered started.

2.3.3. Running operation.

Following the warm-up period the main operating function during a reforming run was to ensure that the required conditions throughout the equipment were maintained. Particular attention had to be given to the flowrator in maintaining the float setting, and also to the condensate removal system. In the case of the latter the 'drip' removal rate had to be adjusted so that the input of condensate to the knock-out vessel was approximately balanced by the offtake, otherwise flooding of the gas line occurred.

At the commencement of reforming and at every half hour interval thereafter, operating conditions throughout the plant were logged; other relevant data noted are listed as follows:-

Wet test meter reading.

Water feed burette reading.

Catalyst rod temperature survey.

Condensate volume collected.

Product sample analysis.

In the measurement of the catalyst temperature three readings along the length of the rod were usually taken at each survey. To collect the condensate formed during the half hour intervals, at the end of each period the offtake valve was opened further and the knock-out vessel drained completely. Product gas samples were taken to the chromatograph for analysis using the Sample Bottle.

In any run schedule that involved changing an operating variable, the run was arranged so that the changes were done in descending order. For example, if the reactor temperature was the variable, the reactor would be run at the highest temperature for the first test period, then reduced accordingly.

2.3.4. Shut-down procedure.

At the completion of an experimental run the equipment was always shut down for overnight standing. If the catalyst was to be used for further studies the plant was filled with a hydrogen atmosphere, but if a strip-down was to follow, the whole system was purged with nitrogen.

After the last collection of data, the test drying column was isolated and the methane flow substituted with an equal volumetric flow of hydrogen or nitrogen, the water delivery being unchanged. When the methane flame

at the flare disappeared the Steam Generator water inlet valve was closed and the plant power supply turned off. The gas purge was allowed to flow for a further $\frac{1}{4}$ hour in order to completely clear the system of methane, after which the flow was halted and the plant isolation valves closed. The test drying column was weighed after every run, and when the catalyst was removed from the reactor, the pellets were also weighed and sized.

2.3.5. Calculation of results.

For the kinetic analysis, the operating conditions and gas compositions were the data of interest. However, for the purpose of assessing the accuracy of the equipment a number of mass balances were carried out using the results obtained from preliminary runs.

A typical mass balance showing the good agreement that was obtained throughout is given in Appendix C.

CHAPTER 3.

ANALYTICAL EQUIPMENT AND PROCEDURES.

3.1. Analytical Equipment.

3.1.1. The chromatograph.

Product gas analyses were carried out using a Beckman G.C.2 Gas Chromatograph in conjunction with a Honeywell-Brown 0-1 millivolt chart recorder. The bench arrangement is shown in Plate 3.

The G.C.2 chromatograph, illustrated in Figure 7, consists essentially of the following elements: a chromatographic column, a carrier gas flow control, a heated sample inlet system through which measured quantities of sample may be introduced into the unit, a thermal conductivity cell (Katharometer), a controlled heater system, and a regulated voltage supply. An inner insulated compartment, maintained at a set operating temperature by the internal heater, encloses the chromatographic column and the detector cell.

Following sample injection to the GC-2, the components are swept by the carrier gas into the column where they are absorbed by the packing material. The carrier gas continually flows through the column carrying off the individual components at different times. The time required for each component to pass through the column depends on the equilibria between sample components, the carrier gas, and the column packing.

The gases flow from the column through the sensing

PLATE 3

THE BECKMAN GC-2 GAS CHROMATOGRAPH

SOAP BUBBLE
FLOWMETER

THE CHROMATOGRAPH

HONEYWELL-BROWN
CHART RECORDER

GAS SAMPLING
VALVE

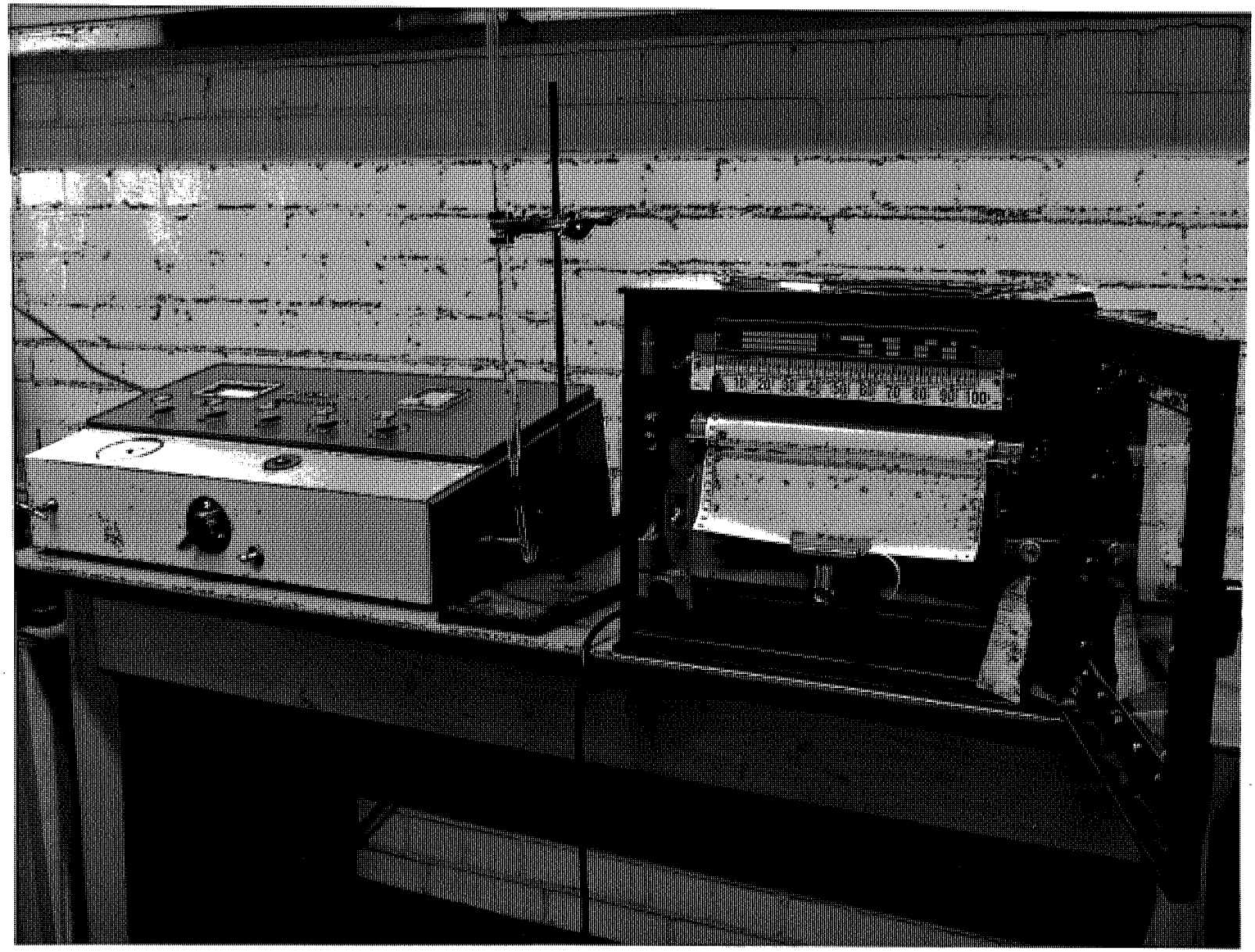

SCHEMATIC LAY-OUT OF THE GC2 CHROMATOGRAPH. FIGURE 7

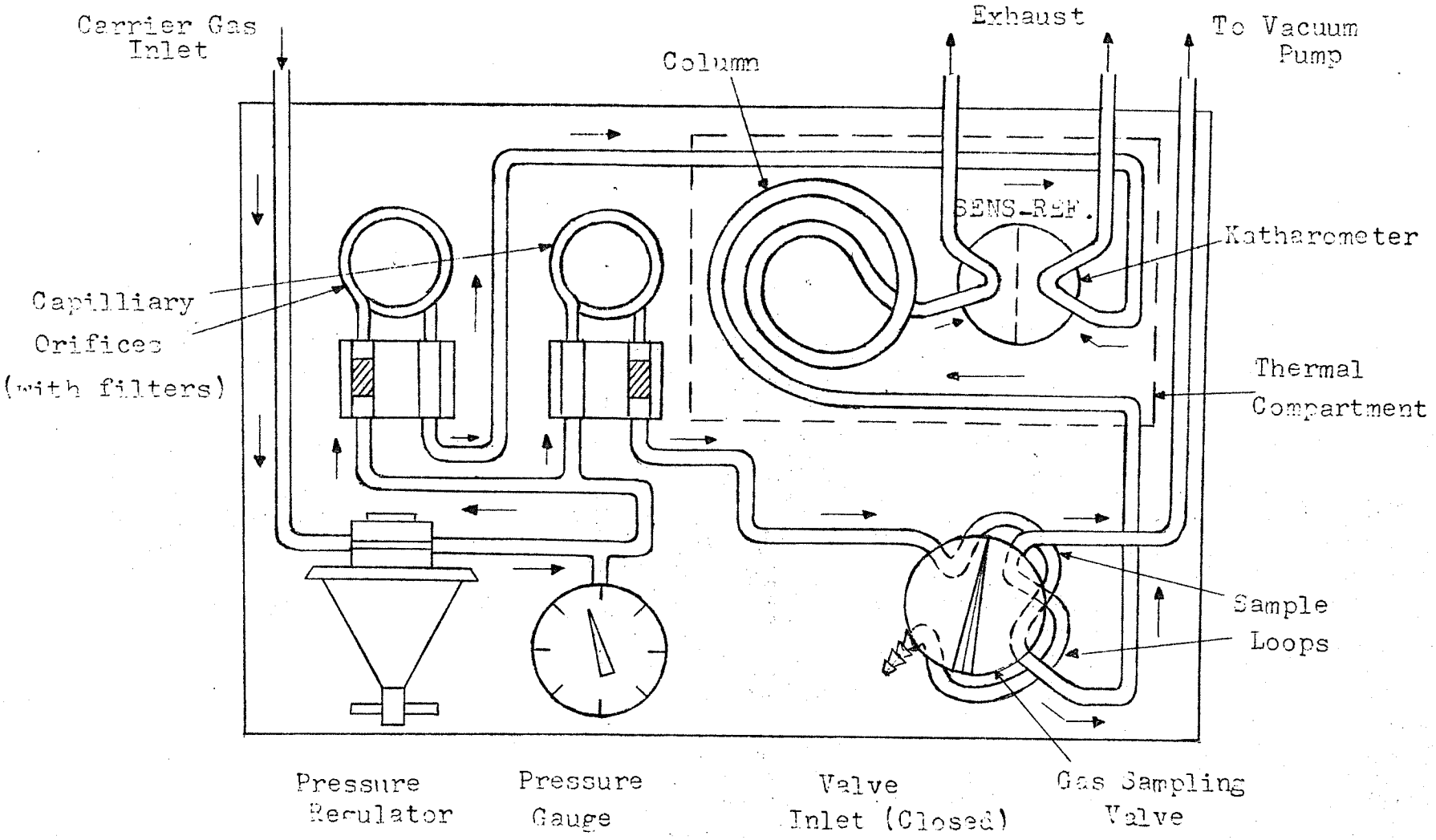

side of the detector cell. A corresponding flow of carrier gas flows through the heating compartment so that it reaches the cell at the same temperature as the sample-carrier gas mixture.

The difference in thermal conductivity between the carrier gas in the reference side of the detector cell and the sample-carrier gas mixtures in the sensing side produces voltage differentials which result in a family of peaks for the various components being produced on the recorder trace. The area beneath each peak on the trace is proportional to the quantity of the component in the sample. However, in many instances it is more convenient to use peak heights as the quantitative measure of each component, and it was this method that was used for the analytical work.

Argon was used as the carrier gas, and the column was wound from a 21 ft. length of $\frac{1}{4}$ inch O.D. stainless steel tube. 'Porapak Q' (Ethylvinyl benzene polymer) beads, 80/100 mesh, were used for the column packing material and were activated before use by heating at 220°C in a carrier gas purge for 4 hours. Sample injection was achieved by means of the Gas Sampling Valve but because of the similarity in thermal conductivity between argon and carbon dioxide, one of the two 1 cc sample loops supplied with the valve, was replaced by a larger loop with a nominal volume of 5 cc. This provided a measurable response for carbon dioxide.

The sampling valve was so constructed that whilst one sample loop was in-line with the chromatograph column, the other was open to atmosphere via a vent tube extending to the rear of the instrument. Turning the sampling valve reversed the positions of the sample loops.

3.1.2. Gas handling equipment.

As stated previously, gas samples were introduced into the chromatograph by means of the Gas Sampling valve. A vacuum method was employed, and a gas handling system was constructed for this purpose. The unit, shown in Plate 4, consisted essentially of a vacuum pump, pressure reduction/control system, a gas sample reservoir, and a mercury filled manometer.

The apparatus is illustrated in Figure 8, and from this it can be seen that the vacuum pump was directly connected to the chromatograph sample loop vent tube. One limb of the manometer was tapped into this line for measuring loop pressures. A valved glass 'Tee' fitting inserted between the manometer tapping and the vacuum pump isolation valve was used as the point for sample introduction.

As it was intended to calibrate the chromatograph with high pressure cylinder gases, a pressure reduction/control system, identical to that used on the reforming apparatus, was incorporated in the equipment. The low pressure end of the cylinder gas line was connected to

PLATE 4

THE CHROMATOGRAPH GAS HANDLING APPARATUS

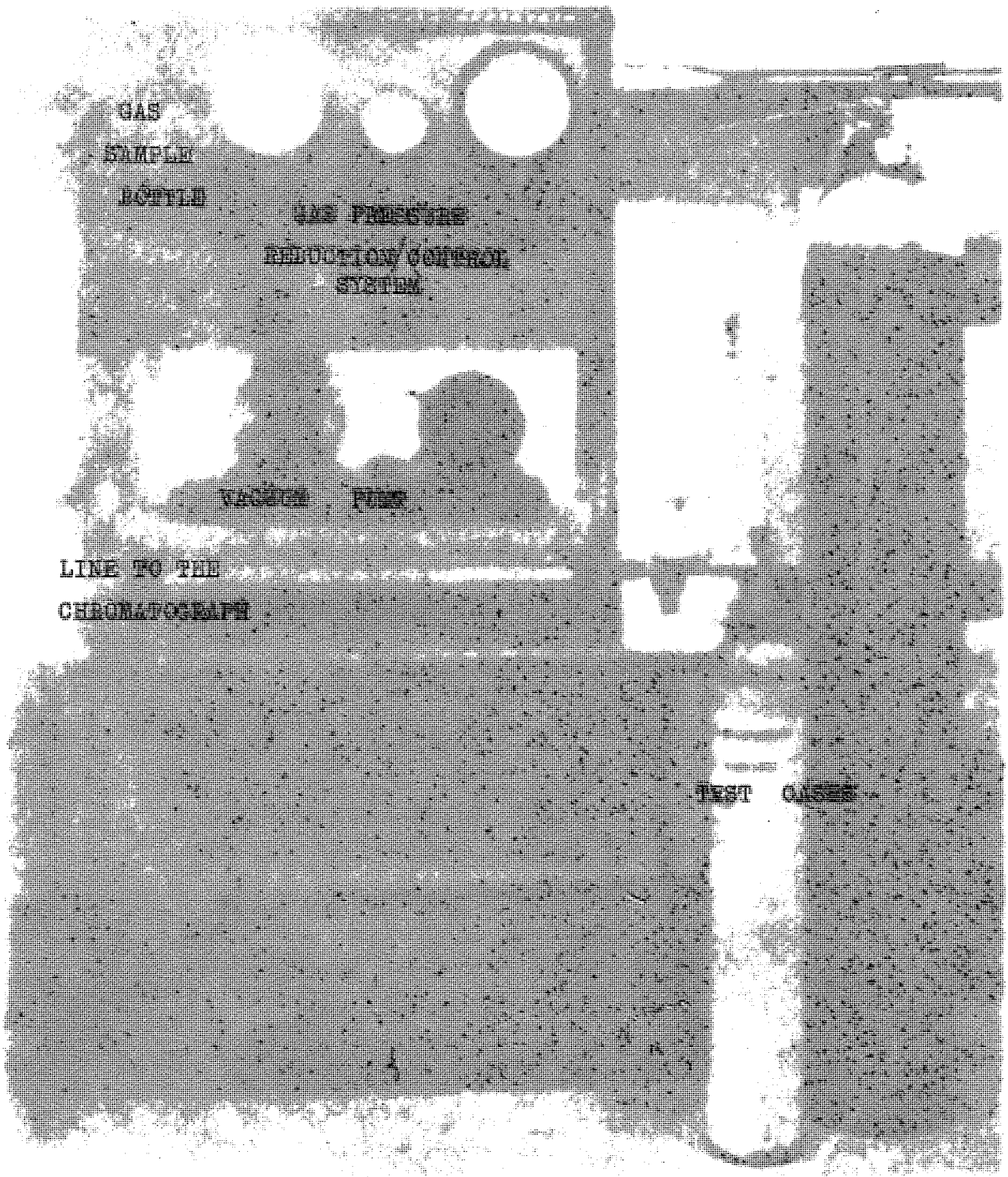

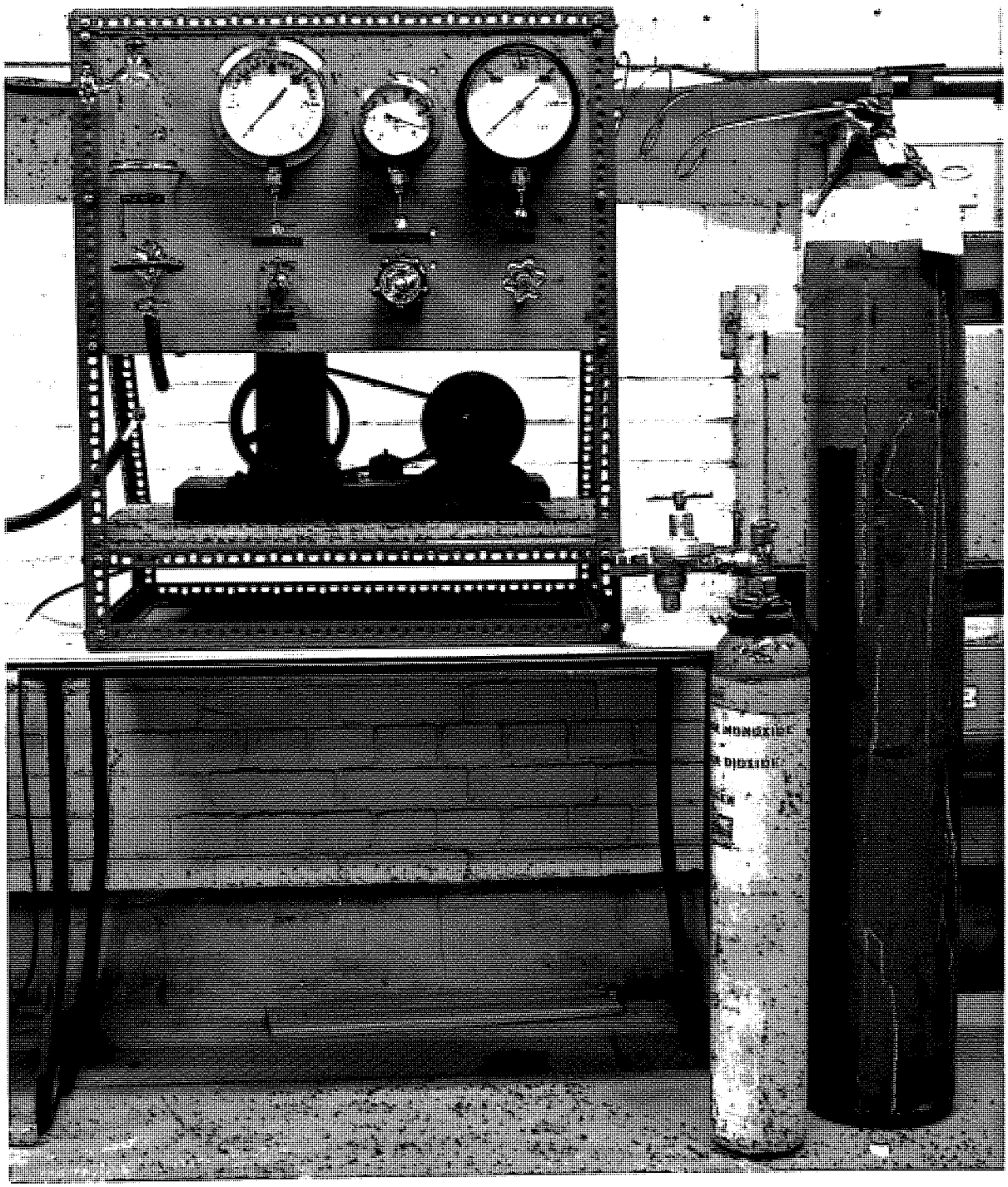
MONOXIDE
DIOXIDE

The Chromatograph Gas Handling Apparatus.

Figure 8

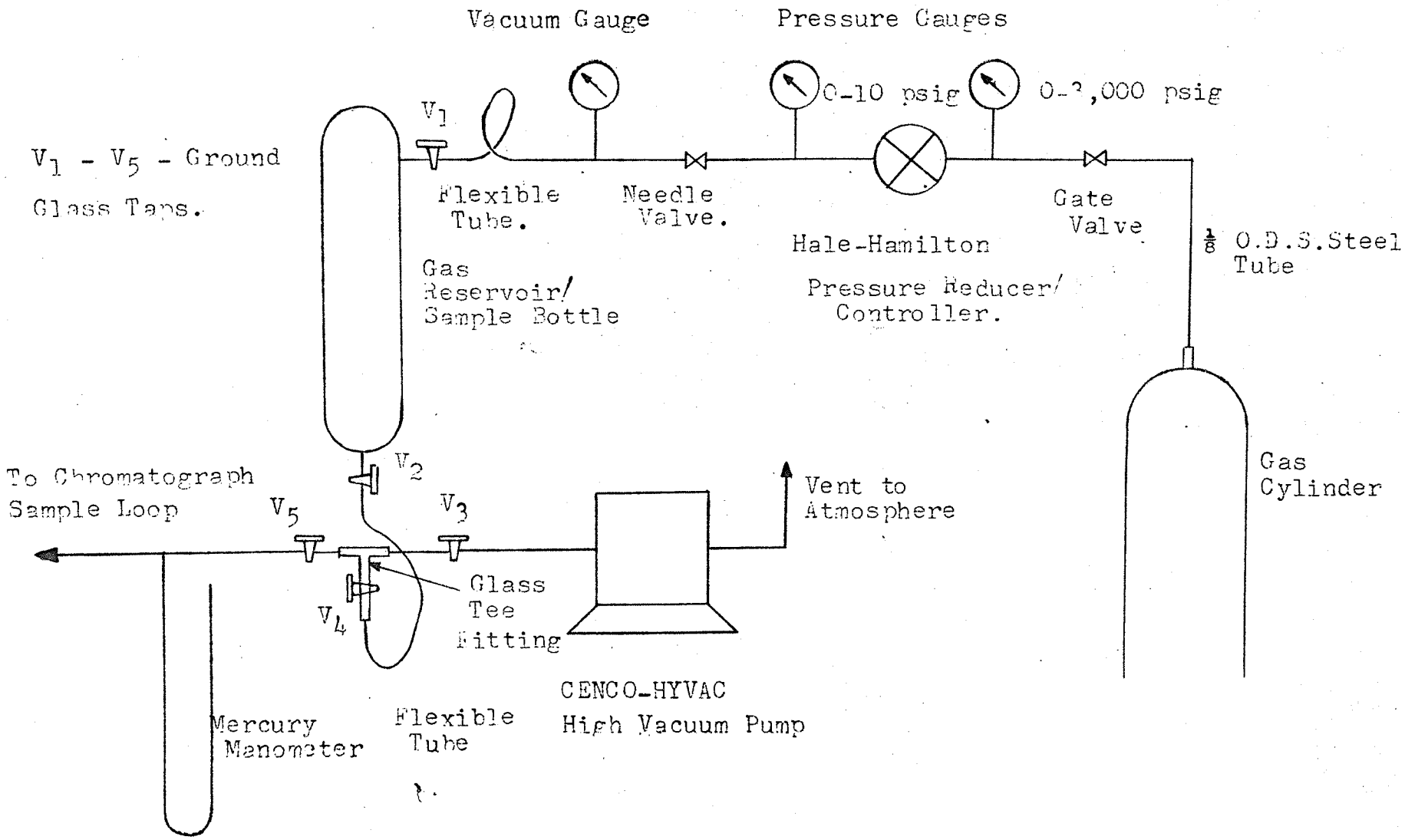

the gas reservoir with flexible tubing, the other end of the reservoir being connected to the injection 'Tee' fitting by more flexible tubing. The gas reservoir was used as the product gas sample bottle during experimental runs, and when employed as such was connected to the 'Tee' fitting in a similiar fashion to that described above.

3.2. Calibration Procedure.

3.2.1. Pre-calibration tests.

Porapak Q was chosen as the column packing material since it offered a complete analysis from a single injection of the type of gas mixtures anticipated from the experimental reforming work. Other factors influencing the choice of Porapak Q may be listed as follows:-

(i) The polymer beads are not coated with a liquid phase, hence, no bleed is obtained from the packing.

(ii) The beads do not react with polar materials, and compounds such as water are eluted as sharp peaks.

(iii) Because of (i) and (ii) there is no tendency for changes in retention times or peak shapes with constant flowrate of carrier gas.

(iv) The mechanism of the separation is such that it permits a rapid recovery if the system is overloaded, i.e. too large a sample for the length of column.

(v) The shape and strength of the beads permit easy column packing.

After selecting the column packing material it was necessary to carry out preliminary commissioning tests in order to ascertain the optimum conditions for operation. These conditions may be summarised as follows.

(i) Column length.

(ii) Oven temperature.

(iii) Carrier gas flowrate.

(iv) Katharometer current.

On reference to the work of Cross (109, 110), it was decided to limit the maximum operating temperature of the oven to 40°C. For maximum sensitivity the Katharometer current was set at 150 ma, this being the level recommended by the instrument manufacturers when Argon is used as the carrier gas. For the initial tests a 9 ft. column was employed with a carrier gas flow of 35 cc/min. A gas mixture containing H_2, CO, CH_4, and CO_2 was used for the test gas sample.

Good peaks were obtained for carbon dioxide and methane. However, with this arrangement it was found totally impossible to obtain a separation between hydrogen and carbon monoxide, the peak for the latter being completely contained within that for hydrogen.

Following the first test, the column length was increased to 12 ft., and further tests carried out with the operating conditions as before. Using the larger

column the H_2/CO separation was improved but nevertheless incomplete. It was found however, that by operating the oven at ambient temperature with a low carrier gas flowrate, a reasonable degree of separation could be obtained. But because the instrument offered no temperature control below 40°C, and a low carrier flow resulted in long analysis times and also enhanced the possibility of Katharometer burn-out, this column was also rejected.

Finally, a 21 ft., column was tried with the oven controlled at 40°C and a carrier gas flow of 35 cc/min. This system gave a satisfactory separation for a minimum analysis time and hence, calibration curves were prepared for these conditions.

3.2.2. Component calibration.

It was correctly assumed at this stage that the dry product gas from the reforming experiments would consist of hydrogen, methane, carbon monoxide, and carbon dioxide and hence, the chromatographic unit was calibrated for the above components.

From the observations made during the pre-calibration tests, the anticipated reformer product compositions, and a consideration of the thermal conductivities of the above gases relative to that of argon (the carrier), the attenuations to be used for each component gas in the

calibration and analyses were selected. Table 2 shows the attenuations selected and indicates the factors in the choices.

TABLE 2

COMPONENT ATTENUATIONS AND SELECTION FACTORS USED FOR THE CHROMATOGRAPHIC ANALYSIS

Gas	Attenuation	Selection Factors
Hydrogen	100	Extremely sensitive with Argon Carrier.
Methane	50	Moderate Sensitivity, high percentages anticipated.
Carbon Monoxide	1 and 5	Moderate Sensitivity, low percentages anticipated.
Carbon Dioxide	1	Poor Sensitivity, low percentages anticipated.

For a given gas, peak height and area increases as attenuation is decreased.

Calibration curves were prepared for each of the four gases in turn, high purity cylinder gases being used as the source of each component.

After switching on the instrument and setting the detector cell current and carrier gas flowrate to the predetermined values, a warm-up period in excess of three hours was allowed in order to obtain a steady base line trace on the chart recorder. During this period

the sampling valve was checked to ensure that the 1 cc sample loop was 'in-line' with the column, and hence the 5 cc loop open to the Gas Handling Apparatus.

When the chromatograph was ready for use, the cylinder containing the gas for calibration was connected to the pressure line of the Gas Handling Apparatus (Figure 8). By use of the appropriate valves and taps in conjunction with the Vacuum Pump, the reservoir was then continually evacuated and filled with the cylinder gas in order to purge residual air from the system. When purging was considered complete, the reservoir was finally filled to atmospheric pressure and then isolated.

Again using the Vacuum Pump and pertinent taps, the 5 cc loop was evacuated until a steady reading was obtained on the manometer. The pump was then isolated and the manometer reading noted. A sample of gas from the reservoir was then introduced into the evacuated line and loop, the manometer reading again being noted. The Gas Sample Valve was then turned, thus putting the sample filled loop 'in-line', and the attenuation control adjusted to the pre-determined setting. During the period between sample introduction and the peak output on the recorder, the 'off-line' sample loop was evacuated and the gas valve position reversed, thus re-exposing the 5 cc sample loop to the gas handling equipment.

This sequence was repeated, increasing the sample quantity each time, until a series of chromatograms had been obtained for corresponding manometer readings. The whole procedure was repeated a further twice in order to ascertain the reproducibility.

By measuring the heights of the peaks obtained, and plotting these against respective loop absolute pressures, the calibration curve was constructed. Calibrations for all of the four gases were carried out in this fashion, and Figures 9,10,11,12, show the final curves.

Following the individual component calibrations, checks were carried out using a standard gas mixture containing all of the gases of interest. The method used for the analysis was identical to that described in Section 3.3.1, after first filling the Gas Sample Bottle with the mixture. The checks proved the calibration to be satisfactory, since the results obtained for a number of analyses were in good agreement with the B.O.C. certified composition. A typical sample of the checks are shown in Table 3.

HYDROGEN CALIBRATION CURVE.

Figure 9.

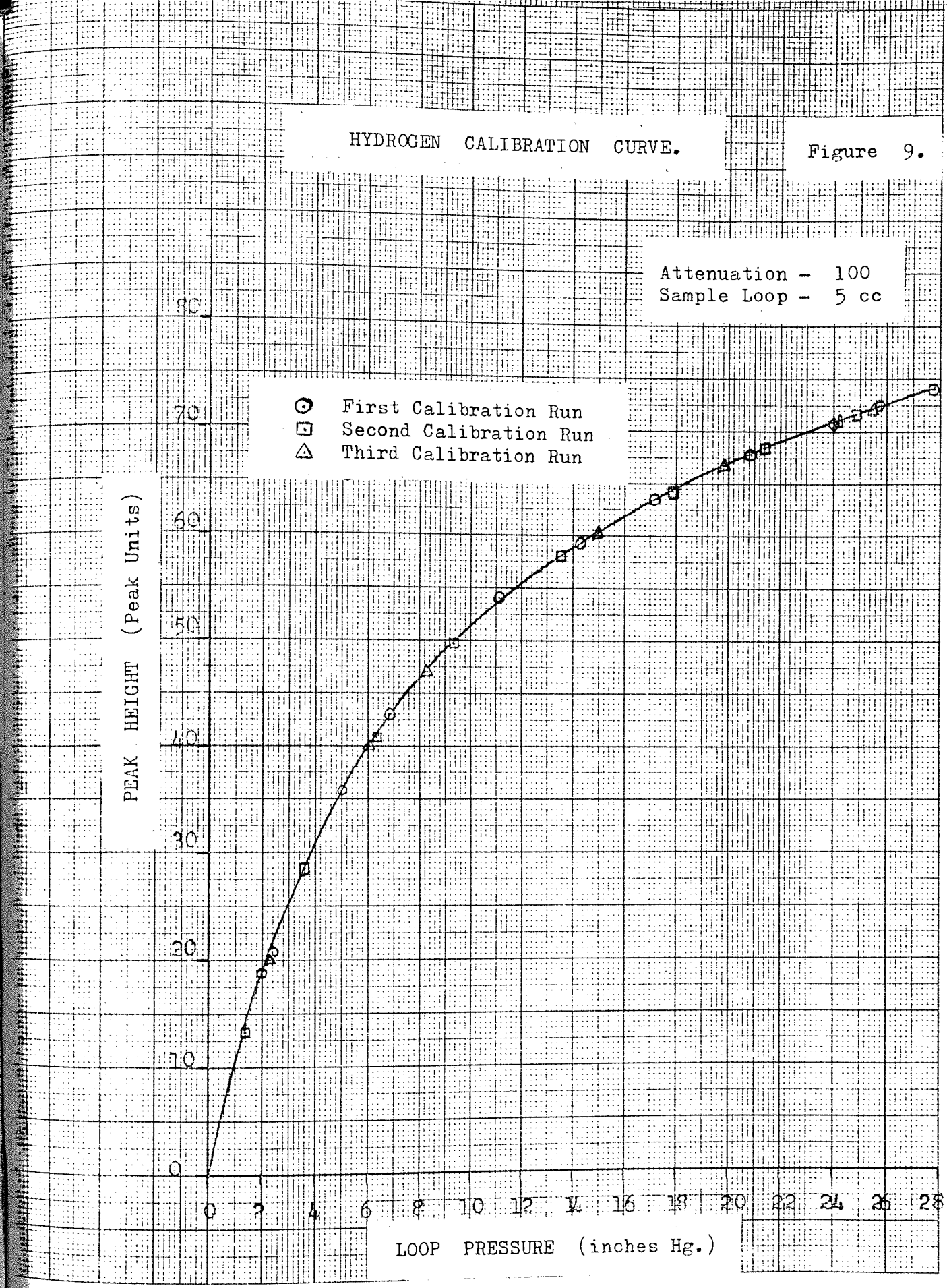

A. CARBON MONOXIDE CALIBRATION CURVE. Figure 10.

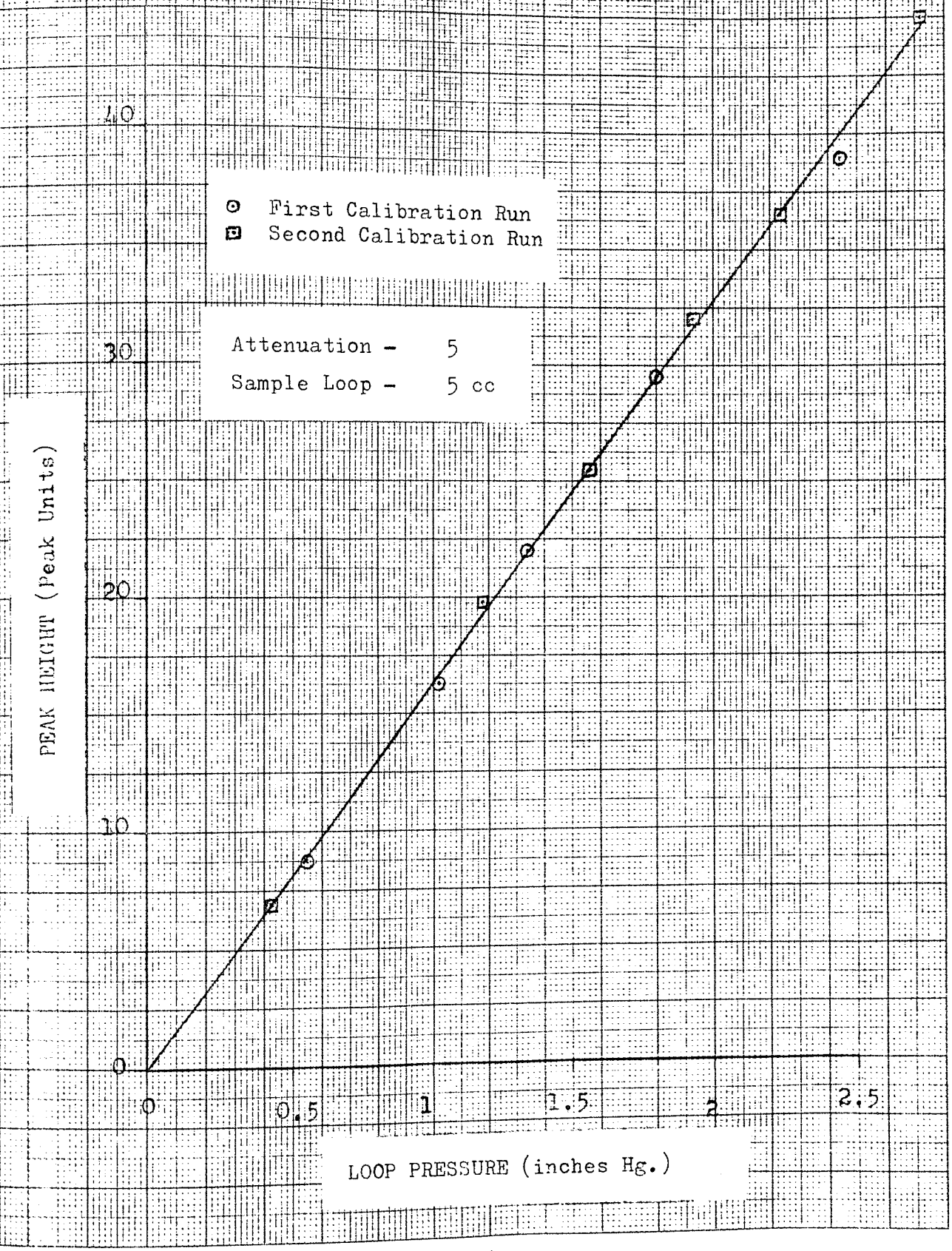

B. CARBON MONOXIDE CALIBRATION CURVE. Figure 10.

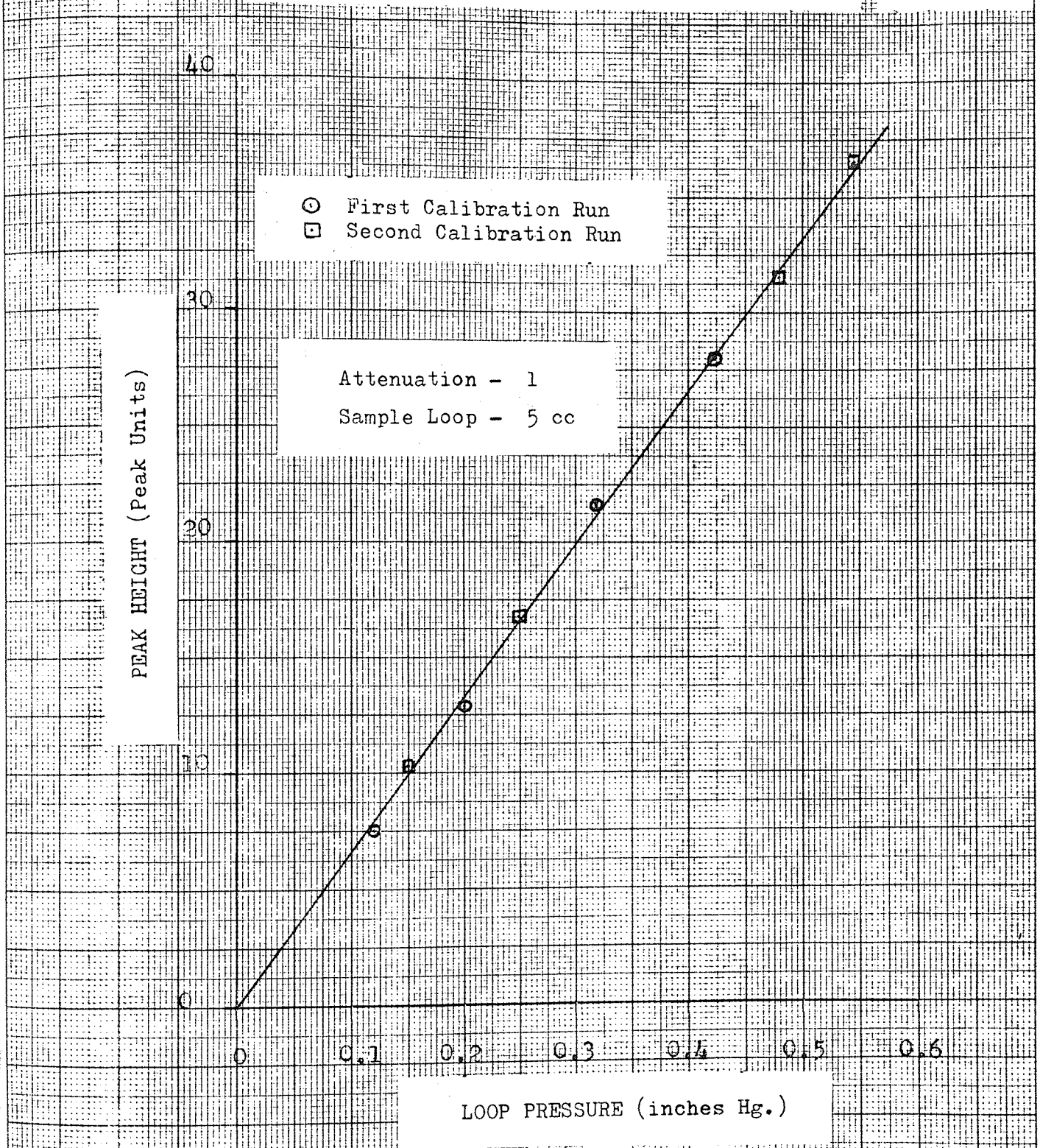

METHANE CALIBRATION CURVE. Figure 11.

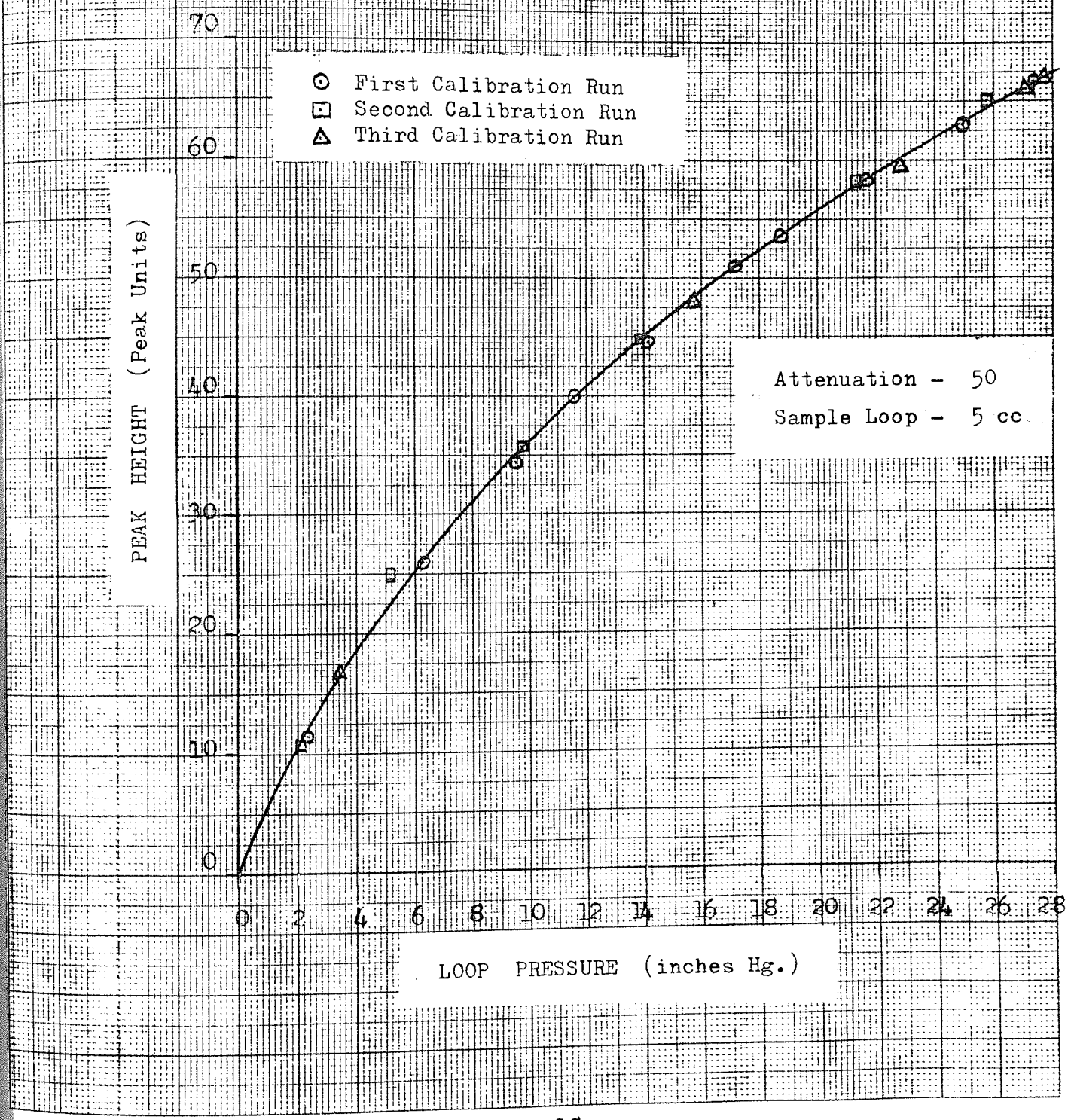

CARBON DIOXIDE CALIBRATION CURVE.

Figure 12.

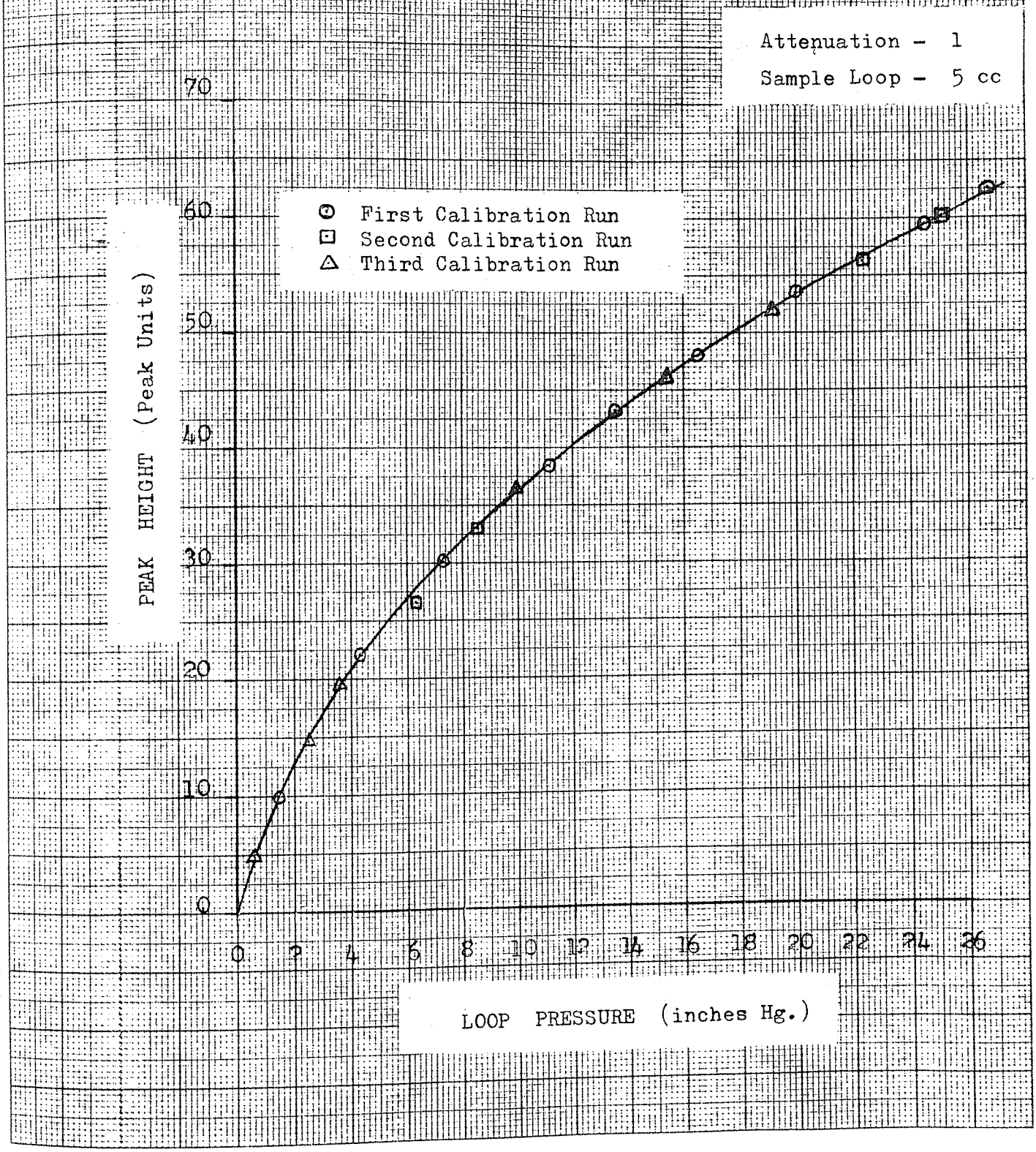

TABLE 3

RESULTS OF CHROMATOGRAPH CALIBRATION CHECKS USING A B.O.C. STANDARD GAS.

Test	H_2	CH_4	CO	CO_2
B.O.C. Analysis	50.2	34.5	10.4	4.9
1	50.1	35.1	9.84	4.96
2	49.72	34.97	10.31	5.00
3	49.89	34.77	10.30	5.04
4	49.92	34.67	10.40	5.01
* 5	50.22	35.08	9.84	4.86
6	50.06	35.02	9.85	5.07

* Used for the model example in Section 3.3.2.

3.3. Analytical Procedure.

3.3.1. Method.

In the experimental reforming work the samples for analysis were contained in the Gas Sample Bottle, hence, for the purpose of sample introduction the pressure reduction line of the Gas Handling Apparatus was not used.

After ensuring that the instrument was ready for use, and the 5 cc sample loop exposed to the vacuum line, one end of the sample bottle was inserted into the flexible tube extending from the injection 'Tee'. After evacuating the whole line and sample loop, the maximum amount of sample possible was introduced into the chromatograph in an identical manner to that used in the calibration, similarly noting the manometer readings for the evacuated and sample filled system.

Upon turning the sampling valve, placing the filled loop 'in-line', stability of the baseline trace was checked at maximum and minimum attenuation settings, adjusting the zero control when necessary. The attenuation control was then set to the desired value for the first component to be eluted (hydrogen). After the first peak had been traced and the pen

returned to the base line, the attenuation control was changed to the value required for the second peak (carbon monoxide). This procedure was repeated for the two remaining elutions (methane and carbon dioxide respectively). Upon the completion of the analysis the 'off-line' sample loop (1 cc) was evacuated and the gas valve turned to make the 5 cc loop available for another analysis.

3.3.2. Calculation method.

From a completed chromatogram the composition of the sample gas was calculated using the calibration curves shown in Figures 9 - 12. A model calculation follows for the B.O.C. standard gas, a scaled diagram of the chromatogram is shown in Figure 13.

Taking the peak height for each component, the calibration curves allow the partial pressure of each gas within the original sample to be found. The volumetric composition is then directly calculated from the partial and total pressures. Table 4 shows a summary of the calculation for the standard gas chromatogram which in a scaled down form, is shown in Figure 13.

Figure 13.

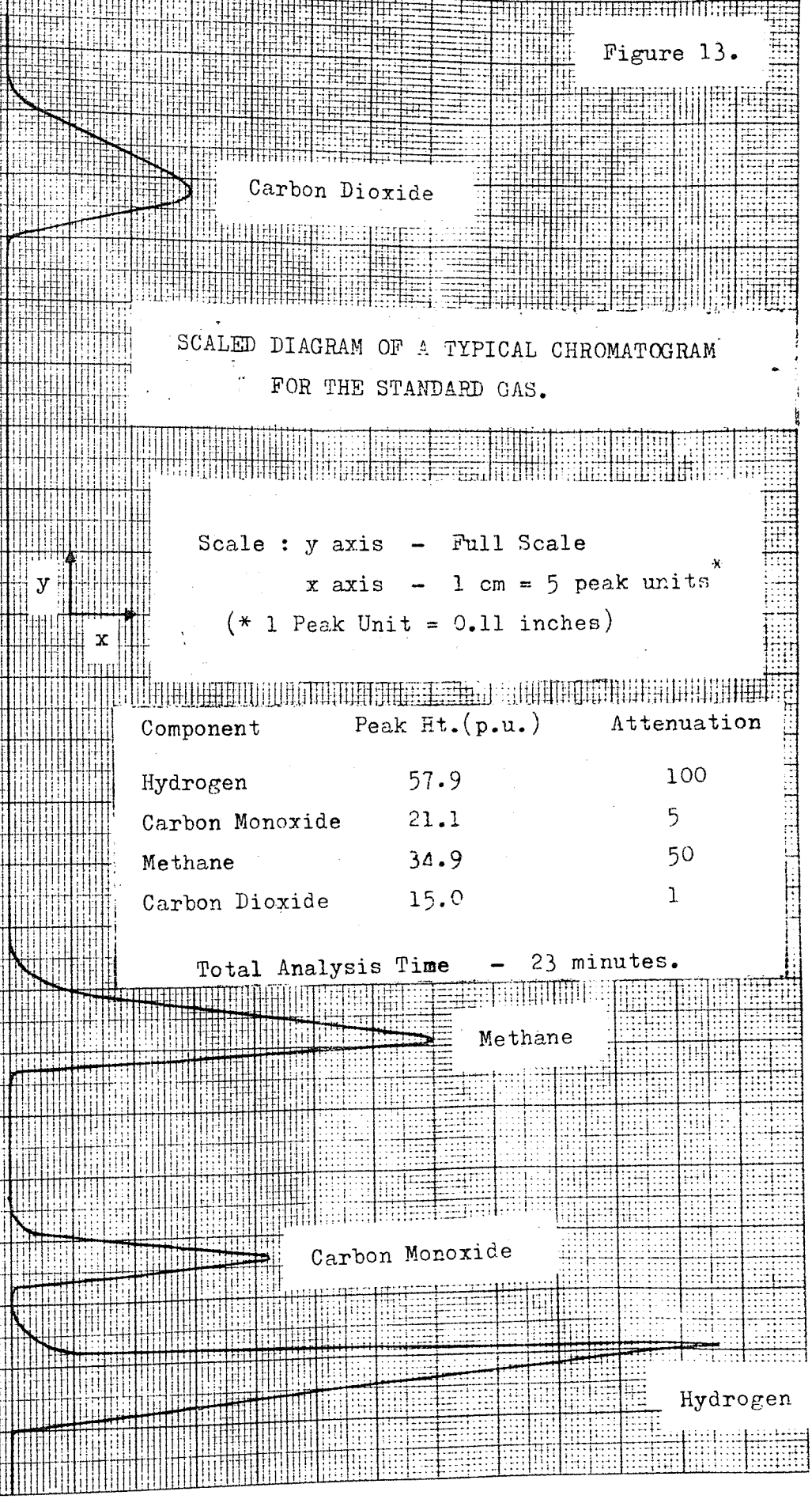

SCALED DIAGRAM OF A TYPICAL CHROMATOGRAM FOR THE STANDARD GAS.

Scale : y axis - Full Scale

x axis - 1 cm = 5 peak units*

(* 1 Peak Unit = 0.11 inches)

Component	Peak Ht.(p.u.)	Attenuation
Hydrogen	57.9	100
Carbon Monoxide	21.1	5
Methane	34.9	50
Carbon Dioxide	15.0	1

Total Analysis Time - 23 minutes.

TABLE 4

STANDARD GAS ANALYSIS CALCULATION SUMMARY.

Component	Peak Height (peak units)	Partial Pressure (in Hg)	% Composition (vol/vol)
Hydrogen	57.9	13.55	50.22
Carbon Monoxide	21.1	1.31	4.86
Methane	34.7	9.47	35.08
Carbon Dioxide	15.3	2.66	9.84
Total Pressure =		26.98	

From the manometer readings taken during sample injection, a simple check on the total loop pressure obtained in Table 4 may be made:-

Evacuated Loop Pressure = 75.2 cm Hg (vacuum)

Filled " " = 7.3 cm Hg (vacuum)

Sample Pressure = 67.9 cm Hg abs.

This value is equivalent to 26.74 in Hg, which compares with 26.98 in Hg obtained from the summation of the

partial pressures. This represents an error in the order of 1%, and since this figure is representative of the majority of analyses, it further illustrates the satisfactory accuracy of the calibration curves and method.

CHAPTER 4.

THERMODYNAMIC STUDIES.

4.1 Introduction.

In the examination of a chemical reaction or group of chemical reactions, it is essential that a thorough study of the thermodynamics and reaction equilibria be carried out. The results from such studies can greatly influence the approach taken in any subsequent kinetic work and may also contribute towards the interpretation of data so obtained.

It must be stated however, that thermodynamic and equilibrium data is not in itself sufficient for predicting reaction routes and mechanisms, but what such data can predict may be summarised as follows:-

(i) The reactions that are thermodynamically feasible, and those which control the final product composition.

(ii) The maximum extent of a reaction or reactions at given operating conditions.

(iii) The overall effect of the operating variables on the system.

Steam hydrocarbon reforming is no exception, and thermodynamic and equilibrium data is not only important with regard to kinetic work but is also essential in the successful design and operation of a reforming process.

4.2. Reactions and Free Energy Survey.

The literature survey shows that the steam-hydrocarbon reforming reaction is somewhat complex due to the numerous possible reactions that may take place and the manner in which the final product is attained. In view of the diversity of opinion that has been expressed, it was decided to investigate the possible reactions on a thermodynamic basis so that the principal reactions may be established and also the benefits outlined in the preceding section gained.

When hydrocarbons and steam are brought into contact over an active catalyst, numerous reactions are possible (43,51,52,73,121). The following list is based on a knowledge of the possible reaction products along with the conclusions that have been made by other workers.

$$Cn\ H_{2n+2} + nH_2O \longrightarrow nCO + (2n+1)\ H_2 \quad - - - - - - - - 1$$

$$Cn\ H_{2n+2} + 2nH_2O \longrightarrow nCO_2 + (3n+1)\ H_2 \quad - - - - - - - - 2$$

$$Cn\ H_{2n+2} + \left(\frac{n-1}{2}\right)H_2O \longrightarrow \left(\frac{3n+1}{4}\right)CH_4 + \left(\frac{n-1}{4}\right)CO_2 \quad - - - 3$$

$$Cn\ H_{2n+2} \longrightarrow x\ CH_4 + y\ H_2 + \text{unsaturated compounds} \quad - 4$$

$$CH_4 + H_2O \longrightarrow CO + 3H_2 \quad - - - - - - - - - - - - - 5$$

$$CH_4 + 2H_2O \longrightarrow CO_2 + 4H_2 \quad - - - - - - - - - - - - - 6$$

$$CO + H_2O \longrightarrow CO_2 + H_2 \quad - - - - - - - - - - - - - 7$$

$$2H_2O \longrightarrow 2H_2 + O_2 \quad - - - - - - - - - - - - - 8$$

$2CH_4 \longrightarrow C_2H_6 + H_2$ - - - - - - - - - - - - - - 9

$C_2H_4 + 2H_2O \longrightarrow 2CO + 4H_2$ - - - - - - - - - - - - 10

$C_2H_2 + 2H_2O \longrightarrow 2CO + 3H_2$ - - - - - - - - - - - - 11

$CH_4 \longrightarrow C + 2H_2$ - - - - - - - - - - - - - - - 12

$2CO \longrightarrow C + CO_2$ - - - - - - - - - - - - - - - 13

$CO_2 \longrightarrow C + O_2$ - - - - - - - - - - - - - - - 14

$2CO \longrightarrow 2C + O_2$ - - - - - - - - - - - - - - - 15

$H_2O + C \longrightarrow H_2 + CO$ - - - - - - - - - - - - - - 16

$C_2H_4 \longrightarrow 2C + 2H_2$ - - - - - - - - - - - - - - 17

$C_2H_2 \longrightarrow 2C + H_2$ - - - - - - - - - - - - - - 18

To predict the thermodynamic feasibility of the above reactions use is made of a method proposed by Dodge (111) :-

For $\Delta G_T^o < 0$, the reaction is promising.

For $\Delta G_T^o > 0$, but $< + 10{,}000$, then the reaction is doubtful but warrants further study.

For $\Delta G_T^o > + 10{,}000$, the reaction is very unfavourable and would only be feasible under unusual circumstances.

It must be emphasised that while this method is only indicative, it does however provide a quick and useful means of analysing a family or group of reactions.

Table 5 gives the standard free energy changes (ΔG_T^o) of the reactions listed. The temperature range chosen is that which is thought to be relevant to the operating ranges for the various existing reforming processes.

The values quoted in Table 5 are for the reactions proceeding in the direction as written in the list on page 118; it follows therefore if any particular reaction has a high positive ΔG_T^o value it will be numerically equal but opposite in sign in the reverse direction. Hence, if a reaction is unlikely to proceed in the forward direction it is likely that the reverse reaction may take place.

Table 5 shows that over the whole temperature range, reactions 8,9,14, and 15, have relatively high positive ΔG_T^o values, therefore it may be concluded that these reactions do not take place. In the case of reactions 8,14, and 15, these are all of the oxygen producing reactions, and since there is no oxygen as O_2 present in a steam-hydrocarbon feed, the reverse reactions may also be eliminated; if O_2 were present, however, its reaction would be highly probable. The result obtained for reaction 9 indicates that the reverse reaction is more favoured than the forward one. This conclusion is not unexpected since it has been established (39,40,51) that the instability of the

TABLE 5

ΔG_T° FOR THE VARIOUS REACTIONS POSSIBLE DURING STEAM-HYDROCARBON REFORMING.

Reaction	Temperature °K							
	700	800	900	1000	1100	1200	1300	1400
1 C_7	-11,378	-58,938	-94,699	-136,562	-178,421	-220,331	-262,216	-304,029
2 C_7	-32,784	-68,471	-104,590	-140,986	-177,539	-214,297	-251,191	-288,076
3 C_7	-78,863	-86,605	-94,195	-101,672	-109,136	-116,557	-123,905	-131,282
4 C_7	-5,956	-20,582	-35,184	-49,757	-64,301	-78,821	-93,306	-107,766
5	+11,437	+5,516	-479	-6,522	-12,573	-18,644	-24,736	-30,812
6	+8,378	+3,297	-1,890	-7,418	-12,437	-17,771	-23,143	-28,508
7	-3,058	-2,219	-1,413	-632	+126	+862	+1,575	+2,279
8	+99,824	+97,836	+92,688	+87,462	+82,200	+76,890	+71,534	+66,182
9	+17,000	+17,020	+16,980	+16,910	+16,840	+16,750	+16,620	+16,510
10	-5,904	-14,558	-23,288	-32,061	-40,846	-49,656	-58,358	-67,264
11	-27,726	-33,246	-38,816	-44,416	-50,025	-55,655	-61,182	-66,913
12	+3,050	+550	-2,010	-4,610	-7,220	-9,850	-12,500	-15,140

TABLE 5 (Cont.)

ΔG_T° FOR THE VARIOUS REACTIONS POSSIBLE DURING STEAM-HYDROCARBON REFORMING.

Reaction	Temperature °K							
	700	800	900	1000	1100	1200	1300	1400
13	-11,444	-7,185	-2,946	+1,274	+5,469	+9,645	+13,793	+17,962
14	+94,496	+94,539	+94,578	+94,610	+94,637	+94,661	+94,677	+94,690
15	+83,052	+87,354	+91,632	+95,884	+100,106	+104,306	+108,470	+112,616
16	+8,386	+4,966	+1,533	-1,906	-5,343	-8,783	-12,218	-15,647
17	-22,676	-24,490	-26,354	-28,249	-30,160	-32,090	-34,030	-35,970
18	-44,498	-43,178	-41,882	-40,604	-39,339	-38,089	-36,854	-35,624

ΔG_T° REACTION = $\sum \Delta G_T^\circ$ PRODUCTS - $\sum \Delta G_T^\circ$ REACTANTS

Data taken from references (117) and (118)

hydrocarbon molecule and its ease to reform increases with the number of carbon atoms. This point is further illustrated by comparing the standard free energy changes involved in the hydrocarbon-steam reaction yielding carbon monoxide and hydrogen. It can be seen from Table 5 that thermodynamically the reaction for heptane, 1, is far more feasible than the same reaction for methane, 5.

Considering the initial reactions that may take place during reforming, i.e. reactions 1-4, it can be seen from Table 5 in which heptane is taken as an example for these reactions, that all of the standard free energy changes are numerically high and negative in sign, and therefore are very feasible. This possibly helps to explain why opinions are so diversified with regard to the initial reactions. Since all are feasible on a thermodynamic basis, it is likely that they all take place to a lesser or greater degree depending on operating conditions and relative reaction rates.

For reactions 1,2,3,4,10,11, and the reverse of 9, the thermodynamic equilibrium constants K_T will be high over the range of temperature considered since K_T is related to ΔG_T^o by the following expression :-

$$\Delta G_T^o = - RT \ln K_T \quad ------ \quad 4.1$$

Therefore it follows that with sufficient residence time and favourable kinetics, these reactions will go to completion. Hence, the only hydrocarbon to remain in the final reformed product will be methane.

The reactions that involve carbon, i.e. 12, 13, 16,17, and 18, all fall essentially into the bounds of thermodynamic feasibility. Reactions 17 and 18 have high negative standard free energy changes over the whole temperature range, and therefore may be considered possible and at the same time tending towards completion. Reactions 12 and 16 have standard free energies that are positive in sign at lower temperatures, but become negative at the higher temperatures. A sign reversal of the standard free energy is also obtained with reaction 13, but in this case it is the opposite way round, that is, negative at low temperatures and positive at high.

With regard to the latter three reactions, the results are interpreted as follows. In the lower temperature region carbon may be formed by reaction 13 and the reverse of reaction 16, carbon removal will be achieved by the reverse of reaction 12. This is also the view expressed by Hebden (86) who studied the synthesis gas reaction at temperatures in this lower region. At higher temperatures reaction 12 becomes the carbon forming reaction whilst 16 and the reverse of 13 will remove any carbon deposits.

The standard free energy changes of the remaining reactions, 5, 6, and 7, all undergo a sign change within the selected temperature range. At low temperatures the reverse of reactions 5 and 6 are favoured, and at high temperatures the reverse of 7 is more promising than the forward reaction. It follows therefore at low temperatures that methane formation is favourable but carbon monoxide formation is not. This is due to the reverse of reaction 5 producing CH_4 at the expense of CO, reaction 7 consuming CO, and reaction 6 using CO_2 and H_2 to yield CH_4 and H_2O. At the higher temperatures, the situation is reversed. This explains the results obtained by Pease and Chesebro (112) who in studying the steam-methane equilibria postulated that for temperatures up to 500°C the equilibrium composition is controlled by reaction 6. However in acknowledging the presence of small quantities of CO in the product, these authors stated that above this temperature the reactions involving carbon monoxide must be taken into consideration.

With regard to carbon dioxide formation it is impossible to draw any conclusions since at all temperatures it is simultaneously produced and consumed. Therefore a knowledge of rates of the CO_2 participating reactions would be required before any analysis could be made.

It can be seen from Table 5 that the standard free energy changes of reactions 5, 6, and 7 are such that relative to the other reactions postulated, the equilibrium constants will neither be excessively high nor excessively low. Therefore the components taking part in these reactions will be present as finite measureable quantities in the equilibrium product.

The deductions that have been drawn from the free energy survey are in agreement with results that can be found in the literature. However, it must be re-emphasised that these conclusions can only be considered as general since they are based solely on the thermodynamics of the individual reactions, and no account of reaction rates and the effect these may have on each other has been made.

4.3 Reaction Equilibria.

4.3.1. Introduction.

Workers who have studied the equilibria of the reforming process, have in general produced tabulated and graphical methods of establishing equilibrium compositions for various hydrocarbon feeds at given operating conditions, or alternatively, produced methods for calculating equilibrium compositions for different values of the operating variables. Lihou (83) for example, presents a graphical method

incorporating numerous calculations; whilst he has shown the method to be accurate, the number of manipulations that have to be performed make the technique tedious. Similarly, Ribesse and Van Maele (115) present a method for calculating equilibrium compositions and thermal energies for an autothermic system. Again the technique does not lend itself to obtaining rapid solutions. Somer (52), produces tabulated results for various ranges of the operating parameters; the obvious limitation with this type of presentation is that it has to be more or less specific, otherwise the volume of tabulation required to cover all of the operating conditions currently employed for the various processes will be large.

Considering that reforming plant operators are likely to require readily accessible equilibrium data, it was decided to obtain such data over wide ranges of the operating variables which may be presented in a compact graphical form.

4.3.2. Mathematical formulation of the equilibrium equations.

It has been established by others (23, 24, 49, 51, 52, 83), and also in the free energy survey, that when hydrocarbons are reformed with steam over an active catalyst, the equilibrium product contains CO,

CO_2, H_2, CH_4, and H_2O. In the absence of permanent carbon deposition, the equilibrium composition must be controlled by reactions 5,6, and 7 since these are the only reactions solely involving all or some of the above products. Since reaction 6 may be considered as the sum of reactions 5 and 7, it can be eliminated leaving the steam-methane and carbon monoxide shift as the controlling reactions. Hence, it follows that these two may be used to calculate equilibrium composition data.

For feedstocks higher than methane in the paraffin homologous series, account has to be made of the initial reaction. As stated earlier, considerable differences in opinion exist as to the way in which this reaction should be represented. Unfortunately the free energy survey does not provide any indication with regard to this since all of the four reactions postulated have high negative free energies and are therefore feasible. However, it was indicated that all of the initial reactions would go to completion, and therefore, for the purpose of calculating equilibrium compositions any one may be selected to represent a system as long as the calculations are carried out on the chosen basis and the stoichiometry is satisfied.

The following development for a $C_n H_{2n+2}$ hydrocarbon considers the initial step to be represented by the completion of reaction 3 :-

$$C_n H_{2n+2} + (\frac{n-1}{2}) H_2O \longrightarrow (\frac{3n+1}{4})CH_4 + (\frac{n-1}{4})CO_2 \quad -- \quad 3$$

Consider 1 mole of methane being formed by reaction 3:-

$$(\frac{4}{3n+1})C_nH_{2n+2} + (\frac{2(n-1)}{3n+1})H_2O \longrightarrow CH_4 + (\frac{n-1}{3n+1}) CO_2$$

If N is the moles of steam left after the initial reaction, then the steam:carbon feed ratio R (moles steam:atom carbon) is represented by:-

$$R = \frac{N + 2(\frac{n-1}{3n+1})}{4n/(3n+1)}$$

At equilibrium the product composition is controlled by the steam-methane and the carbon monoxide shift reactions:-

$$CH_4 + H_2O \rightleftharpoons CO + 3H_2 \quad -------- \quad 5$$

$$CO + H_2O \rightleftharpoons CO_2 + H_2 \quad -------- \quad 7$$

Let x be the moles of CH_4 that react according to 5 and y be the moles of CO that react according to 7 Then at equilibrium the gas mixture will be :-

CH_4		$1 - x$	moles
CO		$x - y$	"
CO_2		$y + \frac{n-1}{3n+1}$	"
H_2		$3x + y$	"
H_2O	N	$- x - y$	"
Total	$N + 1 + 2x + \frac{n-1}{3n+1}$		"

If Kp(5) and Kp(7) are the partial pressure equilibrium constants for reactions 5 and 7 respectively, and P the total pressure, then:-

$$Kp(5) = \frac{pCO \times p_{H_2}^3}{pCH_4 \times p_{H_2O}}$$

$$= \frac{(3x+y)^3 (x-y)}{(1-x)(N-x-y)} \left[\frac{P}{N+2x+(1+\frac{n-1}{3n+1})}\right]^2 \quad - - 4.2$$

and $$Kp(7) = \frac{pCO_2 \times pH_2}{pCO \times pH_2O}$$

$$= \frac{(y + \frac{n-1}{3n+1})(3x+y)}{(x-y)(N - x - y)} \quad - - - - - 4.3.$$

By putting $(n-1)/(3n+1) = A$, and expanding the above partial pressure functions for the two equilibrium constants the following polynomial expressions are obtained :-

For function 4.2

$$f(xy) = 0 = x^4\left[4K_{p(5)} - 27P^2\right] + 4x^3K_{p(5)}\left[y + A\right] + x^2\left[K_{p(5)}\left(-3N^2-2N+4Ny-3-2NA-2A+4yA+A^2\right) + 18P^2y^2\right] + x\left[K_{p(5)}\left(-N^3+N^2+N+N^2y-2Ny-3y-1-2A-A^2 -2Ay-2N^2A-NA^2+2NyA+yA^2\right) + 8P^2y^3\right] + K_{p(5)}\left(N^3+2N^2-N^2y+N-2Ny-y+2N^2A+2NA +NA^2-2NyA-2yA-yA^2\right) + P_y^{2\,4} \quad - - - - - \quad 4.4$$

For function 4.3

$$g(xy) = 0 = -x^2K_{p(7)} + x\left[K_{p(7)}N-3y-3A\right] + K_{p(7)}\left(y^2-Ny\right) - \left(y^2+yA\right) \quad - - - - - - - \quad 4.5$$

By using a suitable mathematical technique equations 4.4 and 4.5 may be simultaneously solved for x and y. Hence, for any saturated hydrocarbon feedstock it is possible to calculate equilibrium compositions for given values of the variables N, P, $K_{p(5)}$, and $K_{p(7)}$.

4.3.3. Digital computer solution.

In order to test the mathematical analysis a computer program was written (Program 1) and run on the Elliott 803 B computer at the University of Aston in Birmingham, the language used being Elliott Algol 60. The simultaneous solution of equations 4.4 and 4.5 was achieved by using a Newton-Raphson iteration. The method is well described in Lapidus (116), but essentially involves a continual improvement on an initial guess of the roots x and y using correction terms derived from the two functions and partial differentials of the same. Figure 14 shows the flow diagram for Program 1, and includes the stages involved in the iteration.

For both methane and heptane feedstocks, selected values of P, N, $K_{p(5)}$, and $K_{p(7)}$ were used as input data for the computer program. $K_{p(5)}$ and $K_{p(7)}$ values were calculated from data given in Table 5 and equation 4.1. In all cases the results obtained agreed with those reported in the literature (23).

4.3.4. Equilibrium constants as functions of temperature.

It can be seen from the preceding section that for the determination of equilibrium compositions, subsidiary manual calculations and 'read-in' of

Flow Diagram for Program 1. Figure 14.

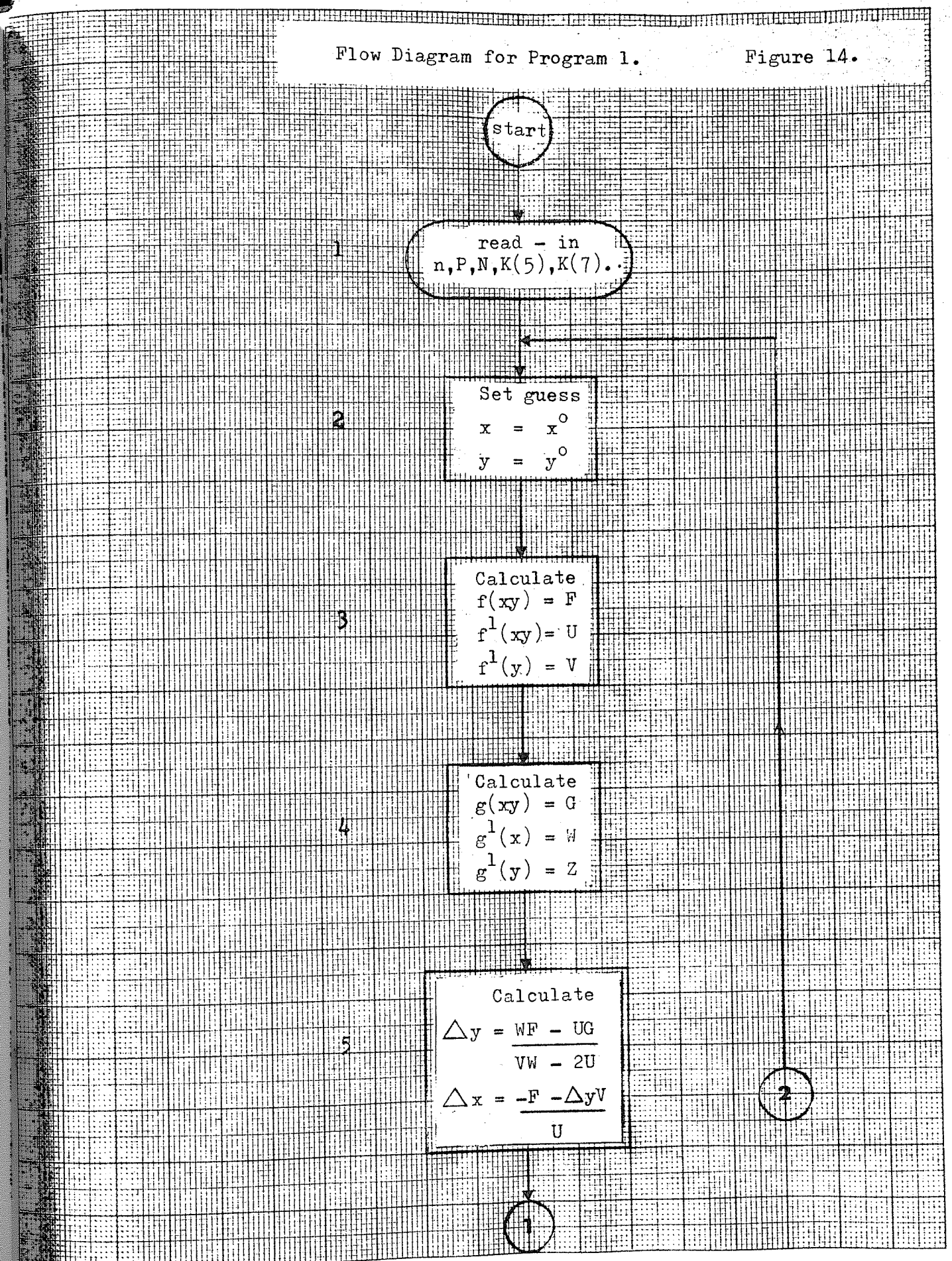

Figure 14 (Cont.)

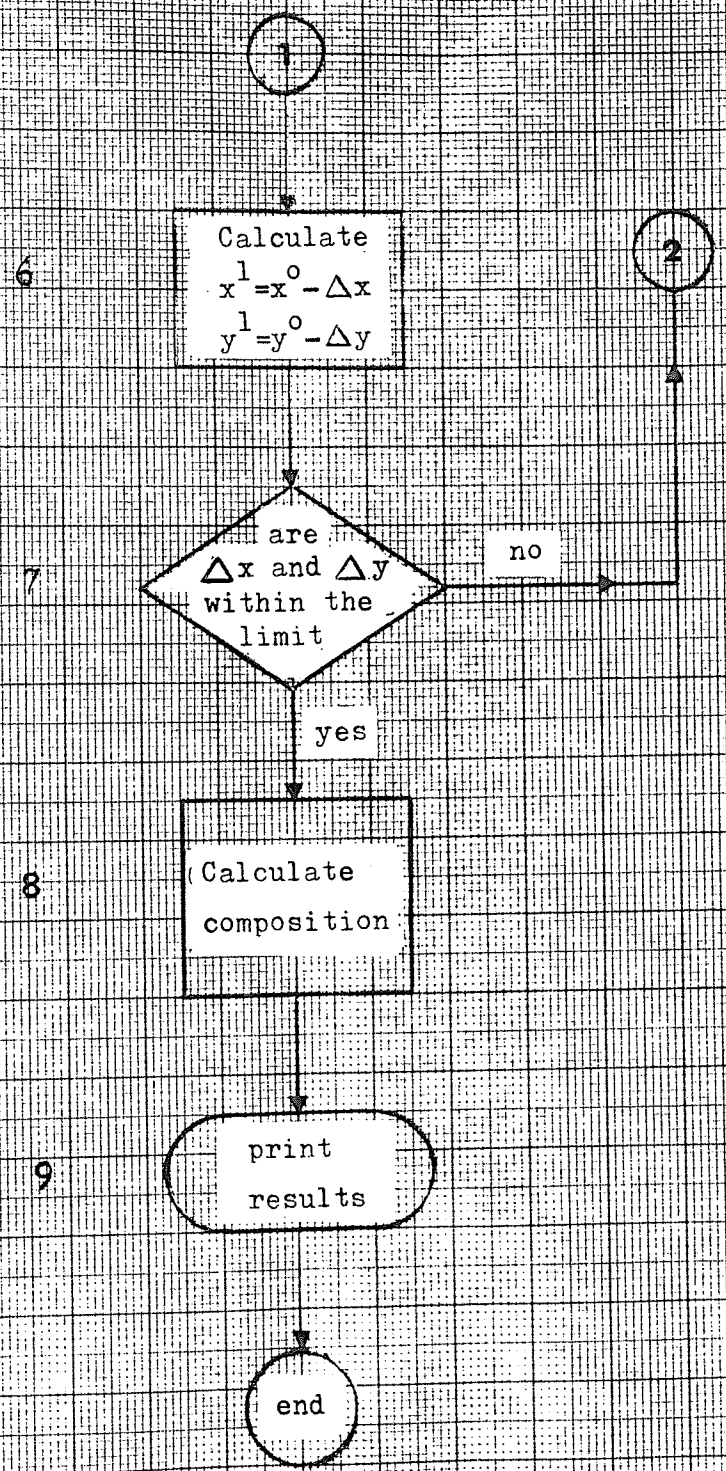

Stages 2 through 7 represent the Newton - Raphson iteration procedure.

respective equilibrium constants is required. Therefore, in order to obtain equilibrium data for ranges of the variables without such subsidiary work, the computer program was modified by the inclusion of a step to calculate the constants from temperature functions.

In the following development of the temperature functions, it is assumed that K_p, the equilibrium constant based on partial pressure, is equal to K_T, the thermodynamic equilibrium constant. Relevant thermodynamic data (117) over a temperature range 700°K - 1400°K for reactions 5 and 7 is shown in Table 6. Heats of formation, ΔH_T^o, and standard free energies, ΔG_T^o, were calculated from the following general expression :-

$$\Delta G_T^o \text{ reaction} = \sum \Delta G_T^o \text{ products} - \sum \Delta G_T^o \text{ reactants}$$

The values of the equilibrium constant $K_{p(5)}$ were calculated from equation 4.1 and the values of $K_{p(7)}$ were taken directly from Spiers (117).

The relationship between K_p and temperature, T, at a fixed pressure is represented by the Vant Hoff equation :-

$$\frac{d \text{ Ln } K_p}{dT} = \frac{\Delta H_T^o}{RT} \quad - - - - - - - - \quad 4.6$$

integration of which yields K_p as a function of temperature. However, Table 6 shows that the heats of formation for both reactions are themselves functions of temperature, therefore the respective functions must be established and inserted into equation 4.6 prior to integration.

Heats of formation and temperature are related by the Kirchoff equation :-

$$\left(\frac{d\ \Delta H_T^o}{dT} \right)_P = \Delta C_p \text{ reaction} \quad - - - - - - 4.7$$

where C_p is the specific heat at constant pressure and ΔC_p reaction = $\sum C_p$ products - $\sum C_p$ reactants. Integration of the Kirchoff equation between the limits T and T_{Datum} yields :-

$$\Delta H_T^o = \Delta H_{T_D}^o + \int_{T_D}^{T} \Delta C_p \, dT \quad - - - - - 4.8$$

By using specific heat data from Hougen (119), reproduced in Table 7, the following specific heat function is obtained for Reaction 5 :-

$$\Delta C_p = 16.848 - 0.019827\ T + 5.5937 \times 10^{-6} T^2 \quad - - 4.9$$

Integration of equation 4.8 using the ΔC_p function represented by equation 4.9 and standard ΔH_T^o data from Spiers (117) at a datum temperature of 298°K, gives the following ΔH_T^o function for reaction 5:-

TABLE 6

THERMODYNAMIC DATA FOR THE METHANE-STEAM (5) AND CARBON MONOXIDE SHIFT (7) REACTIONS.

	Reaction 5				Reaction 7			
T °K	ΔH_T°	ΔG_T°	$K_T(5)$	log $K_T(5)$	ΔH_T°	ΔG_T°	$K_T(7)$	log $K_T(7)$
700	52,690	11,437	2.661×10^{-4}	-3.5749	-	-3,058	9.009	0.9546
800	53,194	5,516	3.112×10^{-2}	-1.5069	-8,822	-2,219	4.032	0.6055
900	53,586	-479	1.307	0.1162	-	-1,413	2.208	0.3439
1000	53,876	-6,522	2.673×10^{1}	1.4270	-8,334	-632	1.372	0.1373
1100	54,101	-12,573	3.162×10^{2}	2.500	-	126	0.9434	-0.0253
1200	54,231	-18,644	2.500×10^{3}	3.3979	-7,857	862	0.6944	-0.1584
1300	54,300	-24,736	1.459×10^{4}	4.1641	-	1,575	0.5435	-0.2648
1400	54,359	-30,812	6.531×10^{4}	4.8150	-7,394	2,279	0.4405	-0.3560

$$\Delta H_T^o(5) = 45079.48118 + 16.848T - 0.0099135T^2 + 1.86456 \times 10^{-6} T^3 \quad \text{- - - - - - - - - - 4.10}$$

TABLE 7

STANDARD HEATS OF FORMATION AND SPECIFIC HEAT CONSTANTS FOR THE RELEVANT GASES.				
GAS	a	$b \times 10^3$	$c \times 10^6$	ΔH_T^o DATUM = 298°K
CO	6.35	1.811	-0.2675	-26.4157
CO_2	6.339	10.14	-3.415	-94.0158
CH_4	3.204	18.41	-4.48	-17.865
H_2	6.946	-0.196	-0.4757	0
$H_2O(g)$	7.136	2.640	0.0459	-57.7979
	$C_p = a + bT + cT^2$			

For reaction 7, the heat of formation data given in Table 6 shows a linear relationship with temperature :-

$$\Delta H_T^o (7) = 2.4\ T - 10,740 \quad \text{- - - - - -} \quad 4.11$$

Integration of the Vant Hoff equation substituting the respective functions 4.10 and 4.11 for ΔH_T^o and using data from Table 6 to determine constants of integration, gives the following relationships between the respective equilibrium constants and temperature :-

$$K_{p(5)} = -28.07905 - 22687.2078/T + 8.479114 \ln T - 0.0049892\ T + 0.469212 \times 10^{-6} T^2 \quad ---- \quad 4.12$$

and

$$K_{p(7)} = -13.43 + 5405/T + 1.208 \ln T \quad ----- \quad 4.13$$

Values of $K_{p(5)}$ and $K_{p(7)}$ generated from equations 4.12 and 4.13 are shown in Figure 15 plotted against temperature, together with values taken from Table 6. It can be seen that for both reactions the two sources of data are coincident, thus showing that the two functions 4.12 and 4.13 are satisfactory for obtaining equilibrium constants from temperature.

4.3.5. Carbon formation boundaries.

Permanent deposition of carbon on the catalyst during the course of reforming can arise in the following two ways :-

(i) By rapid thermal decomposition of the hydrocarbon leading to polymerisation and carbonaceous tar formation.

Figure 15

$LOG_{10} K_p$ AGAINST TEMPERATURE ^{o}K FOR :-

REACTION (5) $CH_4 + H_2O \rightleftharpoons CO + 3H_2$

REACTION (7) $CO + H_2O \rightleftharpoons CO_2 + H_2$

DATA AS GIVEN IN TABLE 6

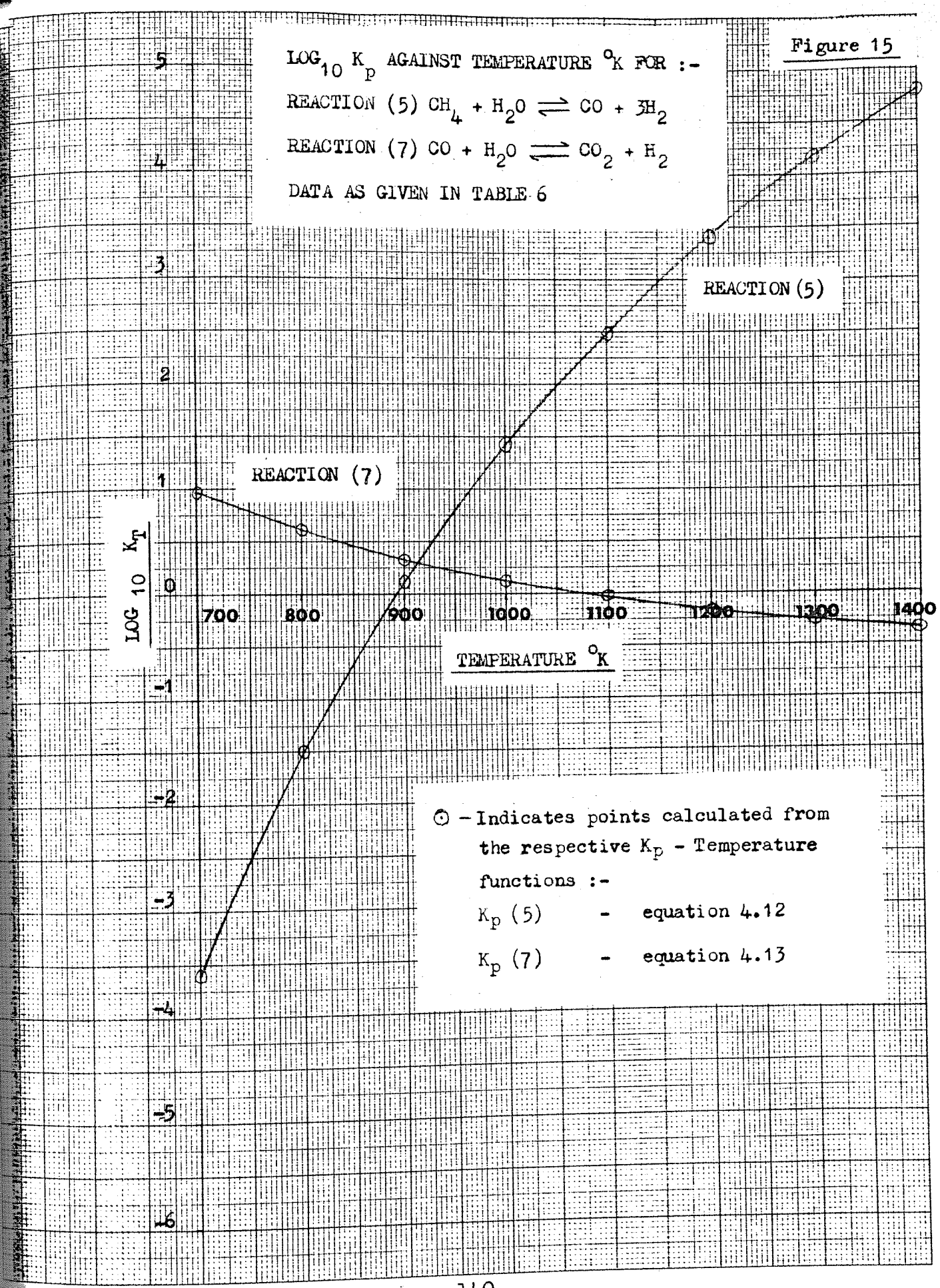

⊙ – Indicates points calculated from the respective K_p – Temperature functions :-

K_p (5) – equation 4.12

K_p (7) – equation 4.13

(ii) By the relative partial pressures of the components in the system, and their effect upon the carbon forming reactions.

Conditions for the first type of deposition will arise at the inlet region of the reactor whilst the initial reactions are taking place, and will be a function of the operating conditions and relative rates of the reforming and degradation reactions. The lack of information available concerning the initial reactions render theoretical predictions on this phenomenon virtually impossible; however, it has been established (24) that this type of deposition may be avoided by using either high steam-hydrocarbon feed ratios or low reforming temperatures.

With respect to the second type of deposition, it is shown in the literature survey that the Bouduard reaction :-

$$2CO \rightleftharpoons CO_2 + C \quad - - - - - - - - - - \quad 13$$

is the one of major importance in controlling the lower limit of deposition. Therefore, in order to establish conditions that are likely to give rise to this type of deposition, use is made of reaction (13) since the relative partial pressures of CO_2 and CO determine the existence or otherwise of carbon. Thus, if the value of $pCO_2/(pCO)^2$ exceeds the equilibrium constant $K_p(13)$, the reaction will move away from carbon formation and vice versa.

A further modification of Program 1 was an inclusion of a step to compare the value of $pCO_2/(pCO)^2$ with $K_{p(13)}$, and to indicate the point at which the two values are equal, thus predicting the conditions that give rise to an equilibrium carbon deposition.

As the program had been modified to calculate values of $K_{p(5)}$ and $K_{p(7)}$ from temperature data, it was desirable to have $K_{p(13)}$ also calculable from temperature. The function for $K_{p(13)}$ was established in an identical manner to those for $K_{p(5)}$ and $K_{p(7)}$.

Values of $K_{p(13)}$ calculated from the derived temperature function, represented by equation 4.14,

$$K_{p(13)} = -22.7164 + 21183.26/T + 0.05212 \ln T + 5.3096 \times 10^{-4} T \quad \text{- - - - - - - -} \quad 4.14$$

were found to be identical to published data (117), thus showing equation 4.14 to be satisfactory.

4.3.6. The final computer program.

In addition to the modifications made to Program 1 as described above, the calculation for obtaining the feed ratio R from the variable N was also included. With the exception of an identifier (n) for the hydrocarbon feedstock, data input was eliminated by writing in cycling routines which incrementally stepped through pre-set ranges of the

three operating variables. The ranges were selected as being representative for the reforming of hydrocarbons, and are as follows:-

(i) Pressure, P,— 10 to 25 atm in increments of 5 atm

(ii) Temperature, T,— 723 to 1173°K in increments of 25 deg K

(iii) Feed Ratio —From 5:1 to the point of carbon deposition in increments of 0.1.

Figure 16 shows the flow diagram for the final program (Program 2); it can be seen that N which is a function of the feed ratio is incrementally changed in the inner loop, temperature in the middle loop, and pressure in the outer loop. A copy of the program, written in Elliott Algol 60 is given in Appendix (D).

It has been shown by Dent (23) and also Hebden (86), that the equilibrium constant appertaining to the Bouduard reaction over catalyst differs from that over graphite (Figure 3), and therefore a second version of Program 2 was written to enable Dent's published values of $K_p(13)$ (catalyst) to be used in the calculations.

Because of the large number of calculations involved in the running of Program 2 only initial testing of the program was performed at Aston. The computation of the results was then carried out on the Atlas computer belonging to the Science Research Council, Didcot, Berks.

Flow Diagram for Program 2. Figure 16.

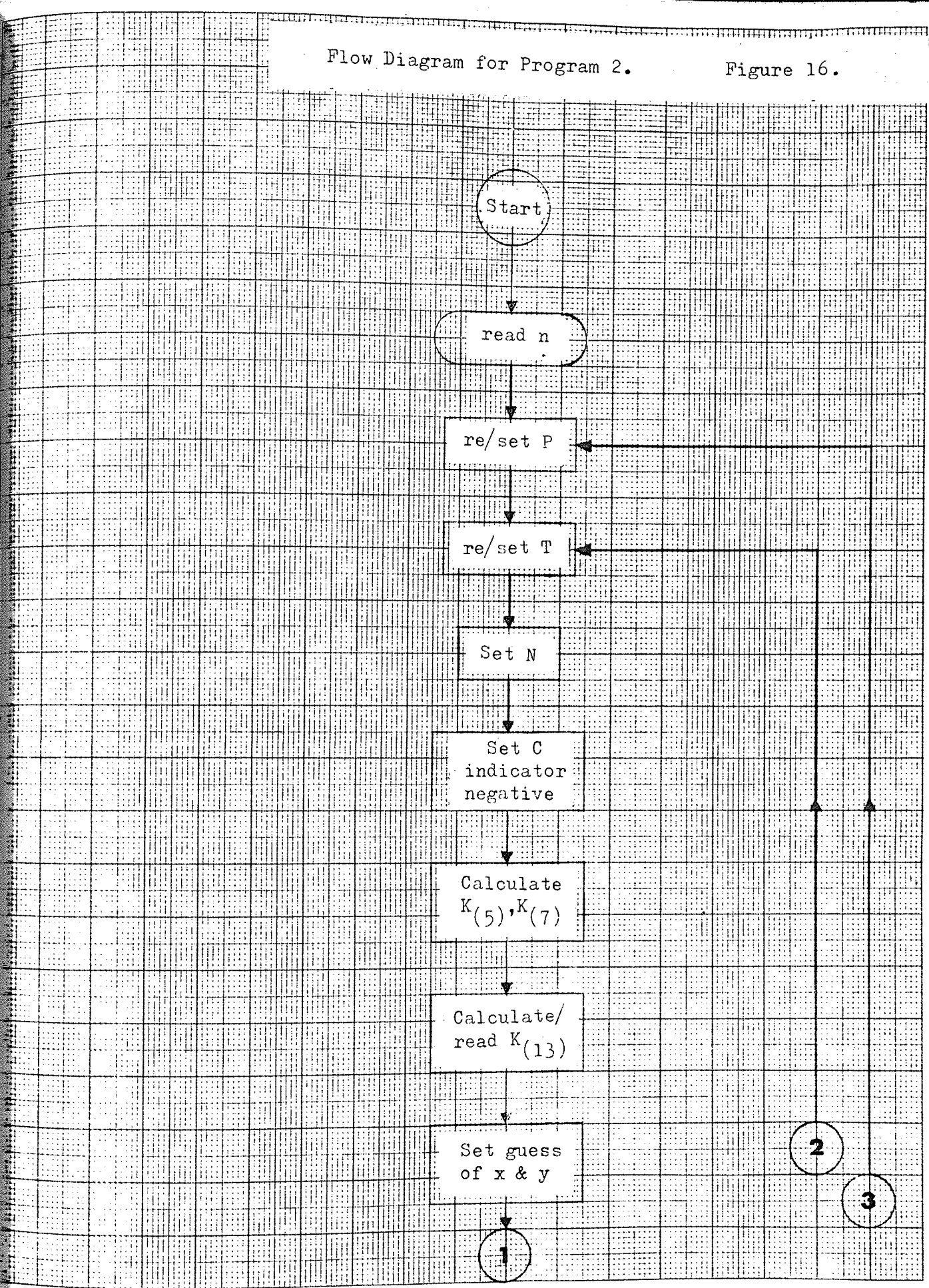

Figure 16. (Cont.)

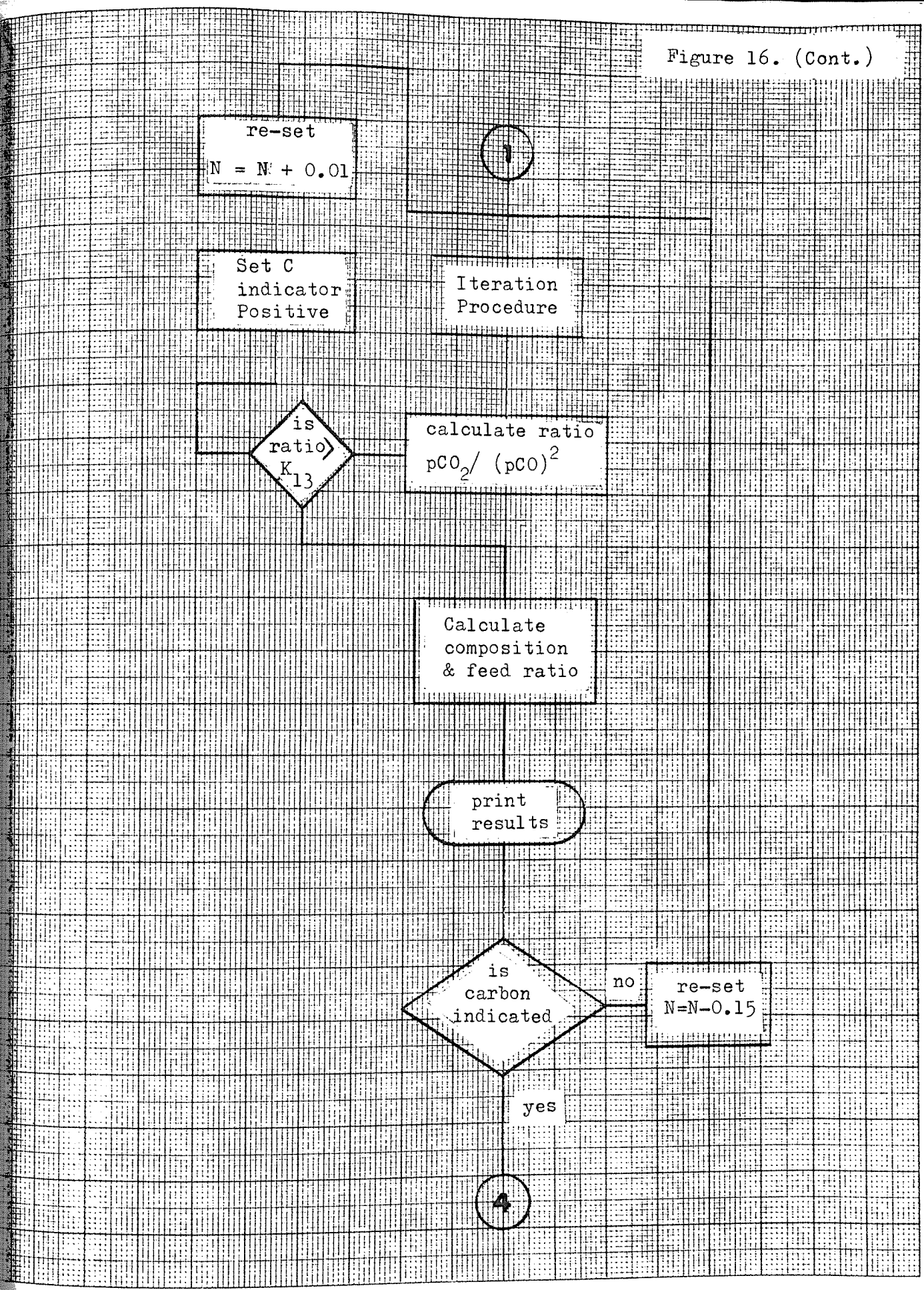

Figure 16. (Cont.)

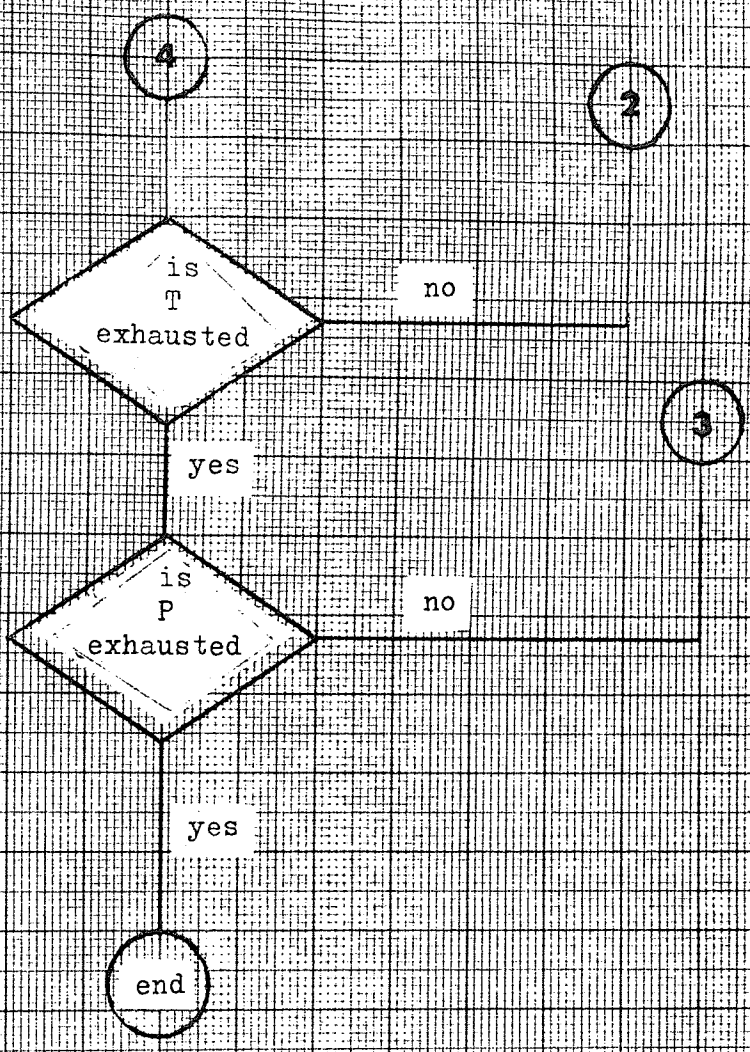

4.4. Computer Results and Discussion.

4.4.1. Effect of the variables on the reforming equilibria.

To illustrate the effect of the operating variables on the reforming equilibria, Figures 17,18, and 19 were prepared from results obtained by the execution of Program 2. All of the above figures are for conditions outside those that give rise to carbon deposition, and embrace the operating conditions that are used industrially for the various applications of the reforming process.

The effect of temperature upon equilibrium compositions for both methane and heptane reforming is shown in Figures 17A and 17B. Both diagrams confirm the conclusions derived from the Free Energy Survey, in that at low temperatures the presence of CH_4 is favoured. At higher reforming temperatures the methane 'slip' is considerably reduced and the concentration of the other constituents is increased, hydrogen becoming the major single constituent at temperatures above 600°C. Figures 17A and 17B also show that throughout the whole temperature range, the equilibrium CO_2 yield is greater for the higher hydrocarbon whilst the H_2 yield is somewhat lower. This is due to the initial H : C ratio of the feedstock which decreases with increasing

EQUILIBRIUM GAS COMPOSITIONS
STEAM – METHANE

Figure 17A

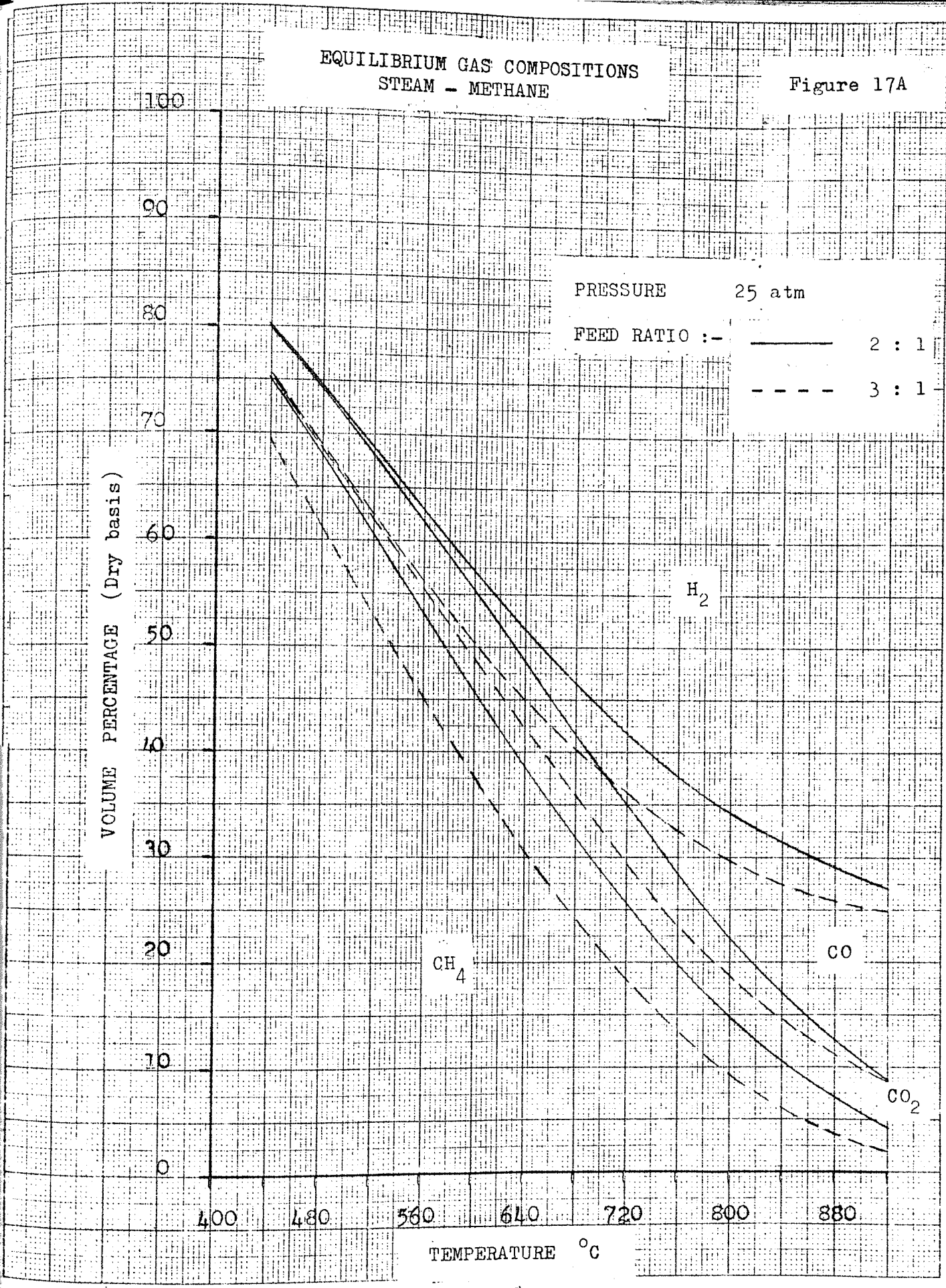

EQUILIBRIUM GAS COMPOSITIONS

STEAM - HEPTANE

Figure 17B

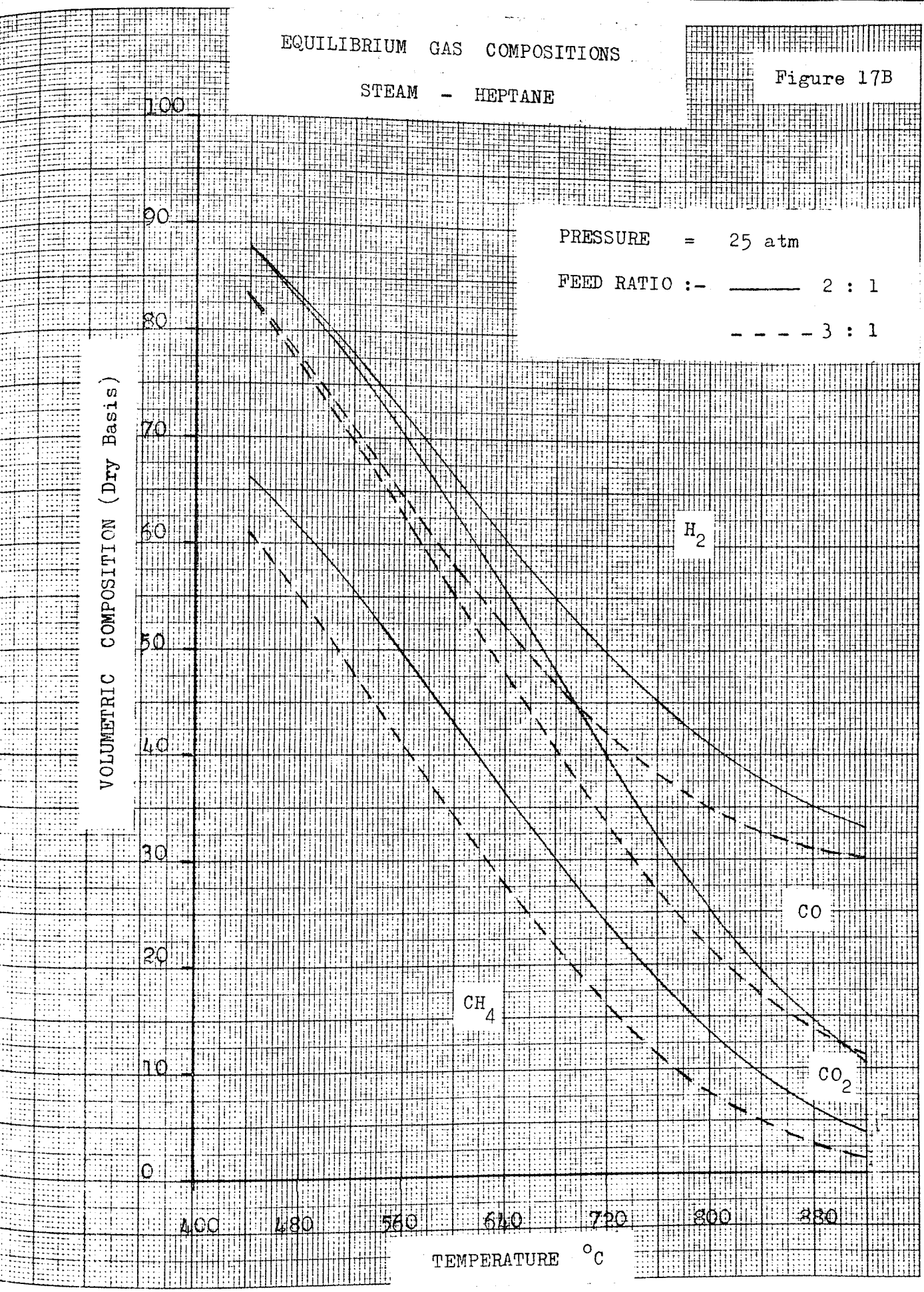

chain length. Therefore, for each carbon atom that reacts, the proportion of hydrogen that is liberated will be greatest for a methane feed and will decrease as the feedstock chain length increases. The greater proportion of hydrogen obtained with a methane feed will reduce the carbon dioxide yield by supressing the principal equilibrium reactions in the forward direction, and hence giving the greater proportion of CO_2 when reforming heptane.

Figures 18A and 18B show the effect of the steam-hydrocarbon feed ratio, and it can be seen that the resultant changes are less severe than those for temperature variation. The results are as anticipated in that the forward direction of reactions 5 and 7 will be encouraged by greater proportions of steam thereby increasing the yields of H_2 and CO_2 and reducing those of CH_4 and CO.

A comparison of Figures 17 and 18 for respective feedstocks shows that in obtaining a required hydrogen or methane content in the product gas, the temperature necessary at a given feed ratio may be reduced by increasing the latter variable. However, thermal considerations made by Dent (23) have shown that the amount of steam supplied for reforming should be as low as possible in order to achieve maximum

Figure 18A

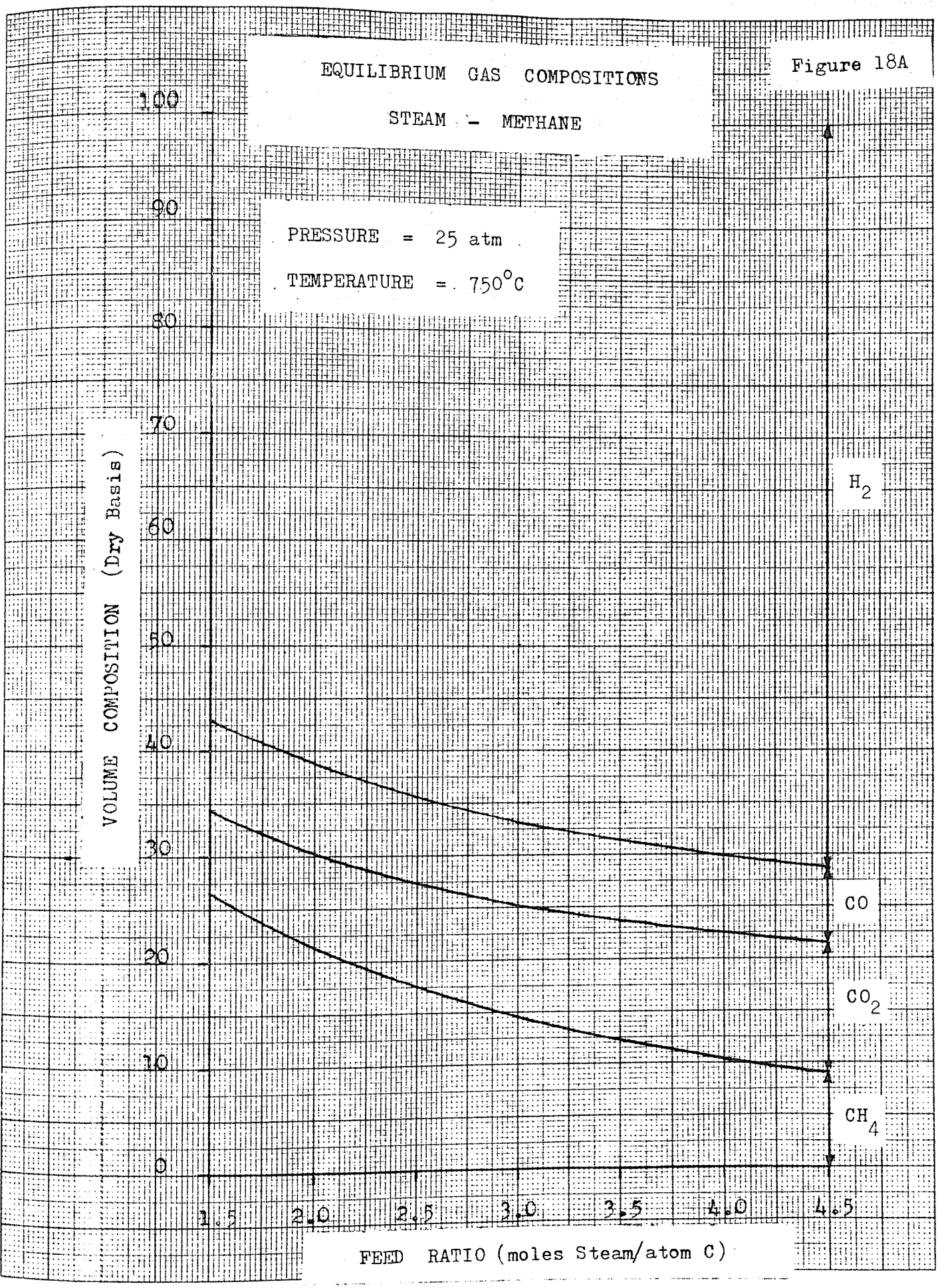
EQUILIBRIUM GAS COMPOSITIONS
STEAM - METHANE
PRESSURE = 25 atm
TEMPERATURE = 750°C
VOLUME COMPOSITION (Dry Basis)
100
90
80
70
60
50
40
30
20
10
0
1.5
2.0
2.5
3.0
3.5
4.0
4.5
FEED RATIO (moles Steam/atom C)
H2
CO
CO2
CH4

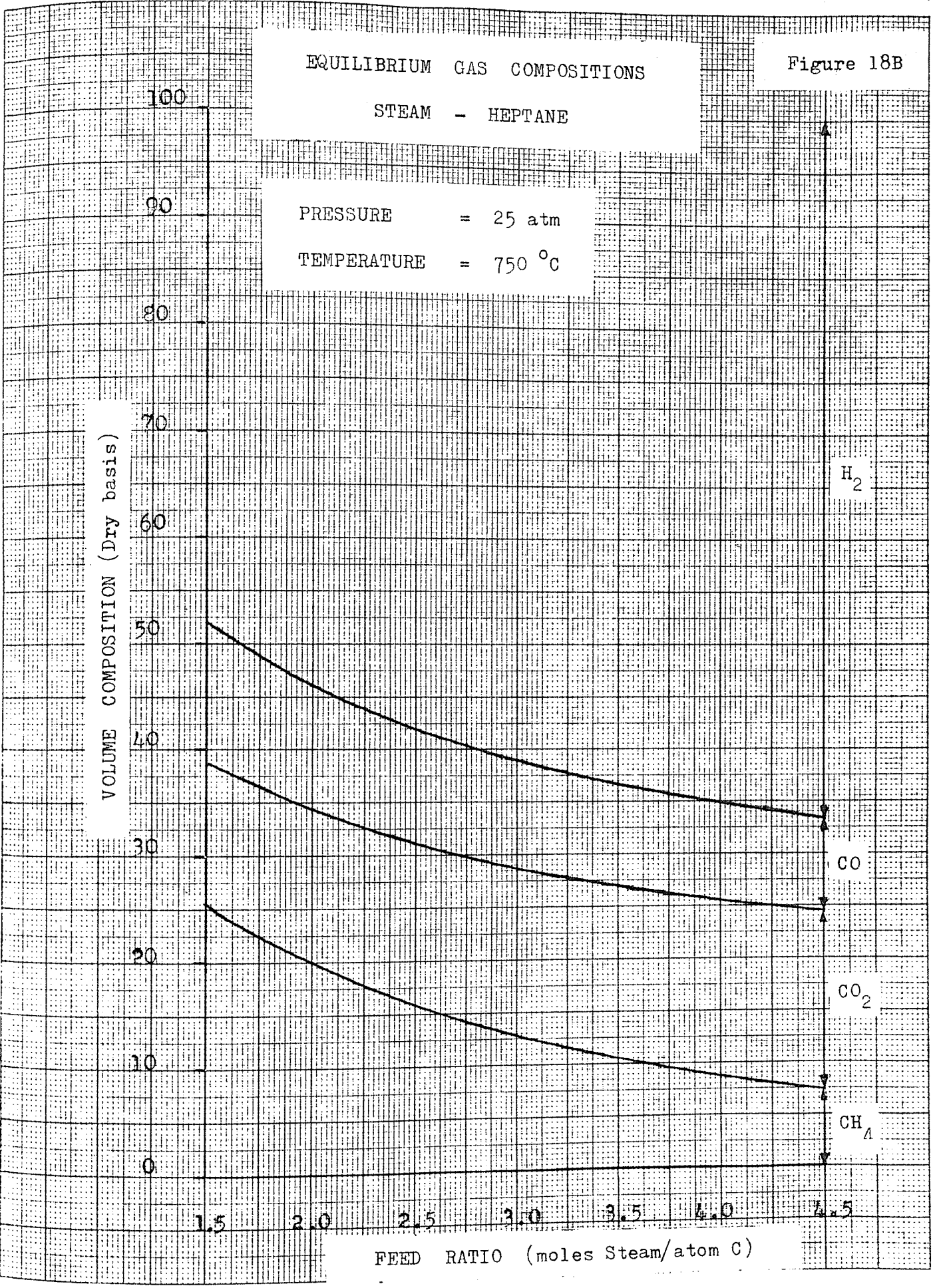
EQUILIBRIUM GAS COMPOSITIONS
STEAM - HEPTANE
PRESSURE = 25 atm
TEMPERATURE = 750 °C
VOLUME COMPOSITION (Dry basis)
100
90
80
70
60
50
40
30
20
10
0
H2
CO
CO2
CH4
1.5
2.0
2.5
3.0
3.5
4.0
4.5
FEED RATIO (moles Steam/atom C)

Figure 18B

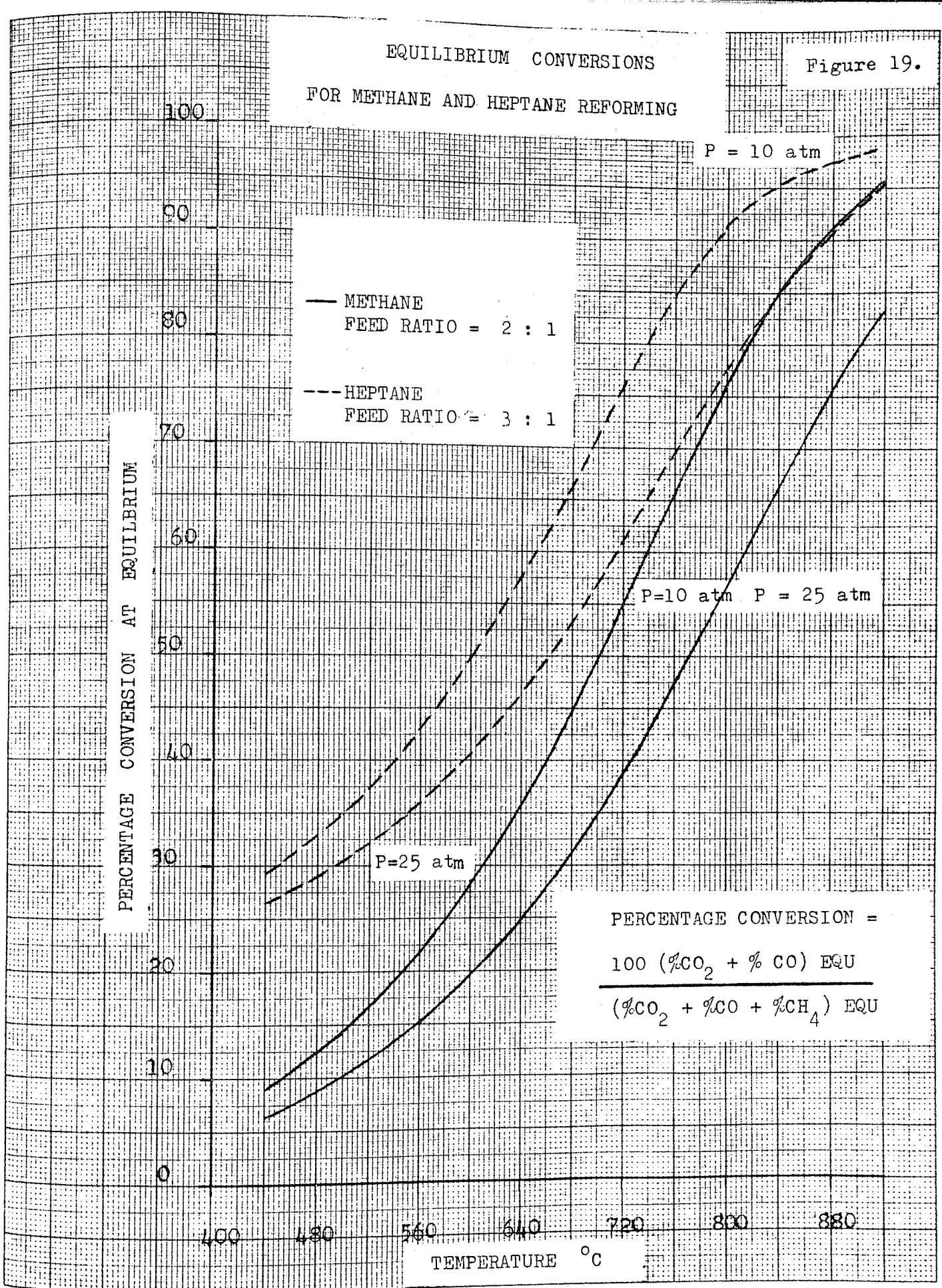
EQUILIBRIUM CONVERSIONS
FOR METHANE AND HEPTANE REFORMING
Figure 19.
P = 10 atm
METHANE
FEED RATIO = 2 : 1
HEPTANE
FEED RATIO = 3 : 1
P=10 atm
P = 25 atm
P=25 atm
PERCENTAGE CONVERSION AT EQUILIBRIUM
100
90
80
70
60
50
40
30
20
10
0
400
480
560
640
720
800
880
TEMPERATURE °C
PERCENTAGE CONVERSION =
100 (%CO2 + % CO) EQU
(%CO2 + %CO + %CH4) EQU

efficiency. While high temperatures and low feed ratios are therefore more favourable, the minimum operable feed ratio will be limited by carbon deposition considerations.

The two principal reactions involved in the equilibria give rise to an increase in moles, and therefore increased operating pressure will reduce the extent of reforming. This is illustrated in Figure 19 and it can be seen that in order to maintain conversions at elevated pressures it is necessary to increase the reforming temperature. It was indicated in the Literature Survey that the tendency in the design of reforming plant has been to increase operating pressures. This has necessitated corresponding increases in the temperatures of operation, and metallurgical limitations of steels available for tube construction have fixed the maximum temperatures and pressures.

4.4.2. Equilibrium summary chart.

In an attempt to present extensive equilibrium composition data in a compact and readily accessible form, Figures 20 and 21 were prepared for heptane and methane reforming respectively. It can be seen that they show equilibrium methane yields over large ranges of the operating variables, and it follows that these charts together with similar ones

EQUILIBRIUM CHART FOR STEAM–NAPHTHA REFORMING

FIGURE 20

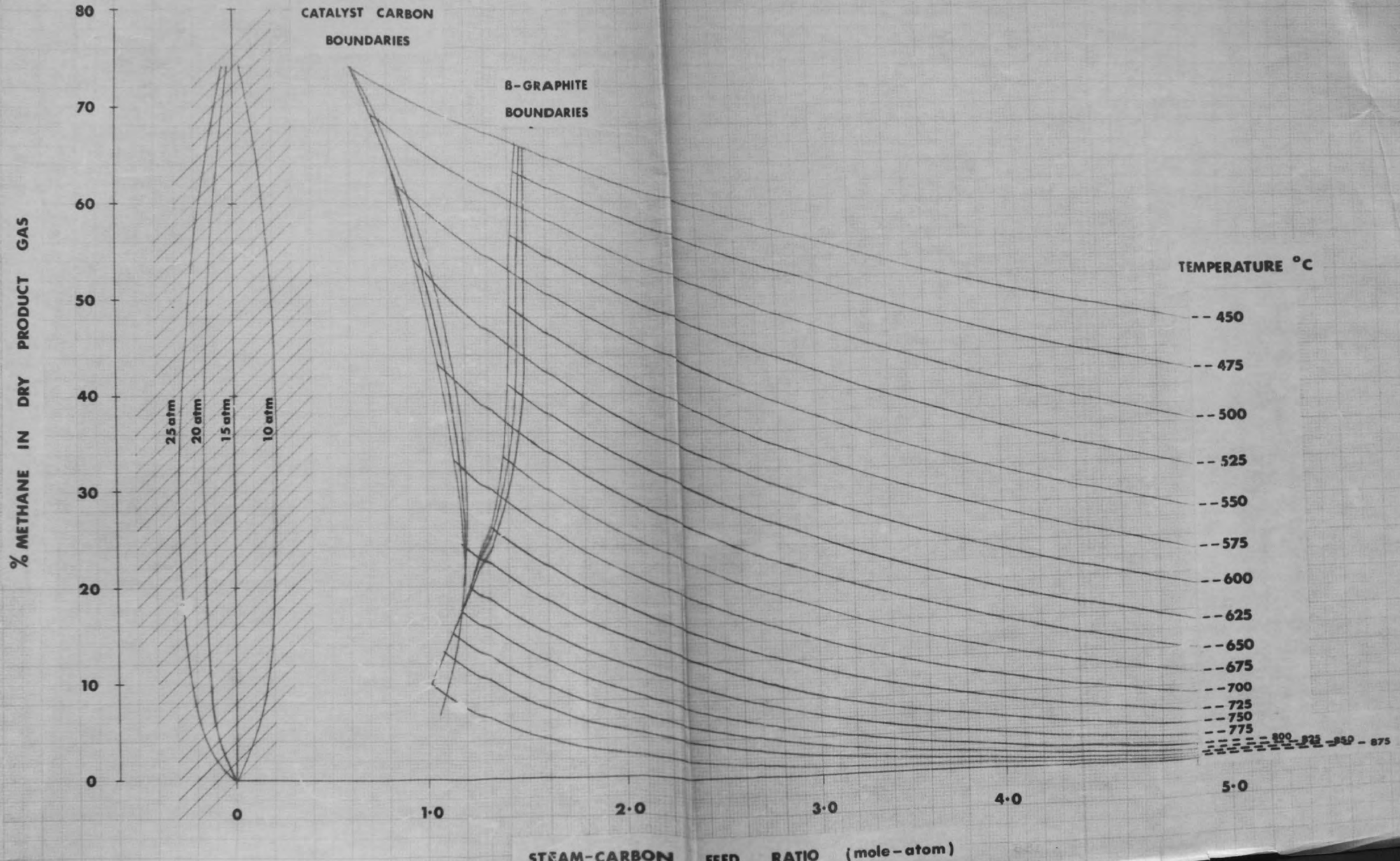

EQUILIBRIUM CHART FOR STEAM – METHANE REFORMING

FIGURE 21

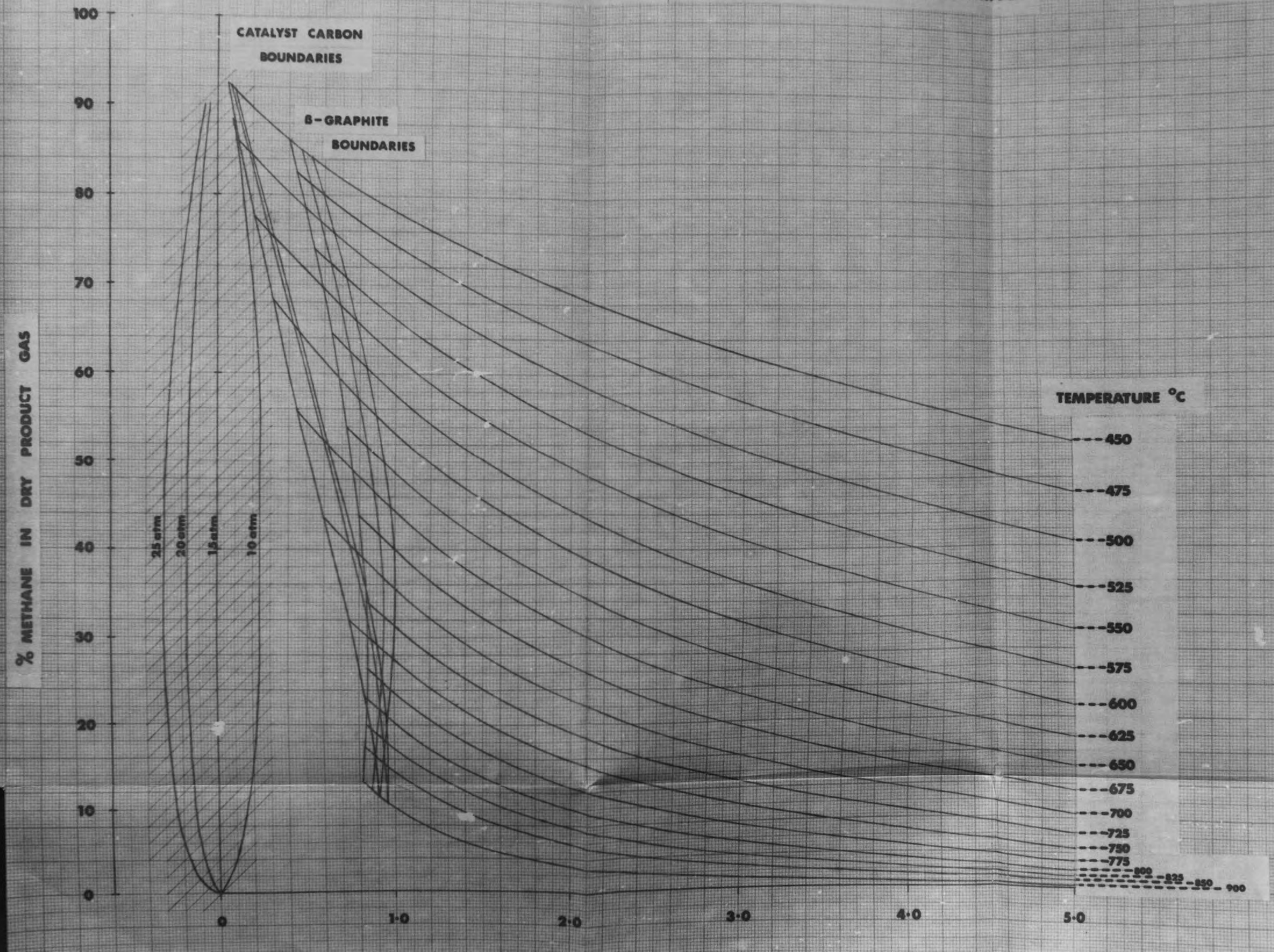

for two of the three remaining gases in the dry product are all that are needed to determine complete equilibrium compositions.

Assuming it is required to find the percentage methane in the dry product for given operating conditions, the charts are used in the following manner:-

(i) Locate the intersection of the appropriate temperature curve and a vertical line drawn from the known point on the Feed Ratio axis.

(ii) From the intersection project a horizontal line across to the point where the required pressure curve is cut.

(iii) For pressures less than 15 atm, move down a 45^{o} line from the point on the pressure line and read the percentage CH_4 on the vertical axis. For pressures greater than 15 atm the 45^{o} line is traversed in an upward direction. The vertical axis is calibrated directly for 15 atm.

To establish feed ratios for given values of temperature, pressure, and methane 'slip', the reverse procedure is used.

Carbon deposition boundary curves for both β-graphite and 'catalyst carbon' are also included in Figures 20 and 21. At low temperatures the difference between the two carbon boundary curves is considerable,

whereas at the higher temperatures the limiting values are approximately equal. This form of relationship is as indicated in Figure 3 which compares K_p — β-graphite with K_p — catalyst carbon over a similar range of temperature. In the discussion accompanying Figure 3 it was stated, that from an industrial standpoint the difference between the two limiting curves is not significant for feedstocks such as heptane since the limiting ratio is fixed by thermal decomposition considerations. However, for methane reforming at the lower temperatures in processes such as the 'Catalytic Rich Gas' the difference in the minimum feed ratios offers an opportunity for improvement to the thermal efficiency. By basing the operating feed ratios on catalyst carbon data rather than that for β-graphite a considerable saving in process steam consumption may be made.

4.4.3. Equilibrium operating chart.

For the prediction of methane percentages from known values of the operating variables, the accuracy of Figures 20 and 21 is to within $\pm$ 3.0%. However, for a specific process the accuracy can be improved by confining the variables to the ranges of interest. Figure 22, in which the arrangement has been modified from that in Figures 20 and 21, shows

OPERATING CHART FOR STEAM—NAPHTHA REFORMING

FIGURE 22

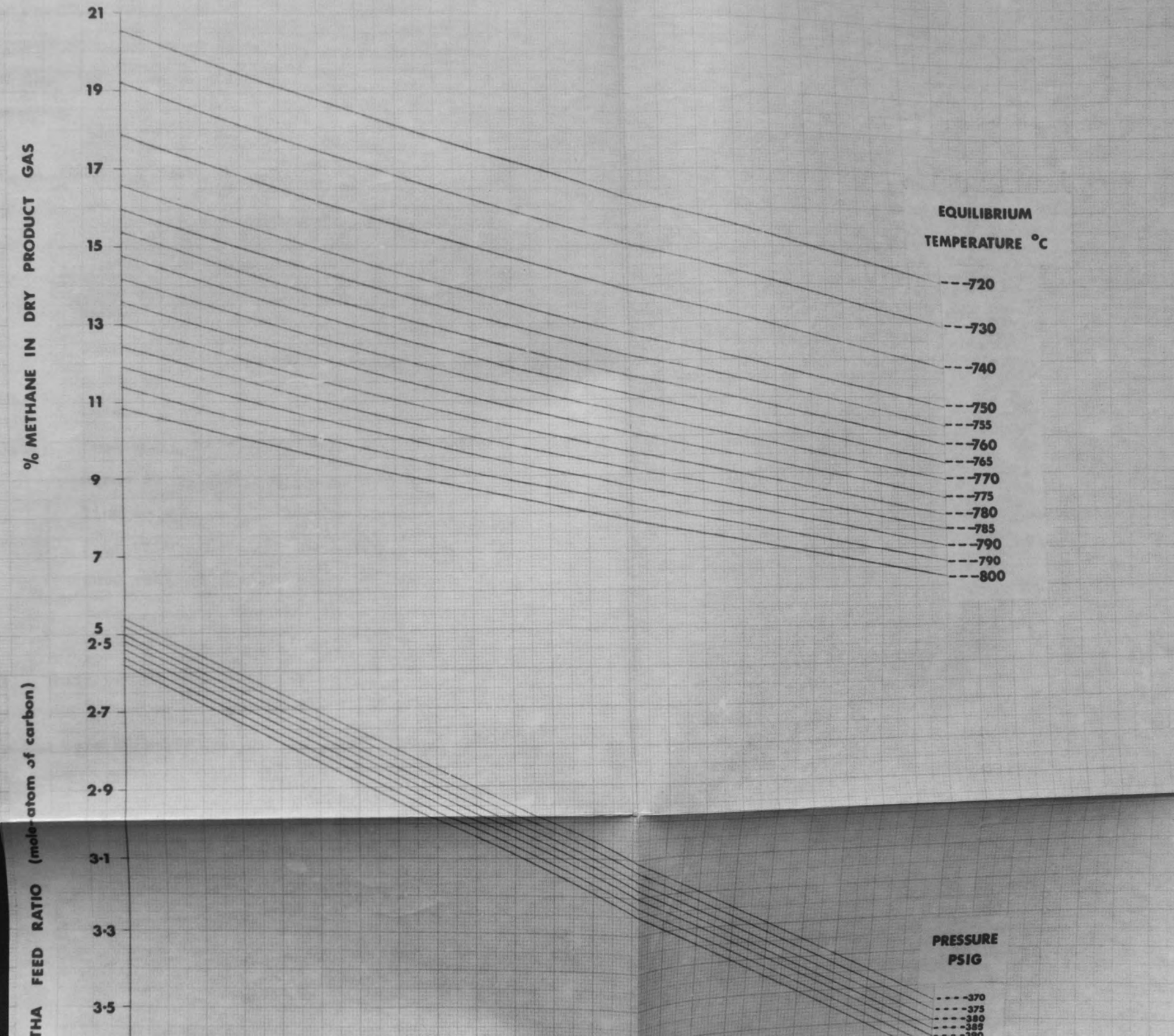

such a chart for an ICI Lean Gas Plant using a naphtha (heptane) feed, and it provides a means of easily back-checking feed ratios being used in a working process. The exercise was considered worthwhile since feed ratios derived from flow recorder readings can be inaccurate, and therefore a means of checking such readings is essential.

In using the chart to perform such a check, the percentage methane in the dry product is required and also the reformer operating temperature and pressure. The feed ratio is then found in the following manner:-

(i) Locate the intersection of the appropriate temperature curve with a horizontal line drawn from the known point on the methane axis.

(ii) From the intersection project vertically downwards to a point where the relevant pressure line is cut.

(iii) From this point project across and read the feed ratio from the lower part of the vertical axis.

To assess the practicability of Figure 22, daily run records from the W.M.G.B. I.C.I. naphtha reforming plant at Coleshill were analysed, and feed ratios were determined. Table 8, which gives the

results obtained for one of the two reformer streams, shows chart ratios, corresponding ratios derived from calculations normally carried out at the plant for checking purposes, and ratios derived from flow recorder readings. Similar data for the second stream was also obtained, but it was subsequently found (120) that the tube temperature recording instruments were faulty and thus rendered the results unuseable. Nevertheless, Table 8 does show that the feed ratios given by Figure 22 are in good agreement with the calculated values, and hence, it is considered that the chart provides a simple speedy method for checking indicated feed ratios.

TABLE 8

FEED RATIO CHECKS CARRIED OUT WITH DATA FROM THE W.M.G.B. ICI REFORMING PLANT COLESHILL.

Calculated Ratio (At Plant)	Recorded Ratio (At Plant)	Chart Ratio (Refer to Fig.22)
2.88	3.10	2.88
2.62	-	2.58
2.56	2.74	2.54
2.66	2.91	2.67
2.74	2.88	2.71
2.88	2.86	2.92

TABLE 8 (Cont.)

FEED RATIO CHECKS CARRIED OUT WITH DATA FROM THE W.M.G.B. ICI REFORMING PLANT COLESHILL.		
Calculated Ratio (At Plant)	Recorded Ratio (At Plant)	Chart Ratio (Refer to Fig.22)
2.79	2.86	2.80
2.81	2.82	2.85
2.48	2.87	2.52
2.61	3.00	2.76
2.34	2.80	2.40
2.53	2.70	2.48

4.5. Significance of Non-Ideal Gas Behaviour.

In the development of the above mathematical equations relating equilibrium composition to the process variables, it was assumed that the equilibrium constants, K_p, based on the partial pressure of the components were equal to respective thermodynamic equilibrium constants K_T. This assumption is only valid if all of the participating components behave as ideal gases throughout the ranges of the variables.

If non-ideal behaviour occurs, reliable equilibrium composition data can only be obtained by using K_p values derived from K_T and K_α, where K_α is the fugacity coefficient equilibrium constant. The relationship between K_p, K_T and K_α is shown in equation 4.15, and from this it follows that K_p is equal to K_T only when K_α equals unity.

$$K_T = K_p K_\alpha \quad \text{- - - - - - - - -} \quad 4.15$$

To assess the significance of non-ideal gas behaviour, K_α values for reactions 5 and 7 were calculated, and for the conditions giving the greatest deviation of K_α from unity, equilibrium compositions were computed with K_p values derived from equation 4.15. The results were then compared with others obtained for the same conditions but based on the assumption that $K_p = K_T$.

For reactions 5 and 7, K_α is related to fugacity coefficients by the following equations respectively.

$$K_\alpha(5) = \frac{\alpha CO \; \alpha H_2^3}{\alpha CH_4 \; \alpha H_2O} \quad \text{- - - -} \quad 4.16$$

and $$K_\alpha(7) = \frac{\alpha CO_2 \alpha H_2}{\alpha CO \; \alpha H_2O} \quad \text{- - - -} \quad 4.17$$

If non-ideal behaviour occurs, reliable equilibrium composition data can only be obtained by using K_p values derived from K_T and K_α, where K_α is the fugacity coefficient equilibrium constant. The relationship between K_p, K_T and K_α is shown in equation 4.15, and from this it follows that K_p is equal to K_T only when K_α equals unity.

$$K_T = K_p K_\alpha \quad \text{- - - - - - - - -} \quad 4.15$$

To assess the significance of non-ideal gas behaviour, K_α values for reactions 5 and 7 were calculated, and for the conditions giving the greatest deviation of K_α from unity, equilibrium compositions were computed with K_p values derived from equation 4.15. The results were then compared with others obtained for the same conditions but based on the assumption that $K_p = K_T$.

For reactions 5 and 7, K_α is related to fugacity coefficients by the following equations respectively.

$$K_\alpha(5) = \frac{\alpha CO \; \alpha H_2^3}{\alpha CH_4 \; \alpha H_2O} \quad \text{- - - -} \quad 4.16$$

and

$$K_\alpha(7) = \frac{\alpha CO_2 \; \alpha H_2}{\alpha CO \; \alpha H_2O} \quad \text{- - - -} \quad 4.17$$

Using reduced temperatures and pressures, fugacity coefficients for the participating gases were obtained from a generalised fugacity chart (119), K_α values were then calculated for reactions 5 and 7 using the above equations. Table 9 shows those values obtained having the greatest deviation from unity, and the conditions of temperature and pressure at which they occur. Also included are corresponding values of K_T and K_T/K_α .

TABLE 9

K_α , K_T, AND K_T/K_α VALUES FOR REACTIONS 5 and 7 WHEN K_α HAS THE GREATEST DEVIATIONS FROM UNITY.

T (°K)	P (atm)	K_T (Kcal/mole)	REACTION 5		REACTION 7	
			K_α	$K_T/K_\alpha = K_p$	K_α	$K_T/K_\alpha = K_p$
600	50	4.989×10^{-7}	1.17	4.264×10^{-7}	1.06	4.707×10^{-7}
700	50	2.661×10^{-4}	1.105	2.406×10^{-4}	1.041	2.557×10^{-4}
800	50	3.112×10^{-2}	1.045	2.979×10^{-2}	1.025	3.037×10^{-2}
900	50	1.307	1.017	1.285	1.020	1.281
1000	50	2.673×10^{1}	0.985	2.714×10^{1}	1.015	2.634×10^{1}

It can be seen from Table 9 that the pressure at which the greatest deviations occur is well outside the range considered in the equilibrium study. Therefore, if the differences in equilibrium composition at the conditions of temperature and pressure given in Table 9 are negligible, then for the ranges considered in the equilibrium study the assumption that the influence of fugacity may be neglected is valid.

Using Program 1, equilibrium compositions were calculated for the conditions given in Table 9; methane was selected as the feedstock, and 3.0 as the feed ratio. The computer results are shown in Table 10.

It can be seen from Table 10 that at pressures of 50 atm the influence of non-ideal behaviour is only slight. Therefore it may be assumed that within the ranges of the variables considered in the equilibrium study, the components behave as ideal gases.

TABLE 10

EQUILIBRIUM COMPOSITIONS FOR METHANE REFORMING.

- PRESSURE = 50 atm - FEED RATIO = 3.0 -

	ASSUMING $K_p = K_T$					ASSUMING $K_p = K_T/K\alpha$				
T °K	600	700	800	900	1000	600	700	800	900	1000
CO	-	0.02	0.12	0.88	3.43	-	0.02	0.12	0.88	3.44
CO_2	0.81	1.63	2.74	4.24	6.10	0.78	1.57	2.70	4.20	6.06
CH_4	23.79	22.68	20.72	17.03	10.70	23.82	22.65	20.77	17.07	10.75
H_2	3.23	6.48	11.29	21.28	34.69	3.13	6.39	11.16	21.14	34.57
H_2O	72.17	69.19	65.13	56.57	45.08	72.27	69.37	65.25	56.71	45.18

CHAPTER 5.

CATALYST REDUCTION.

5.1 INTRODUCTION.

The ICI 46-1 catalyst which was used for the experimental work is a nickel catalyst on a refractory support consisting essentially of alumina, silica, and magnesia. Potash is also incorporated into the support in order to make the material alkaline and thereby reduce the possibility of complete degradation of the feedstock to carbon. As supplied, the catalyst is in an oxidised state which is relatively inactive for reforming, and therefore the nickel oxide present must be reduced to nickel metal before the catalyst may be used. Also, fresh catalyst contains small traces of sulphur which must be removed before the material is used, otherwise poisoning of the active sites would occur and result in a loss of activity.(130)

These two operations may be carried out simultaneously by heating the catalyst in a reducing atmosphere of steam and hydrogen at a temperature slightly higher than that intended for reforming. Sulphur impurities are removed as hydrogen sulphide and analysis of the exit reducing media for this compound may be used to establish the completion of sulphur removal. The reduction of the nickel oxide

is represented by the following reaction:-

$$NiO + H_2 \rightleftharpoons Ni + H_2O \quad ----- \quad (19)$$

and the equilibrium constant for the reaction, $K_{p(19)}$, is related to the partial pressures of hydrogen and steam by the equation :-

$$K_{p(19)} = \frac{pH_2O}{pH_2}$$

It follows therefore that the value of pH_2O/pH_2 determines whether the mixture is of an oxidising or reducing nature. Figure 23 shows $K_{p(19)}$ plotted against temperature, and from this, maximum steam-hydrogen feed ratios for reduction may be established.

While steam is undesireable thermodynamically its presence prevents fast reduction and structural rearrangement.

5.2. Experimental.

Experiments designed to determine the reduction time required for the catalyst were based on the resulting activity of reduced material. Thus, reforming data obtained from batches of catalyst which had been reduced for varying periods were used to determine a satisfactory reduction period. However, the apparatus could not be operated continually round the clock, and so it was impossible to carry out a reforming sequence immediately after a reduction.

Figure 23

K_p vs Temperature for the Reduction of NiO

$$NiO + H_2 \rightleftharpoons Ni + H_2O$$

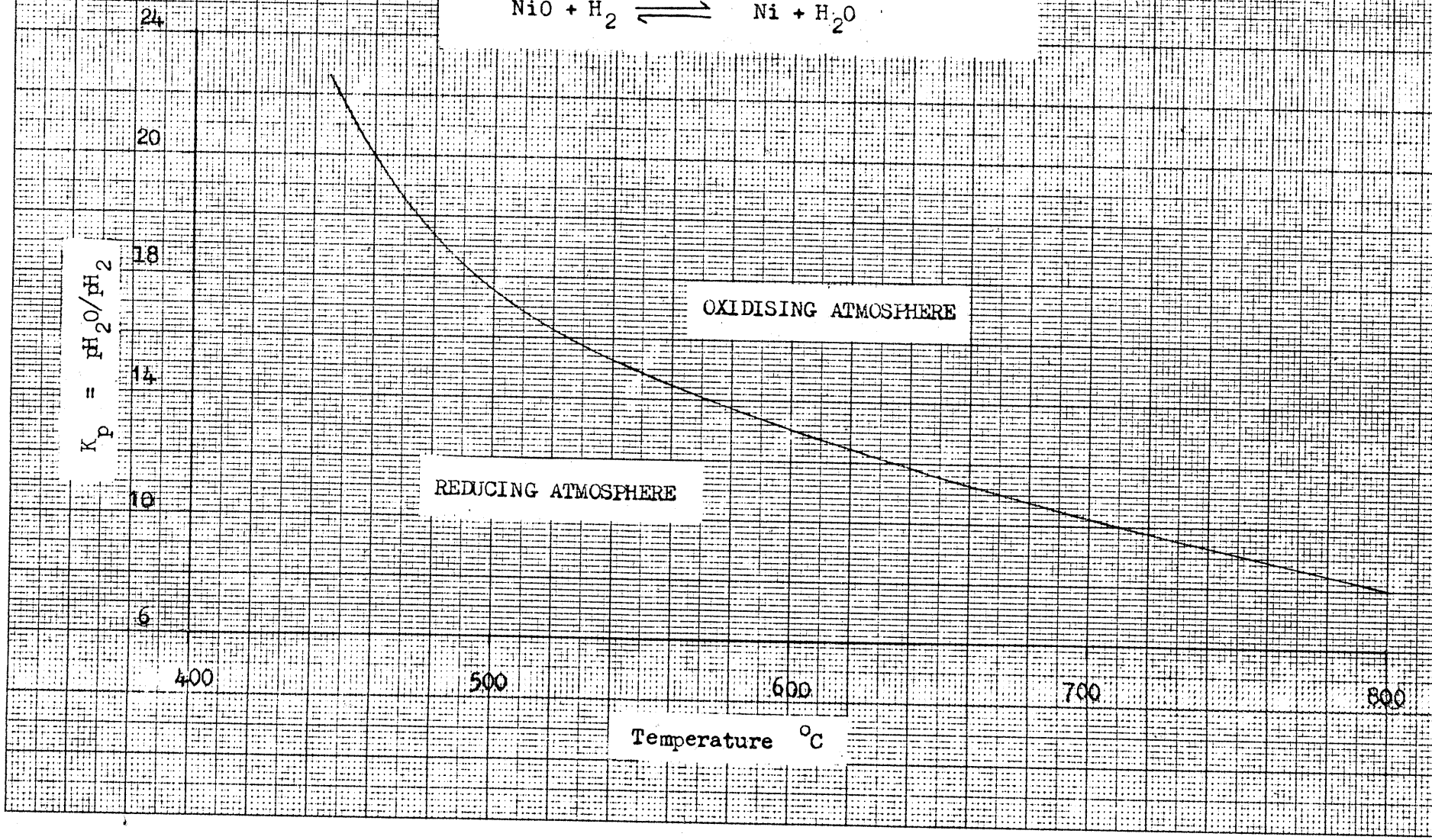

Hence, prior to establishing a satisfactory reduction procedure it was necessary to examine the effect on the catalyst of start-up and shut-down operations which were necessary between reduction and reforming.

5.2.1. Effect of start-up and shut-down procedures.

To assess the effect of the operating procedures, two series of experiments were run to reform methane over catalyst that had been reduced for an arbitrarily selected period of 24 hours. In both series of experiments reforming was carried for three consecutive days with the catalyst charges and operating conditions used at the start of each series maintained throughout. For the first series of experiments the start-up and shut-down media used between each day of operation was a mixture of steam and nitrogen, ie. an oxidising atmosphere. For the second series, a reducing media of hydrogen and steam was used. Within each series the levels of un-reformed methane (methane 'slip') obtained during each day were compared with each other.

5.2.2. Effect of reduction time.

Once a suitable method for carrying out start-up and shut-down procedures had been established, (see Sec.5.3.1.), the catalyst reduction period was

examined from the standpoint of obtaining a satisfactory period to bring about complete activation.

This was achieved by carrying out reforming runs under similar conditions on batches of catalyst that had been reduced for different periods and examining the resulting conversions. Although the diameters of the catalyst rods used in each experiment were constant, the lengths, and hence mass of catalyst, differed within the limits of manufacture. Therefore in order to relate each test, the ratio W/F, where W is the mass of catalyst and F the methane feed rate, was maintained constant.

5.3. Results and Discussion.

5.3.1. Start-up and shut-down procedures.

Figure 24 shows the percentage methane slip obtained in the reformed product gas from three consecutive periods of reforming when using a steam-nitrogen atmosphere for start-up and shut-down operations. The reforming was carried out at 250 psig and a temperature of 600°C with the steam-methane feed ratio fixed at 3:1 (mole:mole). The reforming period between each successive start-up and shut-down was $2\frac{1}{2}$ hours.

It is obvious from Figure 24 that the start-up

% Methane 'Slip' obtained during three consecutive Reforming Periods.

Figure 24.

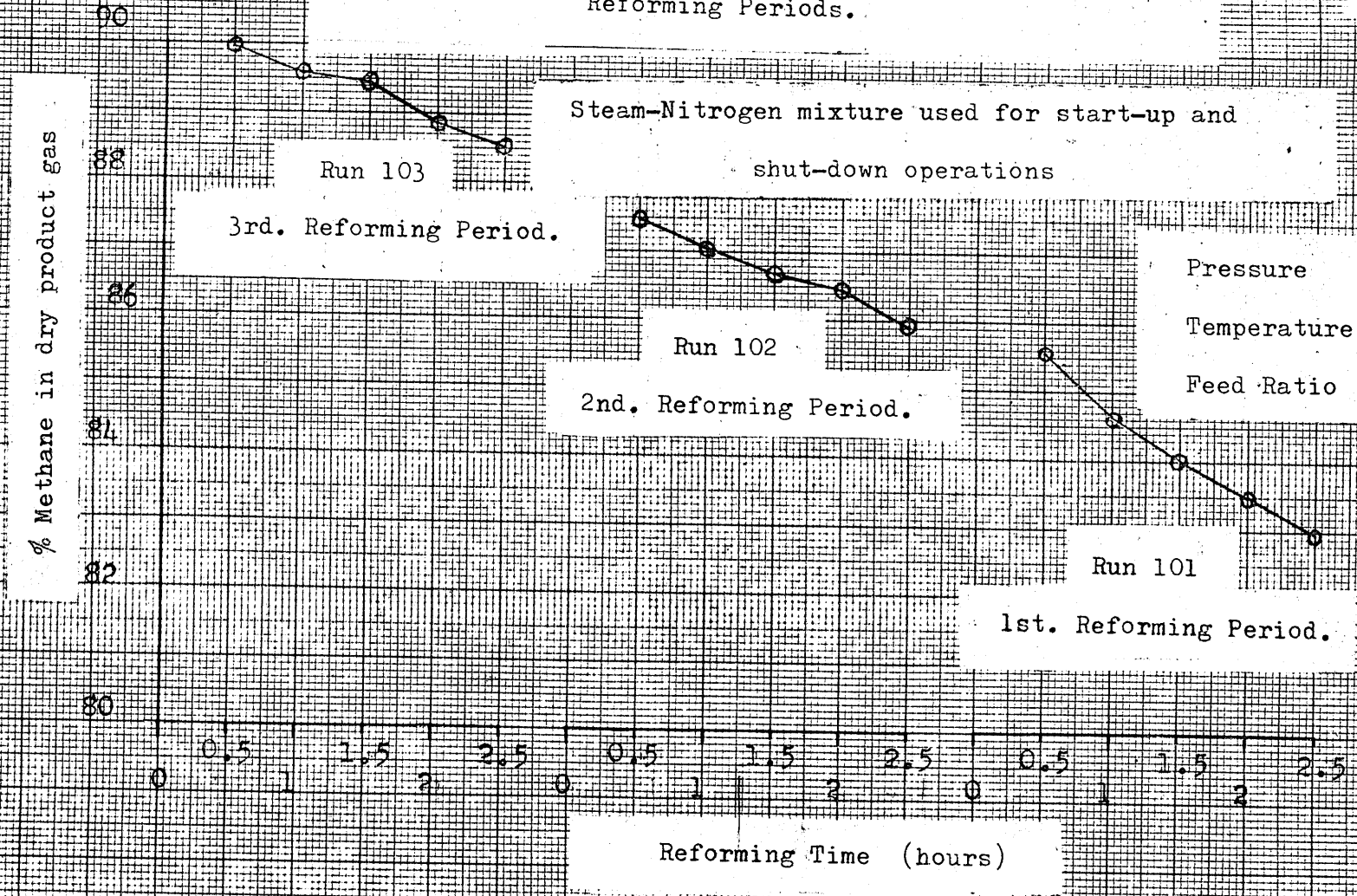

Steam-Nitrogen mixture used for start-up and shut-down operations

Pressure - 250 psig.

Temperature - 600°C

Feed Ratio - 3 : 1

and shut-down procedures as used in the experimentation are detrimental to the catalyst since the methane slip obtained at the start of each run progressively increases. This phenomenon can only be attributed to the operating procedures and not to a loss in activity brought about by the actual reforming process for the following reasons :-

(i) Each individual run indicates that a gradual increase in catalyst activity takes place during reforming, which would not be the case were the catalyst being deactivated by the reforming reactions.

(ii) Since the percentage methane slip obtained at the start of each run does not continue at the level at shut-down of the preceding run but in fact increases, it is evident that the start-up and shut-down procedures bring about a reduction in the catalyst activity.

It was stated in the introductory section that the catalyst must be activated by reduction before it can be used for reforming. The reduction process which is represented by reaction (19) is reversible, and it therefore follows that if a reduced catalyst is exposed to an oxidising atmosphere the reverse reaction will be favoured and the catalyst will be de-activated.

It can be seen from Figure 24 that the activity of the catalyst continually improves during the course of reforming. However, no indication of a steady activity level was obtained, which in the limit is what would be expected. Hence, it is concluded that the rate of recovery at the conditions chosen is such that a considerable amount of reforming time is required in order to obtain constant conversion levels. Therefore, in view of the limited time available per day for reforming experiments, it was deemed necessary to find an alternative start-up and shut-down media that would not de-activate the catalyst.

If as stated above, the catalyst is de-activated by exposure to an oxidising atmosphere, then a reducing media used for start-up and shut-down procedures would be expected to eliminate the problem. Hence, a steam-hydrogen reducing mixture was examined.

Figure 25 shows the results obtained from experiments carried out under identical conditions to those used for the steam-nitrogen mixture. It can be seen that the progressive loss in activity with each successive run found with the oxiding atmosphere is completely eliminated when using the reducing mixture. Further, within the limits of the temperature control and accuracy of the analytical equipment, the activity remains essentially constant throughout

Figure 25

% Methane 'slip' obtained during three consecutive reforming periods.

Steam-hydrogen mixture used for start-up and shut-down operations.

Pressure - 250 psig
Temperature - 600°C
Feed ratio - 3 : 1

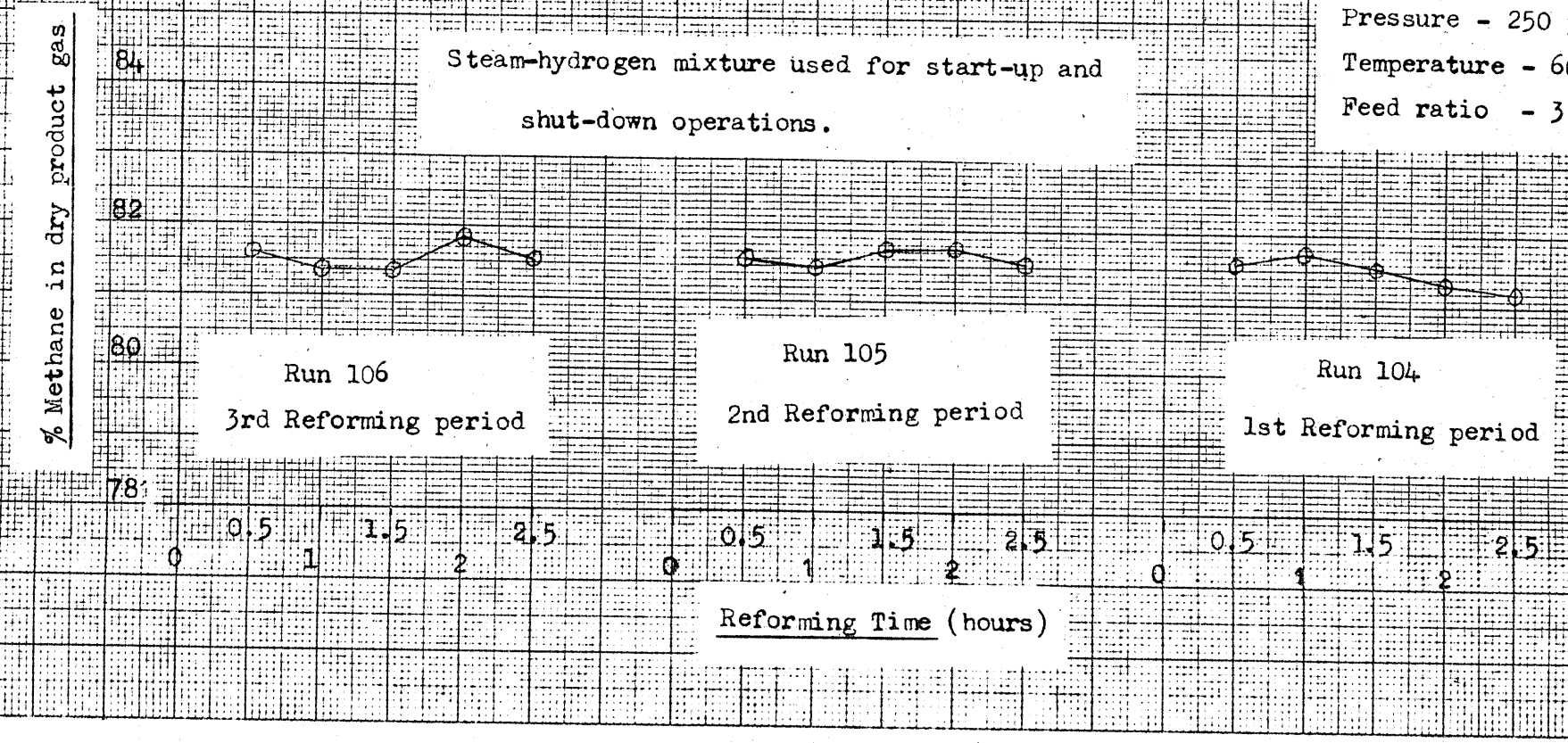

all three runs.

Hence, on the basis of the experimental results discussed above it was decided to use a reducing atmosphere for all start-up and shut-down procedures associated with subsequent reforming experiments.

5.3.2. Effect of reduction time.

The results from the tests carried out in the work discussed in the preceding section (runs 104, 105, 106, shown in Figure 25) indicated that a 24 hour catalyst reduction period allows a constant conversion level to be obtained when reforming. Furthermore, commercial plants which operate with the ICI 46-1 catalyst normally use a 24 hour reduction period for fresh material. In view of the above points and also the consideration of complete sulphur removal, the experiments carried out in this part of the work were designed to establish that a 24 hour reduction period is satisfactory rather than to find the minimum period necessary.

Figure 26 shows the percentage methane slip obtained when reforming methane over catalyst which has been reduced for (i) 8 hours, and (ii) 24 hours. The results were obtained at a pressure of 250 psig, a temperature of 600°C, and a steam-methane feed ratio

Figure 26

% Methane Slip obtained when Reforming with : -

A. Catalyst Reduced for 8 hours.

B. Catalyst Reduced for 24 hours.

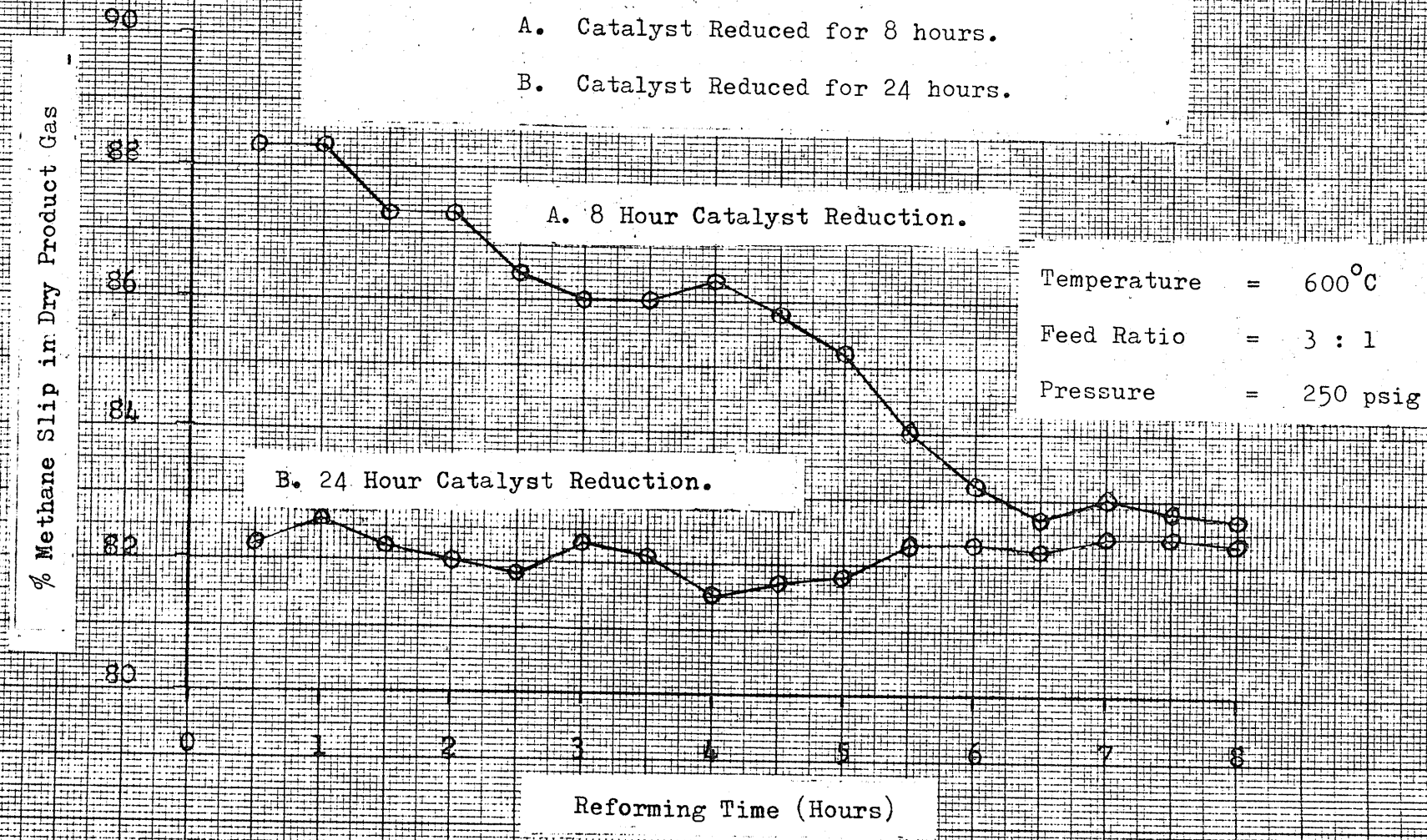

Temperature = 600°C

Feed Ratio = 3 : 1

Pressure = 250 psig

of 3:1; in order to compare the two runs the W/F ratio was maintained constant throughout. Reforming periods of 8 hours were used for the tests so that any trends in activity change would be indicated more so than if short run periods were used.

From Figure 26 it can be seen that when reforming with catalyst which has been reduced for an 8 hour period, the methane slip gradually decreases over the first $5\frac{1}{2}$ hours; however, after this period the slip level remains essentially constant. Alternatively, catalyst which has been reduced for 24 hours gives a conversion which is essentially constant throughout the whole period. Also, within the limits of experimental accuracy, the final steady conversion level obtained with the 8 hr reduced catalyst is the same as that obtained from the 24 hr reduced material.

5.4 Summary.

The above experimentation was carried out as a necessary exercise prior to obtaining reforming data for activity and kinetic studies rather than a specific study of catalyst activation. Therefore the conclusions must be considered on this basis, and it is not intended that they should be relevant to all reforming catalysts.

However, the results indicate that it is necessary to reduce catalyst for a 24 hour period, and

to use a steam-hydrogen reducing atmosphere for start-up and shut-down procedures.

Because the apparatus could not be operated for a continual 24 hour period and reduction for such a period would necessitate a minimum of three preparatory working days prior to each reforming run, catalyst was reduced in bulk and removed from the reforming apparatus for storage in an inert atmosphere until required.

The improvement in catalyst activity observed when using catalyst which was incompletely reduced (ie. 8 hour reduction period and that subjected to oxidising start-up and shut-down conditions), can only indicate that the products of reforming bring about further reduction.

In the literature survey it was postulated that hydrogen results from an initial hydrocarbon decomposition and also from reactions between steam and adsorbed surface species. Such a mechanism would give rise to a surface gas film rich in hydrogen and with a steam:hydrogen ratio much lower than that of the bulk gas phase (which in the above experimentation was of an oxidising nature due to the excess steam).

Hence, it is possible for the catalyst gas film to be of a reducing nature, thus accounting for the continual improvement in catalyst activity observed in the 8 hr reduced material.

CHAPTER 6.

CATALYST ACTIVITY AND KINETIC STUDIES.

6.1. Introduction.

Due to the complexity of a solid catalysed reaction, it is worthwhile to examine the general principles involved and then to develop such principles so that they may be applied to the interpretation of activity and kinetic data. Also such an examination can indicate the way in which experimental work should be directed, and highlight the relevant variables to be examined.

6.2. Mechanism of Catalysis.

6.2.1. Introduction.

In a homogeneous uncatalysed reaction, the arrangement of atoms in the reacting molecules corresponds to a minimum state of potential energy, otherwise the molecules would not be stable. Likewise, the atomic configuration of stable products must also correspond to a minimum state of potential energy. In order for the chemical reaction to take place there is a potential energy maximum corresponding to an atomic configuration through which the reactants must pass.

The potential energy maximum is achieved by

an endothermic activation, and the additional energy required to reach this state is the activation energy. This mechanism is shown schematically by diagram A, Figure 27, which represents an $A + B \longrightarrow C + D$ gaseous reaction. The potential energy maximum or transition state is represented by the activated complex AB^{*}, and the activation energy by E_A. The reaction shown in Figure 27 is exothermic since $E_2 < E_1$, therefore the heat of reaction $\Delta H = E_2 - E_1$, will be negative in sign.

In any system, the greater the activation energy, the greater will be the dependence of the equilibrium concentration of the reacting species upon temperature. Therefore it follows that at high temperatures the equilibrium concentration of the reactants will be low, and a fast reaction rate will result.

Fundamentally a catalyst may be defined as 'any substance that influences the rate of a chemical reaction but itself remains unchanged at the end'. With the exception of negative catalysts, influence on the reaction rate implies a rate increase, and this can only be achieved by reducing the activation energy for the reaction, which, as stated above, controls the rate of the reaction.

In order to reduce the endothermic activation or activation energy, a catalyst participates in the

reaction by adsorbing the activated complex on one or more active sites within the catalyst structure. However, the complex is not formed in the gas phase otherwise the activation energy would not be reduced, but results from interaction between reactants of which some or all are first adsorbed on the catalyst.

Considering the above example for an uncatalysed reaction, the energy diagram (127) for the catalysed system may be represented by diagram B, Figure 27. The additional stages involved in the catalysed reaction can be seen by comparing diagram A and B.

The position A^{*} B^{*} on Diagram B represents the activation step involved in the adsorption of the reactants on the catalyst (chemisorption), and position A (adsorbed) B (adsorbed) represents the point at which the adsorption is complete. The adsorbed reactants must then obtain sufficient energy (E_A^1) to form the adsorbed activated species AB^{*}, which by virtue of its unstable atomic configuration will decompose to yield the adsorbed products of reaction C(adsorbed), D(adsorbed). A third activation barrier exists in the desorption of the adsorbed products to form the final stable gas phase molecules.

Although in diagram B, Figure 27, the formation of the activated complex is shown as the energy barrier of greatest magnitude, any one of the three

Figure 27.

A. Arrhenius Plot for an uncatalysed gaseous reaction

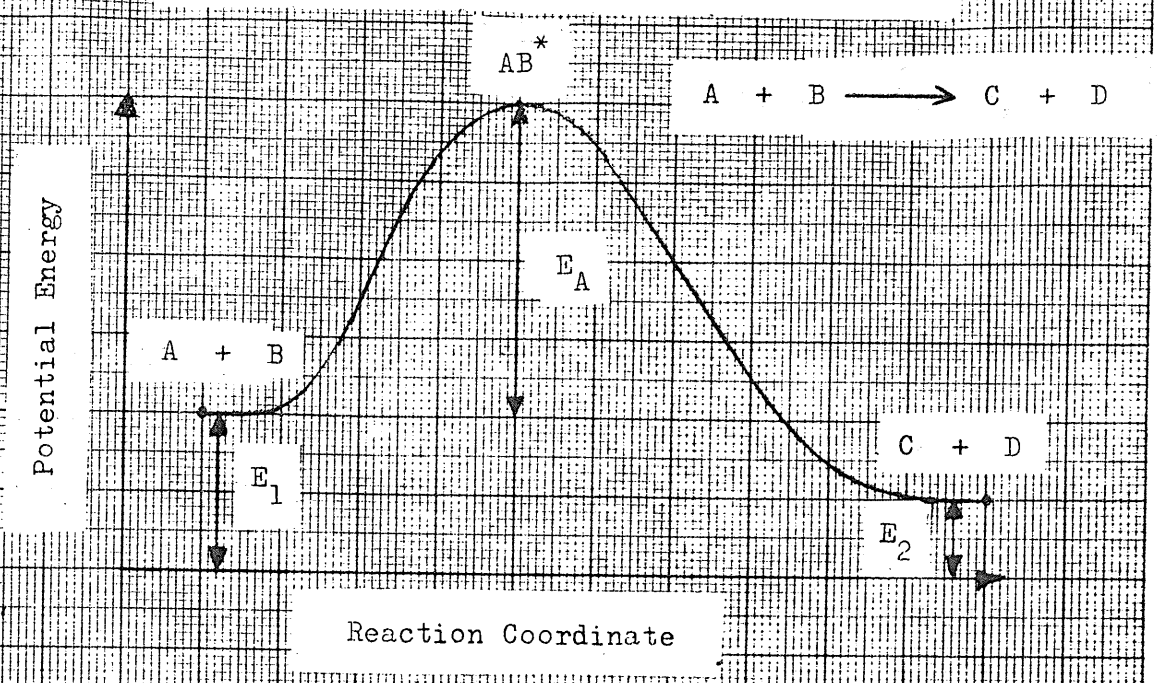

B. Arrhenius Plot for a catalysed gaseous reaction.

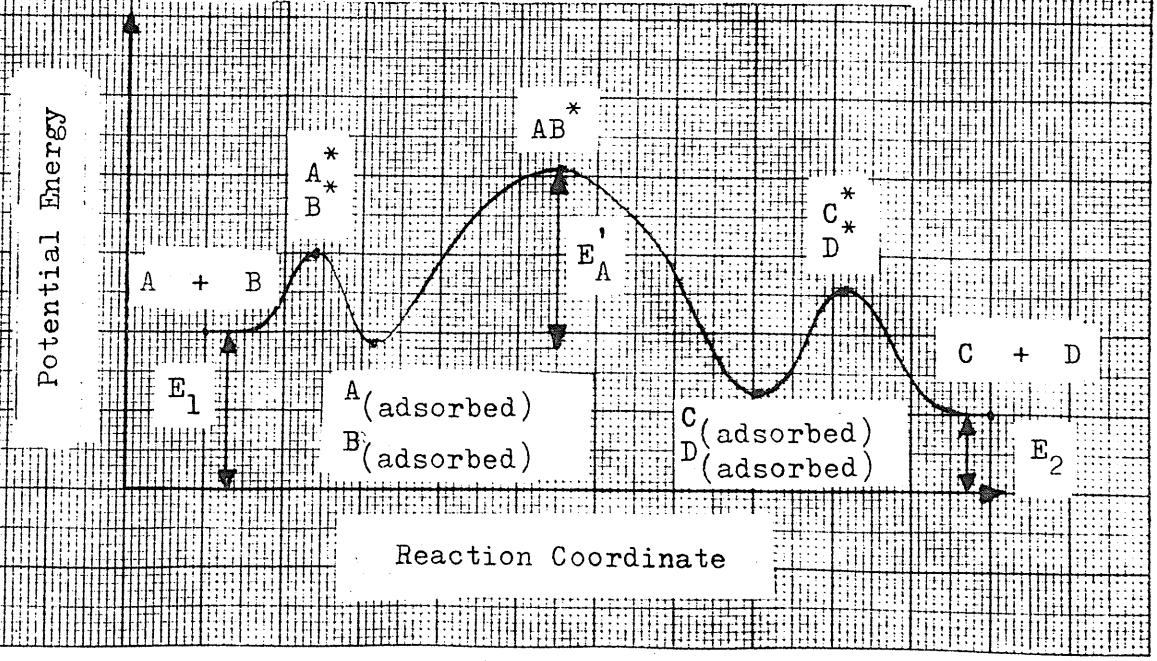

stages could require the greatest activation energy, depending on the specific reaction and catalyst. Nevertheless, whichever is the largest, its magnitude will always be less than the activation energy associated with the uncatalysed reaction. It follows, therefore, that in any particular reaction it will be the relative magnitudes of the activation steps in the individual stages of the reaction, ie reactant chemisorption, formation of the activated complex, and product desorption, that will determine which of the three stages controls the overall reaction rate.

Whilst the above discussion is valid, it is nevertheless confined to the 'chemical' stages of reaction, and in the examination of the kinetics of a catalysed system, the physical steps involved must also be considered. These are the transport of the reactant and product molecules to and from the catalyst surface, which are diffusional and hence physical steps. Since these are themselves rate processes, like the three stages involved in the chemical reaction they can influence and control the overall reaction rate, and hence the concentrations within the system.

Because of the different nature of the mechanisms involved with a catalysed reaction, in any examination it is convenient to classify the various stages sequentially as follows:-

(i) Mass transport of the reactants to the catalyst surface from the bulk gas phase.

(ii) The transfer of reactants through the pore structure of the catalyst to the active sites.

(iii) Activated adsorption of the reactants at the active sites on the catalyst.

(iv) Surface reaction of the adsorbed species.

(v) Activated desorption of the products.

(vi) The transfer of the products out of the catalyst pore structure.

(vii) Mass transfer of the products into the bulk gas stream.

All of the above steps will be governed by a rate equation, and at given conditions it is the slowest step that will control the overall rate at which the reaction proceeds.

6.2.2. Diffusional effects.

In any solid-gas flow system it is convenient to consider that there exists a film of fluid at the interface which exhibits laminar flow conditions, and it is through this film that the reactants and products must diffuse for the reaction to proceed. Further, since mass transfer takes place across the film, the

concentrations within the film will differ from those within the bulk gas stream.

The laminar film represents a resistance to mass transport, and this resistance decreases with decreasing film thickness. It follows therefore that when the bulk gas flow is highly turbulent and hence the laminar film thickness low, the resistance to the rate of molecular diffusion will be less than when low flows which give rise to thicker boundary films are employed.

In a system where the diffusion of one of the reactants is the rate controlling step, the following general rate equation may be written :-

$$r_A = k_G a \, (p_A - p_{Ai})$$

When the catalyst is highly active, p_A will be very much greater than p_{Ai}, therefore the rate expression may be simplified to:-

$$r_A = k_G a \, p_A$$

Therefore the rate expression approximates to a first order equation, and is proportional to the partial pressure of A in the bulk gas (p_A); the mass transfer coefficient (k_G) corresponds to the reaction velocity constant.

It is worthwhile noting the effect of temperature on the diffusion controlled reaction.

The mass transfer coefficient may be represented by (128) :-

$$kG = \frac{D_{AV}\ P}{RTB_G\ p_f} \qquad \text{- - - - - - - (6.1)}$$

From equation (6.1) it can be seen that the temperature dependence of k_G is controlled by the presence of D_{AV} in the numerator, and temperature T in the denominator. A relationship for D_{AV} proposed by Gilliland (129) shows $D_{AV} \propto T^{3/2}$, therefore it follows that k_G, and hence the reaction rate will be proportional to $T^{1/2}$.

In solid catalysed reactions the reaction rate per unit mass of catalyst is influenced by the surface area of the catalyst. For a non-porous solid the reaction is confined to the external surface, and therefore the rate will be a function of the external surface area, but when a catalyst with a high degree of porosity is employed, the external surface area becomes insignificant in comparison to the total area per unit mass.

If the diffusion of reactant and product molecules is such that the activities within the catalyst pore structure equal those in the bulk gas stream, the overall rate of reaction will be identical to that of an impervious system of comparable

surface area. However, in systems where concentration gradients exist within the pore structure because of resistance to the diffusional flow of reactants and products in and out of the catalyst, the reaction rate will differ throughout the whole mass. At the centre of the catalyst the rate will be at a minimum and at the surface a maximum, hence the overall rate in this case will be less than the system where the bulk and internal activities are equal. The ratio of these two rates, ie the actual reaction rate per unit mass of catalyst to the rate that would be obtained when internal and external concentrations or activities are the same, is called the Effectiveness Factor.

In general, the internal transport of molecules is by conventional diffusion or, when the catalyst pores are extremely small in diameter, by Knudsen diffusion in which individual molecules disperse in and out of the pore structure against resistance offered by the wall effect. Unlike film diffusion, the rate of internal diffusion will not be affected by changes in the bulk mass flow velocity. It follows that the effectiveness factor is a measure of the extent to which diffusion within the catalyst retards the overall rate, and will be a function of the size of the reactant and product molecules, the pore dimensions, the pore structure, and the diffusion coefficients of

the reactants and products.

When a catalyst is very active and molecules react within a short contact time, very few reactant molecules will be able to penetrate well into the pore structure. Conversely a less active catalyst will have penetration of the pore structure before reaction occurs.

When a system has an effectiveness factor of unity, the reaction rate within the catalyst will be the same as that at the external surface. Therefore for this condition to exist it follows from the above, that both of the following conditions must be satisfied:-

(i) All of the diffusion processes are rapid,

and (ii) The surface reaction has a relatively low rate coefficient and is the controlling step in the overall reaction.

6.2.3. Activated adsorption.

Activated adsorption (chemisorption) unlike physical adsorption is highly specific and is analogous to a chemical reaction in that interaction takes place between the adsorbate and active centres on the catalyst surface. Also the activation energies involved are much greater and therefore the rate of chemisorption will be more sensitive to temperature.

In a reaction where the rate is controlled by the activated adsorption of one or more of the reactants,

the activation energy for this step will be greater than those involved in the surface reaction and desorption processes. This situation can arise when a number of factors are satisfied, the two major ones being :-

(i) When a very active catalyst is employed, ie. the geometric structure and electronic configuration favours reaction of the adsorbed species.

(ii) When the size of reactant molecules and the geometric arrangement of active centres is not favourable for adsorption.

It was stated above that the chemisorption process is analogous to a chemical reaction, and this is reflected in the laws governing the process (128). The rate constants of an adsorption step will be exponential functions of temperature, and therefore in a system that is controlled by chemisorption, the overall reaction rate will be highly sensitive to temperature changes.

6.2.4. Surface reaction.

Surface reactions take place either between adsorbed reaction species and molecules in the gas phase, or between reactants adjacently adsorbed on the catalyst surface. Therefore, as with the

chemisorption process, the rate of a surface reaction will be determined by the geometric structure and electronic configuration of the catalyst surface which controls the concentration of the adsorbed species and the energies required for the formation of the activated complex.

When a catalyst contains few active sites, the surface concentration of reactants will be low, and hence this can make the surface reaction the controlling step. As stated in the previous section, the chemisorption step is highly selective, and therefore if the arrangement of active sites does not permit adsorption to take place in the stoichiometric proportions for the formation of the activated complex, then the surface reaction will be hindered.

Since the surface reaction is 'chemical' in nature, the rate will vary exponentially with temperature, and therefore when a system is controlled by the surface reaction the rate will be very sensitive to temperature change.

6.2.5. Activated desorption.

The activated desorption of product molecules may in general terms be considered the opposite process to activated adsorption. Therefore the same general factors such as geometric structure of the catalyst

and the specific activation energies involved, will govern the rate of the process. Similarly activated desorption will be very sensitive to temperature and the rate will vary exponentially.

For a desorption controlled reaction, the activation energy must be high relative to those involved with the other steps in the overall reaction. This condition will exist when the resultant of the chemisorption and surface reaction steps is exothermic, and also when the desorption is accompanied by molecular association.

6.3. Qualitative Studies.

It was explained in the previous section that the overall mechanism of a gas solid reaction can be conveniently classified into seven distinct stages. Also the independent rates that govern each stage depend on widely differing factors which are functions of the catalyst, flow characteristics of the system, operating conditions, and physical properties of the reactants and products.

A detailed study of each stage, or the factors which govern each stage, cannot be carried out over a relatively short period because of the magnitude and complexity of the work involved. Therefore it was

considered desirable to firstly examine the steam-methane system on a qualitative basis in order to establish likely rate controlling steps for the conditions attainable within the equipment, and then to follow this by a quantitative kinetic study in an attempt to determine a reaction mechanism and overall rate equation that governs the system within these conditions.

6.3.1. Experimental.

6.3.1.1. Effect of W/F ratio.

It was stated in Sec.6.2.2. that a diffusion controlled reaction is influenced by the flow characteristics of the system. Therefore experimentation based on investigation of the effect of the reactant mass flow velocity on the conversion can be used to establish the relative importance of film diffusion.

Consider an element of mass dW across a tubular reactor containing a total mass W of catalyst:-

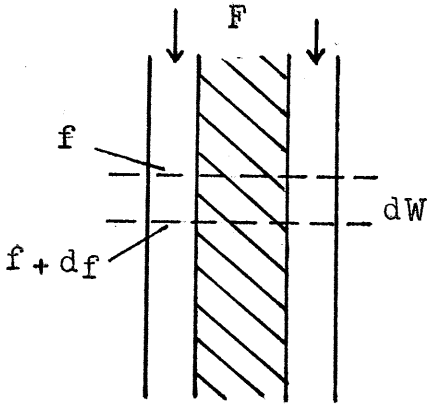

F = Reactant feed rate.

f = Fractional conversion.

r = reaction rate.

From a reactant mass balance over the element, in time dt :-

$$F\,(1-f)dt = F(1-(f+df))dt + r\,dW dt$$

$$Fdf = rdW$$

$$\text{hence } \frac{W}{F} = \int_0^f \frac{df}{r} \qquad \text{- - - - - - (6.2)}$$

Based on the relationship expressed by equation 6.2, two methods may be used to determine the importance of diffusion :-

(i) Carry out experiments in which the flowrate of a given stoichiometric feed of reactants is varied, but the ratio W/F is kept constant. The integral in equation 6.2 is a function of f only, and should remain constant for various values of F provided that W/F remains constant.

If diffusion through the gas film is controlling, the rate will be affected and the conversion f will not remain constant. If below a certain flow rate the conversion starts to decrease, it is at this point that the rate of mass transport through the gas film becomes significant, and will compare with the overall reaction rate.

(ii) In the second method, conversions are compared at given ratios of W/F for various

values of reactant F, ie. the amount of catalyst is adjusted as the flow is changed.

Where the f vs W/F curves coincide it may be concluded that the rate is unaffected by the relative values of F, and therefore the rate will not be governed by diffusion . However, where the curves diverge, the influence of diffusion will be significant.

In the experimentation the tests were designed so that the effect of two or more variables could be assessed from the results of one group of experiments. The first qualitative tests carried out were designed to use the first of the above methods for examining the importance of film diffusion in the system, and in addition, to show the effect of temperature on the reaction.

The details of the experimentation (Runs 201 - 204) are given in the following section dealing with the influence of temperature. However, from the test results fractional conversion data at incremental temperatures within the range 600 - 700°C for four different methane flow rates were obtained at constant pressure, steam-methane feed ratio, and W/F ratio. The relative values of these fixed variables was:-

Pressure - - - - - - - - - - - - - - - - 250 psig

Steam-methane feed ratio - - - - - - - 3 : 1

W/F ratio - - - - - - - - - - - - - - - 3.15 : 1

Subsequent examination of the results from the above tests showed them not to be entirely conclusive, even on a qualitative basis. Therefore it was deemed necessary to carry out a further series of tests (Runs 205 - 208) more specifically aimed at investigating the importance of film diffusion.

In this latter series of tests a temperature of 700°C was chosen in order to obtain higher conversions and thus reduce any analytical error. The other fixed variables were :-

Pressure - - - - - - - - - - - - - - - - 250 psig

Steam-methane feed ratio - - - - - - - - 3 : 1

Fractional conversions over a range of W/F values for five different amounts of catalyst were obtained, Table 11 summarises the runs made.

TABLE 11

Experimental conditions used for establishing the importance of film diffusion.			
Run	Time Factor W/F	Catalyst	
		No.of Pellets	Mass(g)
205	2.5:1,4:1,6:1,8:1,10:1.	1/2	2.5575
206	2:1, 4:1, 6:1,8:1,10:1.	1	5.5886
207	2:1, 4:1, 6:1,8:1,10:1.	2	11.5036
208	2:1, 4:1, 6:1,8:1,10:1.	3	16.6323
209	2:1, 4:1,5.5:1,7:1,9:1.	4	22.2432

6.3.1.2. Effect of temperature.

In the qualitative examination of a catalytic system, temperature is a suitable variable for indicating whether the reaction is diffusion controlled or governed by a 'chemical' step. However when diffusion is not controlling, temperature is not suitable for indicating which actual step or mechanism does control.

It was stated previously that when a reaction is controlled by film diffusion, the rate is proportional to $T^{\frac{1}{2}}$, therefore in this case an increase in rate brought

about by an increase in temperature will be represented by $(T_2/T_1)^{\frac{1}{2}}$. Where T_2 and T_1 are absolute values of the two temperatures under consideration.

The rate equation for a reaction which is controlled by one of the 'chemical' steps may in general be expressed by :-

$$\text{rate } r = \frac{\text{kinetic term x driving force}}{\text{adsorption term}}$$

The kinetic term corresponds to a velocity constant, the driving force will be a function of the component activities and may incorporate the reaction equilibrium constant, and the adsorption term will be a summation of the numerical products of respective component activities and adsorption equilibrium constants.

It follows, therefore, that the relationship between temperature and reaction rate is unlikely to be straightforward, and only when the rate equation may be simplified, will experiments using temperature as a variable be of positive use.

Akers (68) found that the rate equation for a steam-methane system at atmospheric pressure could be simplified to $r = kpCH_4$. The magnitude of the velocity constant k will be governed by an Arrhenius equation and therefore has a simple exponential relationship with temperature.

Acknowledging the discussion above, it was

still considered worthwhile to examine the effect of temperature on the reaction, if only to confirm or reject the absence of diffusion control.

The experiments carried out were designed with a dual purpose :-

(i) To indicate the influence of temperature

and (ii) To indicate the dependence of conversion upon mass flow velocity.

This involved a series of experimental runs at constant pressure and feed ratio in which the flow conditions for each run were varied but the W/F ratio was maintained constant by employing different amounts of catalyst. Within each run, temperature was varied between the limits 600°C - 700°C, thus allowing fractional conversion vs. temperature data to be collected.

6.3.1.3. Effect of pressure.

Pressure is considered by Yang and Hougen (122) to be an important variable in indicating the rate controlling step in the mechanism of a gaseous reaction catalysed by a solid. To illustrate this point they have presented nine types of curve which show for mono- and bi-molecular reactions, the variations of initial reaction rate with total pressure which are obtained when different steps in the possible mechanisms control the reaction rate.

To obtain an indication as to which mechanism steps are likely to control the rate of the steam-methane reforming reaction, experiments were carried out in order to make use of the curves published by Yang and Hougen.

With experimental results at 250 psig already available from runs described previously, it was considered expedient to carry out further runs at 100 psig and 50 psig and analyse the data along with that available at the higher pressure.

The two experimental runs at the lower pressure, Run 210 at 100 psig and Run 211 at 25 psig, were carried out on successive days immediately following Run 207, so as to use the same catalyst. All other variables were maintained the same as those used for Run 207 and are given in Sec. 6.3.1.1.

6.3.2. Results and discussion.

6.3.2.1. Effect of W/F ratio.

The results obtained from Runs 201-204 are given in Appendix E. From these results, fractional conversions were calculated for temperatures of 600°C and 700°C, and used to examine the influence of diffusion.

Figure 28 shows fractional conversion, f, defined as :-

Fractional Conversion vs. Methane Flowrate.

P = 250 psig R = 3:1 W/F = 3.15

Figure 28

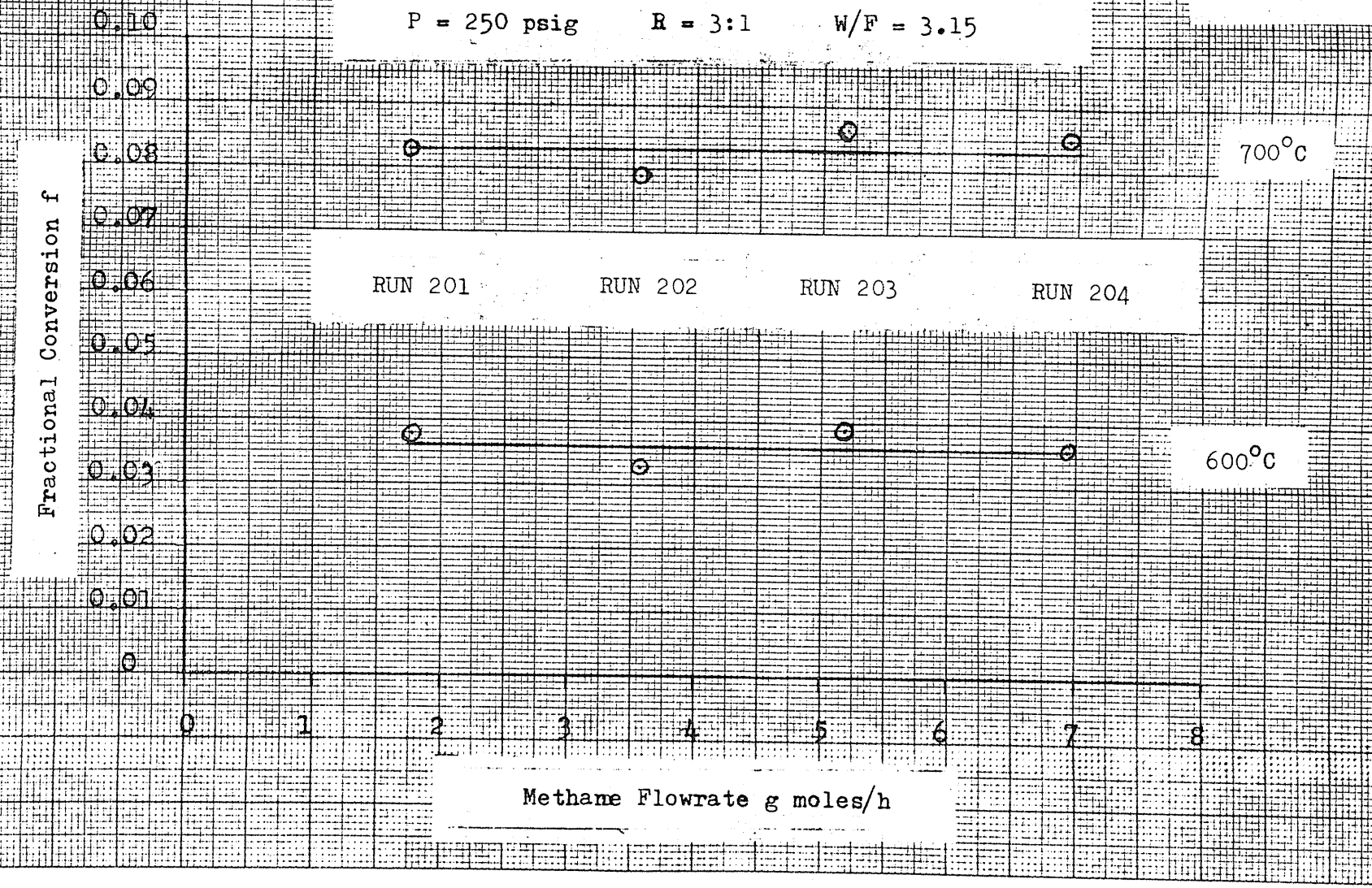

$$f = \left(1 - \frac{pCH_4}{pCH_4 + pCO_2 + pCO}\right)$$

plotted against the respective flow rates used at 600°C and 700°C.

It can be seen from Figure 28 that a straight line relationship at both temperatures is an acceptable representation thus suggesting that diffusion effects are negligible at the temperatures and levels of flow used.

Because of the small number of points on Figure 28 it was considered unwise to draw any definite conclusions, and hence the second series of experiments was carried out in order to confirm or otherwise the relationship indicated.

The results obtained from the second series of experiments are given in Appendix E and included are the fractional conversions calculated from the product composition data.

Figure 29 presents for each experimental run, the fractional conversions obtained plotted against respective W/F ratios. In order to compare this data with that obtained from the first series of results, fractional conversions at a W/F ratio of 3.15 : 1 were taken from the curves, and then Figure 30 constructed from both sets of data.

Fractional Conversion vs W/F Ratio Figure 29.

Runs 205 - 209

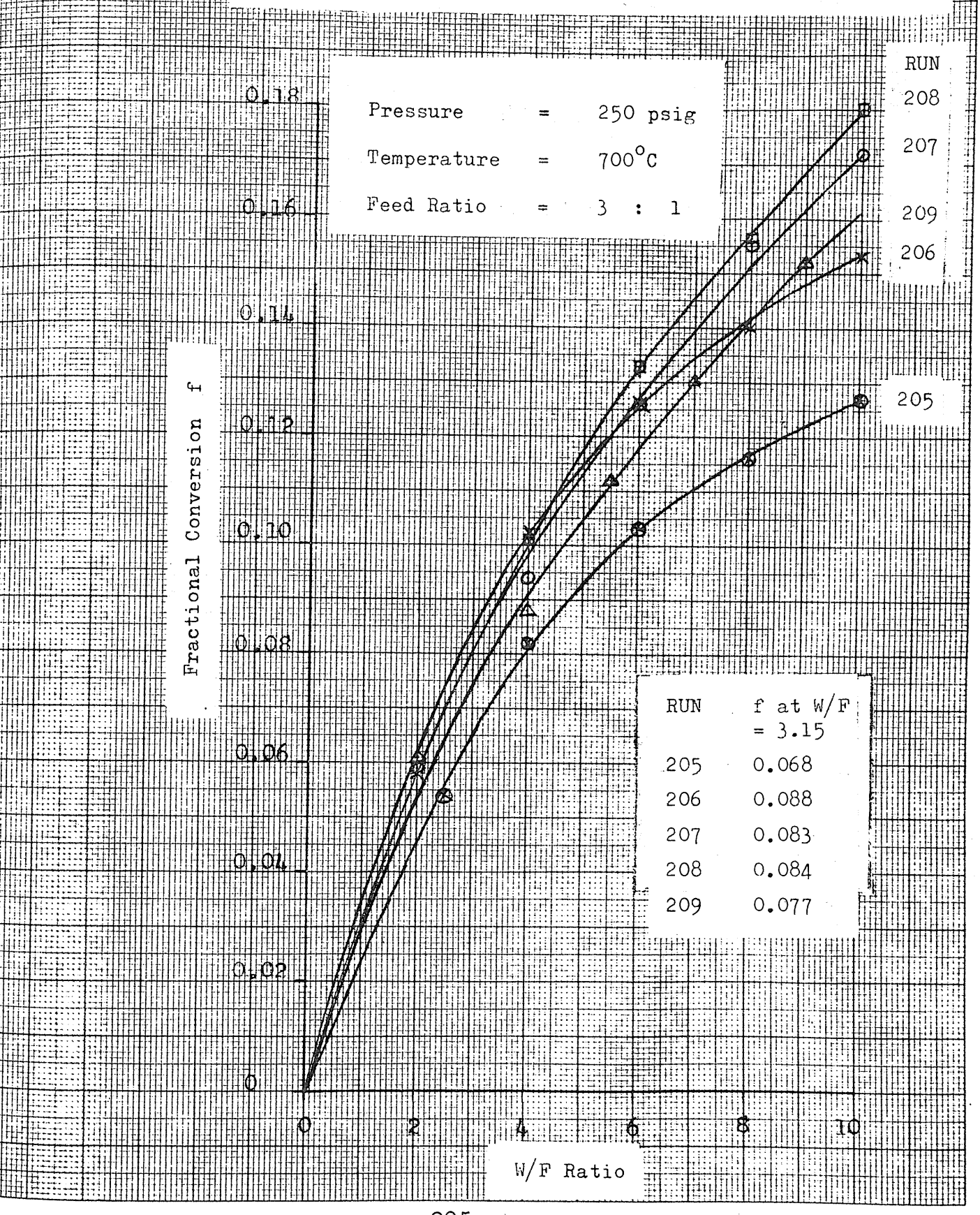

Fractional Conversion vs Methane Flowrate

Figure 30.

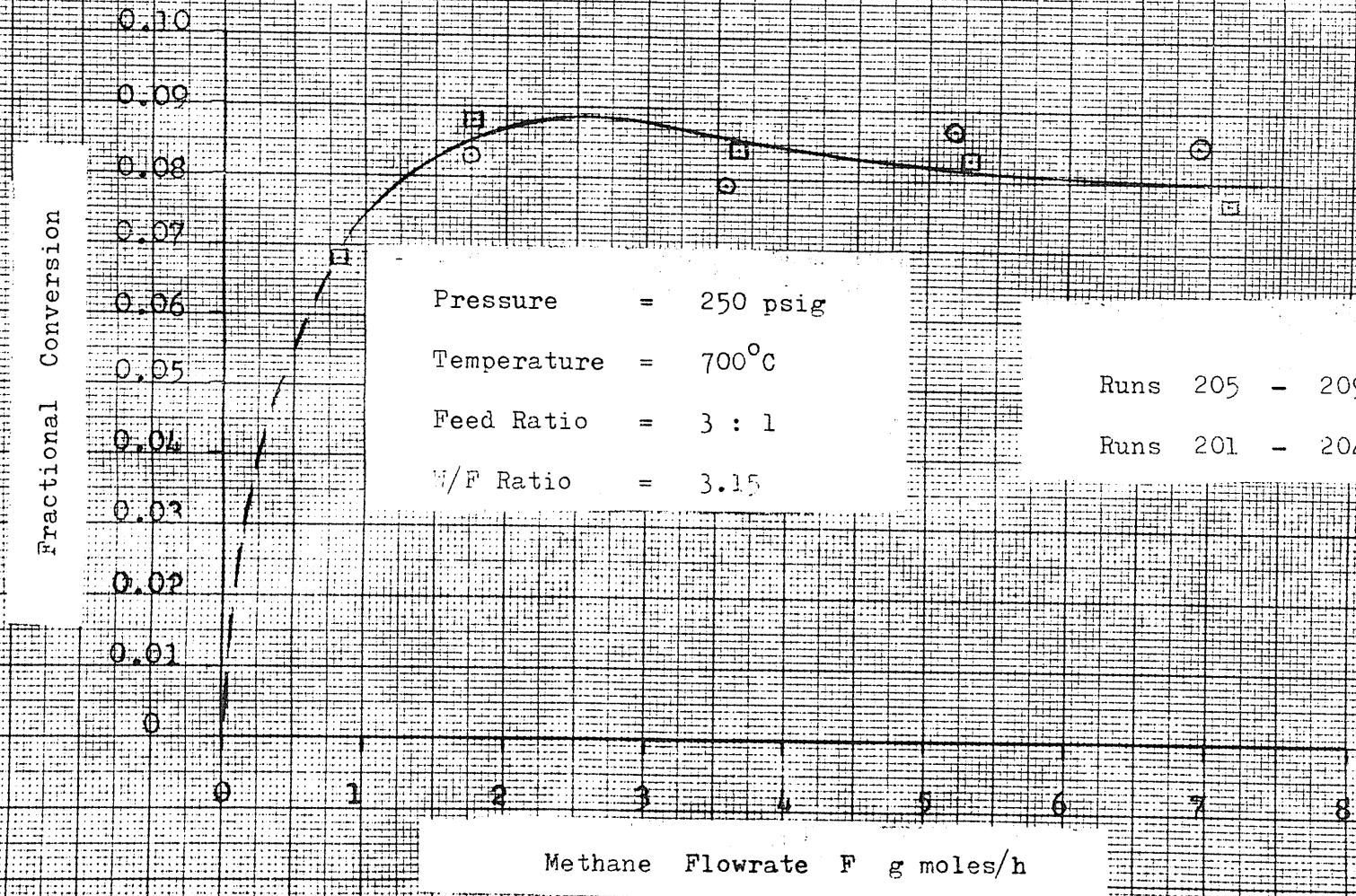

It can be seen that there is a good agreement between both sets of results and the straight line relationship indicated in Figure 28 for $^{W}/_{F}$ values greater than 2.0 : 1 is confirmed.

Other investigators (64,68,76,77) who have examined steam-methane systems at lower pressures than considered here, also show that diffusion effects are negligible. High pressure work has been carried out by Smith (123) using a steam-heptane system, and also by Bhatta and Dixon (78) using a steam-butane system, and it was concluded by both that the influence of diffusion resistance on the overall rate is negligible.

It is difficult to conclude whether the maximum shown on Figure 30 is a true representation or a result of process and analytical deviations. Nevertheless, it is interesting to note that Smith (123) using a packed-bed system obtained a maximum on f vs $^{W}/_{F}$ diagrams at pressures less than 200 psig. However, since he did not obtain a constant regime, it was concluded that the overall shape of the curves was the result of mass velocity effects, ie. channelling through the packed bed.

In the current experimentation, channelling as such could not occur, therefore if it is assumed that the peak obtained on Figure 30 is a true representation, it can only be concluded that it is associated with a range of flow conditions that produce

a critical zone in which the rate controlling step changes.

6.3.2.2. Effect of temperature.

Using the experimental results from the 201-204, run series, which are tabulated in Appendix E, the fractional conversions obtained were plotted against respective operating temperatures. These curves are shown in Figure 31, and it can be seen that they all have the same general form in that the rate of change of f increases with temperature.

If as concluded in the previous section, mass diffusion effects do not control the overall reaction rate, all of the points shown in Figure 31 should lie on a single curve. This follows since the only change in the operating conditions for each series was the methane flow rate and mass of catalyst; therefore outside the diffusion regime these variables will not affect the conversion.

Hence, Figure 32 was constructed using all of the points shown in Figure 31, and it can be seen that essentially they do fall on a single curve. The greater degree of scatter obtained at the low end of the temperature scale is probably attributable to analytical error arising from relatively low amounts of CO_2 and CO which are the least sensitive components for the

Plots of Fractional Conversion vs Temperature for Runs 201 - 204

Figure 31.

Pressure = 250 psig

W/F Ratio = 3.15 g catalyst h/mole CH_4

Feed Ratio = 3 : 1

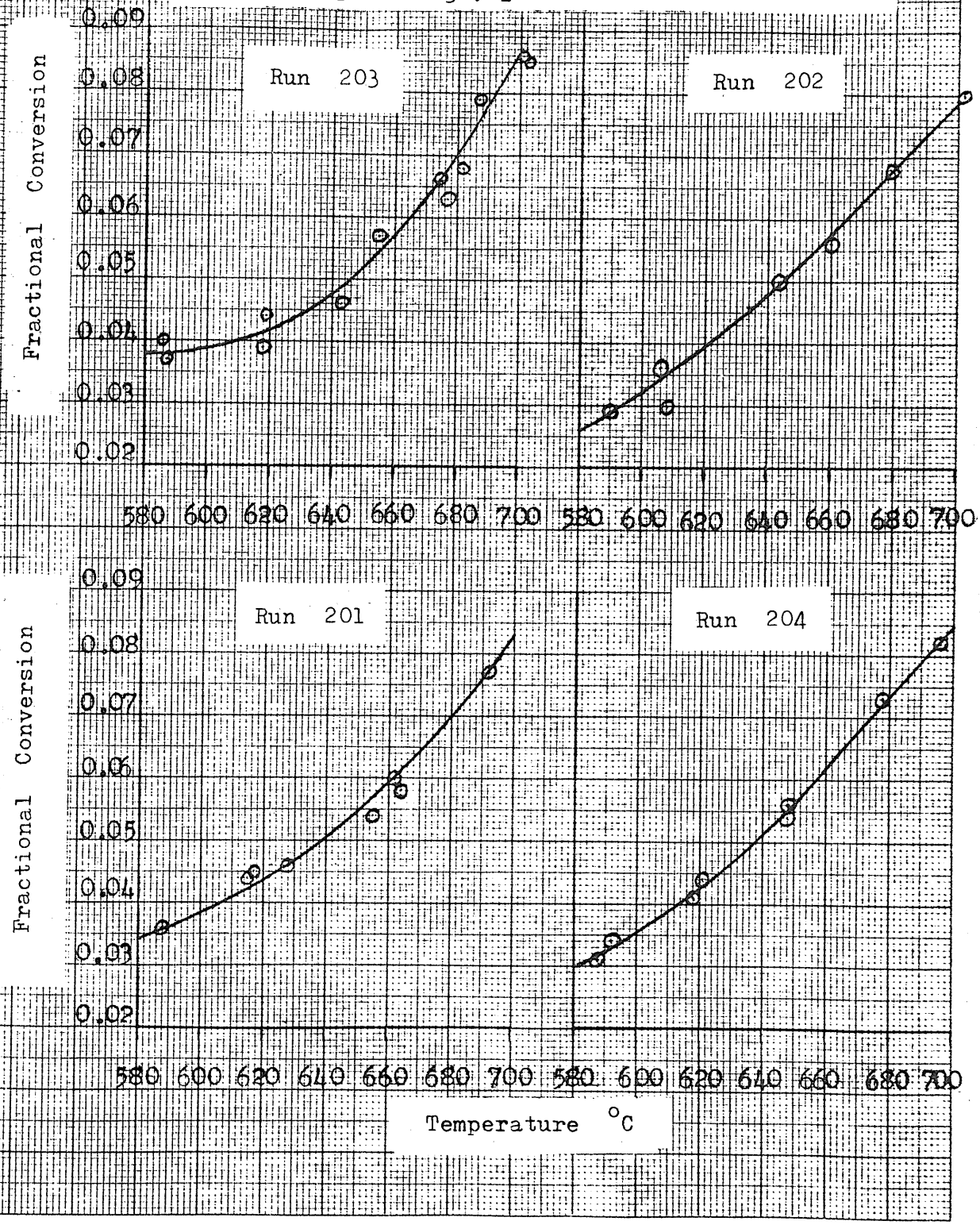

Combined Plot of Fractional Conversions vs Temperature for Runs 201 - 204

Figure 32.

Pressure = 250 psig

W/F Ratio = 3.15 g catalyst/g mole CH_4/h

Feed Ratio = 3 : 1

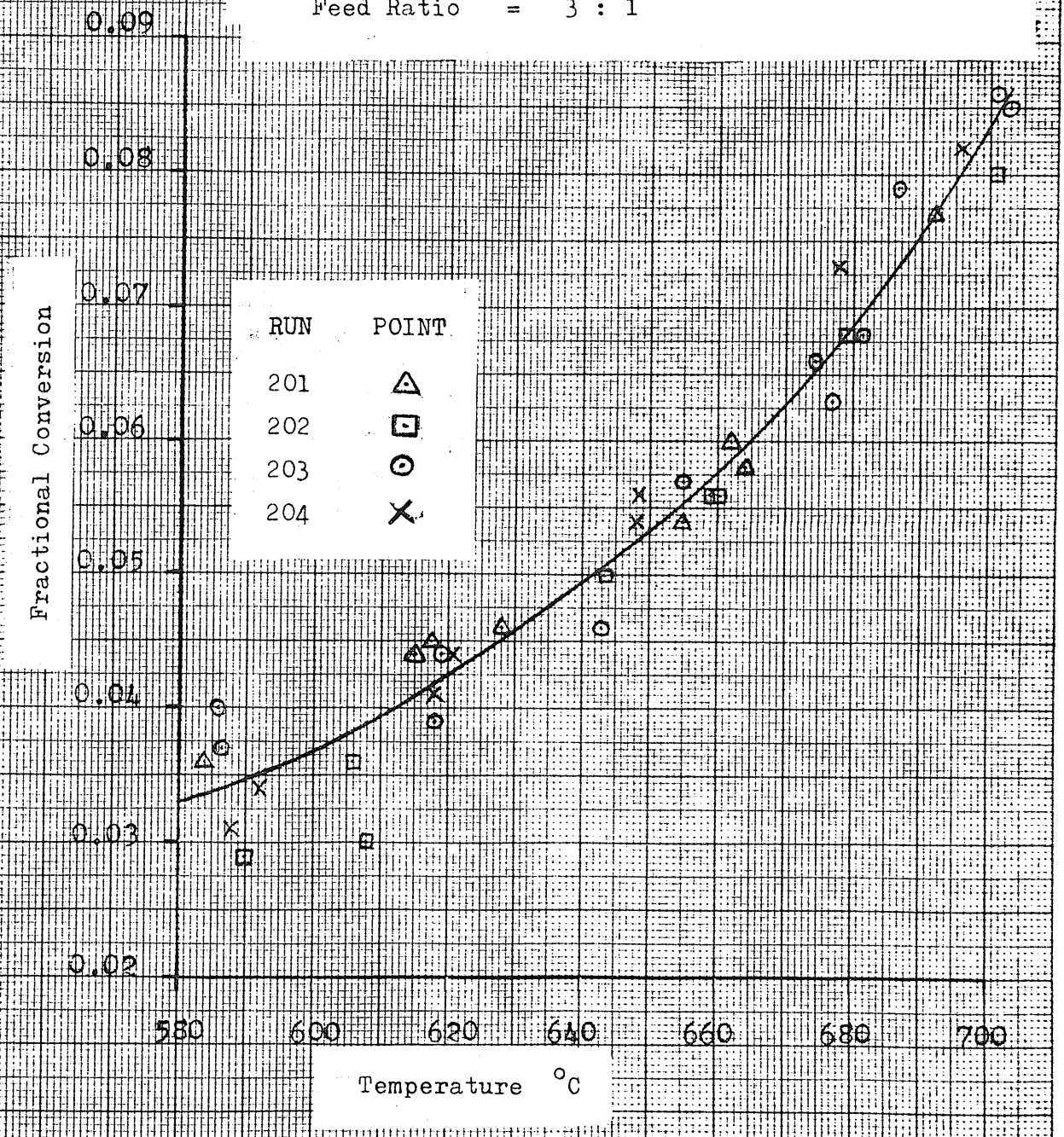

chromatographic unit.

Providing a number of conditions are satisfied, then fractional conversion - temperature data may be treated in an alternative manner to assess the importance of film diffusion control.

It was stated in sec. 6.3.1.2. that when the temperature is increased from T_1 to T_2 then for a diffusion controlled reaction, the rate is increased by a factor equal to $(T_2 \text{ ABS.}/T_1 \text{ ABS.})^{\frac{1}{2}}$.

If for a given mass of catalyst fractional conversion data is collected at differing temperatures with the pressure, feed ratio, and time factor all maintained constant, then the maximum possible increase in f will also be given by $(T_2 \text{ ABS}/T_1 \text{ ABS})^{\frac{1}{2}}$.

From Fig.32 it can be seen that the temperatures over which fractional conversion data range are from 580°C to 700°C. Over these two temperature limits, the expected increase in reaction rate for a diffusion controlled reaction is approximately 7%. However, it can be seen from Fig.32 that the corresponding changes in fractional conversion are 0.0330 to 0.0835 which is an increase in the order of 250%.

This therefore further confirms the absence of film diffusion control and indicates a 'chemically' controlled rate, since with this latter type of control, large increases in reaction rate accompany relatively

small increases in temperature.

6.3.2.3. Effect of pressure.

The experimental results from runs 207, 210, and 211, are given in Appendix E, and the calculated fractional conversions are shown in Figure 33 plotted against their respective W/F ratios.

By re-arranging equation 6.2 it can be seen that reaction rate r may be expressed as :-

$$r = df/d\,(W/F)$$

Therefore the initial reaction rate will be given by the slope of the fractional conversion vs W/F curve at a W/F value equal to zero.

Using the method of slopes which at a value of W/F = 0 is quite accurate, the initial reaction rates for the three operating pressures were established from the curves shown in Figure 33 after firstly extrapolating to a zero W/F value. The results are shown in Figure 34, curve A, plotted against respective pressures.

Although the three experimental points could be considered as on a straight line, this type of relationship cannot be the case since at zero pressure there is no supply of reactants and no conversion, and

Fractional Conversion vs W/F Ratio

Runs 207, 210, 211.

Figure 33.

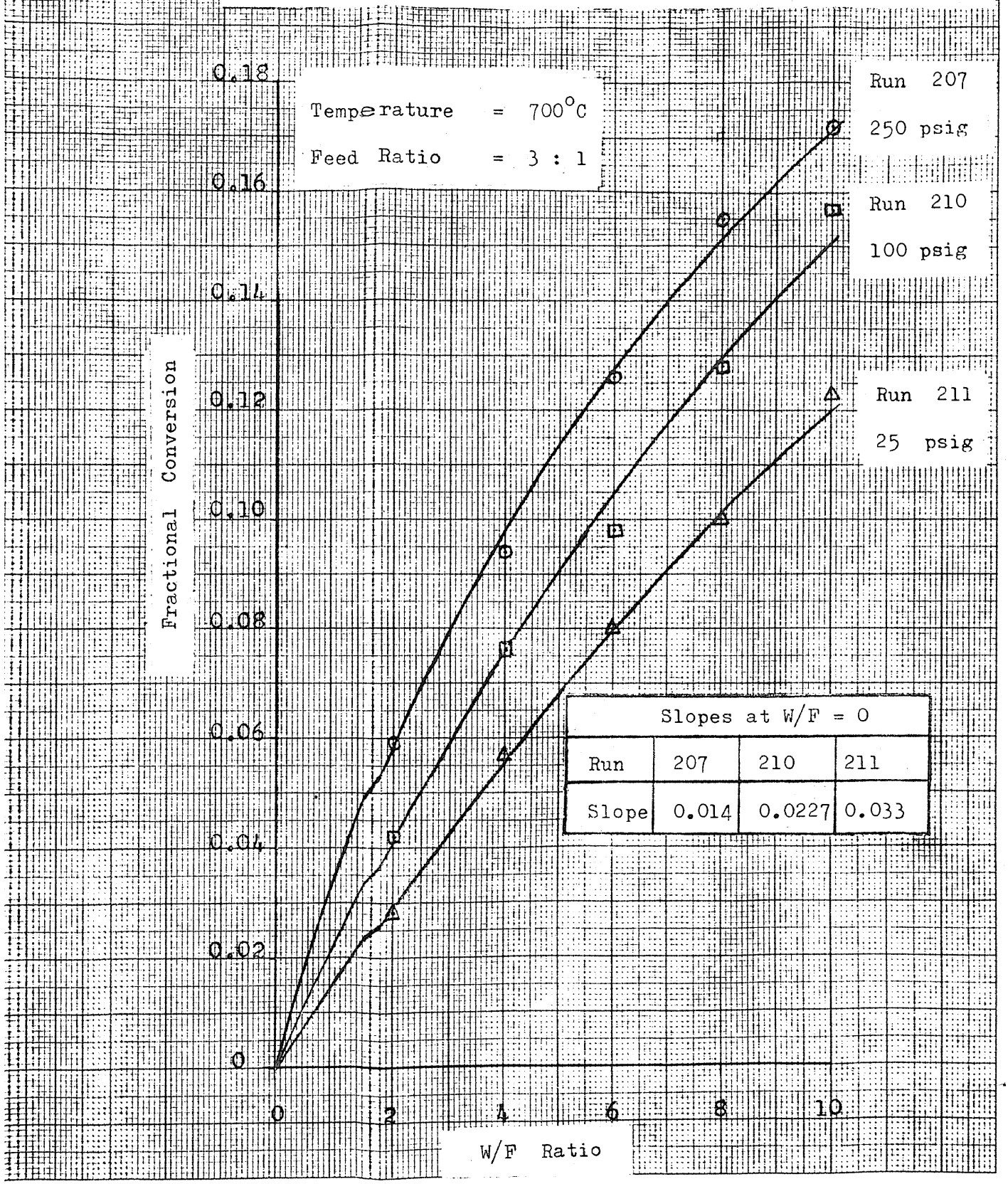

Slopes at W/F = 0			
Run	207	210	211
Slope	0.014	0.0227	0.033

INITIAL REACTION RATE vs TOTAL PRESSURE RELATIONSHIP

Figure 34.

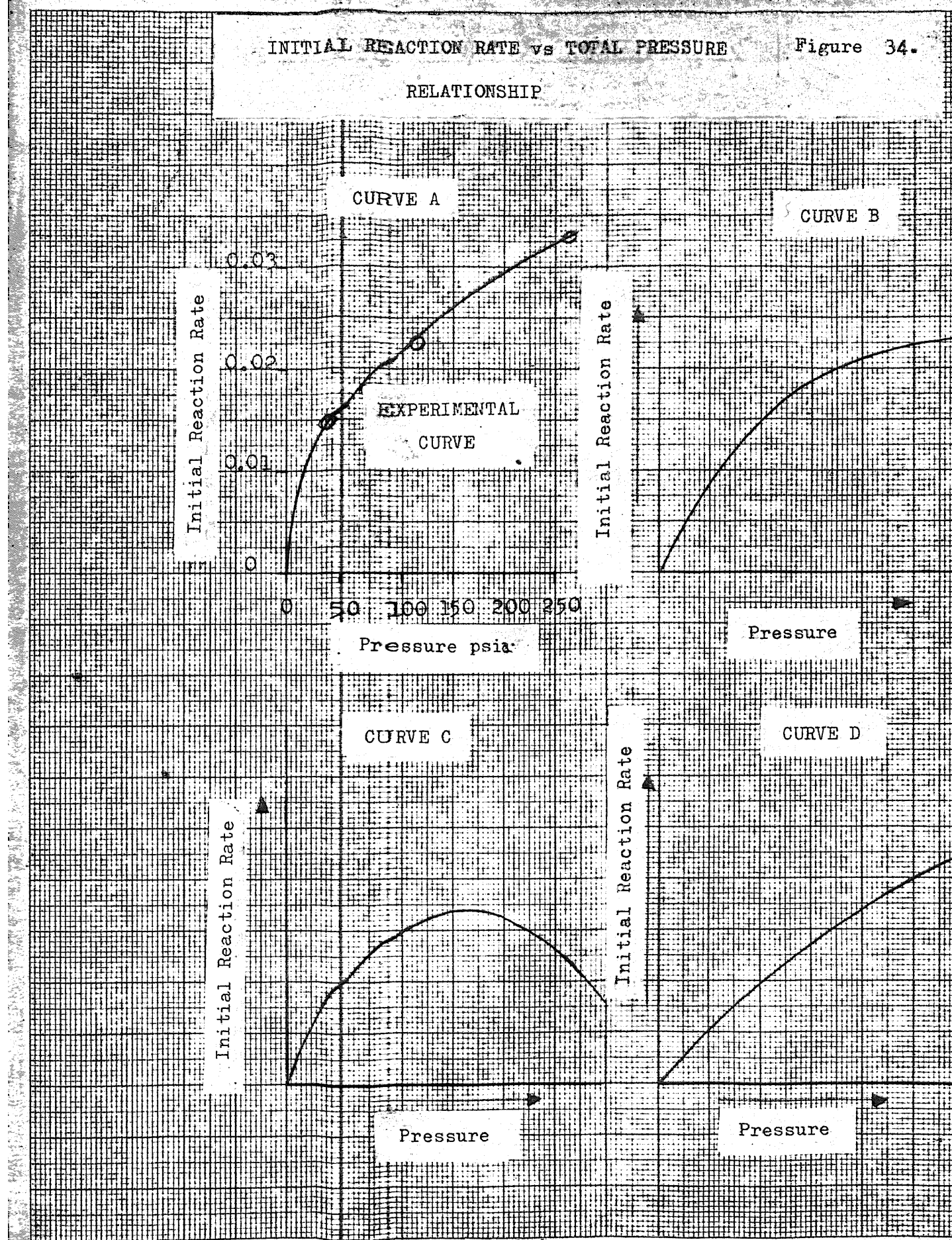

so the origin must be a fourth point. Hence, the resultant plot must be a curve which may have a maximum at a pressure outside the range investigated or continue asymptotically in the horizontal direction.

The three accompanying curves B, C, and D shown in Figure 34 are the only types of curve presented by Yang and Hougen (122) that curve A could represent in part or whole. Therefore according to the above authors, the possible rate controlling steps for the steam-methane reforming reaction may be confined to those listed in Table 12.

TABLE 12

Possible rate controlling steps for the steam-methane reforming reaction.

Curve	Rate Controlling Step.
B	either Adsorption of A controlling $A + B \rightleftharpoons R + S$ or Adsorption of B controlling $A + B \rightleftharpoons R + S$
C	Adsorption of A controlling with dissociation of A. $A + B \rightleftharpoons R + S$

TABLE 12 (Cont'd)

Possible rate controlling steps for the steam-methane reforming reaction.	
Curve	Rate Controlling Step.
D	Adsorption of B controlling with dissociation of A. $A + B \rightleftharpoons R + S$

6.4. Quantitative Studies.

6.4.1. Introduction.

It was shown in the literature survey that numerous studies of the thermodynamics and equilibrium aspects of hydrocarbon reforming have been made. The kinetics of the catalytic reaction of some hydrocarbon feedstocks have also been examined, but the steam-methane system at elevated pressure has received little attention.

Although some rate equations and mechanisms for methane reforming have been proposed, these tend

to be conflicting and mostly confined to low pressure operation. Therefore the present work was undertaken in an attempt to establish a rate equation and mechanism for high pressure reforming.

6.4.2. Experimental.

Because the reactor was of the integral type, it was not possible for reaction rates to be determined directly from the experimentation. Therefore it was necessary to carry out experiments such that reaction rates could be established indirectly from the data.

The method chosen for determining reaction rates was the method of 'slopes' which is described by Hougen and Watson (128), and has been successfully applied by others (68, 125). This method involves obtaining conversion data at different values of the steam-methane feed ratio for various values of the time-factor (W/F), at constant pressure and temperature. By the method of slopes reaction rates may be determined at different operating conditions, and these may then be used to establish a mechanism.

The thermodynamic analysis of the steam-methane reaction showed that at temperatures below 600°C the maximum conversions attainable, ie. equilibrium conversions, are small; therefore it was considered

necessary to carry out the experimentation at a temperature above 600°C.

The feed ratio range chosen for investigation was 8:1 to 2:1 as this was considered to be representative of those used on industrial applications.

The maximum operating pressure was limited to 250 psig because of practical considerations associated with the water supply pump. At this pressure the maximum safe working temperature for the reactor was 700°C but it was considered expedient from a safety point of view to limit the working temperature to 650°C.

Four series of experiments were carried out using the same batch of catalyst, the operating procedures are described in Chapter 2 section 3, and Table 13 summarises the various conditions used in the study.

TABLE 13

Operating conditions used in the Quantitative Experimentation.

Catalyst Weight _____ 10.8616 gm

Temperature _____ 650°C

Pressure _____ 250 psig

Run	Feed Ratio	Time Factors.
301	8:1	4.0:1, 5.0:1, 6.5:1,7.5:1,9.0:1,10.0:1
302	6:1	3.0:1,4.0:1,5.5:1,7.5:1,9.0:1,10.0:1
303	4:1	2.0:1,3.5:1,5.0:1,7.0:1,8.5:1,10.0:1
304	2:1	1.0:1,2.0:1,3.0:1,4.0:1,6.0:1,8.0:1

The time factor (W/F) was varied by changing the methane flow rate, and corresponding changes in the water delivery rate were necessary to maintain the steam-methane feed ratio.

6.4.3. Results and Discussion.

6.4.3.1. Results.

The experimental data from the 300 run series are tabulated in Appendix F. In order to minimise any experimental error associated with the results, product distribution curves were constructed for each component and each run within the series, and resultant composition vs time factor data for use in the rate analysis were taken from respective curves.

A summary of this interpolated data is given in Tables 14 to 17. Also included are (i) fractional conversions and (ii) wet compositions calculated from the dry compositions and knowledge of the steam-methane feed ratio.

TABLE 14

CONVERSION DATA FOR THE 301 EXPERIMENTAL RUN.

FEED RATIO R = 8 : 1

Time Factor W/F	Dry Composition				Fractional Conversion	Wet Composition				
	$\%H_2$	$\%CH_4$	%CO	$\%CO_2$		$\%H_2O$	$\%H_2$	$\%CH_4$	%CO	$\%CO_2$
4	19.30	76.13	0.29	4.28	0.057	86.43	2.62	10.33	0.04	0.58
5	22.67	71.90	0.33	5.10	0.070	85.88	3.20	10.15	0.05	0.72
6	24.62	69.26	0.37	5.72	0.081	85.53	3.56	10.02	0.05	0.83
7	26.25	67.20	0.41	6.14	0.089	85.24	3.87	9.92	0.06	0.91
8	27.80	65.21	0.46	6.53	0.097	84.94	4.19	9.82	0.07	0.98
9	29.33	63.21	0.52	6.94	0.106	84.64	4.51	9.71	0.08	1.07
10	30.88	61.21	0.59	7.32	0.114	84.32	4.84	9.60	0.09	1.15

TABLE 15

CONVERSION DATA FOR THE 302 EXPERIMENTAL RUN.

FEED RATIO R = 6 : 1

Time Factor W/F	Dry Composition %H_2	%CH_4	%CO	%CO_2	Fractional Conversion	Wet Composition %H_2O	%H_2	%CH_4	%CO	%CO_2
3	15.64	80.49	0.27	3.60	0.046	83.30	2.61	13.44	0.05	0.60
4	19.50	75.78	0.32	4.40	0.059	82.57	3.40	13.21	0.06	0.77
5	22.60	71.58	0.38	5.15	0.071	81.94	4.09	12.98	0.07	0.93
6	24.85	68.92	0.45	5.78	0.083	81.44	4.61	12.79	0.08	1.07
7	26.70	66.38	0.54	6.38	0.094	81.01	5.07	12.61	0.10	1.21
8	28.42	64.19	0.61	6.78	0.103	80.59	5.52	12.46	0.12	1.32
9	30.14	62.00	0.68	7.18	0.113	80.16	5.98	12.30	0.13	1.42
10	31.88	59.80	0.76	7.56	0.122	79.71	6.47	12.13	0.15	1.53

TABLE 16

CONVERSION DATA FOR THE 303 EXPERIMENTAL RUN.

FEED RATIO R = 4:1

Time Factor W/F	Dry Composition %H_2	%CH_4	%CO	%CO_2	Fractional Conversion	Wet Composition %H_2O	%H_2	%CH_4	%CO	%CO_2
2	12.55	84.35	0.25	2.85	0.035	77.47	2.83	19.00	0.06	0.64
3	17.08	78.73	0.34	3.85	0.051	76.40	4.03	18.58	0.08	0.91
4	20.70	74.16	0.43	4.71	0.065	75.45	5.08	18.21	0.11	1.16
5	23.51	70.50	0.53	5.46	0.078	74.65	5.96	17.87	0.13	1.38
6	25.60	67.65	0.64	6.11	0.091	74.01	6.65	17.58	0.17	1.59
7	27.28	65.28	0.76	6.68	0.102	73.46	7.24	17.33	0.20	1.77
8	28.85	63.09	0.89	7.17	0.113	72.93	7.81	17.08	0.24	1.94
9	30.40	61.01	1.03	7.56	0.123	72.39	8.39	16.84	0.28	2.09
10	31.98	59.00	1.17	7.85	0.133	71.85	9.00	16.61	0.33	2.21

TABLE 17

CONVERSION DATA FOR THE 304 EXPERIMENTAL RUN.

FEED RATIO R = 2 : 1

Time Factor W/F	Dry Composition %H_2	%CH_4	%CO	%CO_2	Fractional Conversion	Wet Composition %H_2O	%H_2	%CH_4	%CO	%CO_2
1	7.63	90.42	0.02	1.75	0.021	64.42	2.71	32.17	0.07	0.62
2	12.92	83.86	0.35	2.87	0.037	62.70	4.82	31.28	0.13	1.07
3	16.79	78.98	0.51	3.72	0.051	61.31	6.50	30.56	0.20	1.44
4	19.97	74.90	0.68	4.45	0.064	60.08	7.97	29.90	0.27	1.78
5	22.72	71.29	0.84	5.15	0.078	58.92	9.33	29.29	0.35	2.12
6	25.15	68.09	1.01	5.75	0.090	57.84	10.60	28.71	0.42	2.43
7	27.10	65.45	1.18	6.27	0.102	56.91	11.68	28.20	0.51	2.70
8	28.72	63.17	1.36	6.75	0.114	56.08	12.61	27.74	0.60	2.96

In the thermodynamic analysis of the system it was shown that the reforming reaction could be described by two simultaneously occurring reactions, the steam-methane reaction and the CO shift reaction. Whilst it was not implied that these are the only two reactions that actually take place, they do nevertheless represent the summation of the reactions that are feasible on a thermodynamic basis.

Since the slowest step in any sequential reaction will control the overall rate, it follows that if the slower of the above two reactions can be established, the number of possible rate controlling steps will be somewhat reduced.

In order to determine whether the steam-methane or CO shift reaction is the slower, results of alternate tests from the 300 run series were extracted from Tables 14 - 17 and used to calculate the following functions:-

(i) For the steam-methane reaction

$$\frac{p^3H_2 \; pCO}{pCH_4 \; pH_2O} \Big/ K_{p5} \qquad \text{function A}$$

(ii) For the CO shift reaction

$$\frac{pCO_2 \; pH_2}{pCO \; pH_2O} \Big/ K_{p7} \qquad \text{function B}$$

where K_{p5} and K_{p7} are respective partial pressure equilibrium constants.

Table 18 shows component pressures and corresponding values of the above functions for the experimental tests selected.

The value of the functions relative to unity indicates the proximity of each reaction to the equilibrium position. It can be seen from Table 18 that for all W/F ratios the CO shift reaction is by far the nearer to equilibrium, and therefore it is concluded that this reaction is the faster, and the steam-methane reaction or one of its component reactions must be rate controlling.

This result is in agreement with the findings of others (48,49,51,123) who have made studies in the field. It is interesting to note that Dirksen and Riesz (51) also stated that CO_2 was not formed as an initial product, whereas Akers and Camp (68) in extrapolating a plot of $\%CO_2/(\%CO_2 + \%CO)$ vs W/F to zero time factor, obtained values between 1 and 2, and therefore concluded that both CO and CO_2 were initial products. However, the results of the latter could be indicative of a very fast secondary reaction yielding CO_2 at the expense of CO. This is how Topsøe (48) described the rate of the CO shift reaction compared to the methane-steam reaction, and also what a comparison of relative values for the two functions A and B given in Table 18 indicates.

TABLE 18

EXPERIMENTAL COMPONENT PARTIAL PRESSURES AND 'EQUILIBRIUM' FUNCTIONS FOR THE STEAM-CH_4 AND CO SHIFT REACTIONS.

RUN	W/F	pH_2O atm	pH_2 atm	pCH_4 atm	pCO atm	pCO_2 atm	Function A atm	Function B
301	4:1	15.558	0.472	1.859	0.007	0.104	0.911×10^{-5}	0.232
"	6:1	15.397	0.641	1.804	0.009	0.149	3.05×10^{-5}	0.352
"	8:1	15.289	0.754	1.768	0.013	0.176	7.37×10^{-5}	0.341
"	10:1	15.178	0.871	1.728	0.016	0.207	14.4×10^{-5}	0.378
302	3:1	15.010	0.470	2.420	0.009	0.108	0.920×10^{-5}	0.192
"	5:1	14.748	0.736	2.336	0.013	0.167	5.40×10^{-5}	0.327
"	7:1	14.582	0.912	2.270	0.018	0.218	14.75×10^{-5}	0.386
"	9:1	14.429	1.078	2.214	0.023	0.256	32.20×10^{-5}	0.423
303	2:1	13.947	0.509	3.418	0.011	0.115	1.082×10^{-5}	0.194
"	4:1	13.581	0.915	3.275	0.020	0.209	12.33×10^{-5}	0.359
"	6:1	13.322	1.198	3.163	0.031	0.286	45.10×10^{-5}	0.423
"	8:1	13.127	1.407	3.074	0.043	0.349	106.2×10^{-5}	0.442

TABLE 18 (Cont'd)

EXPERIMENTAL COMPONENT PARTIAL PRESSURES AND 'EQUILIBRIUM' FUNCTIONS FOR THE STEAM-CH_4 AND CO SHIFT REACTIONS.

RUN	W/F	pH_2O atm	pH_2 atm	pCH_4 atm	pCO atm	pCO_2 atm	Function A	Function B
303	10:1	12.933	1.620	2.990	0.059	0.398	232.0×10^{-5}	0.434
304	1:1	11.596	0.488	5.791	0.013	0.112	0.805×10^{-5}	0.185
"	2:1	11.286	0.868	5.630	0.023	0.193	8.47×10^{-5}	0.329
"	4:1	10.814	1.428	5.389	0.049	0.320	87.5×10^{-5}	0.432
"	6:1	10.411	1.908	5.168	0.076	0.437	351.0×10^{-5}	0.536
"	8:1	10.094	2.270	4.995	0.108	0.533	894.0×10^{-5}	0.564

6.4.3.2. The method of analysing the results.

The analytical procedure adopted to establish a mechanism and rate expression that represents the experimental data may be summarised as follows:-

(i) All likely mechanisms that represent the overall rate controlling reaction were postulated.

(ii) Assuming in turn that each step in the various mechanisms control the reaction rate, rate equations were derived for each case in a form convenient for solution.

(iii) Unknown constants in each rate expression were calculated from the experimental data, and then by examining the values obtained all of the unlikely mechanisms and controlling steps were eliminated.

(iv) A final check was made on the equation(s) remaining after stage (iii).

In order to describe more fully the method of deriving the rate expressions, the following bi-molecular reaction is considered :-

$$A + B \rightleftharpoons R + 3S$$

It is assumed that a fifth component T is also adsorbed on the catalyst and that the reaction takes place according to the following mechanism :-

1. Reactant A becomes adsorbed.
2. Reactant B becomes adsorbed.
3. Adsorbed A reacts with adsorbed B and two active sites on the catalyst, yielding one adsorbed R and three adsorbed S molecules.
4. Product R desorbs.
5. Product S desorbs.

The above steps may be written symbolically thus :-

1. $A\,(g) + 1 \rightleftharpoons A(1)$
2. $B(g) + 1 \rightleftharpoons B(1)$
3. $A(1) + B(1) + 2l \rightleftharpoons R(1) + 3S(1)$
4. $R(1) \rightleftharpoons R(g) + 1$
5. $3S(1) \rightleftharpoons 3S(g) + 3l$

(where 1 represents an active site on the catalyst surface).

For the case when diffusional resistance effects are negligible and say step 2 is rate controlling, then if all others may be considered at equilibrium, the following development may be made.

The reaction rate r will be the rate at which step 2 proceeds, therefore :-

$$r = k_2 p_B C_1 - k_2' C_B$$

$$= k_2 \left(p_B C_1 - \frac{C_B}{K_2} \right) \qquad \text{- - - - - 6.3}$$

from step 1 $K_1 = \dfrac{C_A}{p_A C_1}$ = adsorption equilibrium constant.

from step 3 $K_3 = \dfrac{C_S^3 \, CR}{C_A C_B C_1^2}$ = surface reaction equilibrium constant.

from step 4 $K_4 = \dfrac{p_R C_1}{C_R}$ = desorption equilibrium constant.

and
from step 5 $K_5 = \dfrac{C_1^3 \, p_S^3}{C_S^3}$ = desorption equilibrium constant.

Therefore, by substitution equation 6.3 becomes :-

$$r = k_2 \left(p_B C_1 - \frac{p_S^3 \, p_R \, C_1}{K p_A} \right) \qquad \text{- - - - - 6.4}$$

where the overall equilibrium constant $K = K_1 \, K_2 \, K_3 \, K_4 \, K_5$.

From equation 6.4 it can be seen that C_1, the concentration of unoccupied active sites on the catalyst is the only variable that cannot be determined experimentally. By equating the sum of C_1 and the concentrations of the reactants and products adsorbed, to the total number of active sites L which will be a

constant, C_1 may be substituted as follows:-

$$L = C_1 + C_A + C_B + C_R + C_S + C_T$$

$$= C_1 + K_1 p_A C_1 + \frac{p_S^3 p_R C_1}{K_1 K_3 K_4 K_5 p_A} + \frac{p_R C_1}{K_4} + \frac{C_1 p_S}{\sqrt[3]{K_5}} + \frac{p_T C_1}{K_6} \quad -- 6.5$$

where K_6 is the desorption equilibrium constant for the fifth component T.

From equation 6.5,

$$C_1 = \frac{L}{\left(1 + K_1 p_A + \frac{p_S^3 p_R}{K_1 K_3 K_4 K_5 p_A} + \frac{p_R}{K_4} + \frac{p_S}{\sqrt[3]{K_5}} + \frac{p_T}{K_6}\right)}$$

Substituting for C_1 into equation 6.4, the reaction rate becomes:-

$$r = \frac{k_2 L \left(p_B - \frac{p_S^3 p_R}{K p_A}\right)}{1 + K_A p_A + \frac{p_S^3 p_R K_R K_S}{K_A K_3} + K_R p_R + \sqrt[3]{K_S} p_S + K_T p_T} \quad --- 6.6$$

where K_A, K_B, K_R, K_S, and K_T are adsorption equilibrium constants for the respective products.

In obtaining a rate expression convenient for solution and subsequent selection or rejection, equation 6.6 is re-arranged as follows:-

$$\frac{1}{r} = \frac{1 + K_A p_A + \frac{p_S^3 p_R K_R K_S}{K_A K_3} + K_R p_R + \sqrt[3]{K_S} p_S + K_T p_T}{k \left(p_B - \frac{p_S^3 p_R}{K p_A}\right)}$$

where $k = k_2 L$

Therefore,

$$\frac{\left(p_B - \frac{p_S^3 p_R}{K p_A}\right)}{r} = R' = a + bp_A + \frac{cp_S^3 p_R}{p_A} + dp_S + ep_R + fp_T - - - \quad 6.7$$

where $a = 1/k$

$b = K_A/k$

$c = \frac{1}{k} \cdot \frac{K_R K_S}{K_A K_3}$

$d = K_R/k$

$e = \sqrt[3]{K_S}/k$

$f = K_T/k$

From equation 6.7 it can be seen that only known or measurable terms are contained in the left hand side, and all of the unknown coefficients are contained in the right hand side; therefore the equation is in a convenient form for determining the unknown coefficients.

6.4.3.3. Analysis of results and discussion.

Based on the previous findings in that the steam-methane reaction is rate controlling, and that the controlling step is 'chemical' in nature ie. the influence of diffusion is negligible, four reaction

mechanisms were postulated and are shown in Table 19.

TABLE 19

POSTULATED REACTION MECHANISMS		
Mechanism	Step	Reaction
I	1	$CH_4(g) + 1 \rightleftharpoons CH_4(1)$
	2	$CH_4(1) + H_2O(g) \rightleftharpoons CO(1) + 3H_2(g)$
	3	$CO(1) \rightleftharpoons CO(g) + 1$
II	1	$CH_4(g) + 1 \rightleftharpoons CH_4(1)$
	2	$H_2O(g) + 1 \rightleftharpoons H_2O(1)$
	3	$CH_4(1) + H_2O(1) + 2\,1 \rightleftharpoons CO(1) + 3H_2(1)$
	4	$CO(1) \rightleftharpoons CO(g) + 1$
	5	$3H_2(1) \rightleftharpoons 3H_2 + 3\,1$
III	1	$CH_4(g) + 1 \rightleftharpoons CH_2(1) + H_2(g)$
	2	$CH_2(1) + H_2O(g) \rightleftharpoons CO(1) + 2H_2(g)$
	3	$CO(1) \rightleftharpoons CO(g) + 1$
IV	1	$CH_4(g) + 1 \rightleftharpoons CH_4(1)$
	2	$H_2O(g) + 1 \rightleftharpoons H_2O(1)$
	3	$CH_4(1) + H_2O(1) \rightleftharpoons CO(1) + 3H_2(g) + 1$
	4	$CO(1) \rightleftharpoons CO(g) + 1$

In developing rate equations for the mechanisms given in Table 19, it was assumed that CO_2 resulting from the CO shift reaction exists at some stage in the reaction as an adsorbed species. Although this assumption may be wrong, for the purpose of developing the rate equations, it is necessary. If it is invalid, then the CO_2 adsorption coefficient in the modified rate equations will be zero and therefore the term will not be included in the final equation. However, if the assumption is not made and yet CO_2 is adsorbed, then the rate equations derived would be fallacious.

The modified rate equations developed for the mechanisms are given in Table 20, and the following subscripts are used to represent the components within the system :-

Subscript A	- - - -	CH_4
Subscript B	- - - -	H_2O
Subscript R	- - - -	CO
Subscript S	- - - -	H_2
Subscript T	- - - -	CO_2

TABLE 20

MODIFIED RATE EQUATIONS FOR THE MECHANISMS SHOWN IN TABLE 19.

MECHANISM	CONTROLLING STEP	RATE EQUATION
I	1	$R' = \left[p_A - \frac{p_R p_S^3}{K p_B} \right] \Big/ r = a + \frac{b p_R p_S^3}{p_B} + c p_A + d p_T$
I	2	$R' = \left[p_A p_B - \frac{p_R p_S^3}{K} \right] \Big/ r = a + b p_A + c p_R + d p_T$
I	3	$R' = \left[\frac{K p_A p_B}{p_S^3} - p_R \right] \Big/ r = a + b p_A + \frac{c p_A p_B}{p_S^3} + d p_T$
II	1	$R' = \left[p_A - \frac{p_S^3 p_R}{K p_B} \right] \Big/ r = a + \frac{b p_S^3 p_R}{p_B} + c p_B + d p_S + e p_R + f p_T$
II	2	$R' = \left[p_B - \frac{p_S^3 p_R}{K p_A} \right] \Big/ r = a + b p_A + \frac{c p_S^3 p_R}{p_A} + d p_S + e p_R + f p_T$
II	3	$R' = \sqrt[4]{\left[p_A p_B - \frac{p_R p_S^3}{K} \right]} \Big/ r = a + b p_A + c p_B + d p_R + e p_S + f p_T$
II	4	$R' = \left[\frac{K p_A p_B}{p_S^3} - p_R \right] \Big/ r = a + b p_A + c p_B + \frac{d p_A p_B}{p_S^3} + e p_S + f p_T$

TABLE 20 Continued

MECHANISM	CONTROLLING STEP	RATE EQUATION
II	5	$R' = \sqrt{\left[\frac{Kp_Ap_B}{p_R} - p_S^3\right]} \Big/ r = a + bp_A + cp_B + dp_R + e\sqrt[3]{\frac{p_Ap_B}{p_R}} - fp_T$
III	1	$R' = \left[p_A - \frac{p_Rp_S^3}{Kp_B}\right] \Big/ r = a + \frac{bp_Rp_S^2}{p_B} + cp_R + dp_T$
III	2	$R' = \left[\frac{p_Ap_B}{p_S} - \frac{p_Rp_S^2}{K}\right] \Big/ r = a + \frac{bp_A}{p_S} + cp_R + dp_T$
III	3	$R' = \left[\frac{Kp_Ap_B}{p_S^3} - p_R\right] \Big/ r = a + \frac{bp_A}{p_S} + \frac{cp_Ap_B}{p_S^3} + dp_T$
IV	1	$R' = \left[p_A - \frac{p_Rp_S^3}{Kp_B}\right] \Big/ r = a + \frac{bp_Rp_S^3}{p_B} + cp_B + dp_R + ep_T$
IV	2	$R' = \left[p_B - \frac{p_Rp_S^3}{Kp_A}\right] \Big/ r = a + bp_A + \frac{cp_Rp_S^3}{p_A} + dp_R + ep_T$

TABLE 20 Continued.

MECHANISM	CONTROLLING STEP	RATE EQUATION
IV	3	$R' = \sqrt{\left[p_A p_B - \frac{p_R p_S^3}{K}\right]} \Big/ r = a + bp_A + cp_B + dp_R + cp_T$
IV	4	$R' = \left[\frac{Kp_A p_B}{p_S^3} - p_R\right] \Big/ r = a + bp_A + cp_B + \frac{dp_A p_B}{p_S^3} + ep_T$

In order to determine the reaction rates r which are required for calculating the values of R' in the modified rate equations, the method of slopes was chosen. For this purpose the curves of fractional conversion vs time factor (W/F) were used since the slope of such curves at any point gives the reaction rate at the respective value of W/F.

Although the curve obtained from a single run can be used to establish reaction rates and hence equations from which the unknown coefficients may be determined, this can give erroneous results because of the inaccuracy in measuring slopes. Therefore it was considered necessary to carry out more than a single run and treat the data collectively in order to minimise the error.

For the purpose of describing the method used to establish values of the coefficients in the modified rate equations, mechanism II with step 1 rate controlling is taken as an example.

$$R' = \left(p_A - \frac{p_R p_S^3}{K p_B}\right) \Big/ r = a + \frac{b p_R p_S^2}{p_B} + c p_R + d p_T \quad - - - 6.8$$

If $p_R p_S^2 / p_B$ is set equal to Θ, then by the method of least squares, the following relationship may be formed :-

$$n\,a + b\sum\theta + c\sum p_R + d\sum p_T = \sum R'$$

$$a\sum\theta + b\sum\theta^2 + c\sum p_R\theta + d\sum p_T\theta = \sum R'\theta$$

$$a\sum p_R + b\sum\theta p_R + c\sum p_R^2 + d\sum p_T p_R = \sum R' p_R$$

$$a\sum p_T + b\sum\theta p_T + c\sum p_R p_T + d\sum p_T^2 = \sum R' p_T$$

From these equations simultaneous solution for the unknowns a, b, c, and d can be obtained.

The method of determinants was used to solve the above equations, and the various known terms were obtained from the data shown in Tables 14 - 17 at selected values of the time factor W/F. Graphs of f vs W/F for each set of data were constructed in order to establish the slopes and hence reaction rates at the particular W/F values chosen. Table 21 shows the individual terms required by the four simultaneous equations, and also reaction rates r as determined from the f vs W/F curves.

The values of all of the unknown rate constants that appear in the modified rate equations listed in Table 20, and determined by the method described above, are summarised in Table 22.

TABLE 21

DATA REQUIRED FOR THE LEAST SQUARES SOLUTION OF EQUATION 6.8

RUN	TIME FACTOR W/F	RATE $r \times 10^3$ h^{-1}	p_R atm	p_T atm	R' atm h^{-1}	$\theta \times 10^3$ atm^2	$\theta^2 \times 10^6$ atm^4	$p_T p_R$ atm^2
301	4	13.21	0.007	0.104	140.7	0.00010	0.0100	0.00073
	6	9.92	0.009	0.149	182.0	0.00024	0.0576	0.00134
	8	8.33	0.013	0.176	212.2	0.00040	0.1600	0.00239
	10	5.35	0.016	0.207	322.8	0.00080	0.6400	0.00331
302	3	13.90	0.009	0.108	174.0	0.00013	0.0169	0.00098
	5	11.93	0.013	0.167	195.5	0.00048	0.0231	0.00217
	7	10.68	0.018	0.218	212.6	0.00103	1.0600	0.00392
	9	8.97	0.023	0.256	246.8	0.00185	3.4220	0.00589
303	2	16.37	0.011	0.115	208.7	0.00020	0.0400	0.00127
	4	13.82	0.020	0.209	236.5	0.00123	1.5120	0.00418
	6	12.04	0.031	0.286	261.2	0.00333	11.1000	0.00887
	8	10.67	0.043	0.349	288.0	0.00648	42.0500	0.01502

TABLE 21 Continued

RUN	TIME FACTOR W/F	RATE $r \times 10^3$ h^{-1}	p_R atm	p_T atm	R' atm h^{-1}	$\theta \times 10^3$ atm^2	$\theta^2 \times 10^6$ atm^4	$p_T p_R^2$ atm^2
303	10	9.33	0.059	0.398	320.0	0.01195	142.900	0.02349
304	1	17.65	0.013	0.112	328.0	0.00027	0.0729	0.00146
	2	14.98	0.023	0.193	376.0	0.00154	2.3720	0.00444
	4	13.41	0.049	0.320	401.5	0.00924	85.0300	0.01570
	6	12.17	0.076	0.437	423.0	0.02654	702.000	0.03323
	8	11.64	0.108	0.533	425.0	0.05510	3040.00	0.05755
		$\sum$ =	0.541	4.337	4871.0	0.12091	4032.4665	0.18597

Overall Equilibrium Constant K = 2.794 atm^2 at 650°C

TABLE 21 Continued.

RUN	TIME FACTOR W/F	$p_R\theta \times 10^3$ atm^3	$p_T\theta \times 10^3$ atm^3	$R'\theta$ $atm\ h^{-2}$	$R'p_R$ atm^2h^{-1}	$R'p_T$ atm^2h^{-1}	p_R^2 atm^2	p_T^2 atm^2
301	4	0.0007	0.0104	0.0141	0.9849	14.6	0.00005	0.0108
	6	0.0022	0.0358	0.0437	1.6380	27.1	0.00008	0.0222
	8	0.0052	0.0704	0.0849	2.7586	37.3	0.00017	0.0320
	10	0.0128	0.1656	0.2582	5.1648	66.6	0.00026	0.0428
302	3	0.0012	0.0140	0.0226	1.5660	17.8	0.00008	0.0116
	5	0.0062	0.0802	0.0938	2.5415	32.7	0.00017	0.0279
	7	0.0185	0.2242	0.2188	3.8268	46.4	0.00032	0.0475
	9	0.0426	0.4738	0.4565	5.6764	63.2	0.00053	0.0655
303	2	0.0022	0.0230	0.0417	2.2957	24.0	0.00012	0.0132
	4	0.0246	0.2570	0.29100	4.7300	49.5	0.00040	0.0436
	6	0.1032	0.9520	0.87000	8.0972	74.7	0.00096	0.0818
	8	0.2786	2.2610	1.86850	12.3840	99.1	0.00185	0.1218
	10	0.7051	4.7580	3.8230	18.8800	123.9	0.00348	0.1582

TABLE 21 Continued.

RUN	TIME FACTOR W/F	$p_R\theta x10^3$ atm^3	$p_T\theta x10^3$ atm^3	$\dot{R}\theta$ $atm\ h^{-2}$	$\dot{R}p_R$ atm^2h^{-1}	$\dot{R}p_T$ atm^2h^{-1}	p_R^2 atm^2	p_T^2 atm^2
304	1	0.0035	0.0302	0.0886	4.2640	36.7	0.00017	0.0125
	2	0.0354	0.2972	0.5785	8.6480	72.5	0.00053	0.0372
	4	0.4528	2.9570	3.7100	19.6735	127.3	0.00240	0.1024
	6	2.0170	11.6100	11.2150	32.1480	171.5	0.00578	0.1910
	8	5.9508	28.4200	23.4500	45.9000	208.0	0.01646	0.2840
	$\sum$ =	9.6626	52.6398	47.1289	181.1774	1292.9	0.03381	1.3060

TABLE 22

DETERMINED VALUES OF THE COEFFICIENTS FOR THE MODIFIED RATE EQUATIONS.

MECHANISM	CONTROLLING STEP	COEFFICIENTS					
		a	b	c	d	e	f
I	1	67.7	-645	31.4	448	-	-
I	2	3578	21.15	-3455	3662	-	-
I	3	102,420	17390	-269.7	-430500	-	-
II	1	-1056.2	-1274.8	65.96	-92.53	-208.3	2070
II	2	2836.1	-243.22	1537.2	359.0	-7555	65.4
II	3	-12.742	0.9222	1.0782	-13.41	4.1	-3.516
II	4	-3283.7×10^4	115.91×10^4	181.6×10^4	0.438×10^4	183.0×10^4	0.0961×10^4
II	5	138.13	3.854	-8.42	-959	4.28	62.32
III	1	216.96	2020	1289	5.725	-	-
III	2	4448.7	298.2	-2824	-6100	-	-
III	3	16,951	-477	164.7	-40450	-	-
IV	1	-6752.4	-14,851.6	341	411	9075	-
IV	2	641.4	152.15	-4080	-4115	1410	-
IV	3	71.80	4.361	-2.07	23.18	1.086	-
IV	4	26.440	-1904	-775.0	171.9	-21820	-

All of the coefficients a, b, c, d, e, and f that appear in the modified rate equations, represent functions of the rate and equilibrium constants relating to each particular mechanism. Therefore, in order for any mechanism to be possible, all but one coefficient in the equation must have a positive identity, the exception being the one relating to the desorption of CO_2, which for reasons stated previously, may also be zero.

Of all the modified rate equations listed in Table 22, it can be seen that only mechanism III with step 1 controlling fulfils the above condition. Therefore the remaining mechanisms can be eliminated as being physically impossible, and the rate equation that best fits the experimental data may be written thus :-

$$r = \frac{k\left(p_A - \frac{p_R p_S^3}{K p_B}\right)}{1 + \frac{K_R p_R p_S^2}{K_2 p_B} + K_R p_R + K_T p_T} \quad h^{-1} \quad ---6.9$$

where K_2 is the surface reaction equilibrium constant.

Using the relationship between the coefficients a, b, c, and d, and the reaction constants, the values of the latter at 650°C and 250 psig are :-

$k = 1/a = 0.004602 \text{ atm}^{-1} \text{ h}^{-1}$

$K_R = ck = 5.994 \text{ atm}^{-1}$

$$K_T = dk = 0.0264 \text{ atm}^{-1}$$

$$K_2 = K_H/kb = 0.6382 \text{ atm}$$

and $$K_P/K_2 = 9.31 \text{ atm}^{-2}$$

The validity of the rate equation was checked by calculating fractional conversions from equation 6.9, and comparing the results with those obtained experimentally. In order to do this, use was made of a re-arranged form of equation 6.2 :-

$$f = \int_0^{W/F} r \, d\,(W/F)$$

which when integrated gives fractional conversions.

By taking experimental data at the same W/F values used in the solution of the modified rate equation, reaction rates r were calculated from equations 6.9. The rates so obtained for the four runs were then plotted against respective W/F ratios, and each curve was integrated graphically to obtain fractional conversions at selected values of W/F.

The results of the integrations are given as points on the experimental fractional conversion vs W/F curves shown in figure 35, curves A to D. The agreement obtained cannot be considered particularly good since considerable differences (up to about 45%) are obtained on three of the four curves.

In view of this poor agreement, and despite the fact that the mechanism is in part or full agreement with the

CALCULATED VALUES OF FRACTIONAL CONVERSION f Figure 35.

COMPARED AGAINST EXPERIMENTAL VALUES.

A - RUN 301 C - RUN 303

B - RUN 302 D - RUN 304

TEMPERATURE = 650°C

PRESSURE = 250 psig

⊙ — CALCULATED CONVERSIONS

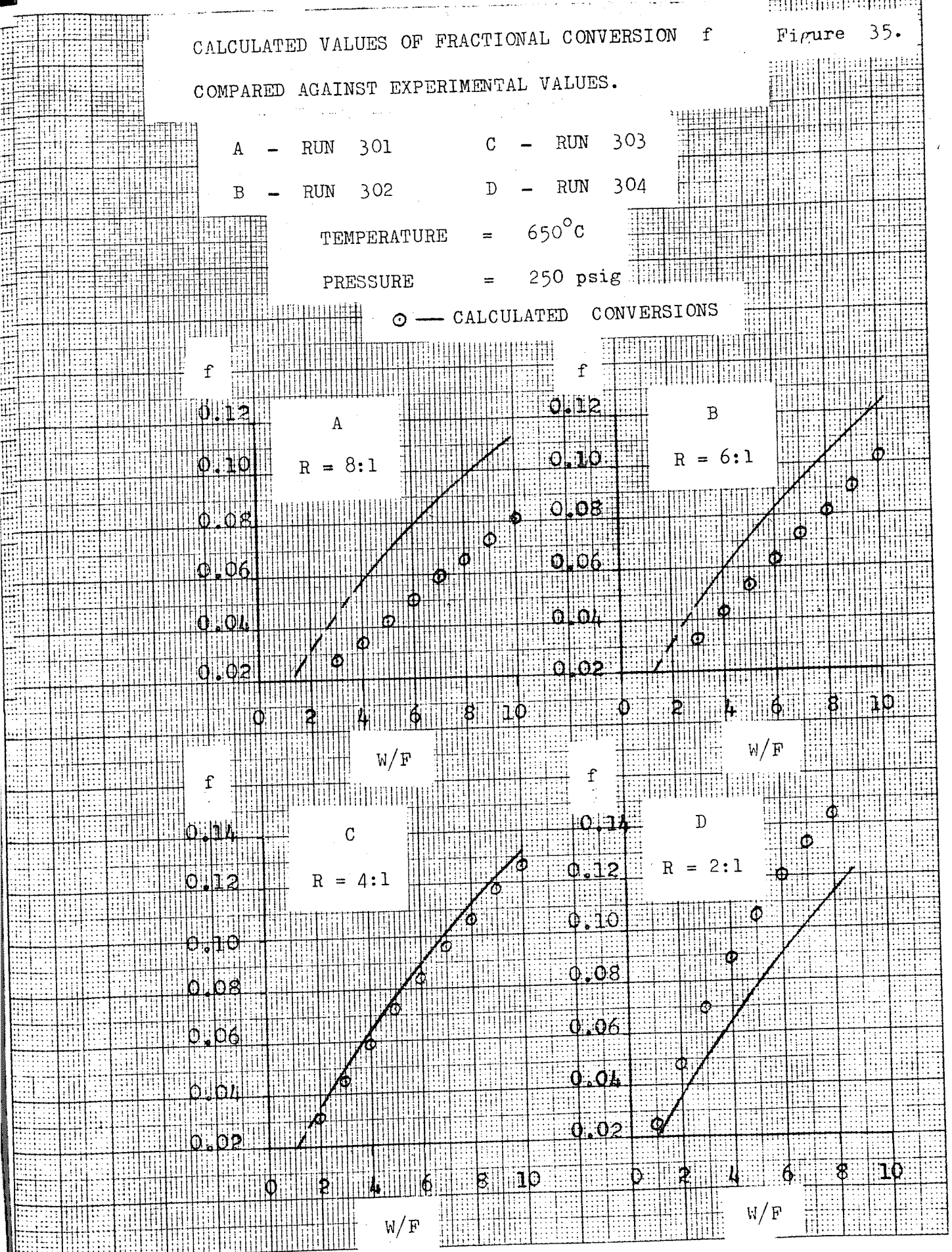

findings of other researchers (66, 67, 68), it was decided to re-examine the data for sources of possible error.

Reaction rates were established from the experimental F vs W/F curves by drawing tangents at respective W/F values, and the positions of the tangents were established by eye. Since it is possible for this method to give erroneous results it was considered necessary to repeat the calculations described above using reaction rates determined by the method of chords which reduces the possibility of error in location of tangents on the F vs W/F curves.

Table 23 compares reaction rates established by both methods for runs 301 - 303, and it can be seen that approximately an 8% difference exists between some values.

TABLE 23

REACTION RATES DETERMINED FROM TANGENTS LOCATED BY EYE (A) COMPARED WITH THOSE DETERMINED FROM TANGENTS LOCATED USING THE METHOD OF CHORDS (B).

RUN	W/F h^{-1}	REACTION RATE (A) h^{-1}	REACTION RATE (B) h^{-1}
301	4	0.01321	0.01300
	6	0.00992	0.0101
	8	0.00833	0.00795
	10	0.00535	0.00601
302	3	0.01390	0.01400
	5	0.01193	0.01211
	7	0.01068	0.01020
	9	0.00897	0.00902
303	2	0.01637	0.01525
	4	0.01382	0.01318
	6	0.01204	0.01175
	8	0.01067	0.01077
	10	0.00933	0.01002

In addition to using the new rates it was decided to exclude all of the data for the 304 run series from the repeat calculations. This is discussed more fully later, but the reason for this is that reaction rates for the 304 run series are essentially the same as those

for the 303 run series, and the dry product gas composition is other than would be expected.

The results of the repeated calculations are given in Table 24 which is similar to Table 22 in showing the calculated coefficients for the modified rate equations.

It can be seen from Table 24 that by using the more accurate reaction rates and excluding the data from the 304 run series, mechanism III with step 1 controlling which previously had all positive coefficients, now has one large negative coefficient. In addition, two other mechanisms namely I with step 1 controlling and IV with step 3 controlling, both have all their modified rate equation coefficients positive in sign.

TABLE 24

DETERMINED VALUES OF THE COEFFICIENTS FOR THE MODIFIED RATE EQUATIONS - REPEAT CALCULATION

MECHANISM	CONTROLLING STEP	COEFFICIENTS a	b	c	d	e	f
I	1	123.96	125.0	7.260	409.0	-	-
I	2	-754.5	1579	-5350	1084	-	-
I	3	19,307	-5,348	183.2	-6,098	-	-
II	1	-4072	11,240	306.2	3512	73,500	-22,720
II	2	520.8	-33.80	27,306	-1193	-143,800	22,180
II	3	8.769	0.1287	-0.1775	-64.42	0.618	8.60
II	4	92,610	42,688	1407	-381.0	-12,710	-661,000
II	5	-114.40	5.225	11.930	92.42	1.541	-48.70
III	1	1006.65	-30,520	4480	14.71	-	-
III	2	8001.2	-60.05	90,600	-26,800	-	-
III	3	-35,858	9,920	167.10	52,900	-	-
IV	1	937.8	41,240	-59.75	-37,660	3873	-
IV	2	630.0	185.0	64,400	-205,600	17,620	-
IV	3	10.531	0.8316	1.785	0.896	46.50	-
IV	4	114,300	-9,192	-5,425	188.0	-34,430	-

Therefore the two rate equations that could possibly fit the experimental data may be written thus:-

(i) Mechanism I 1

$$r = \frac{k\left[pCH_4 - \frac{pCO\,pH_2^3}{K\,pH_2O}\right]}{1 + \frac{KCO\,pCO\,pH_2^3}{KSR\,pH_2O} + KCO\,pCO + KCO_2\,pCO_2} \quad \ldots 6.10$$

Where $k = 1/a = 0.00806$ $atm^{-1}h^{-1}$

$KCO = c\phi k = 0.0586$ atm^{-1}

$KCO_2 = dk = 3.30$ atm^{-1}

$KSR = KCO/kb = 0.00582$ atm^{2}

$K = 2.794$ atm^{2}

and (ii) Mechanism IV 3

$$r = \frac{k\left[pCH_4\,pH_2O - \frac{pCO\,pH_2^3}{K}\right]}{\left[1 + KCH_4\,pCH_4 + KH_2O\,pH_2O + KCO\,pCO + KCO_2\,pCO_2\right]^2} \quad \ldots 6.11$$

Where $k = 1/a^2 = 0.00262$ $atm^{-2}h^{-2}$

$KCH_4 = b\sqrt{k} = 0.0426$ atm^{-1}

$KH_2O = c\phi\sqrt{k} = 0.09145$ atm^{-1}

$KCO = d\sqrt{k} = 0.04595$ atm^{-1}

$KCO_2 = e\sqrt{k} = 2.382$ atm^{-1}

$K = 2.794$ atm^{2}

The validity of these rate equations was checked by the same procedure described earlier for equation

6.0. The results are given in Figure 36 A - C and Figure 37 A - C. The agreement obtained is considered acceptable for both mechanisms, the maximum discrepancy being about 20% for IV 3 and 12.5% for I 1. Furthermore although the integrated results for mechanism I 1 are slightly better at a feed ratio of 8:1, overall the results are so similar that it is not possible to select either mechanism as more valid than the other, and for the experimental results at present available it must be concluded that both are equally possible.

Nevertheless some difference between calculated and experimental conversions does exist, and in addition, the data from the 304 run series for a feed ratio of 2:1 was not included in the above analysis. A brief discussion of possible reasons for the differences follows.

Since the mass balances carried out and the chromatograph calibrations were acceptable, errors or discrepancies cannot be attributed to these sources, and therefore other factors must be responsible.

The possibility of some other 'chemical' reaction mechanism not considered in the above analysis to be rate controlling cannot be completely disregarded. However, the facts and observations of other workers, listed below, were used as the basis for selection of reaction mechanisms, and it is thought that those considered are the most probable.

CALCULATED VALUES OF FRACTIONAL CONVERSION f

COMPARED AGAINST EXPERIMENTAL VALUES.

Figure 36.

A - RUN 301 C - RUN 303

B - RUN 302

MECHANISM I 1

TEMPERATURE = 650°C

PRESSURE = 250 psig

⊙ -- CALCULATED CONVERSIONS

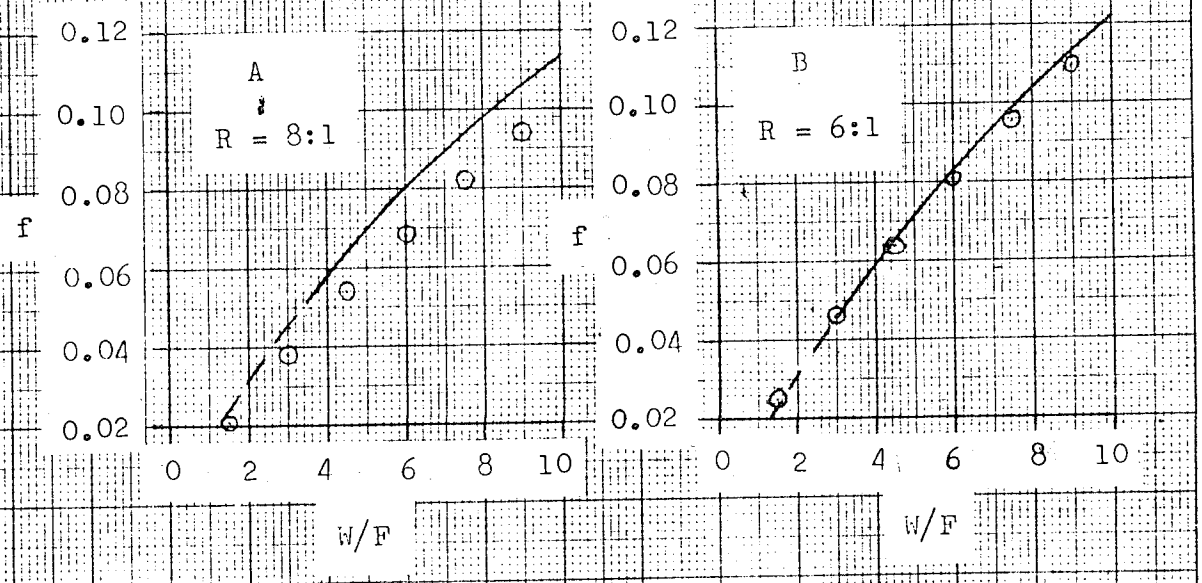

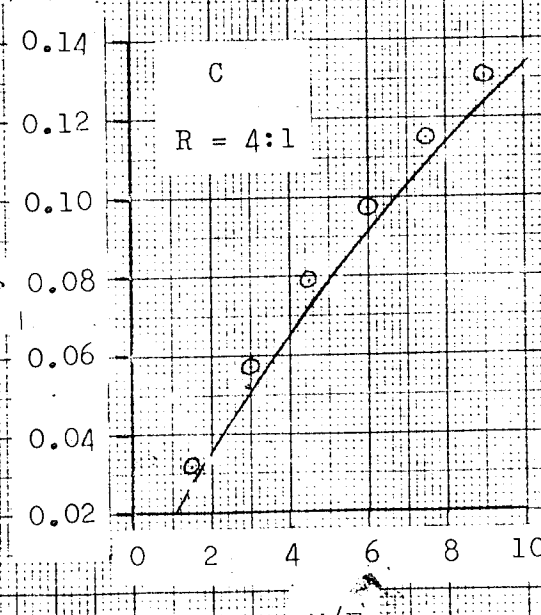

Figure 37.

CALCULATED VALUES OF FRACTIONAL CONVERSION f COMPARED AGAINST EXPERIMENTAL VALUES.

A – RUN 301 C – RUN 303

B – RUN 302 MECHANISM IV 3

TEMPERATURE = 650°C

PRESSURE = 250 psig

Θ — CALCULATED CONVERSIONS

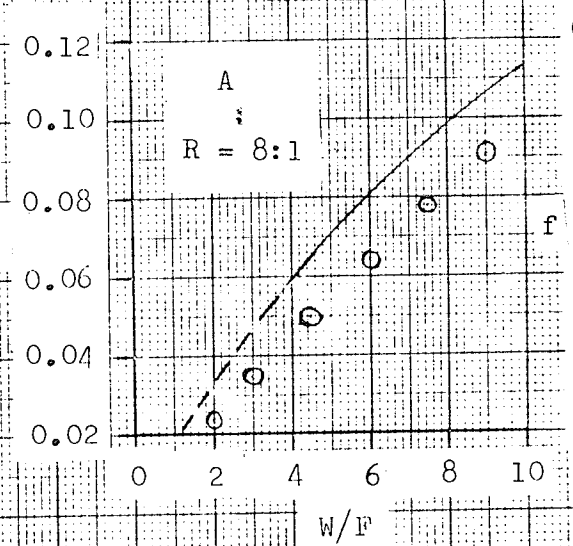

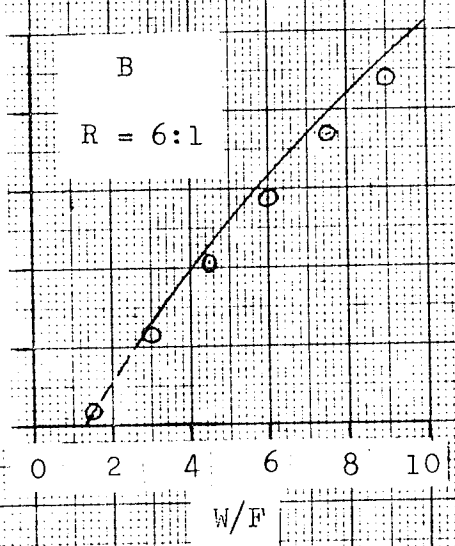

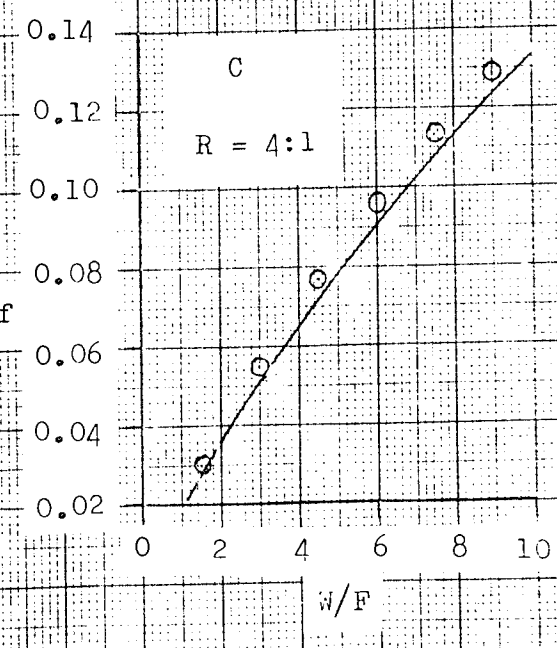

(i) It has been found (57, 63) that hydrogen is an initial product when hydrocarbons catalytically decompose.

(ii) Hydrogen is reported (43, 44, 46, 66, 68) as an initial product of steam-hydrocarbon reforming.

(iii) A mechanism involving radical formation is considered likely by some researchers, (37, 57, 58, 59, 60, 61, 62, 63).

(iv) In the light of (i), (ii) and (iii) a methylene radical is thought to be the most likely.

(v) There is very little evidence in the literature for a mechanism involving a methane decomposition to carbon.

(vi) A steam - CH_4 reaction mechanism involving adsorbed CO product would enhance the CO shift reaction which has been shown to be very much faster than the former.

Since these factors have been taken into account it follows that some other factor could be exerting some influence.

The results obtained in the qualitative studies showed film diffusion resistance to be negligible at the conditions employed. In addition it was shown that the reforming reaction is probably 'chemically' controlled; however, the experimental data from the 304 run series suggest otherwise.

It is considered possible that pore diffusion

resistance exerts some controlling influence over the reaction rate. If pore diffusion resistance alone were rate controlling, the rate of reaction would be expected to rise, assuming similar diffusivities of H_2O and CH_4 molecules, as the steam-methane feed ratio is decreased. However the fact that the reaction rates when operating with feed ratios of 4:1 and 2:1 were the same indicates the possibility of a dual control where the influence of pore diffusion resistance decreases with feed ratio until the point is reached where the 'chemical' resistance is the one of major importance.

6.5. Carbon Deposition.

From experiences gained from the previous experimentation, and considerations regarding the limitations of the apparatus, it was thought unlikely that conditions that give rise to the deposition of equilibrium carbon could be achieved.

Nevertheless, two experimental runs were carried out at 650°C and 250 psig employing feed ratios as low as 0.5:1 and W/F values of 10.35 and 3.50. However, in both cases no outward signs of carbon deposition were obtained, even at the lowest feed ratio which was below the theoretical minimum to prevent equilibrium carbon forming.

When operating with the time factor $(W/F) = 10.35$, the lowest value of the ratio $pCO_2/(pCO)^2$ at 7.525 and calculated from the partial pressures of CO_2 and CO in the product gas was obtained. However, since the equilibrium constant for the Bouduard reaction at the above conditions is :-

(i) over β-graphite $K_p = pCO_2/(pCO)^2 = 2.985\ atm^{-1}$

(ii) over catalyst $K_p = pCO_2/(pCO)^2 = 1.995\ atm^{-1}$

it can be seen that on a thermodynamic basis carbon deposition was unlikely.

Once it was established that deposition could

not be achieved, at the end of the run using a W/F value of 3.50, the water feed was halted, thus allowing methane alone to pass over the catalyst. Within half an hour, the pressure drop across the reactor had changed from zero to 9 psi, and after one hour it had further increased to 19 psi. The run was then terminated and upon dismantling it was found impossible to remove the catalyst rod assembly from the reactor without using force. Therefore it was assumed that the catalyst pellets had expanded and formed a tight 'plug' within the reactor.

By affixing the top of the rod and gently turning the reactor, the assembly was freed. No trace of pelleted catalyst remained on the steel former, and it was found to have broken up completely into a fine powder.

From the above findings it was concluded that carbon deposition must have occurred throughout the catalyst rather than at the pore mouths. This would cause expansion which must have been accompanied by micro-cracking, and hence the complete disintegration into powder when force was applied for removal.

Theories on equilibrium carbon deposition that have been forwarded by researchers (23, 63, 86, 92,93) into this phenomenon, can be used to explain the above observations thus.

In the absence of steam, adsorbed methane decomposes via radical formation to give adsorbed carbon, which, by a structural rearrangement enters the catalyst lattice.

The structural rearrangement must give rise to the expansion, but it is difficult to ascertain whether the cracking was a direct result of this or whether the resistance of the reactor walls to the expansion is the major contributing factor.

6.6. Summary and Conclusions.

The conclusions drawn from the experimental results obtained in the studies described in this chapter may be summarised as follows:-

1. Bulk diffusion resistance was found to be negligible at the conditions of operation, ie. 650°C and 250 psig. This was concluded from the following facts :-

   (i) For varying methane flow rates with the time factor maintained constant, the resulting fractional conversions remained constant.

   (ii) The increase in fractional conversion with temperature was very much greater than that expected from a reaction controlled by film diffusion resistance.

2. The results from the qualitative experiments using temperature as a variable, indicate that the reaction rate is 'chemically' controlled by a simple first order type of equation.

3. Experimental results confirm the findings of other workers in that the steam-methane reaction is very much slower than the CO shift reaction. The former reaction may therefore be considered as rate controlling.

4. The results obtained from the quantitative experimentation show that it is equally possible for two mechanisms to represent the steam-methane reforming reaction:-

Mechanism I

$$(1)\quad CH_4(g) + 1 \rightleftharpoons CH_4(1)$$

$$(2)\quad CH_4(1) + H_2O(g) \rightleftharpoons CO(1) + 3H_2(g)$$

$$(3)\quad CO(1) \rightleftharpoons CO(g) + 1$$

with step (1) controlling.

and Mechanism IV

$$1\quad CH_4(g) + 1 \rightleftharpoons CH_4(1)$$

$$2\quad H_2O(g) + 1 \rightleftharpoons H_2O(1)$$

$$3\quad CH_4(1) + H_2O(1) \rightleftharpoons CO(1) + 3H_2(g) + 1$$

$$4\quad CO(1) \rightleftharpoons CO(g) + 1$$

with step 3 controlling.

5. The reaction rate r for the above mechanisms were found to be represented by:-

Mechanism I 1.

$$r = \frac{k\left(p_{CH_4} - \frac{p_{CO}p^3_{H_2}}{K\ p_{H_2O}}\right)}{1 + K_{CO}p_{CO}p^3_{H_2} + K_{CO}p_{CO} + K_{CO_2}p_{CO_2}} \quad h^{-1}$$

and at 650°C and 250 psig the values of the rate constant and equilibrium constants are:-

$k = 0.00806\ atm^{-1}h^{-1}$

$K_{CO} = 0.0586\ atm^{-1}$

$K_{CO_2} = 3.30\ atm^{-1}$

$K_{SR} = 0.00582\ atm^2$

$K = 2.794\ atm^2$

Mechanism IV 3

$$r = \frac{k\left(p_{CH_4}\ p_{H_2O} - \frac{p_{CO}p^3_{H_2}}{K}\right)}{\left[1 + K_{CH_4}p_{CH_4} + K_{H_2O}p_{H_2O} + K_{CO}p_{CO} + K_{CO_2}p_{CO_2}\right]^2} \quad h^{-1}$$

the values of the constants at 650°C and 250 psig being:-

$k = 0.00262\ atm^{-2}h^{-2}$

$K_{CH_4} = 0.0426\ atm^{-1}$

$K_{H_2O} = 0.09145\ atm^{-1}$

$K_{CO} = 0.04595\ atm^{-1}$

$$K_{CO_2} = 2.382 \text{ atm}^{-1}$$

$$K = 2.794 \text{ atm}^{2}$$

6. The results obtained from the tests carried out to investigate carbon deposition showed that carbon resulting from the catalytic decomposition of methane in the absence of steam, is dispersed throughout the catalyst mass rather than at the pore mouths.

   Carbon deposition was found to cause an expansion of the pellet which was probably due to an adsorption and structural rearrangement and may have given rise to the micro-cracking which occurred in the catalyst pellet.

7. Whilst it cannot be shown conclusively it is considered that pore diffusion resistance exerts some influence over the reaction rate particularly when operating with high feed ratios.

CHAPTER 7.

SUGGESTIONS FOR FUTURE WORK.

It is realised that the investigation described above can only be considered as a small contribution to the knowledge of the mechanism and kinetics of the steam-methane reforming reaction.

The ability to predict product compositions and fractional conversions in relation to time and amounts of catalyst is of great importance in the design of reforming plant. Therefore in order for the kinetic results reported above to have a full practical significance it is necessary that the work be extended to cover ranges of other operating variables and relevant factors.

The following four subjects are those considered the most important and worthy of investigation :-

1. Effect of temperature.
2. Effect of pressure.
3. Effect of flow dynamics.
4. Carbon deposition.
5. Effect of pore diffusion.

1. Effect of temperature.

Each of the equilibrium and velocity constants of the rate equation derived in Chapter 6, will have an exponential relationship with temperature. Hence, rate data collected over a range of temperatures may be used to evaluate the rate constants, thus allowing the relationship between individual constants and temperature to be examined.

Because of the exponential relationships between the rate constants and temperature, as operating temperatures are elevated, it is not impossible for the rate controlling step to change. In the limit, diffusional resistance effects can become controlling, and from the standpoint of catalyst utilisation this can be significant.

For a given catalyst, a diffusion controlled reaction rate is an unsatisfactory condition since this means that whilst the reaction could proceed faster, it cannot because of the physical mass transport of reactants and products.

If in a particular reforming application the product gas requirement is such that the process is operating within the conditions that give rise to diffusional control, by knowing these conditions, requisite changes in catalyst or reactor design to alter the flow characteristics and so move out of the diffusion control region, may be made.

2. Effect of pressure.

Since the development of the process, reformer operating pressures have been gradually increased in order to gain more favourable overall operating efficiencies. It is likely that this trend will continue, therefore a study of the effect of pressure on the reaction rate and mechanism is considered

another worthwhile exercise.

However, because of the unfavourable effect of pressure upon equilibrium product gas compositions it is necessary that operating temperatures also be increased in order to compensate. Therefore the effect of temperature must be established in order that the results of any pressure studies may have a full practical use in design applications.

3. Effect of flow dynamics.

It is obvious from an examination of the literature that few studies relating the flow dynamics of steam-methane reforming systems to the reaction rate have been made. Flow conditions will not only affect the mass transfer of components, but because of the strongly endothermic nature of the reforming reaction, the heat transfer characteristics and resulting temperatures within a reformer tube will also be influenced by flow conditions.

Under some conditions of flow, large radial and longitudinal differences can exist within a reformer tube, and correspondingly give rise to varying reaction rates. Such situations can have serious consequences, not only from the standpoint of achieving required conversions, but in the effect of thermal stresses throughout the reformer tube metal itself. Therefore experimental or theoretical studies that lead to a method of calculating

radial and longitudinal temperature and composition distributions will have a great value in the design field.

4. Carbon deposition.

Carbon deposition is one of the major limiting conditions of the reforming process, since carbon formation not only reduces the activity of the catalyst, but can also reduce its mechanical strength.

It was indicated above that because of pressure considerations, reformer operating temperatures are being increased as the process is developed. Whilst such changes will increase the rate of the reforming reaction, the rate of any catalytic or thermal decomposition reactions will also be increased.

With respect to equilibrium carbon formation, it was shown in the literature survey that a number of workers have found that at certain temperatures, theoretical minimum feed ratios are higher than those determined experimentally. The only publications found that present extensive quantitative data are those of Dent (23) and Hebden (86). Therefore, any studies directed towards establishing mechanisms and relative rates of carbon formation/removal that lead to a precise method of predicting the conditions that give rise to carbon deposition, will be of great importance.

Also the structural rearrangement of the catalyst

that accompanies the formation and adsorption of carbon merits investigation, and techniques such as X-ray diffraction will have to be used for such studies.

5. Effect of pore diffusion.

Pore diffusion resistance can have a marked influence on reaction rates and in addition it can also be an important factor with respect to carbon deposition. If pore diffusion resistance does control the reaction rate, then the gas composition within the catalyst structure will differ greatly from that in the bulk gas stream, and therefore it is possible for carbon deposition conditions to exist within the pores whilst the bulk composition would indicate otherwise.

Knowledge of the extent of pore diffusion resistance would not only eleminate the problem referred to above, but would be important with respect to the design and construction of effecient catalyst pellets.

In order to determine the extent of pore diffusion resistance a number of methods are available, but particularly the determination of effectiveness factors can give a very good indication. A method for doing this is given by Hougen and Watson (128) and essentially it involves differential rate measurement as a function of temperature for two widely different catalyst sizes, holding partial pressures constant at each temperature.

APPENDIX A.

PROCESS FLOW DIAGRAM AND SPECIFICATION.

PROCESS FLOW DIAGRAM

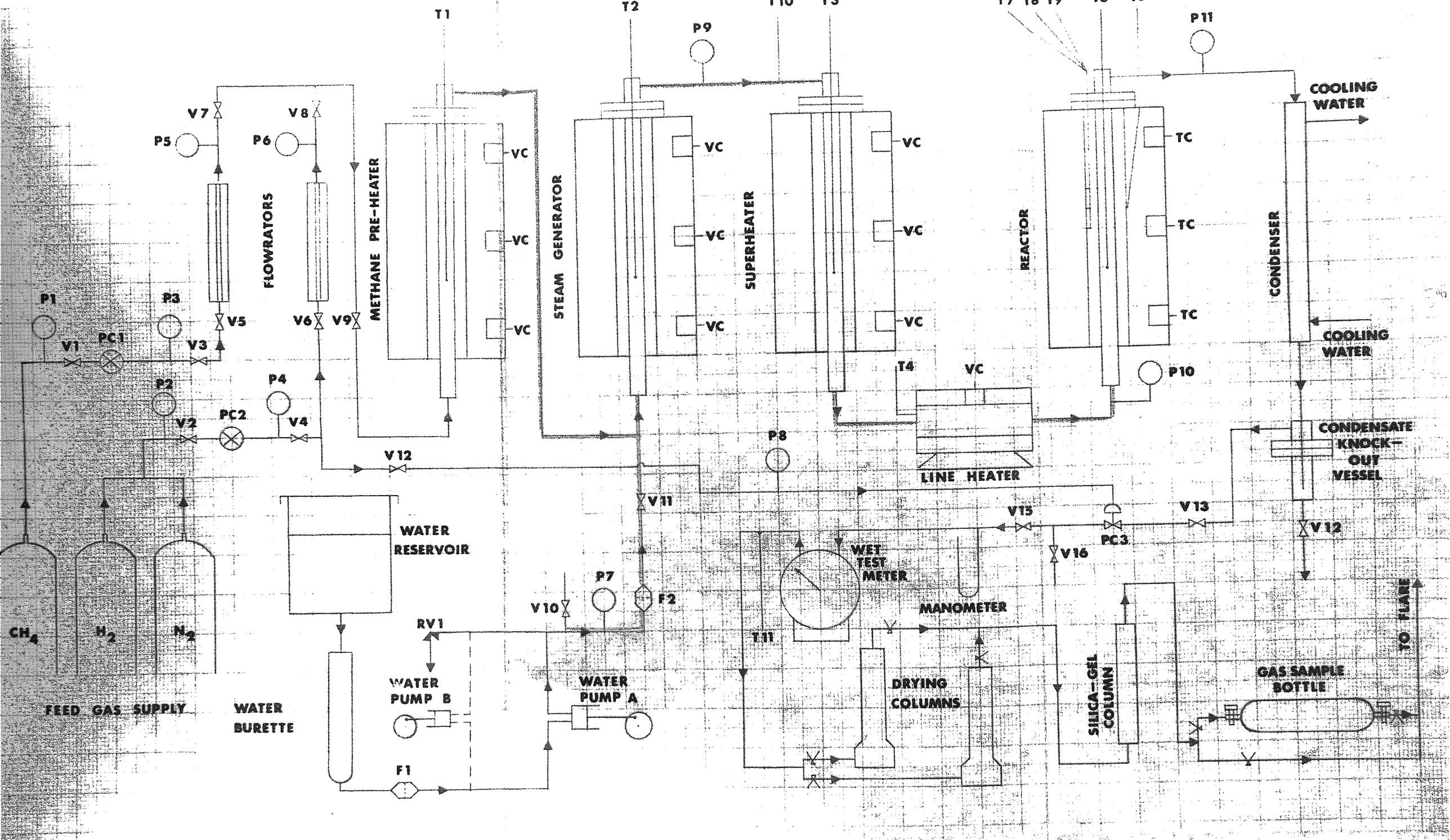

LEGEND AND SPECIFICATION.

P1, P2. Budenberg 0-2000 psig Pressure Gauge.

P3, P4. Budenberg 0-800 psig Pressure Gauge.

P5 - P11. Budenberg 0-400 psig Pressure Gauge.

V1, V2, V11. Hale-Hamilton $\frac{1}{4}$ inch Gate Valve.

V3, V4. Ermeto $\frac{1}{4}$ inch Needle Valve.

V5 - V10, V13 - V16. Ermeto $\frac{1}{4}$ inch Gate Valve.

V12. Ermeto $\frac{1}{8}$ inch Needle Valve.

PC1, PC2. Hale-Hamilton $\frac{1}{4}$ inch Type L15 Pressure Control Valve.

PC 3. Hale-Hamilton $\frac{1}{4}$ inch Type DR2 Pressure Control Valve.

RV1. Ermeto $\frac{1}{4}$ inch Relief Valve.

T1-T5, T10. Pyrotenax 1/16 inch NiCr/NiAl Thermocouple.

T6-T9. Pyrotenax 20/1000 inch NiCr/NiAl Thermocouple.

T11. 0-240°F Hg in Glass Thermometer.

F1. Fritted Glass Filter.

F2. Ermeto $\frac{1}{4}$ inch Brass Mesh Filter.

— Heating Tape and Lagging.

VC. Variac Controlled.

TC. Temperature Controller.

 Heater Winding.

 Mohr Clips.

Feed Gases.

Methane : Supplied by B.O.C. High Purity 99.9%.

Nitrogen : Supplied by B.O.C. 'White Spot'.

Hydrogen : 'High Purity'.

Feed Water.

De-ionised water.

Water Pumps.

1. F.A.Hughes (D.C.L.) 'M' pump, 0-750 cc/h capacity. $\frac{1}{8}$ inch Stainless steel plunger head with micrometer type stroke adjustment.

2. F.A. Hughes (D.C.L.) Micro pump, 0-150 cc/h capacity. Stainless steel plunger head size 2 with micrometer type stroke adjustment.

Water Burette.

Capacity 0 - 2 litres.

Flowrators.

Fischer and Porter 'tri-flat' variable area flowrators.

Ancillary Heating Vessels.

Overall length	-	33 inches.
Outside diameter	-	1 inch.
Inside diameter	-	$\frac{3}{4}$ inch NB.
Construction	-	Stainless steel.
Connections	-	$\frac{1}{4}$ inch OD. 'Ermeto'.
Head Joint	-	$1\frac{5}{8}$ inch 'gramaphone record' flanges.
Gasket	-	1/16 inch, $\frac{3}{4}$ B.S.T.-H Klingerit.
Thermowell	-	$\frac{1}{8}$ inch OD. Stainless steel.
Packing	-	Silica chips.

Reactor.

Overall length	-	33 inches.
Outside diameter	-	1.1/16 inch.
Inside diameter	-	$\frac{3}{4}$ inch N.B.
Construction	-	Stainless Steel.
Connections	-	$\frac{1}{4}$ inch O.D. 'Ermeto'.
Head Joint	-	'Rushton' metal-metal.
Thermowell	-	$\frac{1}{8}$ inch OD. Stainless steel.

Main Furnaces.

All of the main furnaces were of similar construction and had three windings on a $2\frac{1}{2}$ inch ID. silica tube. A Main winding provided the majority

of the heat load, and the remaining two windings provided an end-loss compensation.

The respective out-puts were :-

Main winding 2 Kwatts.

End windings 0.2 Kwatts.

Condenser.

Copper outer jacket, 2 ft.long, $\frac{7}{8}$ inch O.D.

Stainless steel $\frac{1}{4}$ inch OD. centre core.

Wet Test Gas Meter.

Parkinson-Cowan Type A Wet test meter.

Accuracy = $\pm$ 0.1% at 1,000 rev/h.

Capacity = 2o cu.ft/h.

Instrumentation.

Reacter Internal Temperature : Measured using a moveable thermocouple (T6) and a Cambridge portable potentiometer, (workshop pattern).

Other Temperatures : Thermocouples T 1, 2, 3, 5, and 10 fed in parallel to (i) a 'Sangmo-Weston' multipoint switch with a single output on a 0-600°C temperature indicator, and (ii) an 'Electroflow' 0-800°C six point continuous recorder. Thermocouple T4 was fed independently to a second temperature indicator.

Reactor Temperature Control.

The reactor temperature was controlled by Ether Transitrol Type 990 Controllers. Each of the windings in the reactor furnace was connected via a 'Donovan' relay (Size 0) to a controller. Thermocouples T 7 - 9 were the sensing inputs to the three controllers which were modified to operate with the high external resistance (100 Ω) of the thin gauge thermocouples.

APPENDIX B.

MODEL EXAMPLE OF THE CALCULATION REQUIRED TO CALIBRATE THE FISCHER AND PORTER FLOWRATORS.

CALIBRATION OF A FLOWRATOR FOR METHANE.

Tube and Float Data.

Tube diameter	$\frac{1}{8}$ inch
Scale Calibration	0 - 8
Scale length	5 inches
Float material	Sapphire
Float density (ρ_f)	3.98 g/cm^3

Operating Conditions.

Pressure	250 psig
Temperature	Ambient (70°F)

Tube size factors (108).

A - 404

B - 76.8

Fluid properties.

Methane viscosity at S.T.P. = 0.01099 cp

Methane density at S.T.P. = 0.0006653g/cm^3

Standard temperature and pressure (S.T.P.) is :-
70°F and 14.7 psia respectively.

Operating viscosity μ OPT :

From Perry (126), pressure correction to the viscosity is negligible.

Temperature correction is given by :-

$$\mu_{OPT} = \mu_{STP} + (\text{temp coeff})\ (t - 70)$$

where t is the operating temperature.

Since $t = 70^{\circ}F$, $\mu_{OPT} = \mu_{STP} = 0.01099$ cp.

Operating density ρ_{OPT} :

From the Fischer and Porter handbook (108),

$$\rho_{OPT} = \rho_{STP} \times R$$

where $R = \rho_{OPT} / \rho_{STP}$

and $$R = \frac{P}{14.7} \times \frac{530}{460 + t}$$

where P = operating pressure psia.

Hence R = 18.01

Therefore $\rho_{OPT} = 0.0006653 \times 18.01$

$= 0.012\ g/cm^3$

Viscous Influence Number N.

$$N = \frac{A}{\mu_{OPT}} \sqrt{(\rho_f - \rho_{OPT})\,\rho_{OPT}}$$

$$= \frac{404}{0.01099} \sqrt{(3.98 - 0.012)(0.012)}$$

$$= 80.21 \times 10^2$$

Flow Rate W g/min at O.P.T.

$$W = CB\sqrt{(\rho_f - \rho_{OPT})\rho_{OPT}} \quad g/min$$

where C is a flow coefficient

$$W = C \times 76.8 \times \sqrt{(3.98-0.012)(0.012)}$$

$$= 1005.5 \times C \quad g/h.$$

From a Float characteristic curve (108), and using the value of N calculated previously, the following table may be constructed.

Scale Reading	C	W g/h
1	0.0081	8.135
2	0.0321	32.24
3	0.0512	51.40
4	0.0740	74.35
5	0.0998	100.2
6	0.1240	124.5
8	0.1775	178.2

From the above data a calibration curve can be plotted.

APPENDIX C.

MODEL EXAMPLE OF A MASS BALANCE.

Mass Balance for Run 104.

Experimental Data :

Methane flow rate - 83.0 g/h

Water feed rate - 280 g/h

Experimental Results :-

Test	Running Time	Dry Product Composition			
	hr	$\%H_2$	%CO	$\%CH_4$	$\%CO_2$
a	0.5	15.54	0.23	81.59	2.64
b	1.0	15.21	0.24	81.74	2.81
c	1.5	15.14	0.24	81.56	3.06
d	2.0	15.24	0.25	81.31	3.20
e	2.5	15.36	0.23	81.39	3.02
	Average	15.30	0.24	81.52	2.95

Test Meter reading at 0.5 h - 169920

Test Meter reading at 2.5 h - 170423

Metering pressure - 5 inches W.G.

Metering temperature - $72^{o}F$.

Mass Balance over 2h (tests a to e)

Moles methane in = $\frac{83.0 \times 2}{16}$ = 10.375

Moles water in = $\frac{280 \times 2}{18}$ = 31.111

Moles Carbon feed = 10.375

Moles Hydrogen (H_2) feed = 31.111 + 2 x 10.375

= 51.861

Moles Oxygen (O_2) feed = 31.111/2

= 15.556

Product Gas out = Δ Test Meter x meter factor.

= 5.03 x 0.02 ft^3

= 10.06 ft^3

Product Gas out at 32°F and 1 atm pressure is :-

$$10.06 \times \frac{492}{532} \times \frac{401}{396} \quad ft^3$$

At 32°F and 1 atm, 1 lb mole occupies 359 ft^3

$\therefore$ lbs moles product gas is :-

$$10.06 \times \frac{492}{532} \times \frac{401}{396} \times \frac{1}{359}$$

$$= 10.06 \times \frac{492}{532} \times \frac{401}{396} \times \frac{453.6}{359} \quad \text{g moles}$$

= 11.90 g moles.

Based on the average composition and the total moles, the product gas is found to contain :-

1.82	g moles	H_2
0.03	g moles	CO
9.70	g moles	CH_4
0.35	g moles	CO_2
11.90	g moles	Total

Condensate collected = 551 g

= 30.611 g/moles

Moles Hydrogen (H_2) out = 1.82 + 30.611 + 9.70 x 2

= 51.831

Moles Carbon out = 0.03 + 9.70 + 0.35

= 10.08

Moles Oxygen (O_2) out = 0.35 + 0.015 + 30.611/2

= 15.671

Summary

	Moles in	Moles out
Hydrogen	51.861	51.831
Carbon	10.060	10.080
Oxygen	15.556	15.671

APPENDIX D.

THE FINAL COMPUTER PROGRAM (PROGRAM 2).

```
STEAM HYDROCARBON REFORMING
BEGIN REAL  A,N,K5,K7,K13,X,Y,X1,Y1,L,M,Q,R,S,F,U,V,G,W,Z,B,
            C,D,E, CORREX,CORREY,CRATIO,CARBON,RATIO,CATOM'
INTEGER  T,P'
SWITCH SS:=REPEAT,OUT'
READ CATOM'
A:= (CATOM-1) / (3*CATOM+1)'
FOR P:=10 STEP 5 UNTIL 25 DO BEGIN
FOR T:=723 STEP 25 UNTIL 1173 DO BEGIN
N:= 5.0'                          CARBON :=0'
K5:= EXP(-10.09325-23576/T + 5.65408*LN(T) -0.0021022*T)'
K7:= EXP(-13.43 + 5405/T + 1.208 *LN(T))'
K13:= EXP(-22.7164 + 21188.26/T + 0.05212 *LN(T) +5.3096*T/10000)'
PRINT ££L2?CATOM=?,CATOM,££L?T=?,T,££L?P=?,P,££L?K5=?,K5,
      ££S4?K7=?,K7,££S4?K13=?,K13,
      ££L2?CARBON     RATIO     CO     CO2     H2     CH4?'
X1:=0.5'                          Y1:=0.5'
REPEAT :X:=X1'                    Y:=Y1'
L:= X**4*(4*K5-27*P**2)'
M:= X**3*(4*K5*(A+Y))'
Q:=X**2*(K5*(4*N*Y-2*N-3*N**2-3-2*N*A-2*A=4*Y*A+A**2)
         +18*Y**2*P**2)'
R:= X*(K5*(N**2-N**3+N+N**2*Y-2*N*Y-3*Y-1-2*A-A**2-2*A*Y-2*N**2*A
       -N*A**2+2*N*Y*A+Y*A**2)+8*P**2*Y**3)'
```

```
S:= K5*(N**3+2*N**2-N**2*Y+N-2*N*Y-Y+2*N**2*A+2*N*A+N*A**2
      -2*N*Y*A-2*Y*A-Y*A**2)+P**2*Y**4'

F:= L+M+Q+R+S'

U:= (L*4/X)+(M*3/X)+Q*2/X)+R/X'

V:= 4*Y**3*P**2+24*X*P**2*Y**2+36*X**2*P**2*Y+K5*(4*X**3
   +4*N*X**2+4*A*X**2+N**2*X-2*N*X-3*X-2*A*X+2*N*A*X
   +A**2*X-N**2-2*N-1-2*N*A-2*A-A**2)'

G:= (-1)*X**2*K7+X*(K7*N-3*A-3*Y)+K7*(Y**2-N*Y)-(A*Y+Y**2)'

W:= (-2)*X*K7+K7*N-3*A-3*Y'

Z:= 2*Y*(K7-1)-K7*N-(A+3*X)'

CORREY:=(-1)*(W*F-U*G)/(V*W-Z*U)'

CORREX:=((-1)*F-CORREY*V)/U'

X1:=X+CORREX'                    Y1:=Y+CORREY'

IF ABS(X-X1) GR 0.00005 THEN GOTO REPEAT'

IF ABS(Y-Y1) GR 0.00005 THEN GOTO REPEAT'

CRATIO:= (A+Y)*(N+1+2*X+A)/((X-Y)**2*P)'

IF CRATIO GR K13 THEN GOTO OUT'

CARBON:= 1.0'

N:= N+0.01'                      GOTO REPEAT'

OUT:B:=((X-Y)/(N+1+2*X+A))*100'
    C:=((A+Y)/(N+1+2*X+A))*100'
    D:=((N-X-Y)/(N+1+2*X+A))*100'
    E:=((3*X=Y)/(N+1+2*X+A))*100'
    F:=((1-X)/(N+1+2*X+A))*100'
    B:=(B*100)/(100-D)'
```

```
      C:=(C*100)/(100-D)'
      E:=(E*100)/(100-D)'
      F:=(F*100)/(100-D)'

RATIO:=(N+2*A)*(3*CATOM+1)/(4*CATOM)'

PRINT  ££LS2??,  FREEPOINT(2),  CARBON,  SAMELINE,
       ££S5??,   FREEPOINT(3),  RATIO,
       ££S6??,   FREEPOINT(5),  B,
       ££S5??,   FREEPOINT(5),  C,
       ££S4??,   FREEPOINT(5),  E,
       ££S4??,   FREEPOINT(5),  F'

IF  CARBON  LESS  0.5  THEN BEGIN  N:=N-0.15'

GOTO  REPEAT'

END'

END'

END'

END'
```

APPENDIX E.

RESULTS OF THE 200 SERIES OF EXPERIMENTS CARRIED OUT FOR THE QUALITATIVE EXPERIMENTAL STUDIES.

RUN 201

Mass of Catalyst = 5.5565 gms

Operating Pressure = 250 psig

St./CH_4 Feed Ratio = 3/1

W/F Ratio = 3.15 gms catalyst/mole CH_4/h

CH_4 Feed Rate = 1.77 gm moles/h

Test	Product Composition				Operating Temperature	Fractional Conversion
	%H_2	%CO	%CH_4	%CO_2	°C	f
a	12.17	0.18	84.59	3.06	584	0.036
b	15.08	0.22	81.18	3.52	615	0.044
c	14.91	0.22	81.43	3.44	617.5	0.045
d	16.49	0.32	79.60	3.59	628	0.046
e	18.81	0.51	76.94	3.74	655	0.054
f	19.56	0.58	75.49	4.37	662	0.060
g	20.01	0.73	75.33	3.93	664	0.058
h	24.10	0.87	69.96	5.07	692	0.077
i	24.11	0.87	69.98	5.04	692.5	0.077

RUN 202

Mass of Catalyst = 11.2219 gms

Operating Pressure = 250 psig

St./CH_4 Feed Ratio = 3/1

W/F Ratio = 3.15 gms catalyst/g moles CH_4/h

CH_4 Feed Rate = 3.56 g moles/h

Test	Product Composition				Operating Temperature	Fractional Conversion
	%H_2	%CO	%CH_4	%CO_2	°C	f
a	11.63	0.18	85.90	2.29	590	0.029
b	13.11	0.22	83.77	2.90	606	0.036
c	13.69	0.20	83.74	2.37	608	0.030
d	15.45	0.40	80.42	3.72	643.5	0.050
e	18.83	0.51	76.60	4.06	659	0.056
f	18.99	0.51	76.48	4.02	660	0.056
g	21.28	0.66	73.47	4.59	679	0.068
h	23.98	0.88	70.00	5.15	701	0.080

RUN 203

Mass of Catalyst = 16.3031 gms

Operating Pressure = 250 psig

St./CH_4 Feed Ratio = 3/1

W/F Ratio = 3.15 gms catalyst/g mole CH_4/h

CH_4 Feed Rate = 5.18 gms/h

Test	Product Composition				Operating Temperature	Fractional Conversion
	%H_2	%CO	%CH_4	%CO_2	°C	f
a	15.19	0.08	81.44	3.29	586	0.040
b	15.54	0.08	81.23	3.15	586.5	0.037
c	16.00	0.11	80.69	3.20	618	0.039
d	15.84	0.11	80.51	3.54	619	0.044
e	18.93	0.23	77.35	3.49	643	0.046
f	19.44	0.26	76.02	4.28	655	0.057
g	21.48	0.53	73.49	4.50	674.5	0.066
h	21.49	0.49	73.56	4.46	677	0.063
i	22.87	0.57	71.89	4.67	681.5	0.068
j	23.42	0.61	71.59	4.38	686.5	0.079
k	26.81	0.95	66.85	5.39	701	0.086
l	26.50	0.91	67.37	5.22	703	0.085

RUN 204

Mass of Catalyst = 21.8028 gms
Operating Pressure = 250 psig
St./CH_4 Feed Ratio = 3/1
W/F Ratio = 3.15 gms catalyst/g mole CH_4/h
CH_4 Feed Rate = 6.925 g mole/h

Test	Product Composition				Operating Temperature	Fractional Conversion
	%H_2	%CO	%CH_4	%CO_2	°C	f
a	13.70	0.18	83.39	2.48	588	0.031
b	13.66	0.18	83.39	2.76	592	0.034
c	15.67	0.37	80.92	3.04	618	0.041
d	15.55	0.37	80.68	3.40	621	0.044
e	18.86	0.51	76.71	3.92	648	0.054
f	18.99	0.51	76.47	4.03	648.5	0.056
g	22.03	0.78	72.38	4.81	678	0.073
h	24.56	0.94	69.25	5.25	696	0.082

RUN 205

Mass of Catalyst = 2.5575 gms

Operating Pressure = 250 psig

St./CH_4 Feed Ratio = 3/1

Temperature = 700°C ± 2°C

Test	Product Composition				CH_4 Feed Rate	W/F Ratio	Fractional Conversion
	%H_2	%CO	%CH_4	%CO_2	g moles/h	h	f
a	19.17	0.33	76.48	4.02	1.0230	2.5	0.054
b	25.21	0.89	68.69	5.21	0.6394	4.0	0.082
c	28.95	1.13	63.89	6.03	0.4262	6.0	0.103
d	30.72	1.35	61.21	6.72	0.3197	8.0	0.116
e	32.60	1.45	58.87	7.08	0.2558	10.0	0.127

RUN 206

Mass of Catalyst = 5.5886 gms.

Operating Pressure = 250 psig

St/CH_4 Feed Ratio = 3/1

Temperature = 700°C ± 2°C

Test	Product Composition.				CH_4 Feed Rate	W/F Ratio	Fractional Conversion
	$\%H_2$	%CO	$\%CH_4$	$\%CO_2$	g moles/h	h	f
a	25.92	0.41	69.75	3.92	2.7943	2	0.058
b	29.48	0.98	63.27	6.27	1.3972	4	0.102
c	32.91	1.44	58.66	6.99	0.9314	6	0.131
d	35.28	1.77	55.67	7.23	0.6986	8	0.140
e	36.49	1.96	53.81	7.74	0.5589	10	0.153

RUN 207

Mass of Catalyst = 11.5036 gms.

Operating Pressure = 250 psig

St/CH_4 Feed Ratio = 3/1

Temperature = 700 ± 2°C

Test	Product Composition.				CH_4 Feed Rate	W/F Ratio	Fractional Conversion
	$\%H_2$	%CO	$\%CH_4$	$\%CO_2$	g moles/h	h	f
a	17.86	0.62	77.40	4.12	5.7518	2	0.059
b	26.11	0.92	66.98	5.99	2.8759	4	0.094
c	32.25	1.18	59.12	7.45	1.9173	6	0.126
d	36.36	1.32	53.91	8.41	1.4380	8	0.155
e	38.41	1.51	51.01	9.07	1.1504	10	0.172

RUN 208

Mass of Catalyst = 16.6323 gms

Operating Pressure = 250 psig.

St/CH_4 Feed Ratio = 3/1

Temperature = 700 ± 2°C

Test	Product Composition				CH_4 Feed Rate	W/F Ratio	Fractional Conversion
	$\%H_2$	%CO	$\%CH_4$	$\%CO_2$	g moles/h	h	f
a	21.70	0.62	73.62	4.06	8.3162	2	0.059
b	28.81	1.09	64.02	6.08	4.1581	4	0.101
c	34.70	1.38	56.62	7.30	2.7721	6	0.133
d	38.66	1.55	51.68	8.11	2.0791	8	0.156
e	40.68	1.83	48.65	8.84	1.6632	10	0.180

RUN 209

Mass of Catalyst = 22.2432 gms

Operating Pressure = 250 psig

St/CH_4 Feed Ratio = 3/1

Temperature = 700 ± 2°C

Test	Product Composition				CH_4 Feed Rate	W/F Ratio	Fractional Conversion
	%H_2	%CO	%CH_4	%CO_2	g moles/h	hr^{-1}	f
a	20.31	0.63	74.80	4.26	11.1216	2	0.061
b	26.49	0.97	67.00	5.54	5.5608	4	0.088
c	30.66	1.19	61.56	6.59	4.0430	5.5	0.112
d	33.78	1.39	57.65	7.18	3.1776	7	0.130
e	37.57	1.63	52.92	7.88	2.4716	9	0.152

RUN 210

Mass of Catalyst = 11.5036 gms

Operating Pressure = 100 psig

St/CH_4 Feed Ratio (mole/mole) = 3/1

Temperature = 700°C ± 2°C

Test	Product Composition				CH_4 Feed Rate	W/F Ratio	Fractional Conversion
	%H_2	%CO	%CH_4	%CO_2	g moles/h	hr^{-1}	f
a	15.11	0.43	81.30	3.16	5.7518	2	0.042
b	23.15	0.72	71.00	5.13	2.8759	4	0.076
c	27.22	0.96	65.62	6.20	1.9173	6	0.098
d	32.96	1.28	58.45	7.31	1.4380	8	0.128
e	37.43	1.34	52.72	8.51	1.1504	10	0.157

RUN 211

Mass of Catalyst = 11.5036 gms

Operating Pressure = 25 psig

St/CH_4 Feed Ratio(Mole/mole) = 3/1

Temperature = 700°C ± 2°C

Test	Product Composition				CH_4 Feed Rate	W/F Ratio	Fractional Conversion
	$\%H_2$	%CO	$\%CH_4$	$\%CO_2$	g/moles/h	hr^{-1}	f
a	10.74	0.33	86.80	2.13	5.7518	2	0.028
b	18.40	0.70	76.98	3.92	2.8759	4	0.057
c	23.09	0.73	70.75	5.43	1.9173	6	0.080
d	26.86	0.95	65.79	6.40	1.4380	8	0.100
e	30.95	1.21	60.57	7.27	1.1504	10	0.123

APPENDIX F.

RESULTS OF THE 300 SERIES OF EXPERIMENTS CARRIED OUT FOR THE QUANTITATIVE EXPERIMENTAL STUDIES.

RUN 301

Mass of Catalyst = 10.8616 gms

Operating Pressure = 250 psig

St/CH_4 Feed Ratio (mole/mole) = 8/1

Temperature = 650°C ± 2°C

Test	CH_4 Feed Rate	W/F Ratio	Product Composition			
	moles/h	h	$\%H_2$	%CO	$\%CH_4$	$\%CO_2$
a	2.7154	4.0	18.96	0.29	76.52	4.23
b	2.7154	4.0	19.02	0.29	76.36	4.33
c	2.1723	5.0	22.77	0.33	71.64	5.26
d	2.1723	5.0	22.48	0.33	71.98	5.21
e	1.6705	6.5	26.05	0.41	67.63	5.91
f	1.6705	6.5	25.02	0.37	68.72	5.89
g	1.4485	7.5	26.94	0.44	66.32	6.30
h	1.4485	7.5	27.05	0.44	66.05	6.46
i	1.2068	9.0	29.59	0.52	62.86	7.03
j	1.2068	9.0	29.14	0.52	63.63	6.71
k	1.0862	10.0	30.88	0.59	61.21	7.32
l	1.0862	10.0	30.88	0.59	61.21	7.32

RUN 302

Mass of Catalyst = 10.8616 gms

Operating Pressure = 250 psig

St/CH_4 Feed Ratio (mole/mole) = 6/1

Temperature = 650°C ± 2°C

Test	CH_4 Feed Rate	W/F Ratio	Product Composition			
	moles/h	h	$\%H_2$	%CO	$\%CH_4$	$\%CO_2$
a	3.6205	3.0	15.85	0.25	80.35	3.55
b	3.6205	3.0	15.74	0.25	80.32	3.69
c	2.7154	4.0	18.95	0.36	76.23	4.46
d	2.7154	4.0	18.84	0.33	76.54	4.29
e	1.9750	5.5	24.35	0.40	69.43	5.82
f	1.9750	5.5	23.54	0.40	70.26	5.80
g	1.4485	7.5	27.69	0.58	65.14	6.59
h	1.4485	7.5	26.64	0.55	66.23	6.59
i	1.2068	9.0	30.79	0.72	61.26	7.23
j	1.2068	9.0	29.70	0.69	62.37	7.24
k	1.0862	10.0	31.08	0.80	60.35	7.77
l	1.0862	10.0	30.45	0.72	61.26	7.57

RUN 303

Mass of Catalyst = 10.8616 gms

Operating Pressure = 250 psig

St/CH_4 Feed Ratio (mole/mole) = 4/1

Temperature = 650°C ± 2°C

Test	CH_4 Feed Rate	W/F Ratio	Product Composition			
	mole/h	h	$\%H_2$	%CO	$\%CH_4$	$\%CO_2$
a	5.4308	2.0	12.68	0.24	84.25	2.83
b	5.4308	2.0	12.60	0.25	84.31	2.84
c	3.1008	3.5	18.92	0.44	76.27	4.37
d	3.1008	3.5	17.71	0.37	77.71	4.22
e	2.1723	5.0	23.88	0.57	70.01	5.54
f	2.1723	5.0	22.75	0.51	71.35	5.39
g	1.5517	7.0	27.41	0.73	65.36	6.50
h	1.5517	7.0	27.36	0.77	65.57	6.30
i	1.2775	8.5	29.66	0.94	62.16	7.24
j	1.2775	8.5	29.61	0.91	62.19	7.29
k	1.0862	10.0	31.40	1.13	59.75	7.72
l	1.0862	10.0	32.45	1.20	58.51	7.84

RUN 304

Mass of Catalyst = 10.8616 gms.

Operating Pressure = 250 psig

St/CH_4 Feed Ratio (mole/mole) = 2/1

Temperature = 650 ± 2°C

Test	CH_4 Feed Rate	W/F Ratio	Product Composition			
	mole/h	h	$\%H_2$	%CO	$\%CH_4$	$\%CO_2$
a	10.8616	1.0	7.24	0.18	91.12	1.46
b	10.8616	1.0	7.52	0.18	90.40	1.90
c	5.4308	2.0	13.03	0.36	83.56	3.05
d	5.4308	2.0	12.84	0.34	84.01	2.81
e	3.6205	3.0	16.87	0.53	78.90	3.70
f	3.6205	3.0	16.54	0.49	79.23	3.63
g	2.7154	4.0	19.41	0.69	75.62	4.28
h	2.7154	4.0	19.19	0.67	75.78	4.36
i	1.8103	6.0	24.77	0.94	68.52	5.77
j	1.8103	6.0	25.35	1.02	67.71	5.92
k	1.3577	8.0	28.33	1.37	63.86	6.44
l	1.3577	8.0	28.15	1.30	64.05	6.50

B I B L I O G R A P H Y

(1) Byrne P.J., Gohr E.J., Ind.Eng.Chem., 24,1129,1932.

(2) Haslam R.T., Russell R.P., Ind.Eng.Chem., 22,1030, 1930.

(3) Murphree E.V., Brown C.L., Gohr E.J., Ind. Eng. Chem., 32, 1203, 1940.

(4) Cope W.C., Chemical Ind.(Phil), 64, 920, 1949.

(5) Arnold M.R., Kenton Atwood, Baugh H.M., Smyser H.D., Ind.Eng.Chem., 44, 999, 1952.

(6) Reed R.H., Am.Inst.Chem.Eng.J, 41, 453, 1945.

(7) Shearon W.H., Seestrom H.E., Hughes J.P., Ind.Eng. Chem., 42, 1266, 1950.

(8) Borgars D.T., Ind.Chemist, April, 177, 1963.

(9) Andrews S.P.S., Chemistry & Industry, 20, 826, 1965.

(10) Andrews S.P.S., Inst.Fuel Proc.(Eastbourne Conf), 1965.

(11) Eickmeyer A.G., Marshall W.H., Chem.Eng.Prog., 51, 419, 1955.

(12) Estruch B., Lyth C., Materials Technology in Steam Reforming Processes, Pergamon, London, 1966.

(13) Clark A.A.H., Roberts G.F.J., Savage P.J., Spivey E., J.Inst.Gas.Eng., 6, 20, 1966.

(14) Eastman D., Ind.Eng.Chem., 48, 1118, 1956.

(15) Milner M.J., Chem.Proc.Eng., 235, May, 1965.

(16) Cribb G.S., Brit.Chem.Eng., 9, 366, 1964.

(17) Twist D.R., Sagar K.J., Chem.Engr., Oct., CE252, 1965.

(18) Fox & Yarze, Ind.Chemist, Feb.,65, 1963.

(19) Edeleanu C., (Ed), Materials Technology in Steam Reforming Processes, Pergamon,, London, 1966.

(20) Milner M.J., Chem.Proc.Eng., 208, April, 1965.

(21) Wilson D.S., The Modern Gas Industry, Arnold, London, 1968.

(22) Gasmaking, B.P. Publication, London, 1965.

(23) Dent F.J., Principles of the New Gas Making Processes, Gas Council, M.R.S.

(24) Cockerham R.G., Percival G., Yarwood T.A., Inst. Gas. Eng. J., 5, 109, 1965.

(25) Cockerham R.G., Percival G., Trans.Inst.Gas.Eng., 107, 390, 1957.

(26) Collins E.E., Wesley M.W., Joint Meeting of Mid.sec. Inst.Gas Eng. and Mid.Jnr. Gas Assoc., 3rd Nov, 1967.

(27) Rooke D.E., Inst.Gas.Engrs. J., 7, 586, 1967.

(28) Steacie E.W.R., Puddington I.E., Can.J.Research, 16B, 176, 1938.

(29) Steacie E.W.R., Puddington I.E., Can.J.Research, 16B, 260, 1938.

(30) Steacie E.W.R., Puddington I.E., Can.J.Research, 16B, 411, 1938.

(31) Kassel L.S., J. Am. Chem.Soc., 54, 3949, 1932.

(32) Storch H.H., J.Am. Chem.Soc., 54,4188, 1932.

(33) Belchetz L., Rideal E.K., J.Am.Chem.Soc., 57, 1168, 1935.

(34) Marschner R.F., Ind.Eng,Chem., 30, 554, 1938.

(35) Roberts R.W., Nature, 191, 170, 1961.

(36) Kemball C., Taylor H.S., J.Am.Chem.Soc., 20, 345, 1948.

(37) McKee D., J.Am.Chem.Soc., 84,1109, 1962.

(38) Greensfelder B.S., Voge H.H., Ind.Eng.Chem., 37, 514, 1945.

(39) Geniesse J.C., Reuter R., Ind. Eng.Chem., 24, 219, 1932.

(40) Anderson J.R., Baker B.G., Proc.Royal Soc., 271, 402, 1963.

(41) Yoshiro Morita, Suemiko Yoshitomi, Konichi Yamamoto, Mem.School Sci. Eng., Waseda Univ., Tokyo, No.26, 27, 1962. (C.A. Vol 60, 10441d).

(42) Suemiko Yoshitomi, Kogyo Kagaku Zasshi, 63, 2134, 1960 (C.A. Vol 57, 114d).

(43) Cryder D.S., Porter D.J., Ind.Eng.Chem., 29, 667, 1937.

(44) Slovokhotova T.A., Ivanov A.P., Vestnik,M.G.U., Ser.Fiz. - Mat.i Estestven, Nauk., No.2, 125, 1951. (C.A. Vol 46 4340a).

(45) Slovokhotova T.A., et.al., Vestnik, M.G.U., Ser., Mat.Mekh., Astron., Fiz.i Khim., 12, No.5, 193, 1957. (C.A. Vol 52 19371d)

(46) Yarze J.C., Lockerbie T.E., Catalytic Steam Reforming of Light Liquid Hydrocarbons, Kellogg Co., Research & Development Dept., N.Jersey.

(47) Rakovskii E.V. et.al., Khim.Tverdogo Topliva,8, 347, 1937. (C.A. Vol.32, 1874[8])

(48) Topsöe H., Inst.Gas.Engrs.J., 6, 401, 1966.

(49) Bridger G.W., Wyrwas W., Chem.Proc.Eng., 48, No.9, 101, 1967.

(50) Lihou D.A., Chem.Proc.Eng., 46, No.7, 487, 1965.

(51) Dirksen D.A., Riesz, C.H., Ind.Eng.Chem.,45, 1562, 1953.

(52) Somer T.G., Brit.Chem.Eng., 8, 7, 1963.

(53) Kiyoshi Morikawa, Trenner N.R., Taylor H.S., J. Am.Chem.Soc., 59, 1103, 1937.

(54) Kiyoshi Morikawa, Benedict W.S., Taylor H.S., J. Am.Chem.Soc., 58, 1795, 1936.

(55) Kiyoshi Morikawa, Benedict W.S., Taylor H.S., J. Am. Chem.Soc., 58, 1445, 1936.

(56) McKee D., J. Am.Chem.Soc., 84, 4427, 1962.

(57) Wright P.G., Ashmore P.G., Kemball C., Trans. Farad.Soc., 54, 1692, 1958.

(58) Jenkins G.I., Rideal E., Chem.Soc., 2490, 1955.

(59) Rice F.O., Herzfeld K.F., Inst.Am.Chem.Soc., 56, 284, 1934.

(60) Kemball C., Proc.Royal Soc., 207, 539, 1951.

(61) Kemball C., Proc.Royal Soc., 217, 376, 1953.

(62) Galway A.K., Kemball C., Trans.Farad.Soc., 55,1959.

(63) Galway A.K., Proc.Royal Soc., 271, 218, 1963.

(64) Leibush A.G., Bergo G.Y., Trans.State Scientific Res.Inst., Nitrogen Industry, No.2, 1953 (C.A. Vol 52, 17919f)

(65) Leibush A.G., Bergo G.Y., J.Chem.Ind.USSR., 15, No.5, 41, 1938.

(66) Bodrov I.M., Apel'baum L.O., Temkin M.I., Kinetics & Catalysis, 5, No. 4B, 1964.

(67) Bodrov I.M., Apel'baum L.O., Temkin M.I. Kinetika i Katalitz, 8, 821, 1967 (C.A. Vol 68, 43553d).

(68) Akers W.W., Camp D.P., Am.Inst.Chem.Eng.J., 1, 471, 1955.

(69) Gordon A.S., Ind.Eng.Chem., 38, 718, 1946.

(70) Gordon A.S., Ind.Eng.Chem., 44, 1857, 1952.

(71) Gordon A.S., J.Am.Chem.Soc., 70, 395, 1948.

(72) Goldstein R.F., The Petroleum Chemical Industry, (3rd Ed.), Spon, London, 1967.

(73) Dirksen M.A., Linden H.R., Pettyjohn E.S., Inst.Gas.Techn., Research Bull., No.4, 1953.

(74) Germain J.E., Bull Soc.Chim., 319, 1953 (C.A. Vol 52, 10543 f)

(75) Lavrov N.V., et al. C.A. Vol 54, 7929c.

(76) Rozhdestuenskii Y.P., et.al., Zhur Priklad Khim, 34, 1834, 1961 (C.A. Vol 56, 55g).

(77) Obolentsev R.D., et.al., J.Appl.Chem. USSR, 29, 1999, 1956.

(78) Bhatta M.S.M., Dixon G.M., Gas Council Basic Research Group, Fulham, 1967.

(79) Quibel J., Chem.Proc.Eng., 50, No.6, 83, 1969.

(80) Grinrod J., Petro. Chem.Engr., Oct, 43, 1964.

(81) Waterhouse J., Gas World, 23rd Jan, 132, 1965.

(82) Bridger G.W., Chem.Proc.Eng., 47, 39, 1966.

(83) Lihou D.A., Chem.Proc.Eng., 46,No.7, 487, 1965.

(84) Levinter M.E., Panchenkov G.M., Tanatarov M.A., Int.Chem.Eng. J., 7, 23, 1967.

(85) Holland D.R., Wan S.W., Chem.Eng.Prog., 59, 69, 1963.

(86) Hebden D., Trans.Inst.Gas Eng., 95, 602, 1945.

(87) Kiyoshi Muraosa, Kogyo Kagaku Zasshi, 64, 1101, 1961. (C.A. Vol 57, 7517a).

(88) Kiyoshi Muraosa, Kogyo Kagaku Zasshi, 64, 1933, 1961, (C.A. Vol 57, 2043b).

(89) Kiyoshi Muraosa, Kogyo Kagaku Zasshi, 64,1770, 1961. (C.A. Vol 57, 3695c).

(90) Kiyoshi Muraosa, Kogyo Kagaku Zasshi, 64, 1776, 1961. (C.A. Vol 57, 3257f).

(91) Reitmeier R.E., Kenton Atwood, Bennett H.A. Junr., Baugh H.M., Ind.Eng.Chem. 40, 620, 1948.

(92) Kemball C., Moss R.L., Proc.Royal Soc., A 238, 107, 1956.

(93) McD.Baker M., Rideal E.K., Trans.Farad.Soc., 51, 1597, 1955.

(94) Hofer L.J.E., Cohn E.M., Peebles W.C., J.Physical Chemistry, 54, 1161, 1950.

(95) Nagakura S., J.Physical Soc.of Japan, 12,482, 1957.

(96) Kiyoshi Muraosa, Kogyo Kagaku Zasshi, 69, 1942, 1961. (.C.A. Vol 57, 2043d).

(97) Lee G.T., Leslie J.D. Rodekour H.M., Oil & Gas Journal, May, 1964.

(98) Coatsworth K., Chem.Engr., C.E.242, July/Aug., 1968.

(99) Schora F.C., Fuel Gasification, (Preface), Advances in Chemistry Series, Am.Chem.Soc., Washington, 1967.

(100) Cottingham P.L., Carpenter H.C., Fuel Gasification, Advances in Chemistry Series, Am.Chem.Soc., Washington, 1967.

(101) Riesz C.H., Batchelder H.R., Lurie P.C., Am. Gas.Assoc. Monthly, 30,17, 1948.

(102) Riesz C.H., Lister R., Smith L.G., Komarewsky V.I., Ind.Eng.Chem., 40, 718, 1948.

(103) Sebastian J.J.S., Riesz C.H., Ind.Eng.Chem., 43, 860, 1951.

(104) Riesz C.H., Dirksen H.A., Pleticka W.J., Inst.Gas.Techy., Research Bull., 20, Oct., 1952.

(105) British Patent. No: 953,877.

(106) Riesz C.H., Dirksen H.A., Kirkpatrick W.J., Inst.Gas.Techy, Research Bull., 10,1951.

(107) Riesz C.H., Am.Gas.Assoc.Proc., 505, 1948.

(108) Fischer & Porter Handbook, 10 A 9010, Warminster, Pennsylvania.

(109) Cross R.A., Nature, July, 211, 409, 1966.

(110) Cross R.A., Private Communication.

(111) Dodge B.F., Chemical Engineering Thermodynamics, McGraw-Hill, New York. 1944.

(112) Pease & Chesebro, J.Am.Chem.Soc., 50, 1464,1928.

(113) Ipatieff V.N., Monroe G.S., Fischer L.E., Ing.Eng.Chem., 42, 92, 1950.

(114) Wellman P., Katell S., Hydrocarbon Proc. & Petrol-Refiner, 42, 135, 1963.

(115) Ribesse J., Van Maele C., Inst.Gas Eng.J. Sept., 1961.

(116) Lapidus L., Digital Computation for Chemical Engineers, McGraw-Hill, New York, 1962.

(117) Spier H.M. (Ed)., Technical Data on Fuel, 6th Edition, London.

(118) Nat.Bur.of Stds., Selected values of Properties of Hydrocarbons, Circular of the Nat. Bur. of Standards, C.461, U.S. Dept., of Commerce, N.B.S.

(120) Stokes B.A., W.M.G.B., Private Communication.

(121) Dodge B., Trans.Am.Inst.Chem.Eng., 54,540, 1938.

(119) Hougen Watson and Ragatz, Chemical Process Principles, Parts I II and III John Wiley, New York.

(122) Yang K.H., Hougen O.A., Chem.Eng.Prog. 46, 146, 1950.

(123) Smith B.D., Ph.D. Thesis, 1967, B'ham. Univ.

(124) Bohlbro H., Acta.Chem.Scand., No.3, 15, 1961.

(125) Barkley L.W., Corrigan T.E., Wainwright H.W., Sands A.E., Ind.Eng.Chem., 44, 1066, 1952.

(126) Perry J.H., Chemical Engineers Handbook 4th Edition, McGraw-Hill, New York.

(127) Guha T., Callow R.B., B'ham.Univ.Chem.Eng. 13, 1, 1962.

(128) Hougen O.A., Watson K.H., Chemical Process Principles, Part III, John Wiley, New York, 1947.

(129) Gilliland E.R., Ind.Eng.Chem., 26, 681, 1934.

(130) West Midlands Gas Board, Private Communications.